MSEL

Materials Science and Engineering Laboratory

CERAMICS

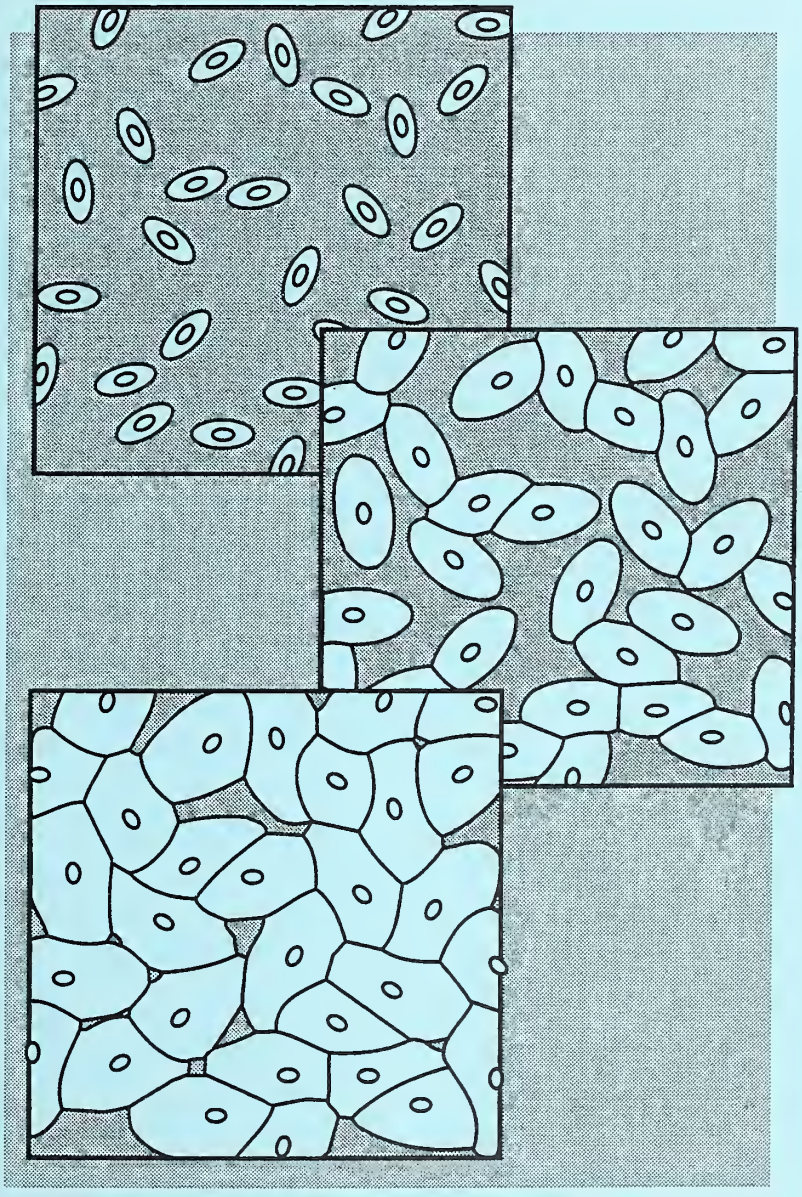

NAS-NRC
Assessment Panel
May 13-14, 1993

NISTIR 4964
U.S. Department of Commerce
Technology Administration
National Institute of Standards
and Technology

Technical Activities 1992

Report Cover: The cover illustration depicts a computer generated graphic simulation of microstructural development in ceramics. The computer based assessment of the role of initial and processing conditions and the application of physical laws allows the rapid evaluation of many process routes which can be verified by experiment. Development of such modeling techniques speeds research through the identification of critical processing conditions.

Materials Science and Engineering Laboratory

CERAMICS

S.W. Freiman, Chief
S.J. Dapkunas, Deputy Chief

NAS-NRC
Assessment Panel
May 13-14, 1993

NISTIR 4964
U.S. Department of Commerce
National Institute of Standards
and Technology

Technical Activities 1992

U.S. DEPARTMENT OF COMMERCE, Ronald H. Brown, Secretary
National Institute of Standards and Technology, John W. Lyons, Director

TABLE OF CONTENTS

OVERVIEW

In 1992 the Ceramics Division continued to develop a technical program which addresses the needs of U.S. industry. This program is made up of tasks involving standard materials development, construction of evaluated databases, and laboratory research focused on topics relevant to the dominant issues affecting commercialization of advanced ceramics, e.g., processing costs and reliability.

A special effort was made this year to hold workshops at NIST with U.S. industrial representatives in a number of materials areas to obtain firsthand knowledge of their research priorities. As examples, workshops were conducted on Photonic Materials (held in conjunction with the Optoelectronic Industry Development Association), Thermal Sprayed Ceramic Coatings, and Intelligent Processing of Ceramic Powders.

The output of the Ceramics Division program is made available to U.S. industry and the ceramics community through a number of avenues including presentations, publications, and direct collaborations with companies and universities. During this past year the research program produced 128 publications, 125 presentations, and led to 7 invention disclosures, 16 Cooperative Research and Development Agreements (CRADAS) were signed with companies and universities.

A significant development during 1992 was the formal inauguration of a consortium devoted to the better understanding of the machining of advanced ceramics. Machining costs can be as much as 80 percent of the total cost of a ceramic product. Now consisting of 17 members from industry and academia, the initiation of this Consortium was highlighted by the signing of one of the CRADA's by Secretary of Commerce, Barbara Hackman Franklin.

Standard materials and data activities continue to represent an important portion of the Division's program. Four new Standard Reference Materials were developed this year. These were: 1) a particle size distribution for silicon nitride powders (SRM 659), 2) a calibration of x-ray intensity for phase composition analysis (SRM 656), 3) an equipment calibration standard for x-ray intensity (SRM 1976), and 4) Abrasive Wear, (SRM 1857). Version 2.0 of the Structural Ceramics Database which contains thermal, mechanical, and corrosion properties of silicon carbide and silicon nitride was released for sale. This is the only publicly distributed database of evaluated materials properties for advanced ceramics. A new program to establish a computerized database for evaluated properties of high T_c superconductors was initiated. An agreement between the Ceramics Division, the Standard Reference Data Program, and the National Research Institute for Metals in Japan has been drafted, which will lead to a shared effort in the development of this database. Several new volumes were published this year as part of the NIST/American Ceramic Society program on phase diagrams for ceramic materials. These include Volume 9 of the series Phase Equilibria Diagrams, an Annual 1992 Volume, a Bibliographic Update, and a Cumulative Index to previous volumes. Finally, one of our staff (E. F. Begley) received a Department of Commerce Pioneer Fund grant to initiate the development of an innovative computer-based tutorial system for phase diagrams.

A major effort over the past few years has involved the NIST leadership of the International Energy Agency ceramic powder characterization program. During the past year characterization procedures developed by the participants from four countries were approved for release to the standard setting bodies in these countries. The implementation of these procedures is expected to lead to more cost-effective ceramic production.

The Division's program on high T_c superconducting materials has continued to focus on research relevant to the production of bulk components such as superconducting wires and magnets. The Division is working closely with the Department of Energy and several U.S. companies to develop the data, measurement procedures, and understanding needed for wire development.

Work on the use of nanosized powders as starting materials for ceramic components has been expanded. Research on the development of magnetic nano-composites has continued. Magnetocaloric measurements of these composites indicate promise for their use as refrigerants. Scale-up of the pressure induced sintering process for producing silicon nitride from nanosized starting powders has been achieved. Three millimeter diameter discs of transparent silicon nitride have been produced. Finally, we have begun to prepare Bi_2Te_3 composites using a chemical approach. These composites which are of interest as components in thermoelectric refrigerators contain nanosized second phase particles which reduce the thermal conductivity of the material, and thereby increase its figure of merit.

This past year has seen a further increase in the modeling efforts in the Division at both the atomic and microstructural levels. These modeling studies include first principle calculations of phase diagrams, molecular orbital calculations of environmental interactions with strained crack tip bonds, micro-mechanics modeling of the fracture process in polycrystalline ceramics, models of high temperature creep, and models relating grain growth to the surface energy of grain boundaries.

In 1992, both funding and staff levels remained relatively constant. Dr. Craig Carter, Dr. Linda Braun, Dr. Larry Rotter, and Dr. Dan Fischer were added to the Ceramics Division staff during the year. Dr. Stephen Hsu returned from his IPA at Penn State and Northwestern Universities to lead the new Surface Properties Group. Dr. Ben Burton transferred to the Ceramics Division from the Metallurgy Division.

Finally, the Division has greatly increased both formal and informal collaborations with awardees of grants from the NIST Advanced Technology (ATP) Program. These collaborations include work directly funded by the ATP to work with Nanophase Technologies Inc. in their effort to develop ceramics from nanosized powders. The NIST research involves using neutron and x-ray scattering techniques to characterize microstructure development. Other collaborations have been initiated with the American Superconductor Corporation, Westinghouse Corporation, and Garrett Ceramic Components.

Stephen W. Freiman
Chief, Ceramics Division

1992 DIVISION RESOURCES

Ceramics Division

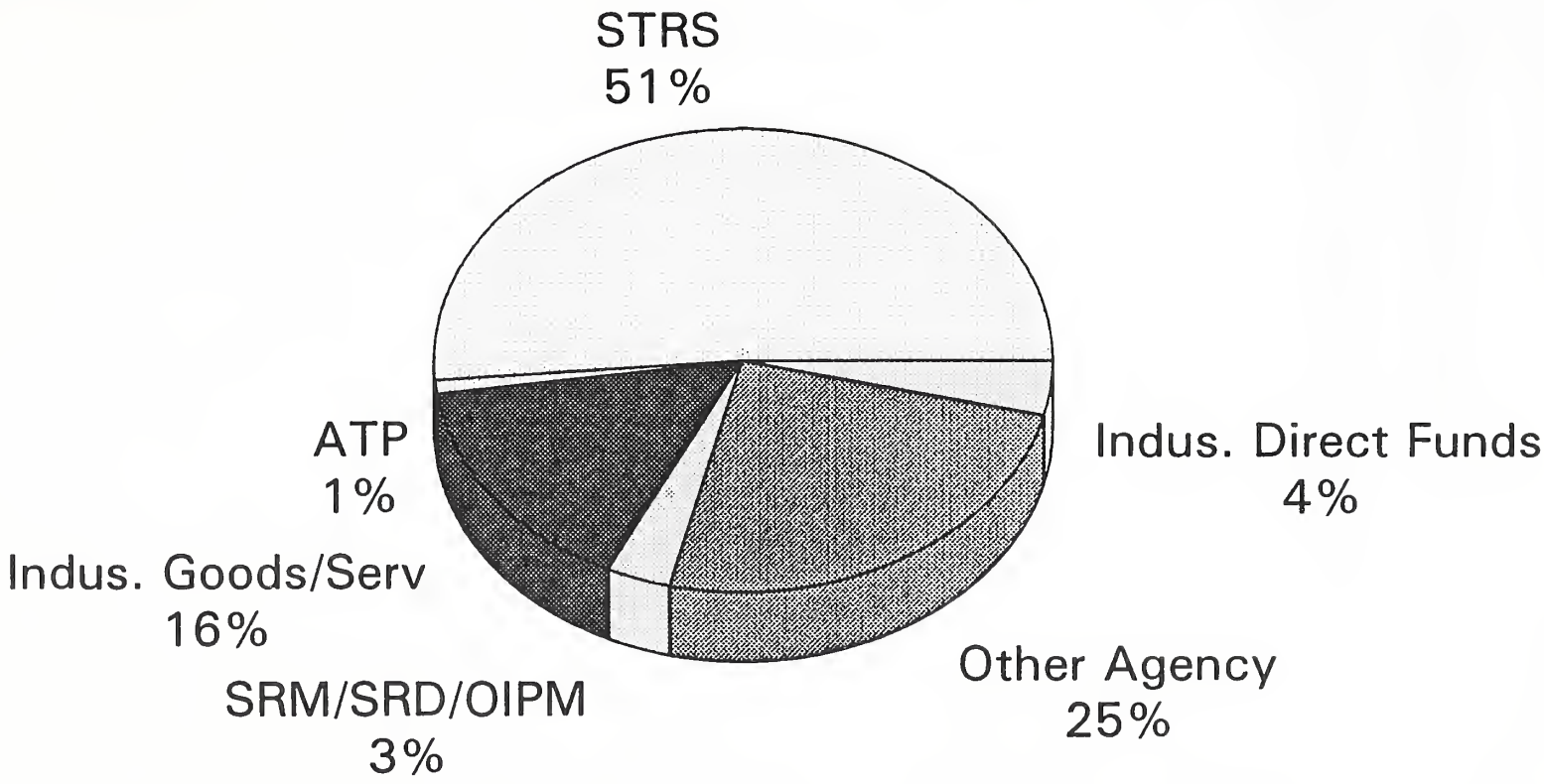

TECHNICAL ACTIVITIES*

Certain trade names and company products are mentioned in the text or identified in illustrations in order to adequately specify the experimental procedure and equipment used.

In no case does such identification imply recommendation or endorsement by the National Institute of Standards and Technology, nor does it imply that the products are necessarily the best available for that purpose.

TECHNICAL ACTIVITIES*

I. DATABASE ACTIVITIES

Research and development efforts in U. S. industries are presenting a rapidly growing demand for both general and specific information on advanced materials. Much of the critical information that is needed is widely dispersed in books, journals, and conference proceedings in a multiplicity of specialized studies. Collecting, synthesizing, and evaluating such data requires a major investment of time and money, and these efforts are frequently, and repeatedly, duplicated by diverse efforts in industry. Often, such data reviews require specialized knowledge to assess the significance and reliability of the data. The Ceramics Division is developing innovative, evaluated, and comprehensive computerized information systems to meet this growing demand.

The Division's activities in the past year have been extended from traditional compilation of data, such as the "Phase Diagrams for Ceramists", to development of better methods to transfer and utilize materials information. These changes increase the impact of work and the degree of interaction with the users of data.

Significant Accomplishments

- The Structural Ceramics Database (SCD), Version 2.0, was released in July 1992 for sale to the public through the NIST Standard Reference Data Program. To date, the SCD is the only publicly distributed computerized database of evaluated materials properties for advanced ceramics. The SCD, which is used in twelve countries around the world, is funded by the Gas Research Institute, the Standard Reference Data Program, and the Ceramics Division. Version 2.0 contains thermal, mechanical, and corrosion properties for both commercial and research grades of silicon carbide and silicon nitride.

- A new program to establish a computerized database of evaluated materials properties for high-temperature superconductors (HTSC) has been initiated with the support of the NIST Standard Reference Data Program. The HTSC program is aimed at providing the essential results of the more than 30,000 publications on these materials that have appeared since 1987. The Ceramics Division and the Standard Reference Data Program are conducting negotiations with Japan's National Research Institute for Metals to establish a collaborative, international agreement on this effort. A tentative agreement has been drafted and is expected to be signed in early FY93.

- A Department of Commerce Pioneer Fund grant was received to initiate the development of an innovative information system that will allow some of the unique expertise gained in NIST research efforts to be preserved and made accessible in an interactive, computerized forum. The new system will utilize the advanced capabilities of digital video interactive technology and expert system software.

- An assessment of the corrosion of advanced ceramics has been conducted under funding from the Department of Energy's Pittsburgh Energy Technology Center. This study is examining the material and performance effects of the corrosion of

various forms of silicon carbide and silicon nitride. These materials are candidates for use in coal-fueled heat exchanger applications in which the temperature exceeds 1000 °C and the environments are often complex gaseous and particulate mixtures. Included in the study are atmospheres of dry and moist oxygen, mixtures of hot gaseous vapors, molten salts, molten metals, and complex environments pertaining to coal ashes and slags.

- Several compilations of phase diagrams for ceramics systems were published: Phase Diagram for Ceramists, Annual '92, Phase Equilibria Diagrams - Volume 9, a Bibliographic Update, and a Cumulative Index.

The Structural Ceramics Database

R. G. Munro and E. F. Begley

The Structural Ceramics Database (SCD) was developed to provide evaluated data for the materials properties of advanced ceramics that could be used in high-temperature environments where other materials might be inappropriate. By design, the SCD is maintained as a reliable source of information that is available nationally and is easy to use on personal computers. The evaluated data of the SCD now provide an important resource for assessing the strengths and weaknesses in currently available data and, in effect, provide a guide to needed future research. More importantly, the availability of evaluated data may assist in materials selection for advanced engineering designs, facilitate new systems developments, and accelerate the introduction of advanced ceramics into industrial applications having high-temperature, aggressive environments.

The first version of the SCD contained data derived from published reports on the thermal and mechanical properties of silicon carbides and silicon nitrides. Most of the data pertained to materials prepared by the researchers themselves and appeared to be of interest primarily to materials research efforts. To address the information requirements of design engineers, the emphasis for the current year was placed on the acquisition of evaluated data for commercially available materials.

Data for numerous commercial materials are now included (15 silicon carbides and 13 silicon nitrides) in the second version of the SCD. A token amount of data is also included for alumina, beryllia, zirconia, aluminum nitride, and boron nitride. The new release of the database also includes two new software features, graphics, to allow on-screen plots of property data versus temperature, and a brief display mode to preview the records retrieved by a user's search of the database.

Corrosion of Advanced Ceramics

R. G. Munro and S. J. Dapkunas

The potential applications of advanced structural ceramics have been widely appreciated for several decades. Characteristics such as high maximum use temperature, strength retention

at high temperature, and chemical stability have held forth tantalizing possibilities for more efficient engines, heat exchangers and recuperators, and for more durable electronic packaging and chemical processing components. The primary barriers that have impeded the widespread development of these applications have been the susceptibility of structural ceramics to brittle fracture and environmentally sensitive corrosion behavior, including the subsequent effects of corrosion on the thermal and mechanical performance of ceramics. The former barrier has received, by far, the greater amount of attention. The corrosion of advanced ceramics, however, has proven to be the more complex problem and has been recognized as a critical consideration in attaining high efficiency applications.

The Ceramics Division is currently conducting a review of the substantial effort that has been made to measure and to understand the effects of corrosion with respect to the properties, performance, and durability of various forms of silicon carbide and silicon nitride. The review encompasses corrosion in diverse environments, usually at temperatures of 1000 °C or higher. The environments include dry and moist oxygen, mixtures of hot gaseous vapors, molten salts, molten metals, and complex environments pertaining to coal ashes and slags.

For both silicon carbide and silicon nitride, corrosion resistance is primarily a result of the formation of silica on the outer surface of the material. An intermediate layer of silicon oxynitride also plays an important role in the case of silicon nitride. To establish a pertinent view of the corrosion of these materials, the formation, dissolution, and stability of these layers must be examined in the context of industrial applications.

There are two primary concerns regarding the selection of a material for use in corrosive environments: the survival of the material, often expressed as the recession rate of the surface, and the mechanical strength of the component. The corrosion rates for ceramics can be relatively small, and, as a result, the recession rates may be tolerable. However, surface pitting and the overall increase in the surface flaw populations generally degrade the strength of the material and reduce its average mechanical lifetime. While some combinations of material and environment may produce a short-term strength enhancement resulting from the healing of surface defects, long-term corrosion generally tends to decrease the strength of the material as the severity of the surface pitting increases.

Results of this review project will provide a coherent foundation for subsequent experimental efforts in the development of coal- and gas-fueled heat exchangers. Quantitative results from this study will be incorporated into the next version of the Structural Ceramics Database.

Phase Equilibria Information System Incorporating Digital Video Interactive Technology

E. F. Begley and C. Lindsay

The rapid growth of materials research in the last decade has involved scientists and engineers from many disciplines. Very often, these researchers have expertise from fields of chemistry and physics in which little or no knowledge of the phase equilibrium diagram has been required previously. In materials research, however, the phase diagram is a critical processing tool. To provide a timely, "on-site" resource for phase equilibria diagrams, the

Ceramics Division has initiated the development of an innovative, computerized information system which eventually will combine expert system software with digital video interactive technology. The first phase of this project is to develop an interactive tutorial on the use of phase diagrams.

Digital video interactive technology allows motion video and audio signals to be digitally compressed and integrated with traditional software applications. In the tutorial, for example, a user who does not understand some aspect of how phase equilibria diagrams are developed could ask the software for an explanation. Rather than responding with simple text, the software would show a short video of an expert in the laboratory demonstrating what is done. This mode of interaction is natural, familiar, and reduces misunderstandings.

Two phases have been planned for this project. The first phase will concentrate on developing an application that will enable individuals to learn or to review how to interpret and use unary, binary, and ternary phase equilibria diagrams. The second phase will concentrate on the implementation of an application that will provide instruction in developing phase diagrams.

With support from the Department of Commerce Pioneer Fund, development of the first phase is underway. The consequences of successful completion are twofold. First, phase diagrams serve as critical roadmaps for materials processing; they are particularly important, for example, in the development of complex electronic ceramics such as high temperature superconductors. U.S. industrial scientists and engineers will have a readily available, high quality system to help them understand these diagrams. Second, understanding phase equilibria is an important aspect of geology, petrology, and materials science programs. Therefore, the tutorial will serve industry and academia, as well as NIST scientists and engineers.

High-Temperature Superconductors

R. G. Munro and J. R. Rumble, Jr.[1]

[1]NIST Standard Reference Data Program

High-Temperature Superconductors (HTSC) comprise one of the most intensely studied classes of materials currently available. Since their discovery in 1986, more than 30,000 reports on the processing, characterization, and properties of these materials have been published in the open literature. This prolific publication rate is evidence of the intense interest in the potential applications of these materials. Developing commercial applications, however, requires the fabrication of HTSC materials into useful forms such as films on non-HTSC substrates or as wires. The fabrication of such forms is highly dependent on the thermal, mechanical, and chemical properties of these materials because HTSC materials are brittle and often reactive with the relevant substrate materials under processing conditions. While extensive bibliographic databases of titles and abstracts of reports are maintained by several public and private agencies, there has been no systematic compilation, evaluation,

and computerization of the numeric data. As a result, there are three major information barriers confronting any designer seeking to develop applications of HTSC materials: (1) the quantity of reports; (2) the reliability of the data; and (3) the currency of the results. These barriers are best resolved through the use of evaluated computerized databases.

NIST, therefore, has initiated the development of a computerized database of evaluated materials properties for HTSC materials. The database will include information on materials processing, composition, structure, and a full range of properties including thermal and mechanical properties as well as the critical characteristics of high-temperature superconductors.

There is worldwide interest in evaluated data for HTSC materials. Negotiations are being pursued specifically with Japan's National Research Institute for Metals (NRIM). Like NIST, NRIM has a strong research program on HTSC materials and would like to optimize the impact of its research results through the development of a computerized information system. A formal agreement between NRIM and NIST is expected to be signed early in FY93 to establish international collaboration on this common goal.

STEP Materials

J. A. Carpenter, Jr. and J. R. Rumble, Jr.[1]

[1]NIST Office of Standard Reference Data

In this period, J. A. Carpenter, Jr., on behalf of the Materials Science and Engineering Laboratory (MSEL), became involved in the national and international thrust on computerized data exchange known as STEP (the STandard for Exchange of Product Model Data). He and J. R. Rumble, Jr. of the NIST Office of Standard Reference Data collaborated with personnel from industry and government, both U.S. and foreign, to further develop the part of STEP dealing with the exchange of materials data and integrate it with the other parts of STEP dealing with exchange of other types of technical data (e.g., drawings, geometry, electrical layout, finite element analyses, etc.) needed to fully describe a manufactured product. In order to promulgate knowledge of STEP to U.S. industry, Rumble and Carpenter co-authored an article on the materials part of STEP that was published in Advanced Materials and Processes magazine (a major national magazine catering to the materials community) and organized and held the National STEP Materials Conference at NIST on Dec. 2-3, 1992. Personnel from other MSEL divisions and the NIST Building and Fire Research Laboratory were also involved in the STEP Materials Conference.

STEP is an international attempt to facilitate the computerized exchange of product data by providing standardized neutral file formats. It is NOT an attempt to provide standardized formats for databases, software, or display, nor to provide nationally or internationally unified databases; it is strictly for the EXCHANGE of data.

Increasingly, products are designed, manufactured, marketed, and tracked via a variety of computer programs and databases. The STEP standard aims to make it easier for these

computer programs to "talk" to one another and access the databases. The current, somewhat chaotic, situation is depicted in Figure I-1 wherein various computer programs try to communicate with each other and several databases; specialized "translator" programs must be written for every possible combination. STEP attempts to replace this with the less chaotic, but still difficult, situation depicted in Figure I-2 in which all the computer programs and databases can communicate through a neutral format; each program or database simply needs one translator from its own format to the STEP format in order to communicate with all the others. An analogy is the agreement by all airline pilots of the world to communicate in English.

STEP is an outgrowth of the Initial Graphics Exchange Specification (IGES) standard, successfully developed and accepted worldwide in the late 1970's and early 1980's for exchange of graphical information, mainly drawings. Buoyed by the success of IGES, the United States decided in 1983-84 to begin development of standards for the computerized exchange of ALL product data, from research and conceptual design, through manufacturing and marketing, even to ultimate disposal. The U.S. designated this the Product Data Exchange Specification (PDES). By about 1987, the International Standards Organizations (ISO) decided to adopt PDES as a world standard and renamed it STEP; PDES now stands for "**P**roduct **D**ata **E**xchange using **STEP**." STEP is officially designated by ISO as Standard 10303. In the U.S., the effort is led by the IGES/PDES Organization (IPO) and PDES, Inc.; IPO is a completely voluntary organization similar to the American Society for Testing and Materials (ASTM) whereas PDES, Inc. is a dues-paying consortium set up by U.S. industrial firms to conduct joint research on data exchange. The U.S. government has also recently launched its own thrust called the National Initiative on Product Data Exchange (NIPDE), mainly aimed at better coordinating all these efforts.

Work on STEP has progressed to the point where initial parts are ready for issue by ISO in January 1993 as Draft International Standards (DIS's), meaning the parts can now undergo widespread trial and revision for a period of time before being finally adopted as worldwide standards. The part dealing with exchange of materials data has not yet reached the DIS stage. Based on the efforts this year, described in the first paragraph above, it is expected that it will become a DIS later in 1993.

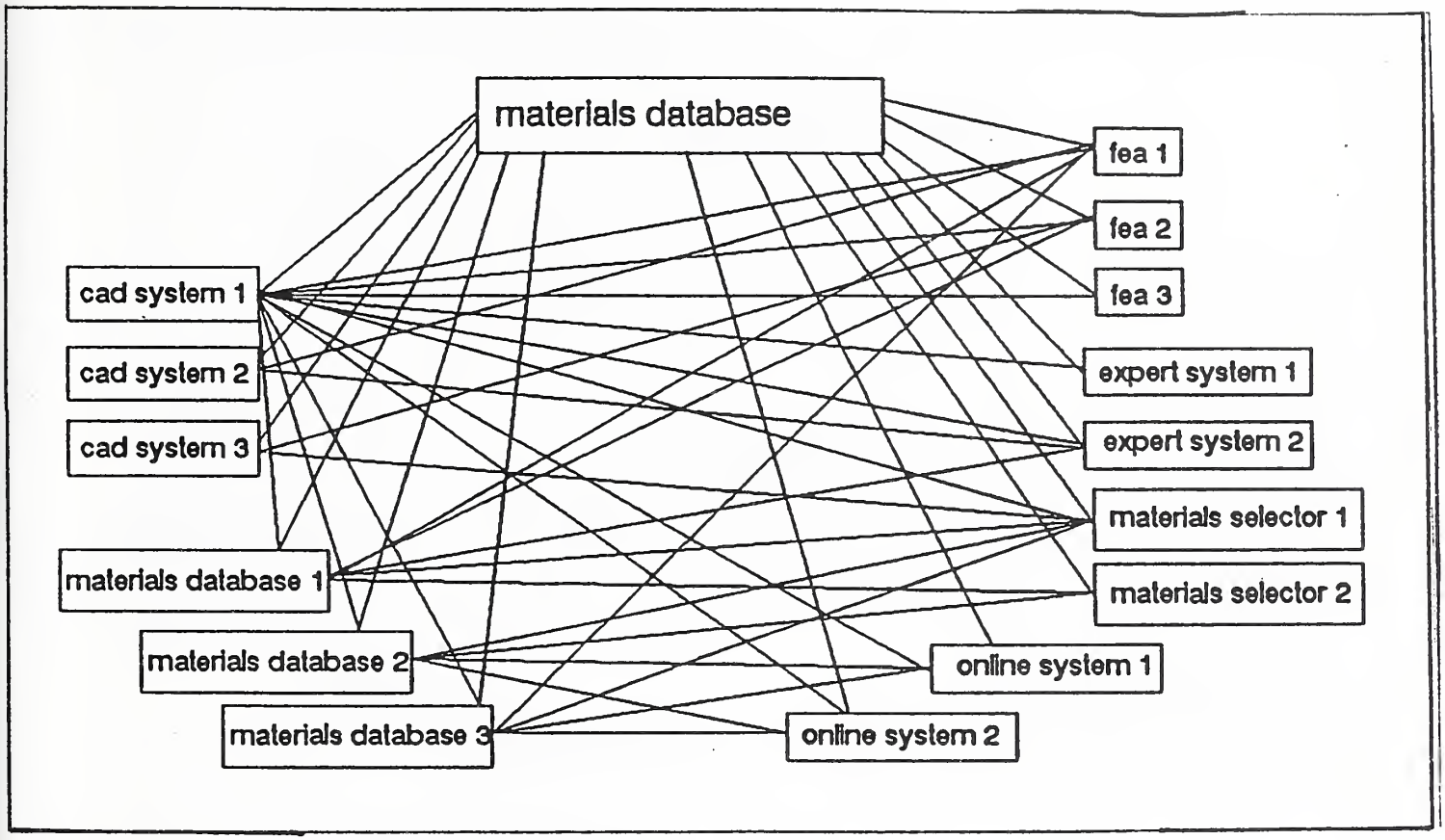

I-1. Currently, in order to exchange data via computer between various software (e.g., computer aided design (CAD), finite element analysis (FEA), expert system, materials selector) and databases, each having different formats, specialized programs called "translators" must be written for each pair. The rather cumbersome and chaotic situation depicted here results.

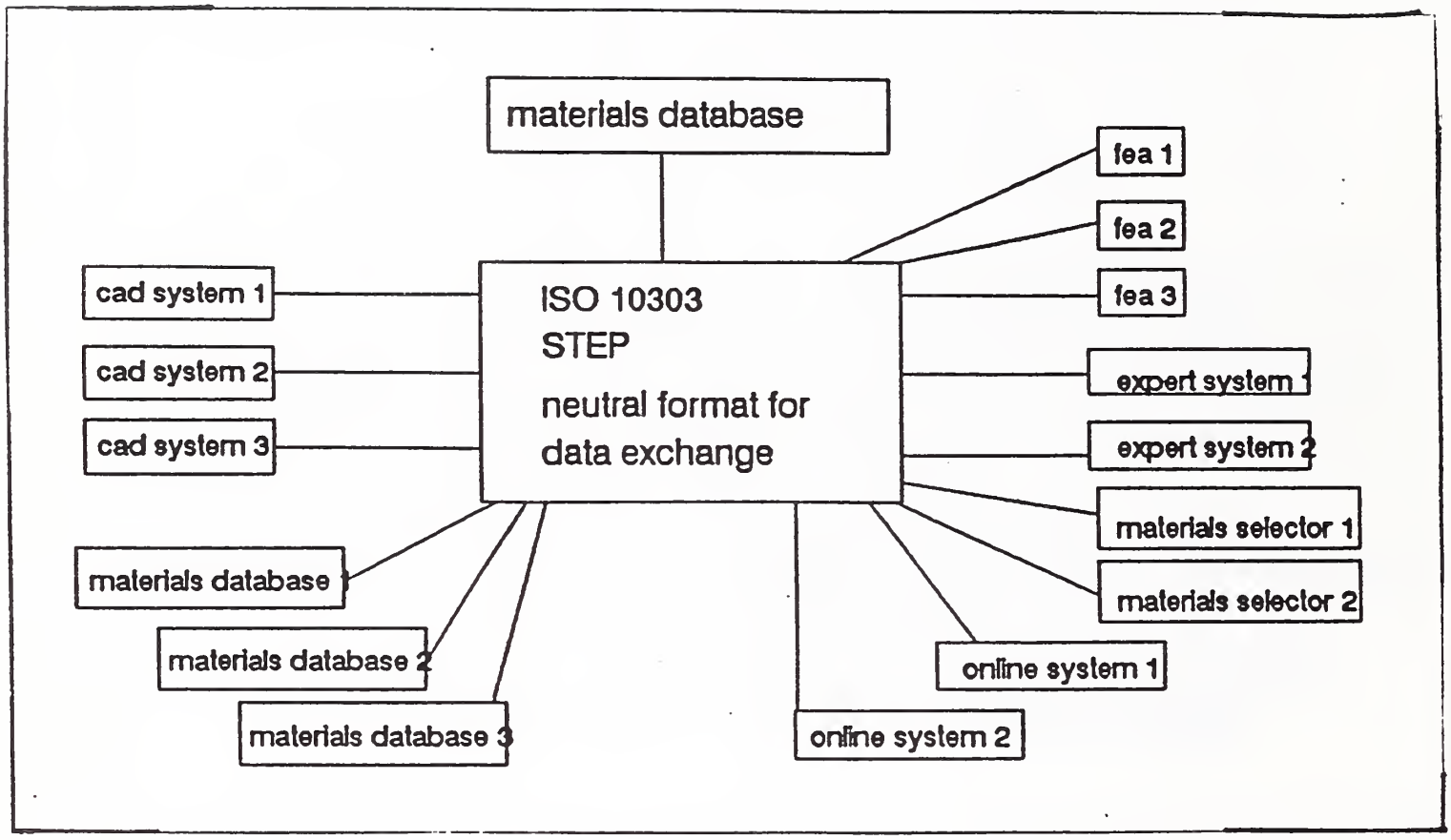

I-2. The intention of STEP is to provide a neutral format into which the data from each piece of software and every database can be translated by a single translator program, thus facilitating communication with all the others.

II. POWDER CHARACTERIZATION AND PROCESSING

Subhas G. Malghan

In the past few years, the U.S. advanced ceramic industry has been able to produce monolithic and composite materials having successively better properties. These improvements have been the result of numerous studies focussing on processing of ceramics. Now cost and reproducibility in obtaining improved properties have become the focus not only in the industrial sector but also in government programs. The 1992 report by the Federal Coordinating Council for Science, Engineering and Technology (FCCSET) of the Office of Science and Technology Policy emphasizes the role of processing in the general arena of materials technology development. In line with such an initiative, a new program has been initiated by the Office of Transportation Technologies, Department of Energy on cost effective ceramics for heat engines. From a technical perspective, processing of ceramics has its roots in powders processing since most ceramics are produced using fine powders.

The Ceramics Division's program on powder characterization and processing is an integrated effort that has been formulated to address critical issues in the processing of powders. This program constitutes research from early stages of synthesis of well-characterized, deagglomerated powders to the understanding of processing effects on the microstructure of ceramics. The underlying hypothesis for this emphasis is that controlled powder characteristics can result in predictable densification and microstructural development, improved ceramic properties, and reproducibility in manufacturing.

The Powder Characterization and Processing group program has emphasized measurement quality, ceramics processing, and chemical synthesis of powders. The overall objectives of the group program are to provide the U. S. ceramic community the ability to control ceramic powder properties so that cost-effective ceramics can be realized. Specifically, the group program consists of the following elements:

1. Development of powders characterization tools such as measurement science, standard methods, and standard reference materials.

2. Processing science to understand interrelationships between powder characteristics, their processing parameters, and densified ceramics.

3. Novel synthesis methods as applied to nano-sized particles and ultra-pure particles for novel processing studies.

Characterization tools are expected to help U. S. industry in the development of powder specifications for particular applications and thereby reduce the cost of processing and waste. An understanding of interrelationships between powder properties and processing has the potential to lead to increased capabilities for microstructural design and improved reproducibility in manufacturing. Nano-powders synthesis is an emerging field where synthesis and processing capabilities can lead to novel materials of unusual mechanical, optical and magnetic properties, as well as possible significant reductions in processing temperatures with concomittant reduction in cost.

With the industrial trend towards cost-effective manufacture of ceramic components for new applications, our focus will continue to be on powder dispersion science in dense slurries, nano-structured powders synthesis and processing, measurement science, and process modelling including on-line measurement of properties for intelligent processing of powders. Further, we plan to strengthen existing collaborations and cooperation with the ceramic coatings and powders processing industry in the U.S.

Significant Accomplishments

- One of the major goals of the IEA powders characterization program was the development of a set of procedures by Subtask 6 participants in the U.S. Sweden, Germany, and Japan. These procedures have been approved for release to the stamdards-setting bodies in the participating countries, thus providing a source of information that was not available. As some of the major goals of this program are coming to fruition, a continuation program is being planned which includes secondary properties of powder, e.g., rheology, compaction density, and agglomerate size. These properties may hold a key to the development of powders specifications for commercial applications.

- Three Standard Reference Materials were developed during this year. Specifically, these were: (1) measurement of silicon nitride powders particle size distribution (SRM 659), (2) calibration of x-ray intensity for phase composition analysis by x-ray diffraction (SRM 656), and (3) calibration of equipment for the intensity variable as a function of 2θ angle, i.e., instrument sensitivity (SRM 1976).

- Design and construction of equipment was completed for compaction of nano-size powders at different temperatures, pressures and environment. This is a major milestone in this project since the equipment allows the study of process variables of nano-size silicon nitride powders densification, and produces 3.0 mm diameter specimens for subsequent evaluation.

- An interrelationship between oxide layer thickness and pH_{iep} was developed for silicon nitride powders. The pH_{iep} is the pH at which particles carry a net zero charge in aqueous suspensions. This interrelationship was established using electroacoustic measurements and x-ray photoelectron spectroscopy data. This information is necessary for the development of highly repeatable processing of powders.

- Several procedures for synthesizing rare earth/transition metal magnetic materials of high magnetization and nano-sized magnetic regions have been developed. One such magnetic nano-composite material, gadolinium gallium iron garnet, $Gd_3Ga_{5-x}Fe_xO_{12}$, is being evaluated in a collaborative effort with the Magnetics Group in the Metallurgy Division. These and similar materials are being considered as a new class of magnetic refrigerants.

- An experimental approach has been developed for the analysis of microstructure and the factors controlling microstructural development in elongated grain silicon nitrides. This approach allows for dissolution of grain boundary phases in Si_3N_4 materials without attacking the Si_3N_4 grains. Use of this technique has allowed the study of factors which

either promote or inhibit production of elongated, fibrous grains.

- A workshop was organized for the U.S. ceramics community to address intelligent processing of powders by the application of electroacoustics for the measurement of surface chemistry parameters, and nuclear magnetic resonance spectroscopy for understanding of defects in processing. Subsequent to this workshop, a number of participants have expressed interest in joining a consortium at NIST to address issues of relevance to silicon nitride powders processing.

International Interlaboratory Comparison of Powder Characterization

S. G. Malghan, L.-H. S. Lum, E. Begley and S. M. Hsu

Cost of production and reproducibility of ceramic components continue to be major issues affecting the widespread use of structural ceramics. Since powders are the starting materials for the production of ceramics, improvements in their characterization and processing hold a key to solving some of the problems of rapid commercialization. This program was initiated in 1986 with the objective of developing pre-standardization procedures for characterization of ceramic powders. The current program, Subtask 6, under the auspices of the International Energy Agency with participation from Germany, Japan, Sweden and U.S., has been in progress since 1989.

The specific objective of Subtask 6 was to improve selected physical and chemical characterization procedures, and conduct a survey of surface chemical analysis procedures. Approximately 25 procedures on five powders were studied by 44 participants in the four countries. Some of the major tasks involved in this project were as follows:

- Procedures collection from participants and development of consensus procedures

- Robustness testing of procedures and development of corrected, consensus procedures

- Preparation of powder samples and their distribution to participants

- Analysis of samples by participants using prescribed procedures

- Collection and compilation of data

- Technical and statistical analysis of data

- Preparation and distribution of preliminary reports on procedures, data analysis and data compilation

At this time, most of the major tasks described above have been completed. In addition, preliminary conclusions and recommendations have been developed.

One of the major tasks this year was to prepare an interim report on Procedures Compilation for approval by the IEA Annex II Executive Committee for release to the standards setting bodies in the participating countries. The purpose of advance release of this report is to assist the standards setting activities which need these procedures to carry out their function in an expeditious manner. This report contains 25 procedures used by the participants of Subtask 6. The early release is in agreement with the goals of the IEA to conduct pre-standardization research and assist downstream activities on standardization. The final report to be released in 1993 will contain detailed analysis of data, procedures compilation, and suggested improvements to the procedures.

The ASTM C-28.05 committee on powders characterization will be given the procedures compilation report. Availability of the IEA draft procedures will accelerate committee activities. The committee has independently developed five draft standards of which three are in sub-committee ballot.

As this phase of the program comes to completion, the technical leaders are developing a program to address two specific issues: (1) ways to improve sample preparation procedures for methods that showed lack of agreement in Subtask 6; and (2) procedures required for powders specification that involve secondary properties of powders. The participants in each country have been discussing these issues and a preliminary program was developed. Recently, this program was approved by the IEA Executive Committee, pending the development of detailed plans by the technical leaders.

Standards for Particle Size Measurement

J. F. Kelly, L.-H. S. Lum and S. G. Malghan

Knowledge of agglomerate and primary particle size distribution is one of the principal requirements in ceramic powders processing. The measurement of particle size distribution is required of the starting powders and during processing so that desired microstructure can be achieved. Accuracy and reproducibility of particle size measurement have been the subject of many publications and studies. The consensus opinion is that lack of suitable standard reference powders for calibration of particle size measurement equipment severely limits our ability to achieve highly accurate and reproducible data. The emphasis of this project, in collaboration with the NIST Office of Standard Reference Materials, has been to develop new standards and to recertify selected existing Standard Reference Materials, SRMs, for the measurement of particle size distribution. These standards have practical utility in the sense that they are more suitable for calibration of instruments and measurement processes, than for absolute measurement. The NIST standards based on latex particles fit in the latter category.

Silicon Nitride Powder SRM 659

SRM 659 was developed by NIST for calibrating sedigraph instruments that are commonly used in the structural ceramics industry. Furthermore, the need for production of SRMs from powders of similar chemical composition as those being processed was identified in the IEA study on ceramic powders characterization. This SRM was developed using a commercially

available powder, the certification of which was carried out by a round robin. The uncertainty in the certified value at the 50th percentile value, 1.43 μm, is 0.10 μm, based on all data. The use of this SRM is expected to provide improved accuracy, repeatability and reproducibility in silicon nitride powder processing. The certification analyses included NIST work as well as results from five other laboratories in the U.S, Japan and Sweden.

Recertification of SRM 1004a and SRM 1003b

A wide range of particle sizes are of interest in materials processing. While SRM 659 provides a standard in the one micrometer range, specifically for the ceramic industry, the requirements for standards in larger size ranges of interest to the mineral and chemical industry are satisfied by several SRMs utilizing spherical glass beads. The NIST OSRM has provided these standards for a number of years. The objective of this study was to recertify the size distribution of these SRMs by using optical image analysis technique. To accomplish this task, we have developed a sample preparation protocol utilizing successive stages of spin rifflers for obtaining representative 6 mg subsamples from 25 g bottles. The glass beads were examined by optical microscopy and digitized images created by optical scanning of photographs. A computer program using commercially available software has been written to analyze the digital image files. This program calculates the projected area of the glass beads and the equivalent sphere diameter for each of approximately twenty thousand particles taken from several samples of the powder. These data are being used to generate the measured size distributions and calculated cumulative weight distributions for the SRM certification.

Powder X-ray Diffraction (XRD) Standard Reference Materials

J. P. Cline

The SRMs from NIST are designed to increase the accuracy and precision of measurements which are pertinent to science and industry. Powder diffraction SRMs consist of stable materials which have one or more diffraction properties measured and certified. The success of an SRM is dependent on the material and certification measurements being of such quality that the accuracy and precision of the certified values allows for the calibration of subsequent measurements made by the user community. The standardization of such measurements is achieved by the performance of a material rather than the standardization of equipment design and/or measurement procedures.

The certification of an SRM for XRD begins with the isolation of a measurement error which may be corrected with the proper use of a standard. A preliminary study is undertaken to determine the feasibility of producing an SRM which will address the problem. Once the decision to produce the SRM has been reached, an "idealized character" of the SRM material is determined from a review of literature. The effects of deviations from this "ideal" character exhibited by available materials are the subject of subsequent experiments. The characteristics investigated are those judged as capable of having an effect on the critical property which is at least as large as the smallest conceivable measurement error of that property. The study may include the development of improved measurement techniques which increase the accuracy and precision of the property determinations.

Line Position SRM

The primary line position SRM, silicon SRM 640b, is the most popular of the NIST powder diffraction standards. SRM 640b consists of a silicon powder, jet milled to a median particle size of about 5 μm from electronic grade single crystal boules and certified with respect to its lattice parameter. The popularity of SRM 640b reflects the widespread adoption of internal and external standard methods for use in lattice parameter measurements. These procedures involve the determination and application of a delta d curve which represents the end result of the various optical aberrations of the particular diffraction equipment. Adoption of the internal standard method has resulted in consistent and routine measurements of lattice parameter to 1 part in 10^4.

SRM 660, LaB_6, is certified with respect to lattice parameter. However, its primary virtue is a lack of size- and strain-induced peak broadening. The SRM displays evenly spaced, non-overlapping, high intensity diffraction lines whose full-width-half-maximum (FWHM) values measured on fixed slit diffraction equipment closely follow the expected quadratic dependence on 2θ angle. These properties also render it suitable for use in determining calibration parameters for a Rietveld refinement.

The Rietveld method uses models of the origins of the specific sources of optical aberration to refine the degree to which they contribute to a delta d curve. The chief factor preventing the realization of the potential increase in accuracy of this method is the lack of fully developed models appropriate for conventional, divergent beam x-ray equipment. This development, in turn, is prevented by the availability of line position SRMs of sufficient quality for this more demanding task. A project has begun to develop a new high accuracy/precision lattice parameter SRM linked to the fundamental length standard via procedures which are independent of the x-ray wavelength determination. This project involves the lattice parameter determination of a silicon single crystal relative to the iodine stabilized HeNe laser length standard with an x-ray optical interferometer (XROI). A second experiment will transfer the lattice parameter measurement from the single crystal of silicon to a crystalline powder via x-ray diffraction equipment of parallel beam optics. Supplemental studies will include an investigation of the effects of crystallite size on lattice parameters. It is anticipated that this project will result in an SRM in about two years.

Instrument Sensitivity SRM 1976

Line position standards are used to calibrate equipment with respect to the angular variable of the goniometer. SRM 1976 is designed to calibrate equipment for the intensity variable as a function of 2θ angle, i.e., the instrument sensitivity. SRM 1976 consists of a sintered α-alumina plate originally manufactured as a micro-chip carrier. The certified values include the lattice parameters, 12 relative intensity values from 25 to 145 degrees 2θ, and absolute variation in intensity. The use of SRM 1976 for evaluation of instrument sensitivity entails the collection of data on the test instrument in a manner analogous to that used in the certification. Graphical evaluation of the performance of the test instrument is accomplished by plotting the ratio of the 12 relative intensities measured from the test instrument to the certified values as a function of 2θ angle. Such a plot is shown in Figure II-1.

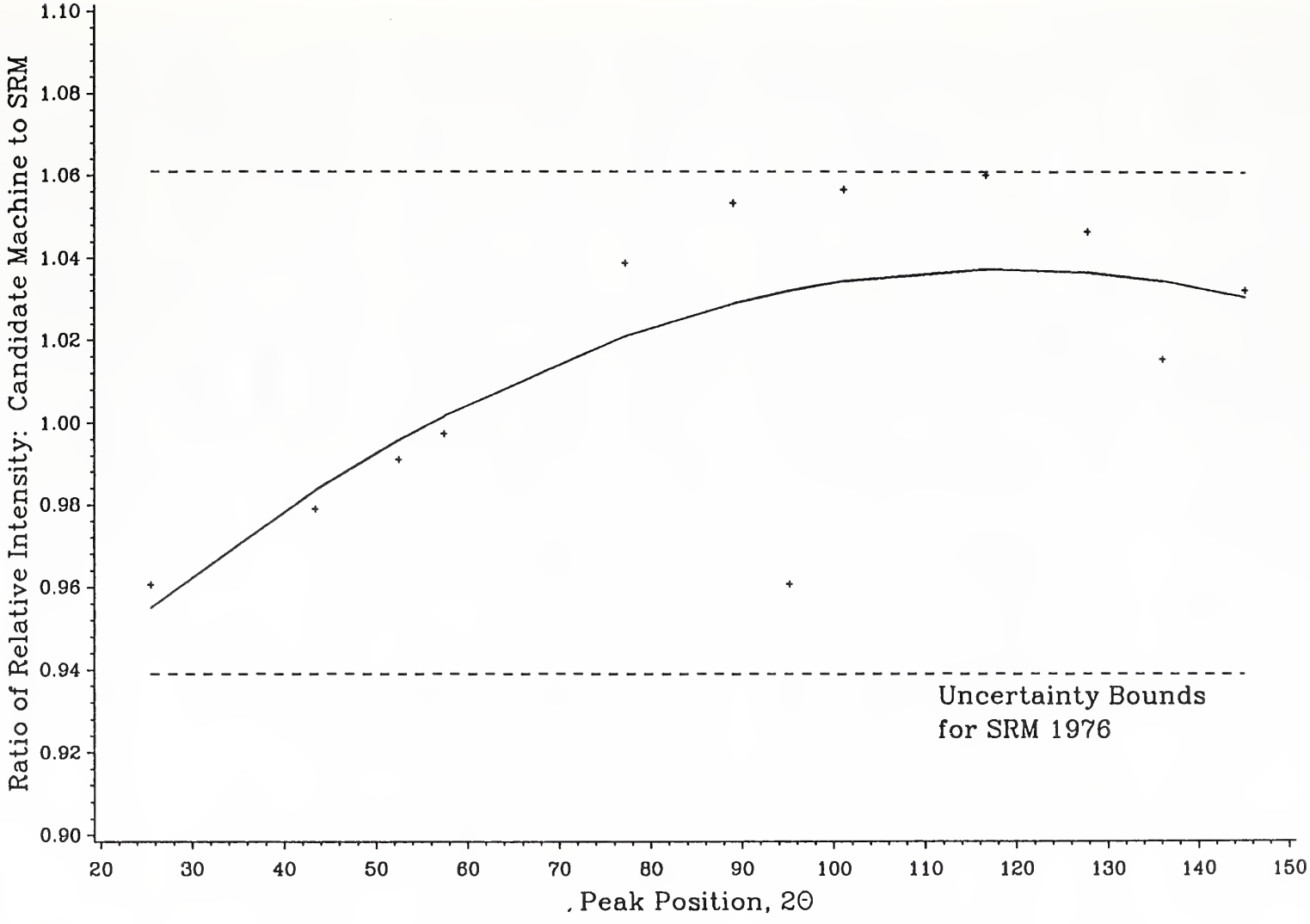

Figure II-1. Utilization of SRM 1976 for Machine Evaluation

Interpretation of the plot may require some scientific judgement on the part of the operator. Patternless scatter within the error bounds indicate the test machine performs in a manner analogous to the reference machine and needs no correction. Patterns observed in the data, even within the error bounds, indicate that a correction may be necessary. The data of Figure II-1 clearly indicate that a correction curve should be applied to intensity data collected from this machine.

Quantitative Analysis SRM 676

Quantitative analysis standards are powders selected to offer a diffraction intensity as close to the "ideal" as possible. They are of high phase purity, small crystallite size, and of isometric particle morphology. Recently SRM 676, an α-alumina powder designed for measurement of I/I_c values, was certified. The certified values included 7 relative intensity values from 24 to 78 degrees 2θ and the lattice parameters. The I/I_c is a constant relating a material's diffraction intensity to that of α-alumina, corundum. The I/I_c has been adopted by the ICDD as one of the material constants which is included in the PDF2 database. The function of this constant is to allow for quantitative information to be gained from routine diffraction scans. Materials to be included in the ICDD database are required to have their I/I_c determined with the use of SRM 676.

Another new quantitative analysis SRM, which is presently being certified, is specific to analysis of silicon nitride. The ceramics industry is interested in silicon nitride due to its desirable high temperature properties. Ubiquitous to processing this material is the transformation of the starting low temperature α phase to the high temperature β phase which occurs during sintering. The α to β ratio of both starting material and the subsequent sintered ware is known to affect properties and is the primary issue addressed by this SRM. However, after discussions with industrial researchers, it became apparent that the ability to analyze for amorphous content was also desired. The SRM itself will consist of two powders, one high in α content, the other high in β. Each is to be certified with respect to α/β ratio and the amorphous content and thus will be suitable for use as a spiking material for user measurements.

The analysis of amorphous content can be performed with the assumption that a spiking phase is 100% crystalline. Samples of the commercial "α" material selected as the SRM powder were spiked with various concentrations of a phase pure β whisker material. XRD samples were spray dried. Rietveld refinements of XRD and time-of-flight neutron data determined a histogram scale factor and the unit cell fraction of the two phases. The use of the Rietveld method circumvents any difficulty caused by the complete interference of the β phase's diffraction profiles with those of the α. The failure of measured unit cell fractions to follow the expected dependence on the concentration of the spiking phase can be entirely attributed to material in the sample not contributing to Bragg diffraction from either phase, defined in this case as the "amorphous phase". The data indicated that phase composition of this powder was 93.8% α, 3.4% β, and 2.8% amorphous.

This technique can be extended to the measurement of the amorphous or impurity level of any material relative to a second material which can be considered phase pure. Additional quantitative analysis SRMs under development include recertification of quartz and cristobalite

SRMs 1878 and 1879, and a new SRM for the measurement of polymorphs of zirconia.

Synthesis of Powders for Nano-Structured Materials

J. J. Ritter

With the Federally mandated phase-out of CFC refrigerants, a search for alternative approaches to accomplish low temperatures has become extremely important. Research on nano-structured materials for two alternative refrigeration processes has been implemented.

1. Magnetic Refrigeration using the Magnetocaloric Effect

Recent theoretical predictions developed at NIST suggest that high magnetization materials with their magnetism focussed in a multiplicity of very small magnetic regions will provide an enhanced magnetocaloric effect. Chemical synthesis procedures based on the controlled pyrolysis of mixed tartaric acid complexes of the metal ions have been developed to generate precursors to rare earth/transition metal garnets. Because of molecular-scale mixing in these precursors, the desired garnets can be produced at temperatures 200 to 400 °C lower than those required in conventional processing. The garnets exhibit high magnetization and nano-sized magnetic regions. A schematic diagram showing the proposed magnetic nano-composite structure for one of these materials, gadolinium gallium iron garnet, $Gd_3Ga_{5-x}Fe_xO_{12}$ (GGIG), is given in Figure II-2.

These prototype magnetic nano-structured materials are being evaluated for performance potential in a collaborative effort with the Magnetics Group in the Metallurgy Division. The measured entropy change as a function of temperature for GGIG is shown in Figure II-3. This garnet shows an enhancement in magnetocaloric effect by a factor of about 3.4 over the best currently-used magnetic refrigerant, gadolinium gallium garnet(GGG), at temperatures around 15 K. Thus, GGIG is an improved substitute for GGG in the $7\ K < T < 20\ K$ range, and may well be useful at temperatures as high as 25 K. In addition, GGIG does not possess a remanent magnetization and; therefore, exhibits no hysteretic losses during field cycling, an important factor to be considered in magnetic refrigerant selection.

2. Thermoelectric Refrigeration using Thermogenic Materials

Theoretical projections indicate that an improved thermoelectric figure-of-merit for known thermogenic materials could be achieved through a decrease in thermal conductivity for these materials. It is believed that the introduction of nano-porosity or a nano-sized second phase, being of the order of the wavelength of phonons, could serve as phonon scattering sites, and thus decrease thermal conductivity. Chemical synthetic procedures amenable to the production of bismuth telluride and related materials as either nano-composites or as nanoporous entities have been developed. Bismuth telluride as a nanocomposite with 5 nm carbon is undergoing evaluation for its thermogenic properties. The program is being conducted in collaboration with, and is partially supported by the Army Night Vision and Electro-Optics Directorate.

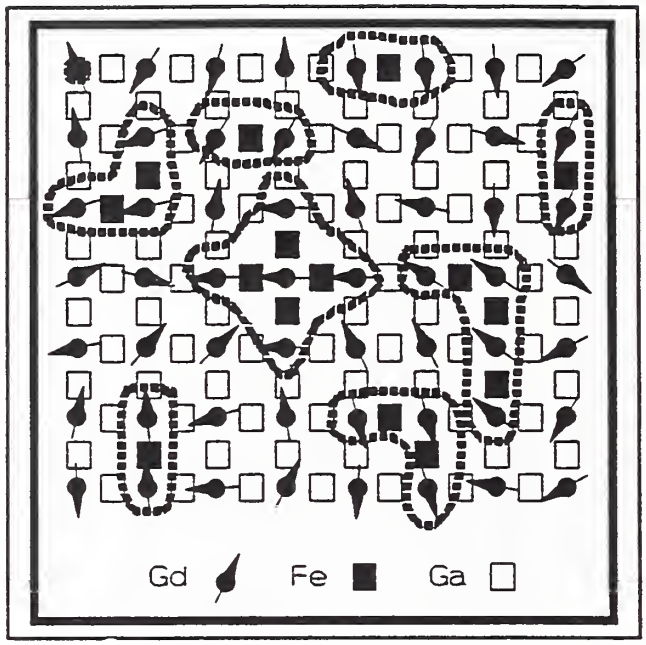

Figure II-2. Schematic of the $Gd_3Ga_{5-x}Fe_xO_{12}$ magnetic nanocomposite structure showing atomic positions, spin directions (via arrows) of the Gd atoms and the locations of magnetic clusters (dashed lines).

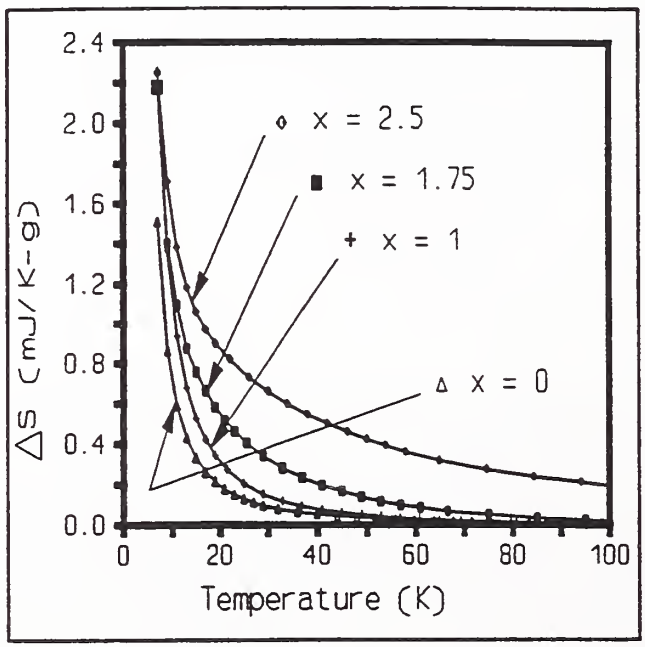

Figure II-3. Measured entropy change vs T for a field change of 800 kA/m for GGG (x=O) and the GGIG magnetic nanocomposites containing 1, 1.75, and 2.5 atomic % Fe.

Microstructural Development in Self Reinforced Silicon Nitride

J. S. Wallace and J. F. Kelly

Silicon nitride materials with remarkably high fracture toughness at room and elevated temperatures have recently been developed. The extraordinary mechanical properties of these materials are related to the development of rod-shaped ß-silicon nitride grains during sintering, producing a composite-like, fibrous microstructure. The result is an improved reliability of the ceramic with a flaw tolerance not commonly associated with brittle ceramic materials. Although the properties of these materials are strongly influenced by the microstructure, the factors controlling development of the desired rod-shaped Si_3N_4 grains are poorly understood. Furthermore, accurate analysis of grain size distribution and the grain shape in these non-equiaxed materials is difficult.

A unique approach is being taken for the analysis of microstructure and the factors controlling microstructural development. First, a technique has been developed for dissolving the grain boundary phase in these Si_3N_4 materials without attacking the Si_3N_4 grains. The liberated grains are then dispersed and filtered, resulting in a single layer of free grains for accurate microscopic characterization of grain size and shape. This allows the effect of changing the sintering process variables, such as time, temperature and dopants, to be quantified.

Development of these microstructural analysis techniques now allows study of the factors which either promote or inhibit production of elongated, fibrous grains. For example, grain growth in traditional monolithic Si_3N_4 bodies, which have 7-12% volume fraction of liquid phase during sintering has been compared to that of oxynitride glass - Si_3N_4 composites which have up to 70 % liquid phase. It has been found that grain-to-grain impingement during growth is a predominant factor in restraining grain growth when low volume fractions of liquid phase are present during sintering. This work continues to examine the effects of bulk chemistry and impurities, as well as advanced processing techniques, on growth of elongated grains. Such information is necessary for not only basic understanding of the processes involved in microstructural development during liquid phase sintering of this important class of engineering materials, but also permits fabrication of controlled, well characterized microstructures for the study of mechanical properties, both at room and elevated temperatures.

High Energy Agitation Milling (HEAM) of Silicon Nitride Powders

D. B. Minor, P. T. Pei and S. G. Malghan,

The HEAM is an attractive technology for deagglomeration and size reduction of submicrometer powders since milling time can be decreased by as much as 75% of that required in conventional milling, and produce slips at high solids content. Our past research has shown that this milling system offers significant advantages in the processing of silicon nitride powders. The current goal of this project is to examine factors affecting repeatability of milling results when using this mill for deagglomeration and size reduction. In addition, a cooperative research project with Saint Gobain-Norton Company's advanced ceramics research center is being pursued with a goal to compare the performance of HEAM with vibratory milling. Dr. V. K. Pujari,

St. Gobain-Norton Company, has been collaborating with us on this project.

An experimental program based on statistical design of experiments has been developed in conjunction with Dr. S. Schiller, Statistical Engineering Division. Experiments have been carried out using samples from a single batch of powder to study variability in the properties of the milled powders. In all of these experiments, the same procedure was used for slurry preparation, milling and measurement of powder properties. The variability in milled powder properties at various intervals of milling time was evaluated by the measurement of particle size distribution, specific surface area, electrokinetic sonic amplitude, conductivity, and pH at which the isoelectric point occurs. These results showed that variability in data was different at different milling times and particle size distributions. A trend was observed in the specific surface area data which consisted of a decrease of surface area over the entire series. This trend was not observed in the particle size distribution data. One major difference between the samples for particle size and surface area is their physical state, i.e., suspension versus dry powder. Hence the measurement process could be influencing the observed variability.

The SEM investigation using backscattered atomic number contrast imaging used in conjunction with automated video image analysis has produced initial evidence of homogeneous distribution of sintering-aid in the green body. Research is in progress to develop a quantitative method of homogeneity description of sintering-aid distribution. In addition, several experimental modifications are under investigation to determine their influence on milling performance and process repeatability.

An example of change in surface properties as monitored by the measurement of electrokinetic sonic amplitude (ESA) of sequential steps involved in slurry preparation step and milling are presented in Figure II-4. In this figure, the ESA response as a function of pH of samples drawn during the milling experiment is presented. The change in pH_{iep} of these samples reflects that dispersion conditions in the slurry are also undergoing changes as the sintering-aid is added and powder is milled for successively longer time. The response of slurry with the addition of surfactant (ammonium polymethacrylate) is shown in curve a and its pH_{iep} is at pH 5.1, and after 20 minutes of milling, the pH_{iep} has remained at pH 5.1, as shown by curve b. After the sintering aid was added to the slurry, the ESA and pH_{iep} change. The pH_{iep} of the powder at first shifted to 6.3 (curve c) at 32 minutes of milling, i.e., 12 minutes after the addition of yttria. At 50 minutes milling or 30 minutes after the addition of yttria, the pH_{iep} has shifted to 6.0 (curve d). Finally, at the end of milling for 80 minutes, the pH_{iep} is at 6.3. The final pH_{iep} of the powder was very reproducible for three consecutive milling experiments where the average pH_{iep} was 6.4 ± 0.1.

This research has established the feasibility of milling slurries containing in excess of 50% solids by volume. This is one of the major accomplishments since the ability to mill such dense slurries in such a short time is not achievable by any other milling method. The high solids loading has been attributed to the use of a combination of an appropriate surface chemistry in the slurry, and optimized milling method. High solids loading has facilitated the study of dense slurries preparation.

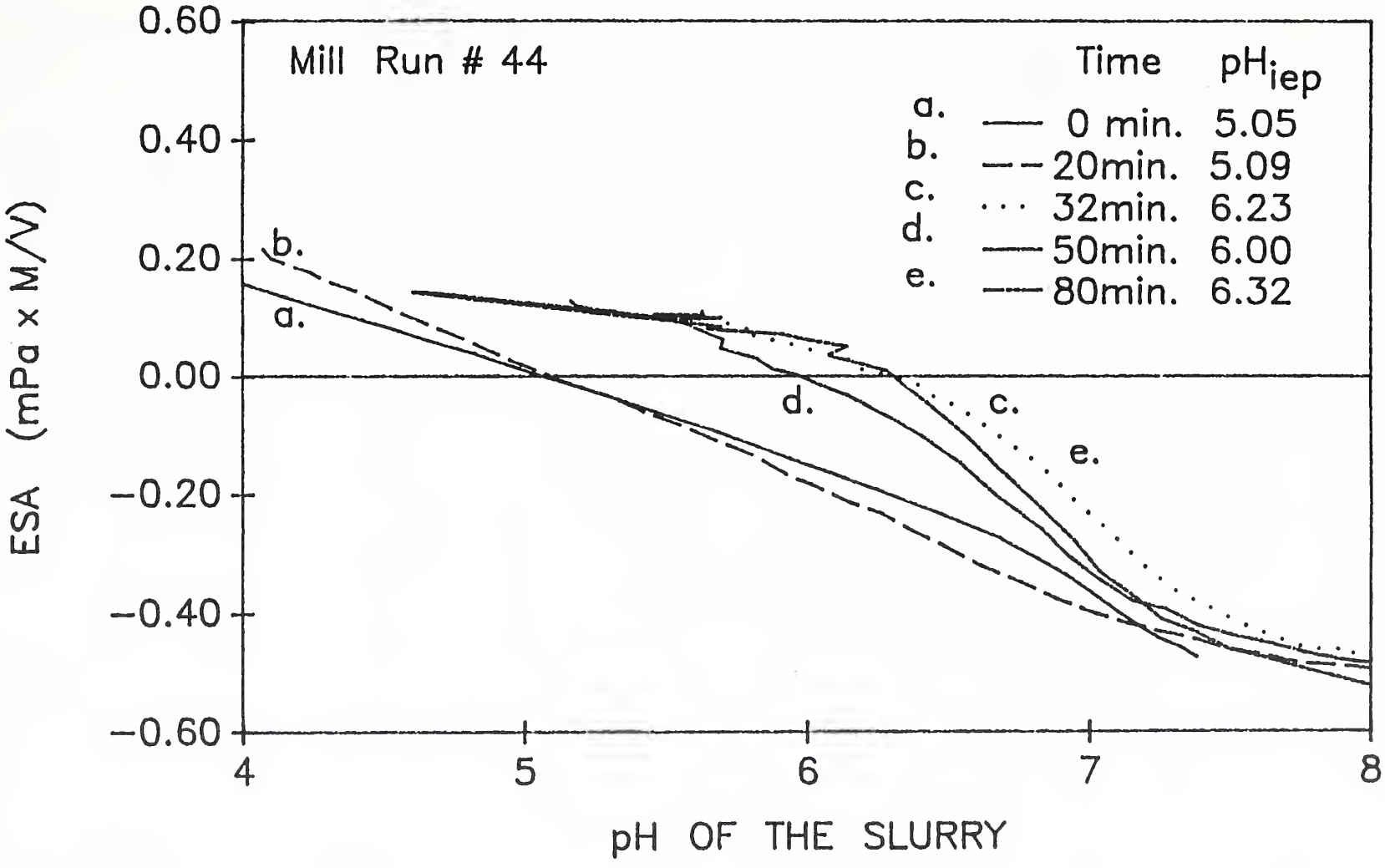

Figure II-4. ESA and pH_{iep} of silicon nitride at different stages of the milling process; (a) 0 minute, (b) 20 minutes, (before the addition of yttria), (c) 32 minutes, (12 minutes after the addition of yttria), (d) 50 minutes and (e) 80 minutes.

Two separate samples of milled slurries and green ceramic formed by slip casting have been sent to Dr. Pujari for densification studies. Early indications are that the green ceramics had higher density than those from vibratory milling, and sintered to full density. Additional evaluation studies are in progress.

Low Temperature Fabrication of Transparent Silicon Nitride

Wei Chen, A. Pechenik, G. Piermarini and S. G. Malghan

Particles with characteristic sizes between 1 and 100 nm are termed nanosize particles. Powders made of nano-size particles offer a number of potential advantages over conventional micrometer-size ceramic powders. When primary particles are small, strong aggregating forces usually prevent them from packing efficiently during compaction. As a result of agglomeration of primary particles, the compacts produced from nano-size silicon nitride particles have low packing density which precludes achieving high density after sintering. Past work at NIST, which utilized a diamond anvil cell for compacting nanosize particles of amorphous silicon nitride, revealed that drastic improvements in the packing density of nanosize particles can be achieved at low temperatures and high pressures. The improvements allowed fabrication of very small dense compacts, which, even prior to sintering, are transparent in visible light. These transparent, densely-packed compacts, allowed pressureless sintering of amorphous transparent silicon nitride at temperatures significantly lower than those used conventionally for hot-pressing of silicon nitride.

The current project takes the above-mentioned work one step further toward fabricating large-size transparent silicon nitride ceramics from the nanosize particles. To achieve this goal of fabricating significantly larger samples than the ones produced using the diamond cell in the previous work, one must understand the rate-dependent or time-dependent behavior of compacting nanosize particles at various temperatures and under a variety of cover gasses used for lubricating the surface of compacting particles. The novel equipment built for this purpose permits the control of: (1) the temperature inside the working chamber, (2) the pressure applied to the compact, (3) the gas pressure of the cover gas, and (4) the rate of compaction. At the same time, the new equipment allows accurate measurements of the rate of compaction, frictional forces between the compacting particles and the walls of the cylinder, and other important parameters which later will be used to understand rheology of the nanosize particles based on the Navier-Stokes equation.

The major activity during this reporting period was fabrication and calibration of the equipment for compacting nanosize particles under controlled atmosphere. The equipment has been fabricated, assembled, and calibrated. Schematics of the experimental set-up are shown in Figure II-5. This equipment allows fabrication of 3 mm-diameter disc-shaped samples from starting powders of nanosize particles under vacuum or in a selected gas environment. Inside the environmental chamber, the piston-cylinder apparatus can be cooled to liquid nitrogen temperature or heated to 200°C for baking under vacuum. Two load cells measure both the load applied to the sample and the frictional force between the sample and the walls of the die for calculation of pressures. A special design allows that the frictional load cell can work at room temperature. A displacement transducer measures displacement of the piston and thus, changes

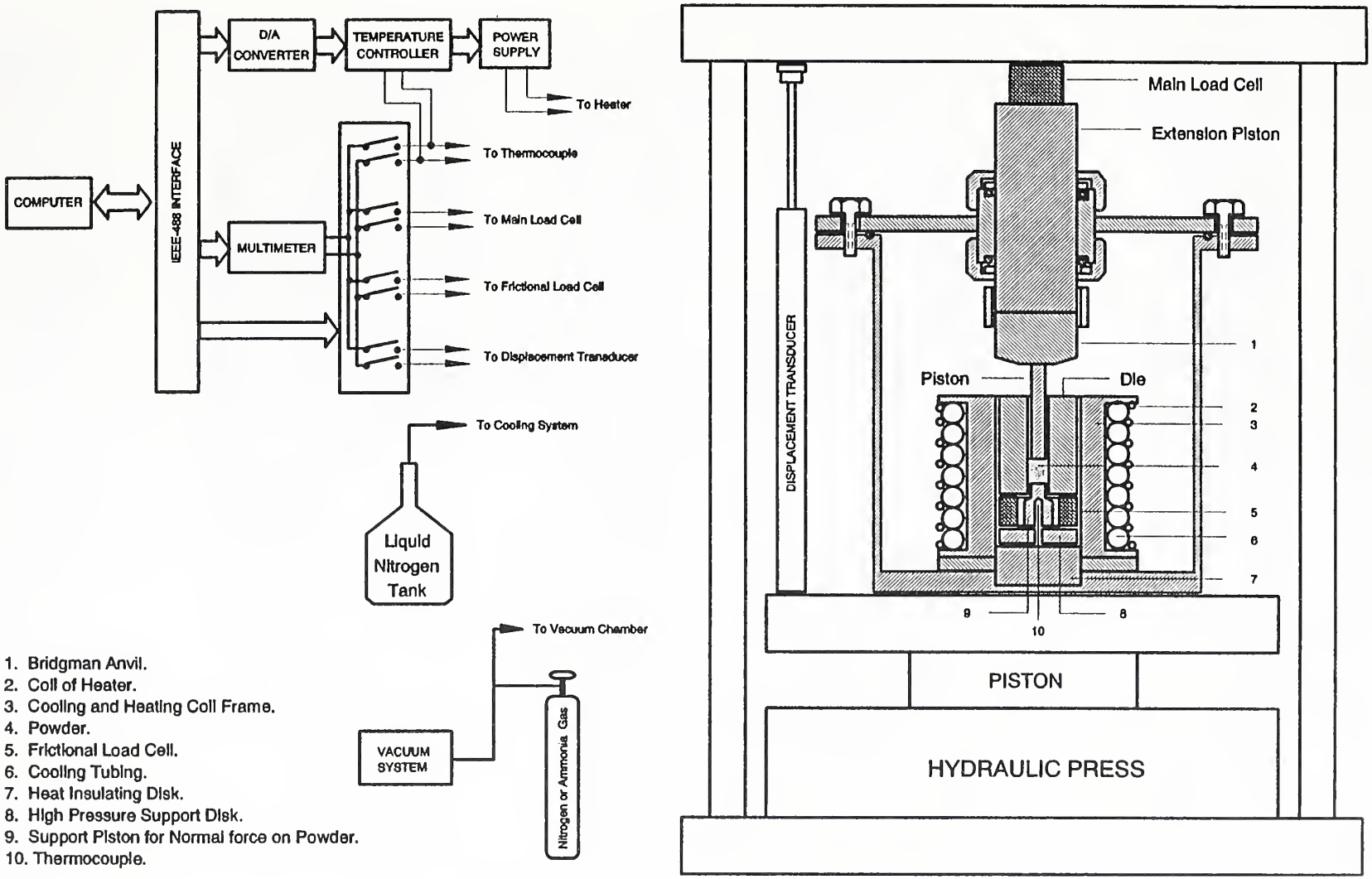

Figure II-5. CONFIGRATION OF THE EXPERIMENT FOR FABRICATION OF TRANSPARENT SILICON NITRIDE

in volume of the sample as a function of time and the applied pressure. Pressure to the top piston is applied using a computer-controlled Instron testing machine, which allows a precise control of the rate of pressure application.

Prior to conducting experiments with silicon nitride powder, a series of experiments with other powders were conducted to check and calibrate the equipment. The data from these experiments are displayed as sample volume vs. applied pressure, density vs. pressure, density vs. time, pressure vs. time, temperature vs. time, and the frictional force. Thus a very accurate description of compaction is possible.

Characterization of Surface Oxide on Silicon Nitride Powders

V. A. Hackley and S. G. Malghan

The microstructure of advanced structural ceramics is greatly influenced by the steps preceding powder consolidation and green body formation. In the case of colloidal processing of Si_3N_4, powders are dispersed in a liquid medium at high solids concentrations. The properties of this suspension (slip) depend critically on the chemistry of the solid/liquid interface. Failure to control surface reactions may result in agglomeration, which promotes poor slip rheology and leads to microstructural heterogeneity in the green body. This problem is compounded by the presence of complex interactions between the primary phase and various additives which are typically present during processing (e.g., sintering aids, binders and dispersants).

Work in our laboratory has centered on the use of electroacoustic techniques for characterizing dense powder slips. Charged particles in an alternating electric field emit an acoustic wave with an amplitude proportional to the electrical potential at the particle surface. This measurement, termed the electrokinetic sonic amplitude (ESA), can be applied to suspensions approaching 40% solids by volume, giving this technique a distinct advantage over others (e.g., electrophoresis) which are generally restricted to dilute systems.

Using ESA measurements, in addition to Auger electron spectroscopy to determine surface oxide content, we have characterized the surface and interfacial properties of five commercial Si_3N_4 powders. The powders were surface-washed by soxhlet extraction, a continuous treatment in which the sample is repeatedly exposed to a distilled aqueous solution which removes surface contaminates and oxidation products. In Figure II-6, results of ESA measurements as a function of suspension pH for these powders, labeled A through E, indicate soxhlet extraction leads to an increase in the isoelectric point (pH_{iep}) for several powders. This is thought to occur due to the removal of surface oxide in the form of SiO_2 during extraction, leaving an increasingly basic surface dominated by amine groups. We find that a linear relationship exists between the oxide layer thickness (t) and the pH_{iep},

$$t\ (nm) = 0.15\ [9.7 - pH_{iep}]$$

and that the extent of surface oxidation can therefore be estimated from relatively accessible electroacoustic measurements. The primary implications of this study, with respect to powder processing of Si_3N_4 by colloidal methods, is that variations in surface chemistry of the starting

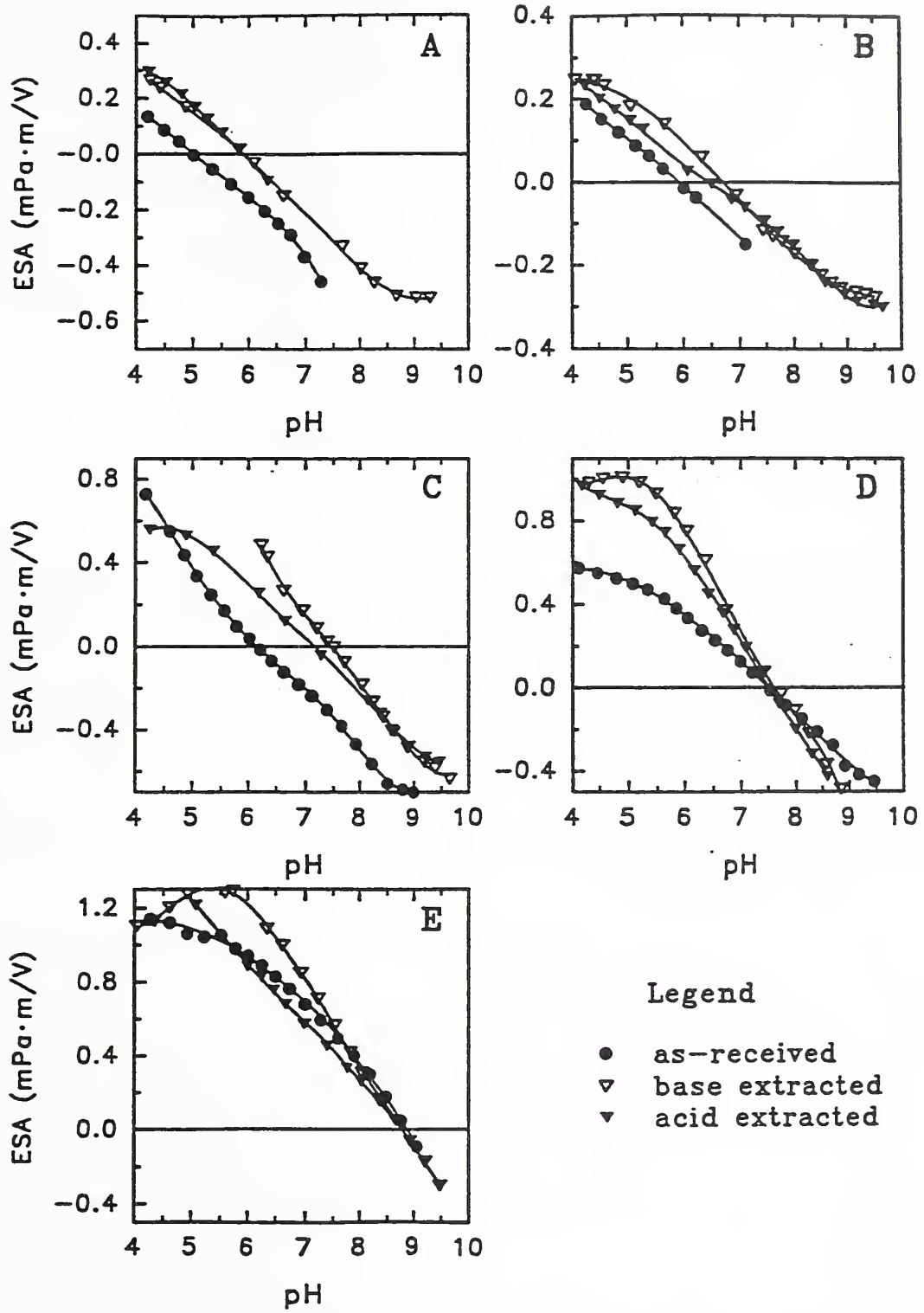

Figure II-6. Titration curves for Si_3N_4 powders A-E. Electrokinetic sonic amplitude (ESA) is plotted as a function of suspension pH for the as-received and extracted samples.

powders are due primarily to differences in the degree of surface oxidation (not bulk oxygen as previously thought), and that suspension behavior can be adjusted to conform to a desired state by controlled removal of the surface oxide layer using aqueous extraction. Conversely, controlled oxidation of the powder surface could be used to obtain a desired oxide thickness. In this way, greater consistency in slip properties and oxygen management should be obtained.

We are also using ESA measurements to examine Si_3N_4 interactions with secondary suspension components. For example, the adsorption of polyelectrolytes such as poly(acrylic acid) modifies the surface charge of particles and is reflected in the magnitude and sign of the sonic amplitude. Chemical absorption of ionic contaminants on the Si_3N_4 surface is also characterized using ESA. Finally, a parametric investigation of the ESA technique is ongoing. In this study, we are relating ESA to sample and system parameters in an attempt to establish a framework necessary for general application of ESA measurements in ceramic powder processing.

Nuclear Magnetic Resonance for Green Ceramics Characterization

Pu Sen Wang

In a ceramic green body, the binder distribution is a critical parameter that affects the final ceramic properties and manufacturing repeatability. An understanding of the interfacial reactions between the binder and ceramic powders under various processing parameters is essential to alleviate problems related to binder distribution in ceramic powder processing. The development of NMR imaging for ceramic materials has been limited due to line-broadening caused by nuclear dipolar interaction in solids. It is even more difficult for the "hard solids" like ceramics which have a spectroscopic linewidth, a few hundred times larger than that in "mobile" samples because of the restriction in atomic motion. In 1992, we accomplished the following: (1) a comparative study of the binder effect in green body homogeneity; (2) improvement of gradient-coils micro-imaging facility for certain solid imaging; and (3) progress towards the development of an ^{27}Al stray-field imaging facility.

Silicon nitride powders with binders, either polyethylene glycol (PEG) or polyvinyl alcohol (PVA), were cast by centrifuging to cylindrical green bodies of 12 mm diameter and 10 mm thickness for stray-field NMR imaging. Samples of both types were fabricated with $10.0 \pm 0.9\%$ wt. of binder. The binder distribution was homogeneous in the PEG sample. However, in the PVA sample, the binder distribution was nonuniform in certain locations. A stationary, nonspinning ^1H NMR spectroscopic study at 400.13 MHz shows that a sharp peak from the residual water was detected in the sample with PVA binder. No such mobile protons from water were observed in the sample with PEG binder. This indicates that the green body with PVA binder has higher water content than that containing PEG. This water content may be responsible for the inhomogeneous binder distribution at certain locations of the sample.

The high-resolution stray-field imaging for solids reported above utilizes projection reconstruction technique. This technique requires long measuring times and complicated data handling. In contrast, the micro-imaging with gradient coils used for slurry mapping utilizes nuclear spin echo technique. One of the advantages of this latter method is short measurement time. In 1992, a multi-slice technique was also developed in our facility. This technique

provides the possibility of examining a number of portions in a sample (e.g. 4, 8, 16, 32,...) in a few minutes. A certain degree of overlapping of neighboring slices is inherent in this method; however, excitation sequence planning can minimize this overlapping. For example, in an eight-slice experiment, the order of excitation is 1-3-5-7-2-4-6-8. In this manner, before slice #2 is excited, slice #1 and #3 have relaxed. Still, this multi-slice spin echo NMR imaging technique is limited to materials with certain relaxation times. We have tested the green samples by this imaging technique and observed internal cracks in some ceramic pieces.

α-Silicon Nitride Powder Surface Oxidation Kinetics

Pu Sen Wang

One of the major technical issues in the processing of silicon nitride ceramics is variability of starting powders sinterability. A large number of powder parameters can affect the sinterability of a given powder. In addition to physical properties, surface and bulk chemical properties and the powder synthesis route are considered to be some of the most important parameters that influence powder behavior during processing-related unit operations. Further, in the case of silicon nitride powder, oxygen, carbon, metallic elements and halides are considered to be the major bulk impurities. However, oxygen is the single most abundant impurity in the commercially produced starting powders, often ranging from 0.3 to 2.0% by weight. Oxygen content of the starting powders and that added via sintering-aids constitute the total oxygen that participates in glass formation at sintering temperatures. Therefore, data on the oxidation of silicon nitride powders and the composition of the oxidized layer are some of the necessary pieces of information required to evaluate powder sinterability. Powders produced from different synthesis routes appear to contain different oxygen concentrations. In the present study, x-ray photoelectron spectroscopy (XPS) and Auger electron spectroscopy (AES) have been used to measure and compare the initial oxidation kinetics of two crystalline α-Si_3N_4 powders. One of the powders was synthesized by direct nitridation and the other had been prepared using a gas-phase reaction. Powder samples were oxidized in air at temperatures between 850°C and 1000°C. The first powder, SNR-1870, was obtained from H. C. Starck which was prepared by direct nitridation; while the second powder, PCR 8-7, was synthesized by Union Carbide by sylane pyrolysis.

XPS and Bremsstrahlung-excited AES data were used to calculate oxide layer thickness and oxidation rates. XPS analysis showed that the average oxide thickness on the as-received SNR-1870 powder was less than that on the as-received PCR 8-7 powder. This is probably a direct result of acid washing process. The oxidation rate of both powders in air was linear in the temperature range between 850° and 1000°C. The activation energy for oxidation was significantly higher on the PCR 8-7 powder. Also, XPS analysis showed that some oxynitride was formed in addition to SiO_2 during oxidation of the PCR 8-7 powder; whereas, oxynitride was not detected on the SNR-1870 powder after oxidation. Different oxidation characteristics of these two powders are believed to be the result of differences in surface chemistry (surface oxide thickness) and/or differences in the levels of bulk impurities, such as oxygen or hydrogen. Thermal decomposition mass spectroscopy showed much higher H_2 evolution from the PCR 8-7 powder than that from the SNR-1870 powder at temperatures above 700°C. The oxide thicknesses determined from the XPS data were systematically 10 - 30% higher than those

determined from the AES data. This may be due to uncertainties in the data analysis procedures.

III. SURFACE PROPERTIES

Stephen Hsu

The introduction of advanced ceramics into industrial applications is dependent on their long term durability and cost-effectiveness. Long term durability includes issues such as strength degradation under cyclic loading, friction, wear, and the effectiveness of the lubrication process to protect the surface. The ability to predict time-dependent property changes is still in its infancy. The interplay between wear and fatigue behavior for structural ceramics is not understood at this time, yet this knowledge is urgently needed to design ceramic components for engine applications. Cost-effectiveness of ceramics addresses the issues in low-cost powder synthesis, optimum microstructural design for a specific property, and low-cost rapid machining with controlled surface properties. The combination of designed surface properties and specific bulk properties in a monolithic ceramic holds promise for optimum cost-effective ceramics.

Optimum ceramic properties depend on the microstructure and the interface properties. Therefore, the ability to understand the basic causes, to be able to measure and observe such phenomena, and to control the properties of surfaces and interfaces is increasingly becoming the key issue for the next generation of ceramics.

Based on these considerations, the tribology effort which primarily deals with surface phenomena was broadened last year and a new surface properties group was established. The objectives of the new group are: (1) to develop new measurement techniques to characterize the physical and chemical properties of ceramic surfaces and interfaces under static and dynamic contact conditions; (2) to understand the relationship between microstructure, chemical compositions of the surface and interface, and the micro-mechanical and tribological properties of ceramics and other materials; (3) to develop the science and technology for the control of surface properties by physical and chemical means, and to develop basic design principles for optimum combination of surfaces and substrates; (4) to provide data, reference materials, and design guidelines for the introduction of such materials in industrial applications.

The technical highlights listed below reflect a year in transition. Some new activities have been initiated and some activities have been expanded. Many of the activities have strong industrial linkage and support as well as connections to other government agencies, especially the Office of Transportation Materials in DOE. As we embark on the new direction, these ties will be maintained and strengthened.

Significant Accomplishments

- Demonstrated the feasibility of chemically assisted machining of ceramics. Based on the results of a prior surface chemistry study focused on effective lubrication of ceramics, chemical compounds were discovered to alter the machining process significantly. Using a simple cutting device, various chemistries at 1% by weight were studied. The most successful compound increased the cutting rate by 60% while simultaneously producing a 40% reduction in surface roughness. This technology, if successfully developed, could reduce ceramic component cost significantly with

current machining tools. This would give the US ceramic industry a competitive advantage. A patent has been filed. Collaborations with industrial partners are being pursued.

- Conducted basic studies of ceramic machining by using a single-point diamond scratching technique. Experiment on a CVD silicon carbide under different environment have shown that a critical load exists, above which significant sub-surface and surface damage is created in the process. That load and associated scratching depth vary considerably among air and different liquid environments. Identification of suitable environments for low damage cutting of brittle materials may be possible with this kind of study.

- Demonstrated that silicon nitrides and silicon carbides can be lubricated by a new generation of lubricant chemistries. Boundary lubrication of ceramics is increasingly a critical issue as ceramics are being considered for use in engines and machineries. Ceramics fail primarily by fracture which in part, depends on the stress intensity. An effective lubricating film can lower the stress intensity at asperity contacts, thus protecting the surface. Current lubrication chemistry is primarily based on phosphorus-containing chemicals, which were developed for steel components, and it generally does not react with ceramics. Our results suggest that the fundamental surface chemical reactions and reaction mechanisms are different for steel and silicon-based ceramic components. New chemistries were discovered that could readily react with silicon-based ceramics and form a reaction film. Several patents have been filed. Successful development of this knowledge could pave the way for wide-spread use of ceramics in engines.

- A new apparatus capable of measuring the shear strength of thin surface films has been designed and built. A ball colliding with an inclined plane is the basic concept behind the design. The inclined plane is mounted on a x,y translation platform, and the ball is anchored on a frame above the platform. Force transducers are installed to measure the forces in the x, y, and z directions. Knowing the exact surface geometry and the forces at a specific location, the normal force and the shear force can be calculated. A monolayer adsorbed film of stearic acid was deposited on the surface of the inclined plane by Langmuir-Blogett technique and the forces when the film ruptures were recorded. This measurement methodology could have significant impact on the magnetic head/disk technology. Collaboration with the US magnetic information industry is being pursued.

- A new method has been developed to measure hardness of relatively soft tribological films on substrates using nano-indentation. The method can treat films as thin as 0.1 μm, and in thicker films can determine hardness variation with depth in the film. The technique is being applied to metal coatings, oxide and sulfide surface layers, and to tribological films produced in situ. It should be a useful analytical method for understanding the mechanisms responsible for low friction, low wear solid films.

- The advanced lubrication technology jointly developed with Akzo Chemicals has recently been validated by full-scale engine testing . Of some 18 candidates submitted, Akzo/NIST chemistry is one of the two best performaners. Futher research is aimed at optimizing the chemistry of the base fluid and the chemical compounds that react with the surface. The project is sponsored by the Office of Transportation Materials in the Department of Energy.

Chemically Assisted Ceramic Machining

T. Ying[1], J. Gu[2], Y. Wang[1], R. S. Gates and S. M. Hsu

[1] Graduate students, University of Maryland
[2] Post-doctoral Fellow, University of Maryland

Machining of hard, tough ceramics is time-consuming and costly, and currently it is one of the major cost components of finished ceramic parts. For tribological applications, the combination of surface finish and tight tolerances pushes the machining cost to about 50-90% of the total cost. Residual surface cracks from machining have been identified as the major factor affecting the reliability of ceramic components. The conventional approach of an ultra-stiff machine with an optimum combination of diamond wheels and bonding substrate often adds cost to the process. The goal of this project is to use chemical means to improve the machining rates and simultaneously reduce the surface damage with machining ceramics such as Si_3N_4 using conventional machining tools.

The initial approach centers on the mechano-chemical effects. Various chemical compounds are used to react with the surface under machining conditions to form soft reaction layers which could be removed at lower stress. In this way, the machining process can proceed much faster. Since the surface being machined is subjected to less stress, the extent of surface damage is reduced. The reactions are activated by mechanical forces which produce localized stresses, high local surface temperatures (flash temperatures), and disrupted (dangling) surface bonds at the machining interface (i.e. diamond-ceramic interface). Once the reactions occur, a boundary film is formed and it modifies the stress distribution, lowering the friction, and reducing surface temperatures. The lower point stress distribution minimizes the formation of residual cracks which weaken the material strength. The key to this approach is to discover which chemical compound can react with the ceramic surface under the machining conditions without causing corrosion or safety concerns.

Experiments conducted on Si_3N_4 have successfully demonstrated the feasibility of this approach. Cutting time was reduced by 60% over the commercially available chemistry, while providing lower surface roughness. Some typical results are shown in Figures III-1 & III-2. Figure III-3 further demonstrates the surface finish potential of this approach. It shows the surface of Si_3N_4 before and after using a current state-of-the-art chemistry. The far left third of the photomicrograph represents the original surface as ground. The middle third of represents the same surface after 2 minutes of the best currently available chemistry. The right third represents the surface after 10 minutes grinding with the same fluid. Note the presence of some residual grinding marks. Figure III-4 presents an identical specimen before and after 10 minutes grinding

using an experimental chemistry, showing the complete removal of any residual grinding marks. Patent applications are being pursued for both the high cutting rate chemistry and new surface finish compounds.

Mechano-chemical Effects Observed Using a Single Diamond Scratch Test

A. W. Ruff, H-J. Shin[1] and E. Whitenton[2]

[1] Graduate Student, University of Maryland
[2] Precision Engineering Division, NIST

A system for nano-indentation and controlled load/depth scratching of materials has been developed. It is being used for characterization of thin surface films and coatings, as well as for bulk materials. The load range of the instrument extends down to 10 mN, and the depth sensitivity to about 1 nm. Both the instantaneous load and the penetration of the indenter into the sample are measured continuously. The specimen can be translated under load to produce controlled scratches in air or under liquids. The system can be used to measure hardness, elastic modulus, ductility, toughness, and scratch resistance of thin films.

Controlled scratching studies were done in collaboration with the Precision Engineering Division on surfaces of CVD silicon carbide to examine the effects of different environments on machining and grinding. A single point diamond turning tool was used, in either air or one of four different fluid environments. Substantial differences in damage to the material were found in using the different fluids. Figure III-5 shows one example of controlled scratching at 200 mN load in a water/oil emulsion. The peaks in the scratch resisting force curve and the valleys in the relative scratch depth curve are the result of severe sub-surface cracking at this level of load. Each local increase in scratch force and its corresponding decrease in scratch depth denotes a burst of subsurface cracking activity and the associated surface uplifting. This damage occurs sporadically along the scratch and appears to involve some damage accumulation process in the material. Lower loads in this example produce little or no damage. Studies will continue next year to further identify critical damage loads for different test and material conditions.

Ceramics Lubrication

R. S. Gates, D. Deckman[1] and S. M. Hsu

[1] PhD Candidate, Chemical Engineering Department, The Pennsylvania State University

The introduction of ceramics into engine applications is severely hampered by the lack of proper means to lubricate the ceramic surface. Successful lubrication of ceramic surface relies on the formation of a thin lubricating film under concentrated contacting conditions, often referred to as the boundary lubrication condition. An understanding of the basic chemical mechanisms between the ceramic surface and various chemistries is essential to develop the necessary lubrication technology for ceramics.

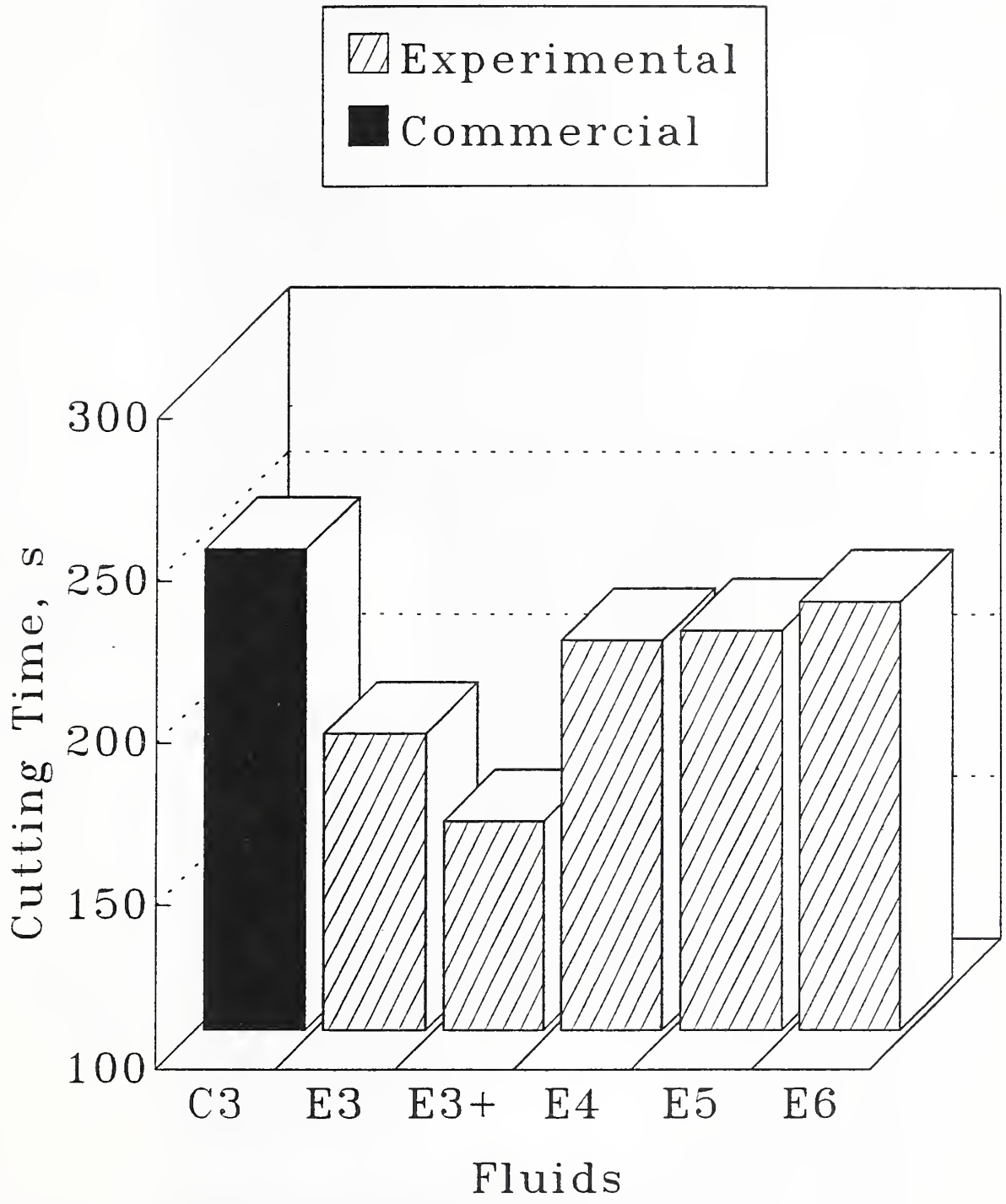

Figure III-1. Silicon Nitride Cutting Experiments using Organic-Based Fluids

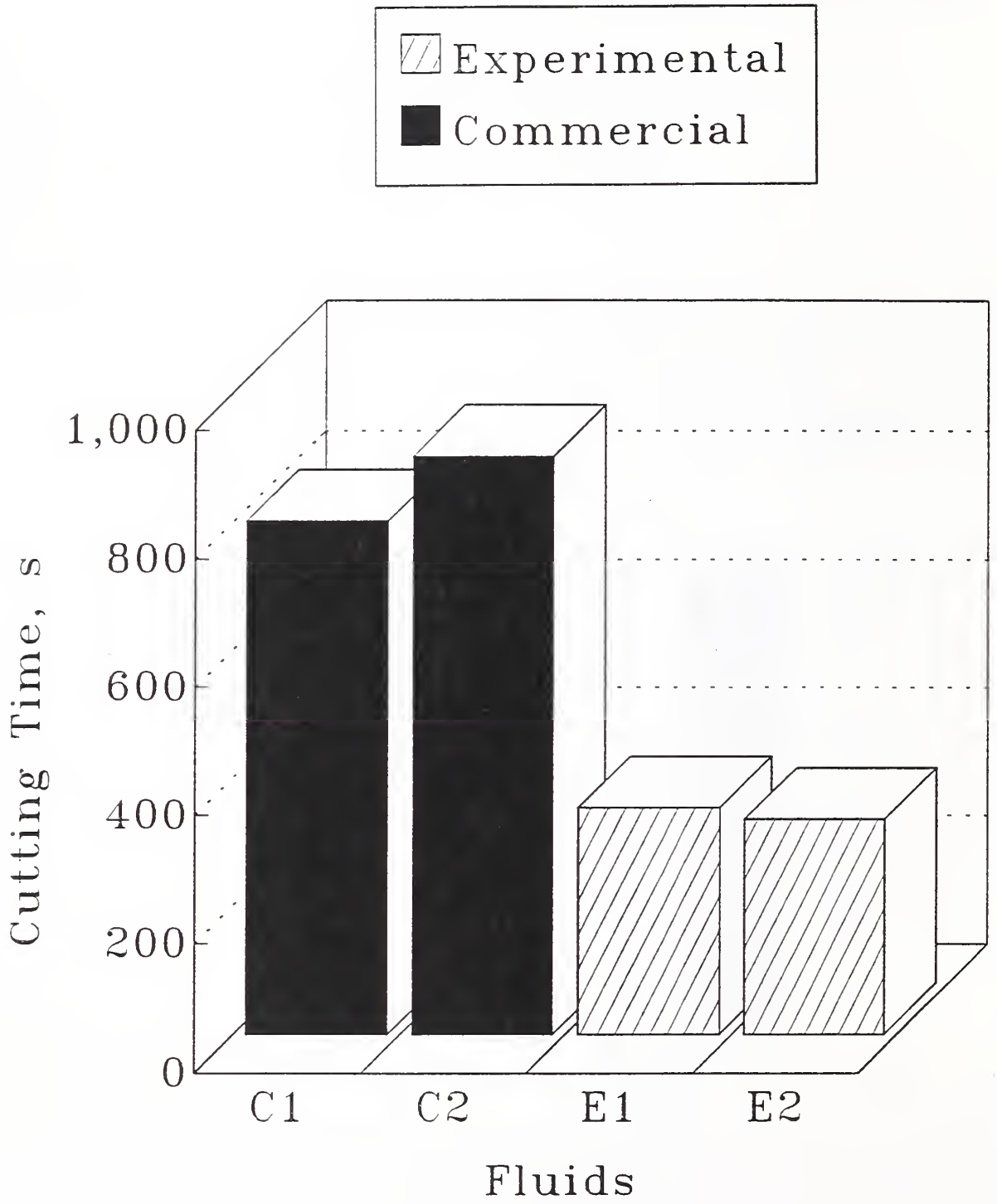

Figure III-2. Silicon Nitride Cutting Experiments using Water-Based Fluids

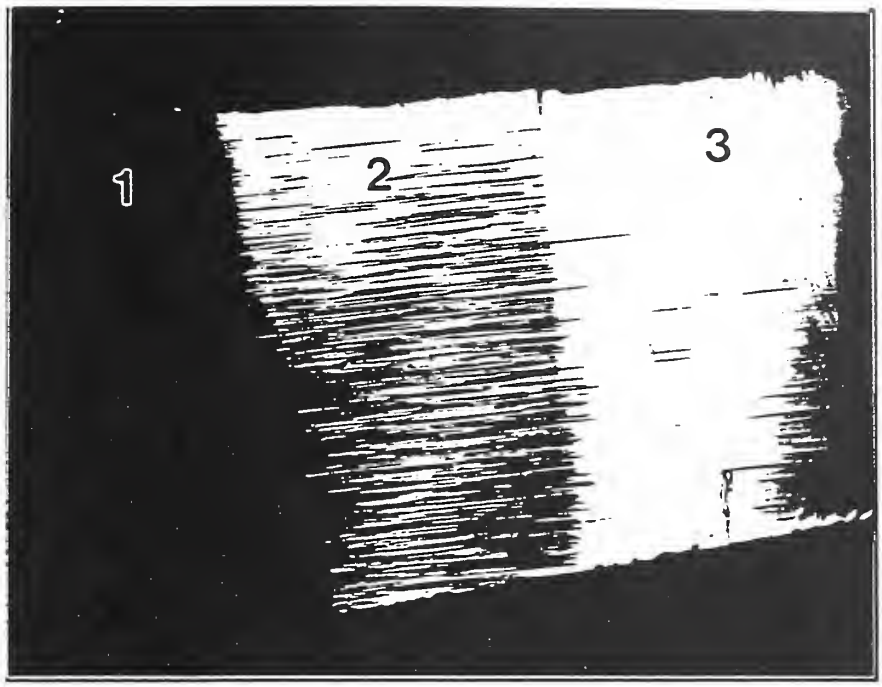

Figure III-3. Si_3N_4 Machining using Commercial Fluid. Region: 1 - original surface, as ground, 2 - original surface after 2 minutes grinding with best available grinding fluid, 3 - original surface after 10 minutes grinding with best available grinding fluid

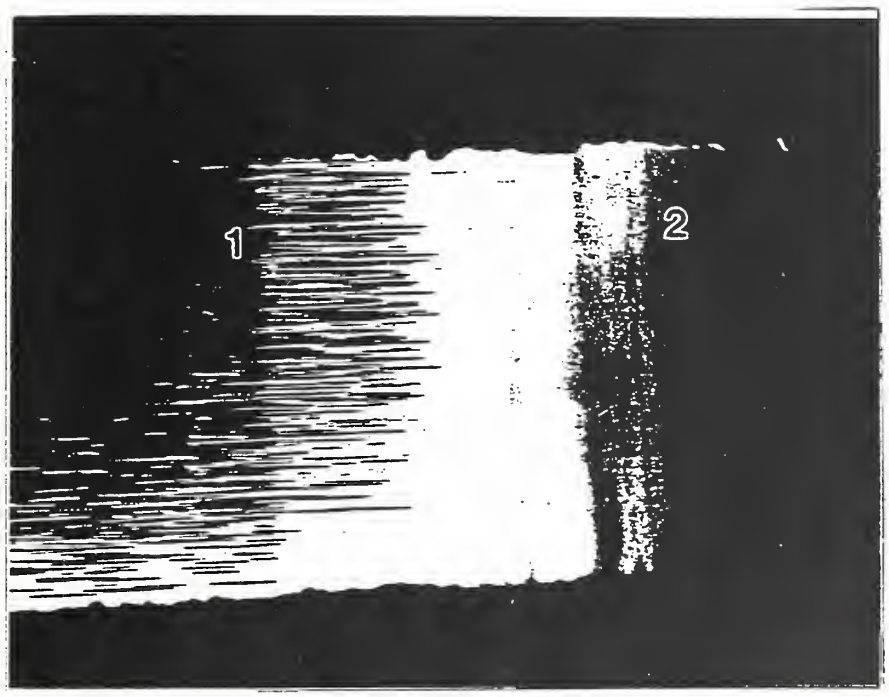

Figure III-4. Si_3N_4 Machining using Experimental Fluid. Region: 1 - original surface, as ground, 2 - original surface after 10 minutes grinding with experimental grinding fluid.

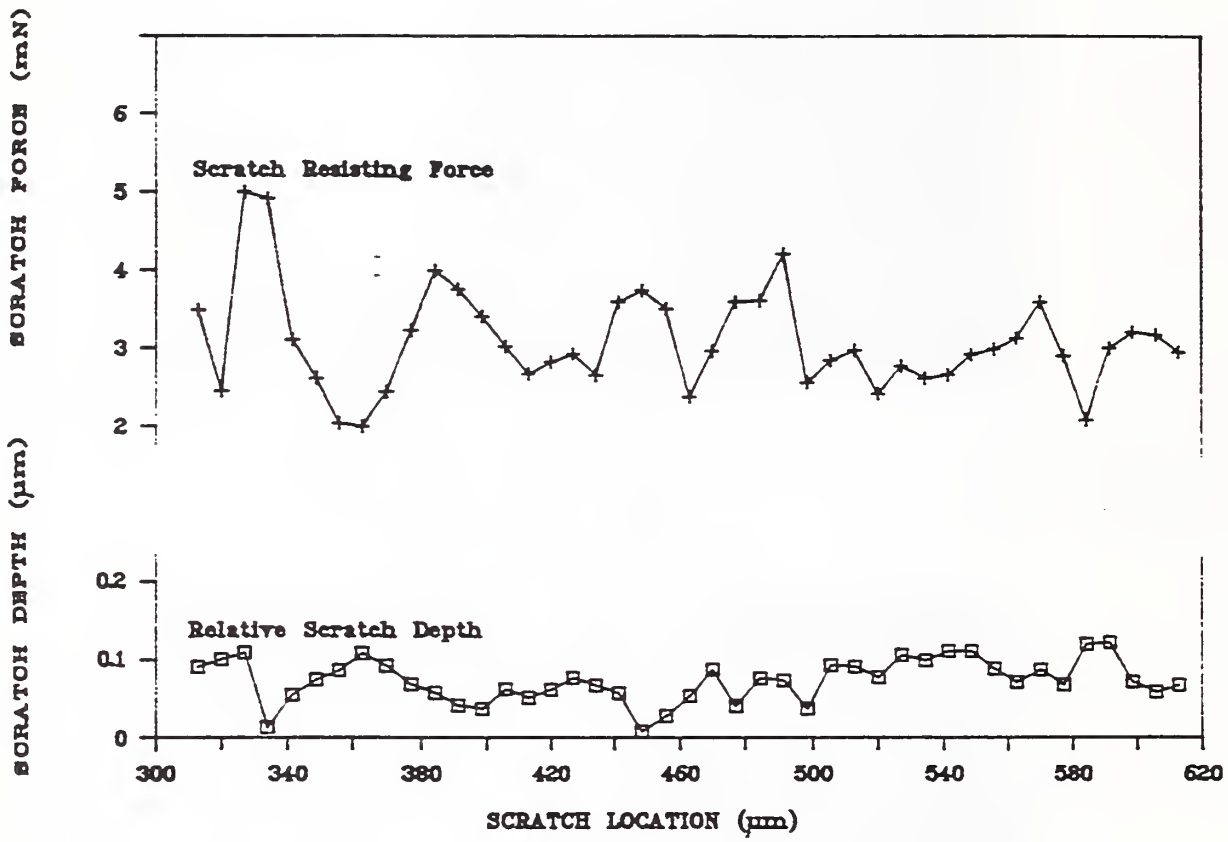

Figure III-5. Controlled scratching experiment on CVD SiC at 200 mN load in a water/oil emulsion. The peaks in the scratch resisting force curve and the valleys in the relative scratch depth curve are the result of severe sub-surface cracking.

The issue of lubricating ceramics is particularly opportune at this time. Facing the continually stringent emission requirements and the need to improve the fuel economy, the US transportation industry is experimenting with various advanced materials to develop the next generation of high efficiency, environmentally compatible engines. The lack of lubrication technology with most of the advanced materials has become increasingly obvious to engine manufacturers. Current lubrication technology is a result of trial and error over the past fifty years focusing on a very limited chemistry: mainly the phosphorus-iron chemistry. The lack of fundamental understanding of how current technology functions inhibits the development of alternate chemistries with very different elements, such as silicon and zirconium in ceramics.

Research conducted in the division has discovered several classes of chemical compounds that are capable of reacting with Si_3N_4 and SiC. Two independent studies have been carried out: one focused on silicon nitride; and one focused on silicon carbide. Fig. III-6 shows results of a screening test on anti-wear activities of different compounds on the two surfaces. The lack of strong correlation suggests that silicon nitride and silicon carbide react differently with the same chemistry. This is surprising since surface analysis results indicate that both surfaces are covered with silicon dioxide. Other studies done abroad also suggest that the silicon nitride surface has different reactivity from silicon carbide surface. This result has significant implications with respect to the development of lubrication technology for ceramic components.

A reaction mechanism study of alcohol functional groups on Si_3N_4 surfaces has been conducted. The results illustrate the complexity of these new chemistries. The surface of Si_3N_4 is actually oxidized and hydroxylated. Static reactions at moderate (80°C - 245°C) temperatures on high surface area Si_3N_4 powders has indicated that the adsorption of the alcohol is followed by reaction to form a bonded surface alkoxide, as shown in the upper illustration to the right. The resulting hydrophobic silicon alkoxide surface can then undergo subsequent reactions, promoted by the high temperature rubbing environment of the contact. The stepwise reaction eventually results in the formation of (free) silicon tetra-alkoxide as shown in the lower illustration. The presence of this reaction product has been demonstrated using secondary ion mass spectroscopy (SIMS). Further heating of the tetra-alkoxide results in condensation reactions and the formation of higher molecular weight silicon-containing organic compounds which subsequently form the lubricating film protecting the silicon nitride surface.

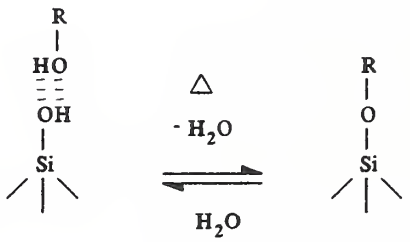

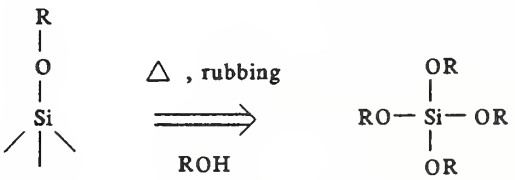

Based on the results to date, four patent applications have been submitted.

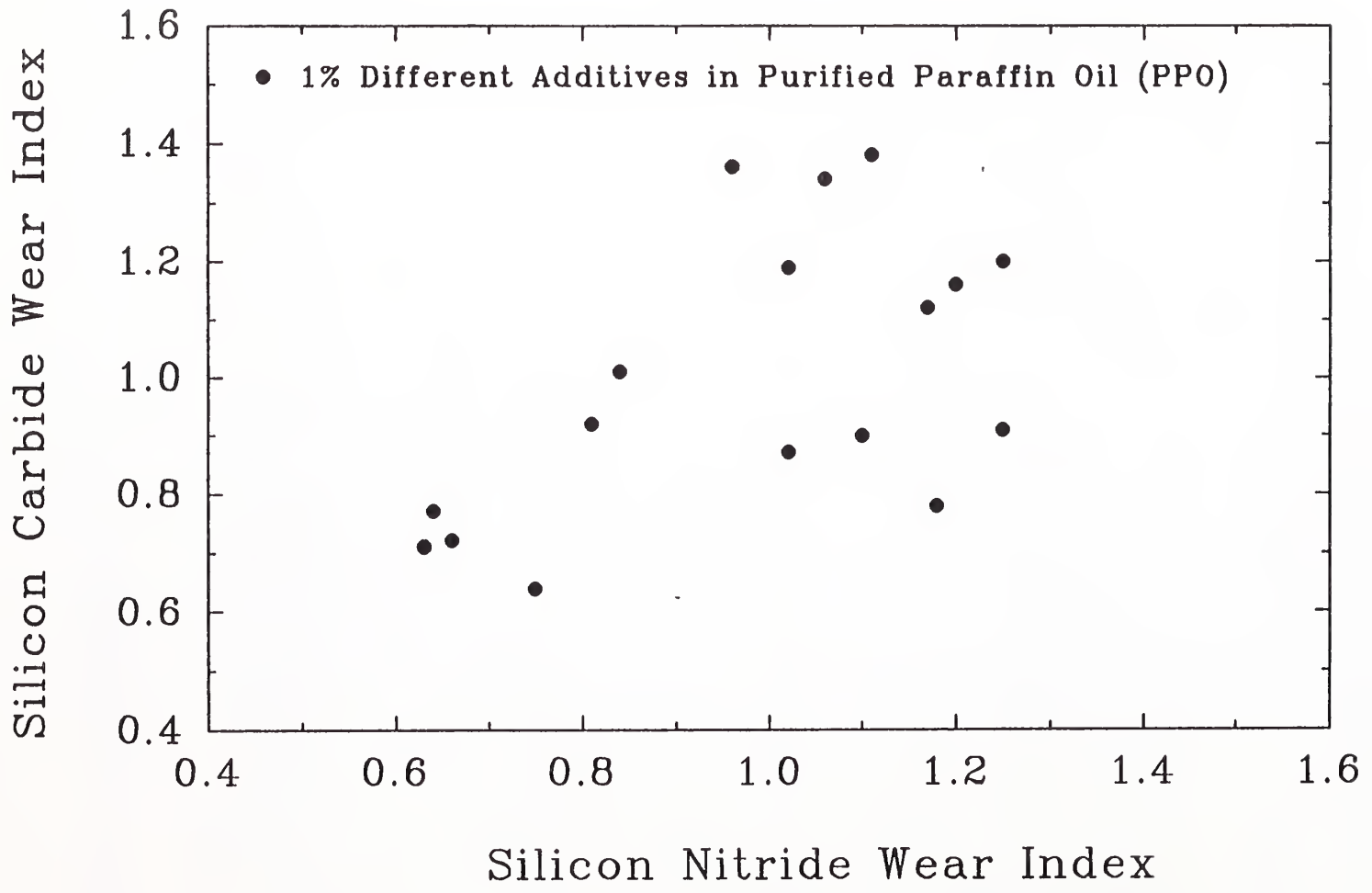

Figure III-6. Comparison of the Response to Different Chemistries by Si_3N_4 and SiC. Chemicals are 1% by Weight in Paraffins. (Wear Index is Defined as the Wear with the Chemical / Wear without the Chemical)

Tribology of Self-lubricating Composites

A. W. Ruff and M. B. Peterson[1]

[1] Guest Scientist, Wear Sciences, Inc., Maryland

Research sponsored by the Air Force Materials Laboratory has been completed on the use of advanced, vacuum-deposited solid lubricant coatings in bearing systems for space satellites. NIST has carried out research to develop an understanding of the tribology of self-lubricating composites and advanced solid lubricant coatings. Several key processes responsible for wear and friction in such materials have been identified. Composite materials consisting of both copper-matrix and bronze-matrix with solid lubricant phases of either intercalated ($NiCl_2$) graphite or molybdenum disulfide were studied in sliding wear. Both uncoated and MoS_2 pre-coated type 440 °C stainless steel rings were used as counterface materials. Friction and wear tests were carried out using a pin-on-ring tribological test system at normal temperatures in both air and dry argon.

The principal mechanism controlling wear of self-lubricating composites involves an interfacial film. The properties and durability of that film depend on film composition, the mechanical conditions present, and the environment. Generation of wear debris particles during service are an important consideration as they change film composition and microstructure. Recommendations have been made to the Air Force concerning hardware design and production procedures for such tribological systems.

Advanced Lubrication for Engines

Z. Hu[1], J. Sun[1], R. S. Gates and S. M. Hsu

[1] Post-doctoral Fellows, University of Maryland

The desire for higher fuel efficiencies and lower emissions has provided the driving force for the development of high efficiency, environmentally compatible engines. Many of these concept engines exploit the higher efficiency from high combustion temperatures. High temperatures necessitate the use of advanced materials such as ceramics, metal matrix composites, and coatings. However, as the temperatures rise, the lack of lubrication at high temperatures adversely affects efficiency due to increase in friction. When the temperatures are lowered, the lack of proper lubrication of the new materials introduced becomes the limiting factor in developing such concept engines.

Emissions requirements for diesel engines in 1994 and 1998 provide another need to analyze and understand the formation mechanism of diesel particulates. The contribution to diesel particulate by the lubricant currently is about 20-25% of the total weight of the particulate. This will go up to about 40-50% in engines that meet the 1994 emission requirements. Most of this contribution is in the form of partially oxidized organic compounds adsorbed and reacted onto the surface of fuel-derived carbon soot particles.

This project is sponsored by the Office of Transportation Technologies in the Department of Energy (DOE). The objectives are two-fold: to explore novel concepts to lubricate new materials used in advanced engines, to provide basic understanding of how the new materials can be lubricated; to develop system concepts that will reduce the diesel particulates. Our efforts have been to develop simulation tests to assist industries to develop the advanced lubricants necessary for the high temperature operations. Several laboratory simulation tests using pressurized differential scanning calorimetry (PDSC), thermogravimetric analyzer (TGA) have been developed. In conjunction with the chemical industry and the diesel engine manufacturers, several advanced lubricants have been developed. Akzo Chemicals has been collaborating with us and a joint fluid recently has been engine tested by the Cummins Engine Co. It is one of the two best performers of the 18 candidates submitted.

The diesel particulate project is to understand the formation mechanisms of diesel particulates. In conjunction with CRC and diesel industry, samples of diesel particulate have been obtained and methods for characterization of the particulate were developed.

A new analytical procedure has been developed that utilizes a simultaneous thermo-gravimetric and differential thermal analyzer (TGA/DTA) to measure the composition of the diesel particulate. A typical analysis, shown in Figure III-7, provides this information in less than an hour. The data shows that there are essentially three main TGA weight loss events associated with heating diesel soot in an oxidizing atmosphere. The related exothermic reactions are apparent in the DTA heat flow measurement. A series of similar analyses of solvent extracted samples, coupled with FTIR and GC-MS analyses demonstrated that the first peak is due to relatively non-polar organic compounds. The second peak is associated with polar and polynuclear aromatic compounds, and the third peak is from carbon itself.

Future efforts will involve developing a simulation test to study the formation of particulates under simulated engine conditions.

Ceramics Wear Maps

M. C. Shen[1], S. W. Lee[1], and O. B. Bogatin[2] and S. M. Hsu,

[1] Post-doctoral Fellows, University of Illinois at Chicago
[2] Visiting Scholar, Institute of Non-Metallic Materials of Russian Academy of Science at Yakutsk

The key to introduce new materials into the product cycle is to provide proper design guidelines for the utilization of the new materials. For tribological applications, the friction and wear characteristics of a new material as a function of speed and load (stresses and temperatures) are vital for successful design. For this purpose, wear maps have been developed providing a comprehensive data base for ceramics under a wide range of operating conditions and environments. Wear maps have been constructed for several aluminas, silicon nitrides, silicon carbides, a yittrium stabilized zirconia, and a SiC whisker reinforced alumina. Operational conditions include dry sliding, water lubricated, purified paraffin oil lubricated, and a commercial lubricant. Wear transitions, different wear levels, and the progression of wear as

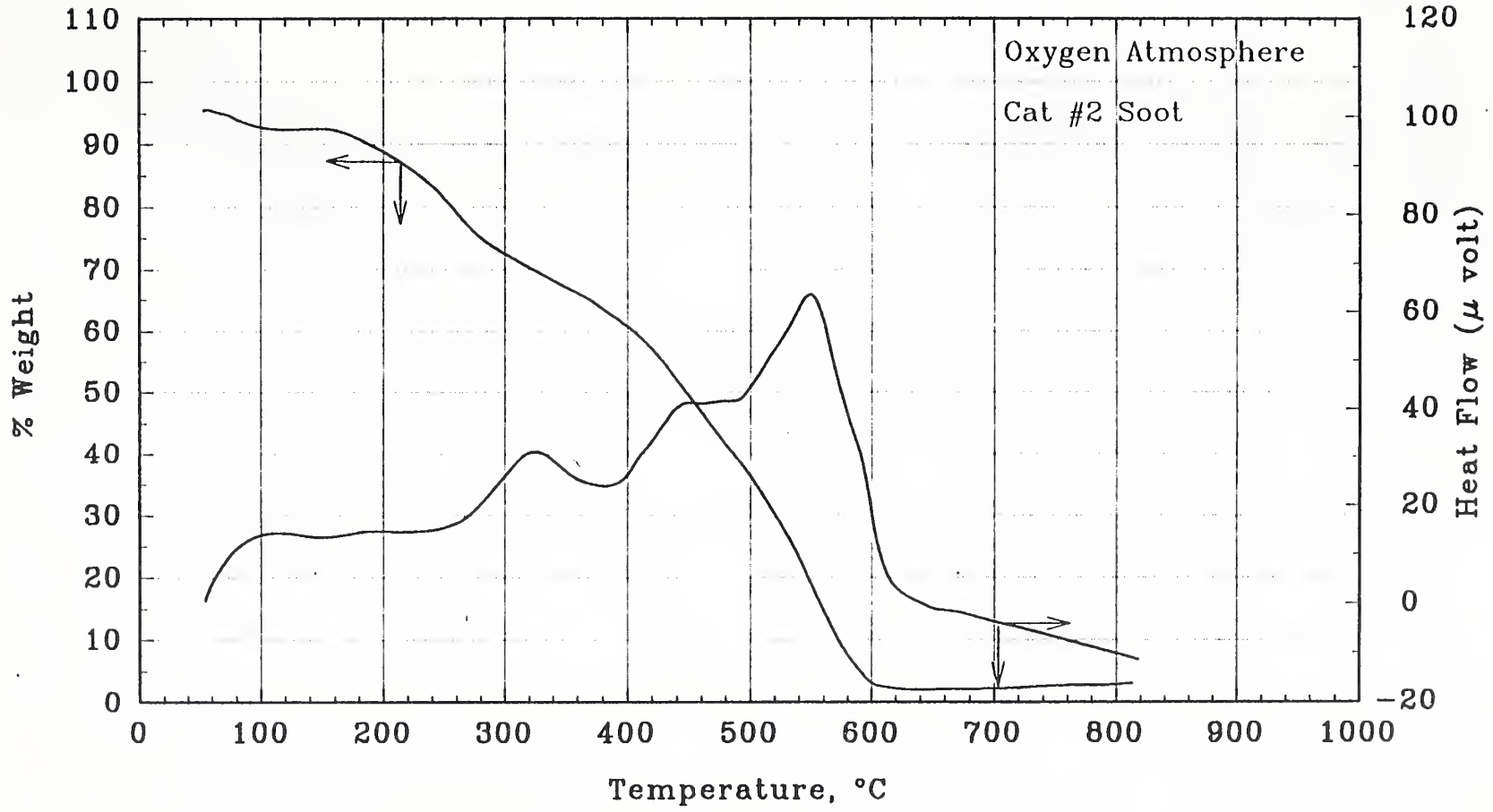

Figure III-7. TGA/DTA Thermogram of Caterpillar Diesel Particulate

a function of speed, load, temperature and environment can be visualized from the maps.

Using such a data base, selections of a ceramic for a particular application can be made. Figure III-8 illustrates the capability of the current methodology: the equal wear rate contour of 10^{-5} mm^3/m of a HIPped Si_3N_4 under various conditions are plotted. Given the wear rate of 10^{-5} mm^3/m, the operative load and speed for unlubricated case are limited to 10 N and 0.01 m/s. The presence of lubricants expands the operating limits to higher loads and speeds.

Detailed wear mechanism studies on various ceramics materials were conducted and some predictive wear models were developed. The wear of ceramics is largely due to tensile cracks at the trailing edge of the asperity contacts. Depending on the surface roughness and the presence of wear particles, plastic deformation has been observed. Large wear particles, once present, cause a large increase in contact stresses due to the decrease in real contact area. The resulting stress is generally sufficient to cause immediate fracture which in turn produces more wear particles. This basically constitutes a wear transition. After such a transition, brittle fracture dominates. Results of SEM observations on worn surfaces indicate that the predominant wear mode changes across the wear transition. Therefore, different predictive wear models have to be developed for different wear mechanisms in different speed and load regimes. Also, we need a model that can predict the onset of the wear transitions.

To describe the brittle fracture dominated wear mode due to the formation of large wear particles from tensile stresses in the sliding contact, a tensile crack wear model based on linear fracture mechanics was developed. The model is described as follows,

$$V = C * \left(\frac{\sigma_{max}}{\sigma_D}\right) * \frac{P*L}{H_V(T)}$$

where
- V = wear volume
- C = a coefficient
- σ_{max} = maximum tensile stress
- σ_D = critical damage-induced stress
- P = normal load
- L = sliding distance
- $H_V(T)$ = temperature-dependent hardness

The tensile crack model successfully describes the wear results of most polycrystalline ceramics under moderate loads. The maximum tensile stress, σ_{max}, is estimated by using Hertzian stress analysis including the tangential force from friction. The critical damage-induced stress, σ_D, is a function of the grain size, the residual stress at the grain boundaries, as well as other geometric factors. The hardness data as a function of temperature are determined independently by hot-hardness indentation tests. Figure III-9 illustrates the model prediction for the wear data of a SiC ceramic under dry sliding condition. As shown in the figure, there is good agreement between the prediction and the data for the intermediate wear level, where surface cracks dominated wear. In the low wear regime, the agreement is not as good. Experimentally, wear was found to be dominated by micro-cutting and plastic deformation. At very high wear levels,

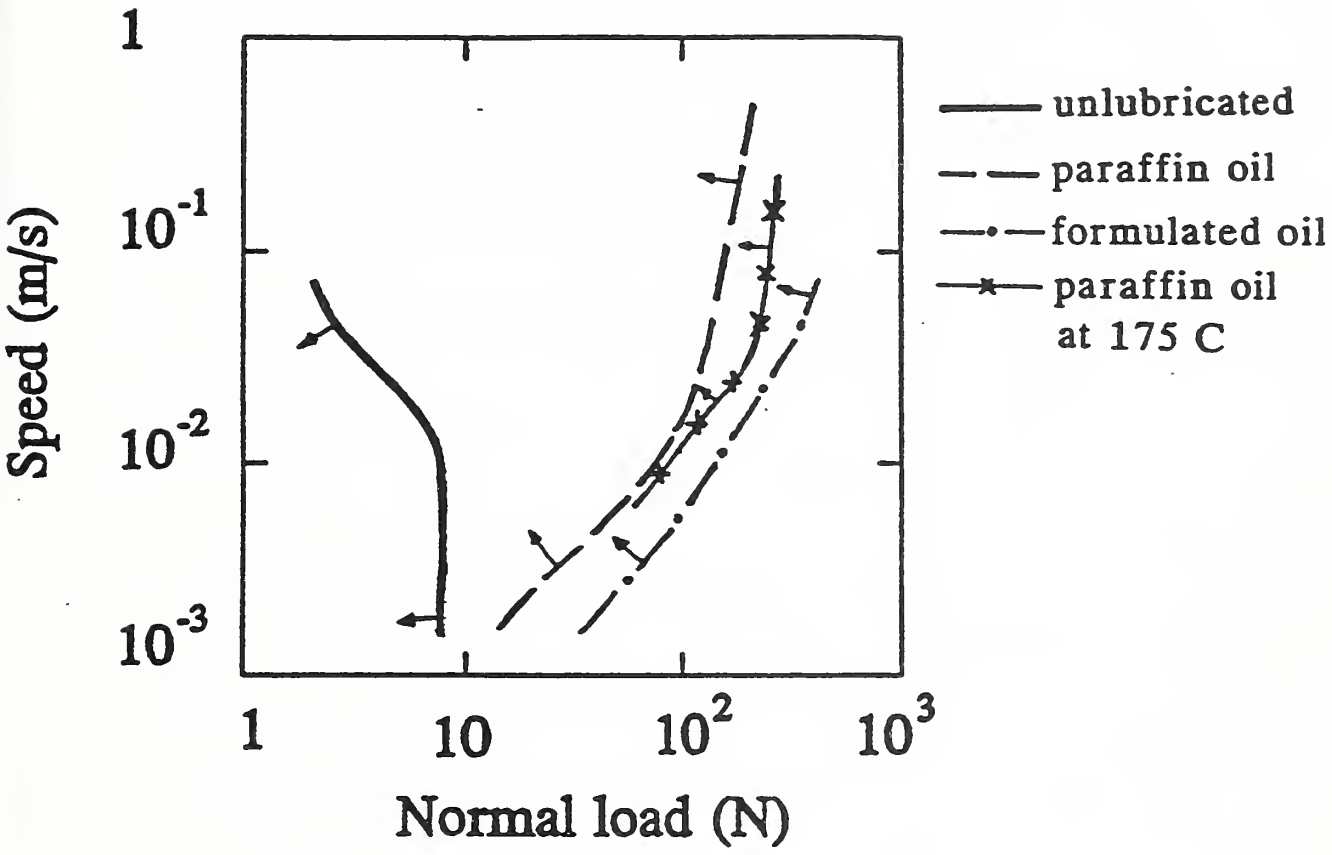

Figure III-8. Contours of wear rate (volume/distance slid) at 10^{-5} mm^3/m for a Si_3N_4 material under various lubrication conditions. The arrows point to the direction of lower wear rate.

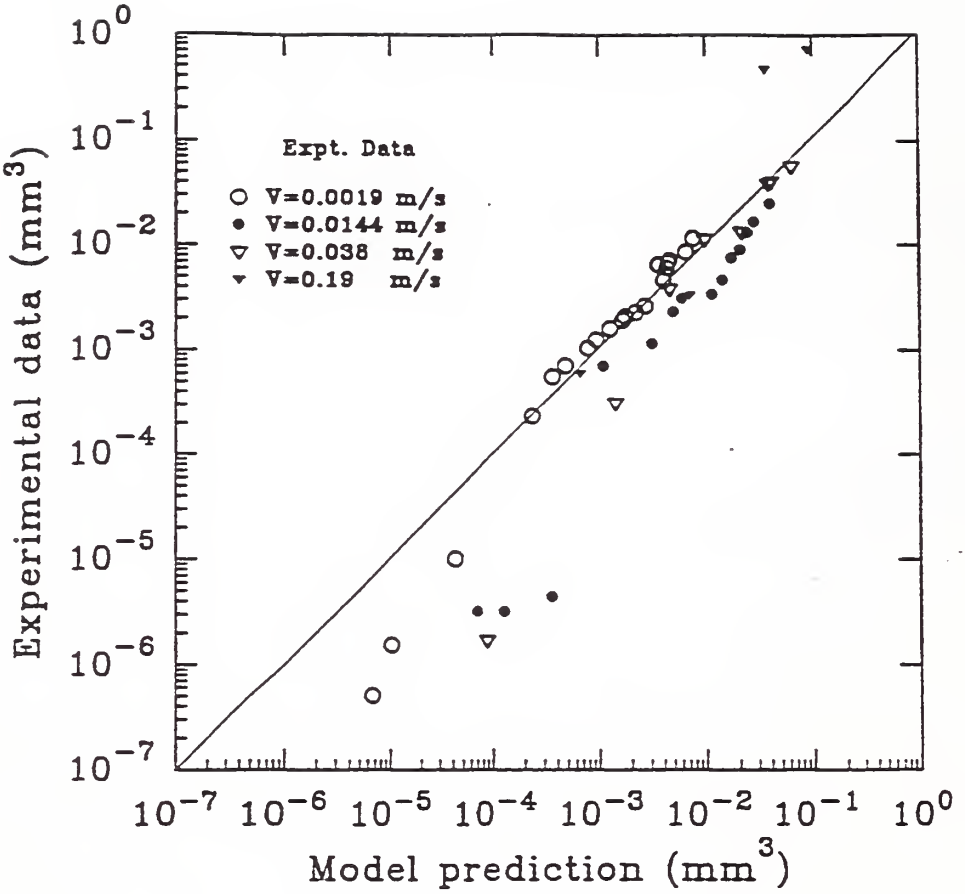

Figure III-9. Model prediction vs. experimental wear data for a SiC material under unlubricated condition by using a tensile crack model.

the model underestimates the wear. Here we found the additional stress due to thermal shock accelerates the wear. Also, in testing the model against various materials, the ratio of σ_{max}/σ_D appears to lie between 1.2 to 1.3 when wear transitions occur. Theoretically, we expect the ratio to be 1.0 for the instantaneous fracture to take place at transitions. The additional 20-30% of stress required for transitions can probably be explained by the microstructural effects, i.e. R curve behavior, crack deflection, and crack bridging effects.

Additional analysis of the wear transition data of various ceramics yields some interesting results. Figure III-10 plots a normalized wear quantity, Z, the ratio of wear depth to the average grain size of the material. Of the three ceramics shown, the wear transitions occur when wear depth is comparable to the grain size. This observation is valid regardless of the lubrication conditions, of course, higher speeds and loads are necessary for the lubricated case to reach the same wear depth. From the tensile crack model, one might speculate that the onset of wear transition is caused by the crack propagation up to one grain size length. At this stage, wear particle(s) of the minimum size of a grain is produced. The generation of this critical size wear particle(s) could change the stress distribution in the contact. The surfaces now could be separated by one or several large third body particles and the stress intensity at the tips of the particles could be very large, much higher than the K_{Ic}. This would cause immediate fracture in the substrate, and produce more wear particles which accelerate the process. Thus, the wear after the transition is usually dominated by brittle fracture.

Future efforts are aimed at developing models describing the low wear regions and examine the details of surface defects on stress distribution in contacts.

Microstructural Design For Wear

C. He[1], H. Y. Liu[2], J. Wallace and S. M. Hsu

[1] Graduate Student, University of Maryland
[2] Postdoctoral Fellow, Northwestern University

The mechanical properties of engineering ceramics are generally influenced by the microstructural features of the material. The wear mechanisms of ceramic materials are complex, but can be classified by one of the two dominant processes: deformation or brittle fracture. The transition from deformation-dominated wear to fracture-dominated wear under increasing load is often severe and generally defines the useful range of the material for a particular application. Previous researchers have shown that a Hall-Petch type relationship exists between wear rate and grain size for polycrystalline ceramics. Therefore, the control of microstructure is an important factor in developing wear resistant ceramics.

Previously, we have studied the wear behavior of an alumina and a partially stabilized zirconia. The alumina exhibits a pronounced wear transition at relatively low loads. The wear behavior of zirconia materials is somewhat different. Low thermal conductivity of zirconia causes severe wear at high sliding speeds due to stresses generated by thermal shock. The addition of a relatively small fraction of zirconia to alumina results in a composite material of increased toughness, commonly known as zirconia toughened alumina (ZTA). The effects of the zirconia

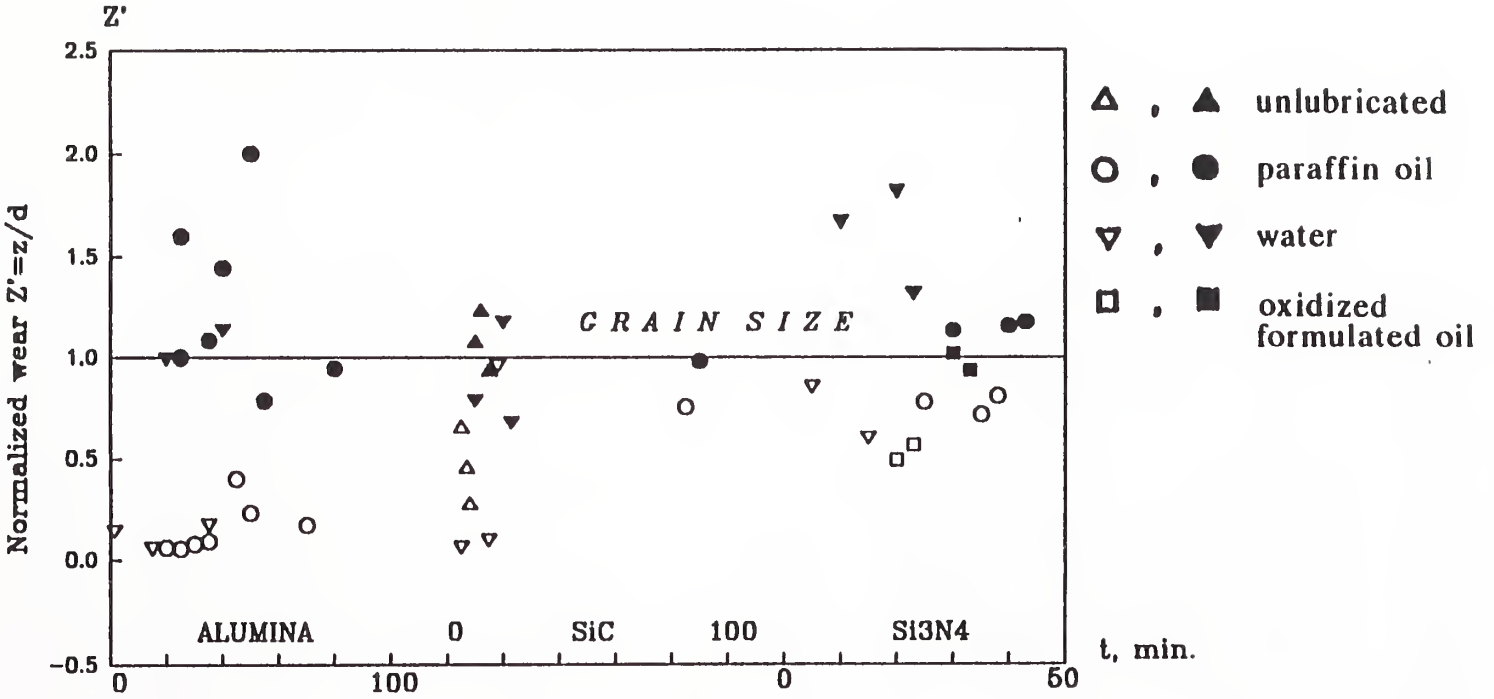

Figure III-10. Plot of normalized wear (z = wear depth, d = average grain size) vs. sliding time before (hollowed symbols) and after (filled symbols) wear transitions in various environments and under different load and speed.

content on microstructure and its toughening mechanism have been extensively investigated by others. We have previously developed a model based on energy balance to predict wear transition from a deformation-controlled regime to a brittle-fracture-controlled regime for alumina. The model has subsequently been modified for ZTA.

In order to understand the effect of microstructure on wear resistance, various samples of controlled microstructure of ZTA were made. Alumina powder was mixed with 5, 10, 15, and 20 vol% undoped zirconia powder (sintered samples were referred to as AZ5, AZ10, AZ15 and AZ20, respectively) through conventional processing.

Wear tests were conducted using a ball-on-flat geometry in a modified four-ball wear tester. A commercial 12.7 mm diameter hot-pressed silicon nitride ball was used. Purified paraffin oil was used as the lubricant. The density, ZrO_2 content, and hardness of the composites are listed in Table III-1. The grain size and width of the grain size distribution of the composite decreases with increasing ZrO_2 content, because the ZrO_2 particles serves as obstacles for the grain growth of Al_2O_3 during sintering. The ZrO_2 grain size increases with ZrO_2 content, resulting in reduction of the t-Zro_2 fraction. In AZ5, a few of the ZrO_2 grains were inside the alumina grains, but the majority of the zirconia grains were at or near the alumina grain boundaries. In contrast, the ZrO_2 grains in AZ10, AZ15 and AZ20 are all intergranular, concentrated along the alumina grain boundaries.

The transition from plastic deformation to a brittle fracture dominated wear process for each of the ZTA materials is characterized by a distinct increase in wear and a concomitant increase in the coefficient of friction at the transition load. The worn surface exhibited massive surface damage and was clearly formed by a brittle fracture process. The transition load as a function of the content of ZrO_2 in the composites is shown in Figure III-11(a). The transition load or micro-fracture resistance increases from 170 N to 350 N as zirconia content increases from 5 vol% to 20 vol%. Figure III-11(b) shows the relationship between the transition load and the d_{90} of the Al_2O_3 grains for each materials. It can be seen that the transition load is inversely proportional to the d_{90} which represents the largest 10% of Al_2O_3 grains in the material. This suggests that the wear transition is dependent on the flaw population and crack propagation along the grain boundaries. The largest 10% of the grains therefore, represent the weakest links and are most likely to fracture under the stress.

Under mild wear conditions the worn surface was found to be very smooth with elongated grooves in the sliding direction suggesting that wear was dominated by plastic deformation. Some isolated grain pullouts were visible, but not dominant. The pre-transition wear resistance of the ZTA composites is plotted in Figure III-12. AZ15 shows the best pre-transition wear resistance of the four materials, while AZ5 the worst. As the zirconia content increases from 15% to 20%, the pre-transition wear resistance decreases even though the transition load increases. In the pre-transition region where gross fracture is not the dominate mechanism, wear of the ZTA composites are controlled by grain size, t-ZrO_2, hardness, Poission's ratio and other parameters. AZ20 has the lowest hardness but the smallest grain size. AZ10 has the highest transformation potential but much broader grain size distribution. AZ15 has higher measured hardness, narrower grain size distribution, and medium transformation potential. In the final analysis, the combination of hardness and grain size gives AZ15 the lowest pre-transition wear.

Table III-1. Compositions and Properties of the ZTA Composites

Material	Tetragoanl fraction in ZrO_2, X_t	ZrO_2 content t* vol%	ZrO_2 content m** vol%	Density g/cm^3	Relative density %	Hardness GPa
AZ5	88%	4.4	0.6	4.04	98.8	17.9±2.0
AZ10	73%	7.3	2.7	4.14	98.7	16.5±1.3
AZ15	19%	2.9	12.1	4.22	98.8	17.2±1.5
AZ20	4%	0.8	19.2	4.29	98.4	14.9±1.5

* Tetragonal phase of ZrO_2

** Monoclinic phase of ZrO_2

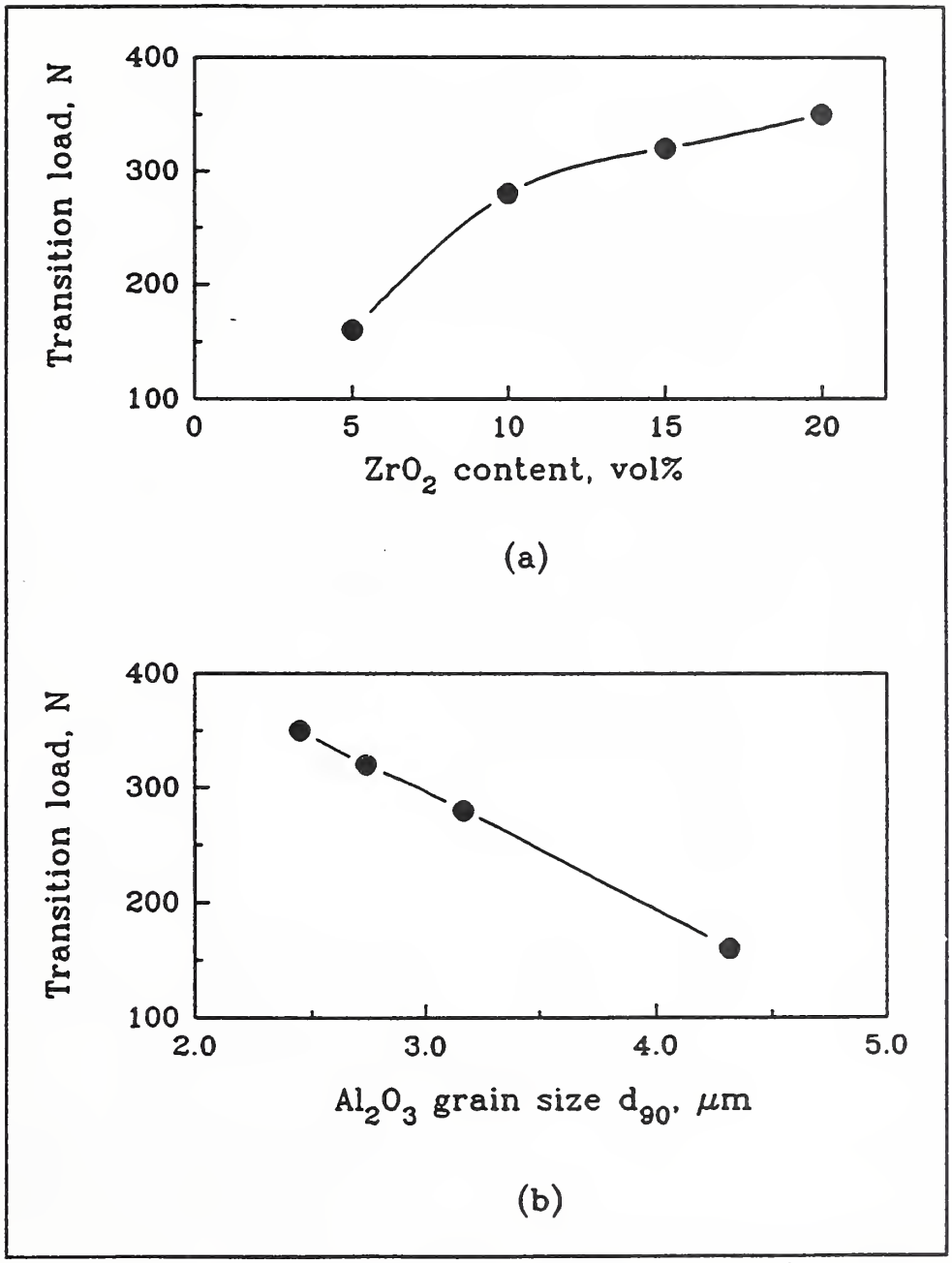

Figure III-11. Wear transition load as a function of: (a) ZrO_2 content, (b) d_{90} of Al_2O_3 grains in ZTA materials (0.23 m/s, paraffin oil)

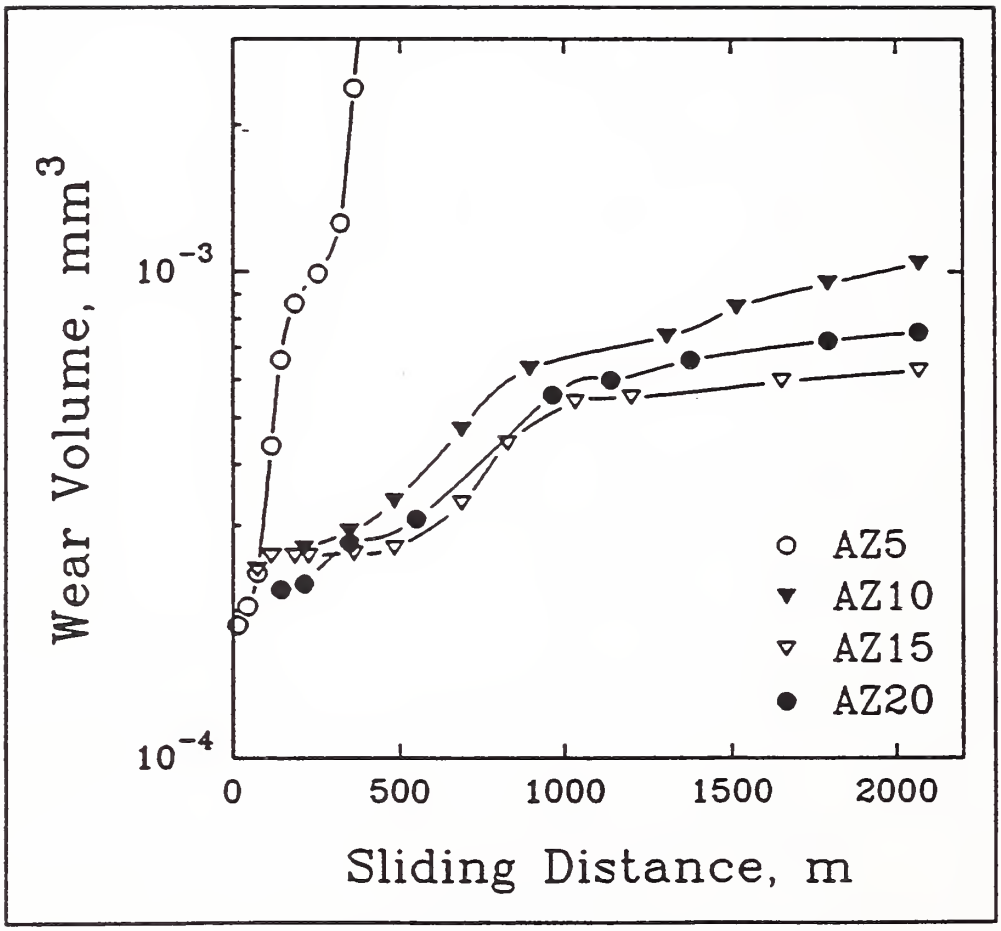

Figure III-12. Pretransition reesistance of ZTA materials sliding at 180 N load and 0.23 m/s with paraffin oil lubrication. Note that AZ20 has higher wear volume than does AZ15 for a given sliding distance.

The microstructural design for optimum wear resistance study is currently being extended to silicon nitride. A critical assessment of various processes and their microstructure has been completed.

Mechanisms of Abrasive Wear in Lubricated Contacts

L. K. Ives

A project involved with evaluating different materials that can resist abrasion by coal particles sponsored by the Fossil Energy Materials Program of DOE was recently completed. DOE is supporting the development of diesel engines capable of direct operation on a fuel incorporated with pulverized coal i.e. a slurry consisting of 50% water and 50% coal. Efficient combustion has been demonstrated with this fuel; however, operating engines have experienced an extremely high rate of wear. One critical area of wear is at the piston ring/cylinder wall contact. Mineral matter in the coal and ash particles generated from the mineral matter during combustion are the primary cause of the high rate of wear.

The goal of the project was to identify the critical parameters controlling the wear of materials under this abrasive action and based on the mechanisms, develop guidelines for new materials. A pin-on-disk wear simulation test was developed. An investigation was also conducted to determine the type, size, shape and relative concentrations of particles that might be present in the combustion chamber of diesel engines operating on coal-fuel. Scanning electron microscopy and associated energy dispersive x-ray analysis were used. The particles analyzed had been collected from the exhaust of diesel engines operating on coal fuel as well as from the oil filters of such engines. It was concluded that quartz and some silicates were the hardest particulate materials present. Thus, in the evaluation of materials and coatings for coal-fuel diesel engine applications abrasives of comparable hardness should be used in testing.

Parameters influencing piston ring and cylinder wall wear in a coal-fueled diesel engine fall into several different categories, namely: 1) those related to particle properties and concentration, 2) contact parameters (load, speed, etc.), 3) the lubricant, 4) the thermal and gaseous environment and 5) the type and properties of the contacting materials. In most cases, as might be expected, there is a strong interdependence among the parameters. Except for component materials and the lubricant, because of other constraints, only limited control can be exercised over the various parameters to reduce wear. Experiments have indicated that the lubricant and associated additives have at most a small influence on wear rate. A major improvement is obtained, however, by employing materials and coatings with hardness significantly greater than that of quartz. In pin-on-disk wear tests employing particles extracted from the oil filter of a diesel engine run on coal-fuel several ceramics and composite materials exhibited sufficiently high wear resistances to be suitable for engine applications. One of the best was sintered tungsten carbide with 6% cobalt binder phase. Coatings of this material are in fact among the strongest candidates for application in prototype coal-fueled diesel engines.

Solid Films and Coatings

A. W. Ruff, L. K. Ives, H-J. Shin[1], N. Vinod[1] and M. B. Peterson[2]

[1] Graduate Students, University of Maryland
[2] Guest Scientist, Wear Sciences, Inc.

This research focuses on tribological characteristics of thin solid lubricating films and of selected wear-resistant coatings. Basic processes that take place in the near-surface regions of particular model materials are studied. Use of model materials facilitates interpretation of the observed phenomena in terms of analytical models of friction and wear.

Studies over the past year has been concerned with tribo-chemical solid state reactions of molybdenum oxides and sulfides, and also copper oxides. It has been possible to generate low friction, durable films in situ during sliding at various temperatures. Oxide and sulfide powders have been applied as lubricants on glass and ceramics (Al_2O_3, Si_3N_4, SiO_2) and studied in sliding at temperatures up to 600 °C. Friction coefficients as low as 0.15 have been achieved so long as sulfur reactions are favorable in competition with some oxidation reactions. Design of alloy compositions to favor such competition in forming surface films seems feasible.

Nano-indentation measurements of copper - copper oxide tribological films about 0.1 to 1 μm thick, formed by sliding in situ on aluminum oxide substrates, have shown increased hardness by a factor of 10 within the wear track when compared to unworn regions, as well as associated easy shear to give low friction values (Figure III-13). Critical issues for these films include cohesion within the film so that traction forces can be supported, film porosity, adhesion to the substrate, and wear debris contamination during sliding that changes film chemistry and properties.

Studies of the relationship between tribological behavior and film properties have been done for a series of copper films formed as coatings on aluminum oxide substrates. The experiments were conducted over a range of temperatures from 23 to 600 °C in air. Film thickness and substrate roughness were also varied in the experiments. In general the coefficient of friction at 600 °C was about two-thirds of that at room temperature. Aluminum oxide substrate roughness was found to have a significant effect. For thin (31 nm) films, the friction rose from an initially low value and became high and unsteady, suggesting that the supply of copper oxide for lubrication was rapidly depleted. In contrast, for thicker films, the coefficient of friction decreased during the test to a low and steady value (Figure III-14), indicating that a sufficient supply of copper oxide lubricant was available from valleys between asperities on the rough surfaces.

Work next year will focus on deposited films of copper-molybdenum having carefully selected compositions that will be slid against polished Al_2O_3 at various loads and temperatures up to 800 °C. Measurements of nano-indentation hardness, elastic module, film thickness, morphology, porosity and composition will be conducted and related to measured friction and wear. Transmission electron microscopy and microchemical analysis methods will be applied to understand relations between film structure-composition and measured properties. An

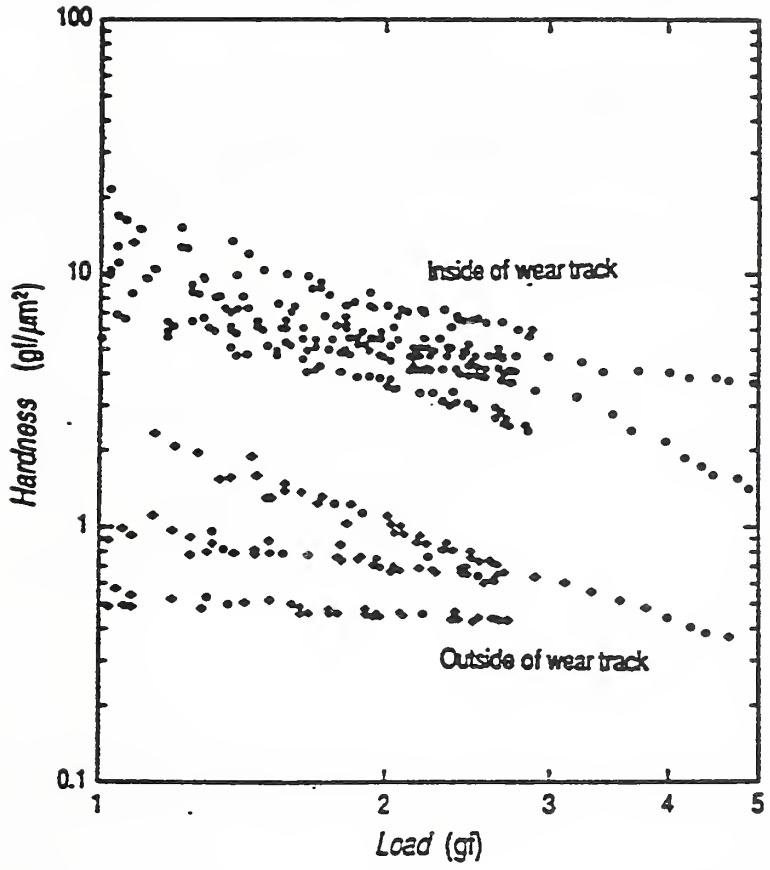

Figure III-13. Film hardness changes associated with sliding measured by nanoindentation for copper oxide films.

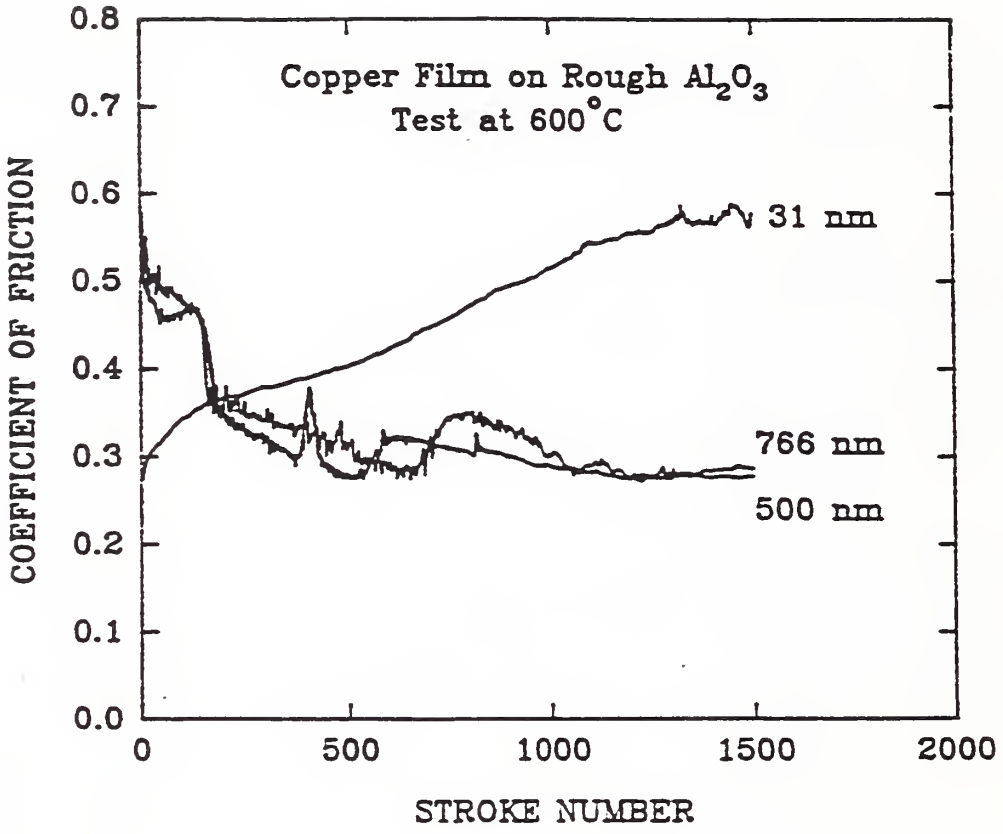

Figure III-14. Friction changes with sliding distance for three copper film thicknesses.

analytical model of a tribological film will be developed to bring together the measured results on physical, chemical and tribological properties.

A Computerized Tribology Information System

A. W. Ruff and S. M. Hsu

The second phase of work on the computerized tribology information system, ACTIS, has been completed. It involved development of six new computer modules: an improved central access module, two rolling element bearing modules, an advanced gear module, a lubricant database, and a lubricant expert system selector module. These modules are now additional to the original ACTIS set: a numeric database on tribological materials, and four design calculation codes for contact stress, lubrication conditions, gear systems and journal bearing systems. All modules work together within one central PC-based system.

The overall plan for the ACTIS system was developed from a workshop held at NIST in 1985. The work has been funded since then by NIST, other federal agencies (Department of Energy - Office of Energy Conversion and Utilization Technologies, Air Force Wright Aeronautical Labs, Army Belvoir Research and Development Center, National Science Foundation), and two professional societies (the Society of Tribologists and Lubrication Engineers, and the American Society of Mechanical Engineers). The ACTIS system is presently being marketed by a not-for-profit corporation, ACTIS, Inc.

A related on-going NIST activity, the Tribology Data Center, supported by the Ceramics Division and the Standard Reference Data Office, continues efforts to obtain, evaluate, and disseminate critical data on tribo-materials. A database on ceramic tribological materials has been completed this year and plans are being formulated for its distribution.

Wear Standards and Measurement Activities

A. W. Ruff

Standards development has continued in the area of computerization of wear test systems, databases of tribological information and statistical analysis of wear data. The new sub-committee on Computerization in the ASTM G-2 Committee on Wear and Erosion leads that work, and is chaired by an NIST staff member. Draft standards have been written on a database format for wear and on wear data analysis methods. The drafts are undergoing committee ballot. The work is also coordinated with ASTM Committee E49 on Computerization of Material Property Data.

A project is being conducted in the VAMAS Wear Test Method group to establish a uniform methodology for organizing wear test data. The effort involves representatives from 9 countries and over 35 laboratories around the world and is the first attempt to reach an international consensus on the evaluation and dissemination of wear data.

Another project nearing completion concerns preparation of an atlas of worn surfaces. The work involves experts at NIST, Battelle Columbus Labs, and BAM in Germany. The atlas will consist of two parts; one is a collection of data and micrographs of worn surfaces on a variety of materials under different exposure conditions. The second part will be a computerized database of over 300 records drawn from publications from the International Conference on Wear of Materials, 1977-1991. The database will permit searching that literature source for particular tribology information.

IV. MECHANICAL PROPERTIES

David Cranmer

The reliable application of structural ceramics depends upon the ability to control and predict mechanical properties. Knowledge of processing-microstructure-property-performance relationships is the basis for this control and is the focus of our program in mechanical properties. Our program on mechanical properties has as its broad objectives: (1) the generation of new models and supporting data to elucidate fracture and deformation mechanisms in brittle materials at both ambient and elevated temperatures; (2) the development of fracture methodology for studying the fundamental forces that exists between two near surfaces; (3) the investigation of ceramic microstructures and their relationship to mechanical behavior; and (4) the development of standard test methods.

The advanced ceramics and ceramic composites industries needs for such a program are reflected in their extensive participation in workshops held at NIST in the past two years, in the broad agenda and industrial participation in ASTM Committee C28 on Advanced Ceramics, and in the formation 18 months ago of ASTM Subcommittee C28.07 on Ceramic Matrix Composites.

Development of test procedures and methodologies under this program serves a number of different purposes. It allows systems and components designers and product developers to obtain design properties of these materials; it allows materials developers and producers to reliably and reproducibly obtain important mechanical properties such as tensile strength, toughness, and creep; and it allows theoreticians and analysts to acquire the information to verify models and theories of behavior. Acquisition of the differing types of data and materials required by each of the above communities leads to very different testing a requirements, and dictates a broad-based program in mechanical property testing, test development, and standardization activities. Testing for design data is usually the most difficult to do because of the range of tests required and the need for repetitions to ensure reliability. Testing to validate/verify theories and models can also be very demanding due to the range of materials structures and compositions which may be required.

The issues to be considered in designing test procedures and methodologies, including specimen design, specimen gripping arrangements, load train design, heating method, temperature measurement, and strain measurement constitute areas of focus for the group. Specific projects are focussed on the processing-property relations between microstructural features and resulting properties including toughening behavior in structural ceramics and development of models for the fracture behavior of continuous fiber-reinforced, ceramic matrix composites. This latter work involves test development as well as preparation, characterization, and testing of composite systems.

Significant Accomplishments

- Two microstructural, micro-mechanics fracture models have been formulated algebraically, initial computer code has been developed, and several initial simulations have been performed. In one model, anisotropic thermal strains were introduced to elucidate the influence of the strain, grain size and Poisson's ratio on microcrack density; in the other the evolution of a three-dimensional crack front in a microstructure with

random-strength grain boundaries resulted, in the development of a R-curve.

- The influence of fiber inclination angle of reinforcement toughening in ceramic matrix composites was elucidated with a model composite system. The fiber bridging force of inclined fibers was measured as a function of crack opening displacement for different fiber inclination angles using a fracture mechanics approach. Localized matrix cracking was also observed for inclined fibers and was related to fiber inclination angle.

- A technique has been developed to significantly enhance the adhesion between two similar insulators (smooth silica sheets) by treating one surface with a covalently bonded monolayer of a silane. This monolayer, only 0.7 nm thick, is sufficient to change the electrical potential of the treated surface from negative to positive, resulting in a strong electrostatic attraction between a treated and an untreated surface, both in air and in aqueous solutions. This is the first direct experimental evidence that a single monolayer treatment is sufficient to cause this surface-charge-induced adhesion, and a patent on the technique is being filed.

- A generic model for long-term creep rupture in ceramics matrix composites has been proposed. Transmission microscopy has shown that actual damage occurs in agreement with the model.

- A methodology was developed for evaluating short-crack toughness curves for ceramics. Such data is important for the determination of strength and wear resistance. Experimental data are being obtained for more lithic ceramics and ceramic composites.

- Small angle neutron scattering (SANS) and small angle x-ray scattering (SAXS) have shown that large cavities develop in silicon nitride due to creep stain. Heretofore, these isolated cavities were never observed using other experimental techniques.

- A "Ceramic Machining Consortium" was begun during this past year. This consortium now consists of 17 members. The goal of the consortium is to provide measurement methods, data, and mechanistic information needed by industry to develop cost-effective machining methods for advanced ceramics.

Creep Life Estimation on Fiber Reinforced Ceramic Composites

Tze-jer Chuang

Because they offer superior mechanical properties at ultra high temperatures, continuous fiber reinforced ceramic composite materials have been identified as candidate turbine engine materials for high speed supersonic flight vehicles required by NASA and USAF. To provide a reliable estimate of the service life, NIST has conducted a program to develop a methodology for lifetime estimation on these materials under long-term sustained loading conditions. Evidence collected from microscopy indicated that materials behave differently among long-term and short-term responses. For example, the failure mode in a typical (short-term) strength and/or toughness test consists of macrocrack growth with fiber bridging and pull-out; whereas that in

a typical (long-term) creep test consists of nucleation, growth and linkage of interfacial microcracks (see Figure IV-1). Thus, enhanced strength/toughness often leads to deteriorated durability. The service life is the sum of times spent in each developmental stage. A time-dependent theory based on mass transport kinetics has been developed which is capable of predicting microcrack growth rate if temperature and external loads are given.

A generic model has been proposed for assessing lifetime of this class of materials when subjected to long-term creep rupture conditions. This two-dimensional model consists of interfacial cracks growing between square grains and rectangular fibers in the direction normal to the principal tensile stress axis. Neglecting transient effects, the total lifetime is derived based on the criterion that rupture is due to coalescence of adjacent cracks. It is found that lifetime is inversely proportional to crack growth rate, volume fraction, and aspect ratio of the fibers; but extremely sensitive to the applied stress owing to the high power of the V-K_I law. This lifetime estimation seems to be in fair agreement with the creep rupture data of SiC_w/Si_3N_4 composite with 0 and 30 vol% reinforcement tested at 1250°C in air. Furthermore, TEM performed on the post-crept specimens revealed that creep damage occurs predominantly in the form of microcracks at matrix/matrix as well as fiber/matrix interfaces, approximately in accord with the model simulation.

Asymmetric Tip Morphology of Creep Microcracks Growing Along Bimaterial Interfaces

Tze-jer Chuang, June-Liang Chu[1] and Sanboh Lee[1]

[1]Dept. of Materials Science & Engineering
National Tsing Hua University, Hsin-chu, Taiwan

The asymmetric tip morphology of a creep microcrack propagating along a bimaterial interface is presented based on the assumptions that the near-tip shapes are developed from surface diffusion controlled crack growth and that a steady state prevails. Following Chuang and Rice, a single master curve can adequately describe the near-tip shapes to within 6 percent accuracy, but four cases of crack-tip morphology emerge depending on the ratios of surface to interfacial free energy and diffusivity of the adjoining phases. For fixed ratios of the two surface diffusivities, crack tip morphology maps in the space of specific surface energies are constructed with which areas associated with each individual case are indicated. Predicted cases on a set of bimaterial systems are tabulated and discussed. TEM photos of creep crack tips in alumina and silicon nitride are presented for illustration. The information given here is essential to a coupled analysis of diffusion and elastic deformation at a composite interface which may ultimately yield predictions of the delamination rate between the reinforcing phase and the matrix phase as a function of applied stress, temperature and other relevant materials' constants.

Surface Forces Between Dissimilar Ceramic Materials

D. T. Smith, R. G. Horn, A. Grabbe and J.-P. Chapel

The surface force apparatus has been used successfully for more than a decade to make fundamental measurements of forces between molecularly smooth mica surfaces in a variety of

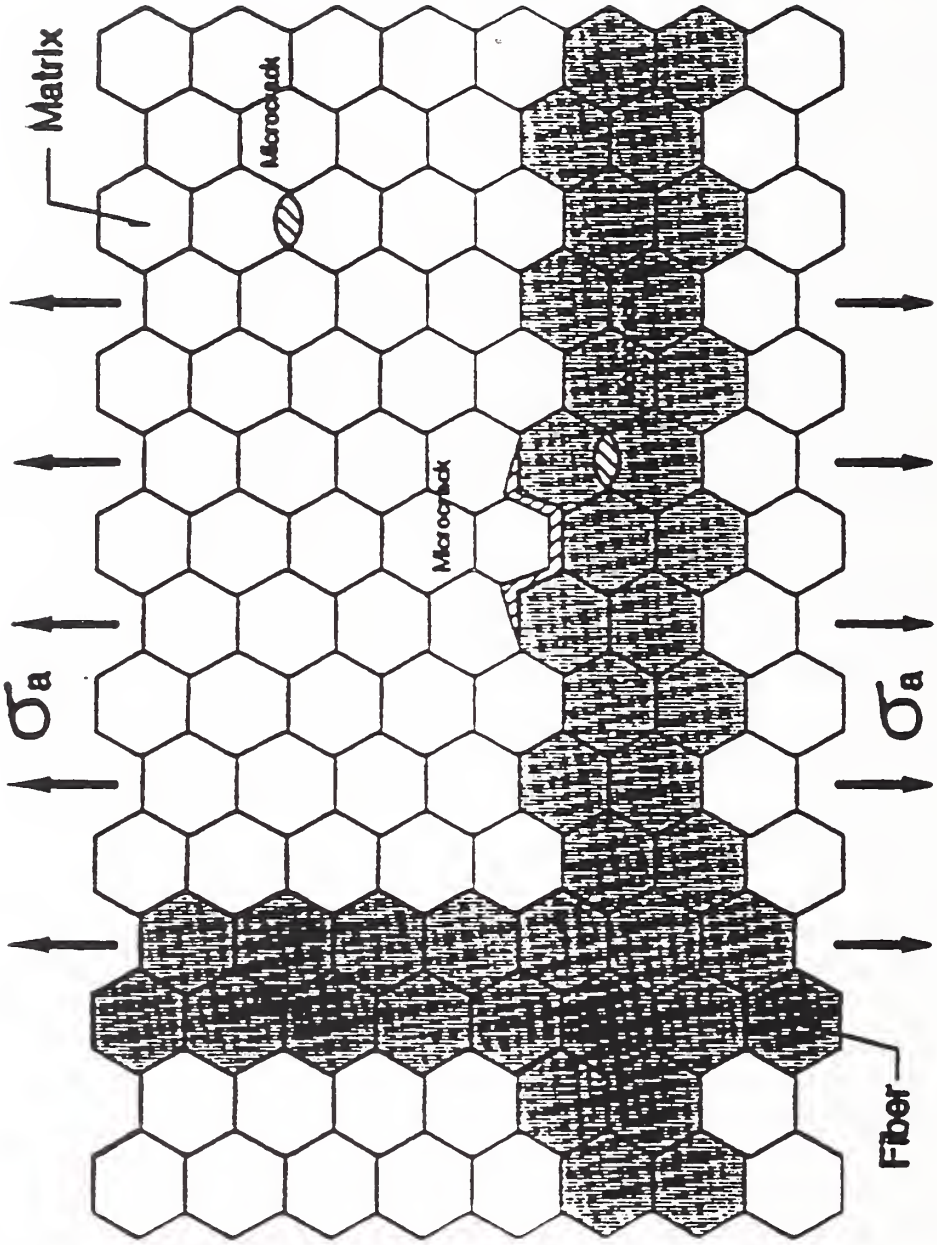

Figure IV-1. Schematic of possible sites for microcrack formation during creep of a fiber reinforced ceramic.

liquid and vapor environments. Recently at NIST, a method was devised to extend these measurements to silica surfaces. This development greatly extends the range of possible studies which can be made with the apparatus, and in particular it has opened the way to investigating forces between dissimilar materials. Such forces play a vital role in areas such as intergranular fracture, the mechanical properties of composite materials, colloidal processing of mixed powders and composites, and the adhesion of coatings.

In 1992 the work has focused primarily on forces between silica surfaces, which are used either as-prepared (using an oxy-hydrogen flame) or after being subjected to one of several surface treatments that chemically modify the surface. Forces are measured both in "symmetric" systems, where the two silica surfaces are identical, and in "dissimilar" systems, where opposing silica surfaces have received different treatments.

Forces in symmetric silica systems are of interest because they model the forces between small silica particles in suspension, and allow prediction of the stability of a given colloidal suspension. The symmetric systems studied included as-prepared silica, surfaces which had been exposed to steam for 150 hours, and surfaces which had been exposed to ammonia vapor. Both the steam and ammonia treatments were chosen because they in theory should change the density of surface silanol groups. Analysis of the electric double-layer forces in aqueous NaCl solutions for these three silica systems indicated that steam treatment does indeed increase the density of silanol groups, while exposure to ammonia vapor etched the surfaces slightly and rendered them porous. In all three systems, a hydration repulsion was observed at short range, indicating that suspensions of particles with any of the three surface conditions would be stable, i.e., would not tend to form agglomerates. This result is more or less independent of the concentration of the intervening NaCl solution. Work is currently underway to systematically study the double-layer and hydration forces for the full range of monovalent cations (Li^+ through Cs^+) as a function of salt concentration and pH.

Forces have also been measured in several dissimilar silica systems, both in air or dry nitrogen gas and in salt solution. Several striking effects have been observed. The dissimilar system which has received the most study is one where one silica surface is used as-prepared and the other is given a covalently bonded monolayer of an aminosilane (thickness 0.7 nm) that changes the surface potential of that surface from negative to positive. Force measurements in water indicate a long-range attractive double-layer interaction, and no hydration repulsion. Comparison of the data with theoretical calculations using fully retarded van der Waals interactions and the non-linear Poisson-Boltzmann equation indicates that the amino-functional surfaces exhibit charge regulation behavior.

When the forces in the silica/aminosilane-silica system described above are measured in dry air or nitrogen, a strong, long-range attraction is observed after contact. This attraction is the result of the spontaneous transfer of charge from one surface to the other during contact. A modification of the Surface Force Apparatus, developed at NIST, permits the in situ measurement of the amount of charge transferred. This contact electrification phenomenon, usually observed only between two macroscopically different materials, is possible here because the single monolayer silane treatment of one surface causes a modification of the surface electronic states of that surface that is sufficient to drive charge transfer. This is the first direct

experimental evidence that a simple monolayer is sufficient to cause this effect, and the technique could be of considerable value in fields such as microelectronic device construction. A patent application is in progress.

Additional modifications to the Surface Force Apparatus are almost complete that will allow the sliding of one surface over another for the study of friction, ultra-thin film lubrication and tribocharging. The design will permit the automatic regulation of a constant applied load.

Thin Film Indentation Studies

D. T. Smith, G. S. White

An instrumented indenter capable of measurements down to 0.01 kg full-scale load was used to investigate the mechanical properties of Bi-Sr-Ca-Cu-O high-T_c film on a polycrystalline MgO substrate. By comparing the data from the film-substrate system to similar measurements on bare MgO, and applying a volume fraction model for the composite system, it was possible to determine the hardness of the 5μm-thick films (Figure IV-2). It was also possible to study delamination of the film, which occurred at the perimeter of the indentations of 0.050 kg load or higher. The use of both instrumented indentation and volume fraction models for composite indentation will be used much more extensively in 1993, when the Nano Instruments nano-indenter facility becomes operational.

Ceramic Matrix Composites

C. P. Ostertag and L. M. Braun

Successful development of reliable ceramic composites depends on an understanding of matrix cracking, damage mechanisms and failure modes in these materials. This program addresses these issues by examining initiation, propagation and accumulation of cracks in the matrix of continuous fiber-reinforced ceramic composites.

Custom-designed devices which enable *in situ* SEM and optical microscope examination of the crack tip interaction with fibers and subsequent fiber pull-out during loading, were used to investigate crack propagation. These devices enable direct qualitative observations of the crack shielding zone at the microstructural level during loading, the crack profile, and the bridging/pull-out mechanisms at and behind the crack tip. Microstructural parameters that influence cracking and propagation, such as fiber volume fraction, fiber spacing, fiber/matrix interface, and matrix toughness, were investigated directly from experimental results of the crack profile, the crack opening displacement close to the fibers, and hence, the crack closure forces. Compact tension specimens were used to study the propagation of long-cracks, and biaxial and/or four point bend flexure were used to investigate the propagation of short-cracks (Figure IV-3). Specimens were precracked with either notches or indentations prior to stressing. These in situ stressing experiments were also used to investigate crack-front versus crack-wake phenomena. Crack-front behavior is defined as crack propagation prior to the crack being bridged by the fibers, and crack-wake behavior as crack propagation after the crack is bridged by the fibers.

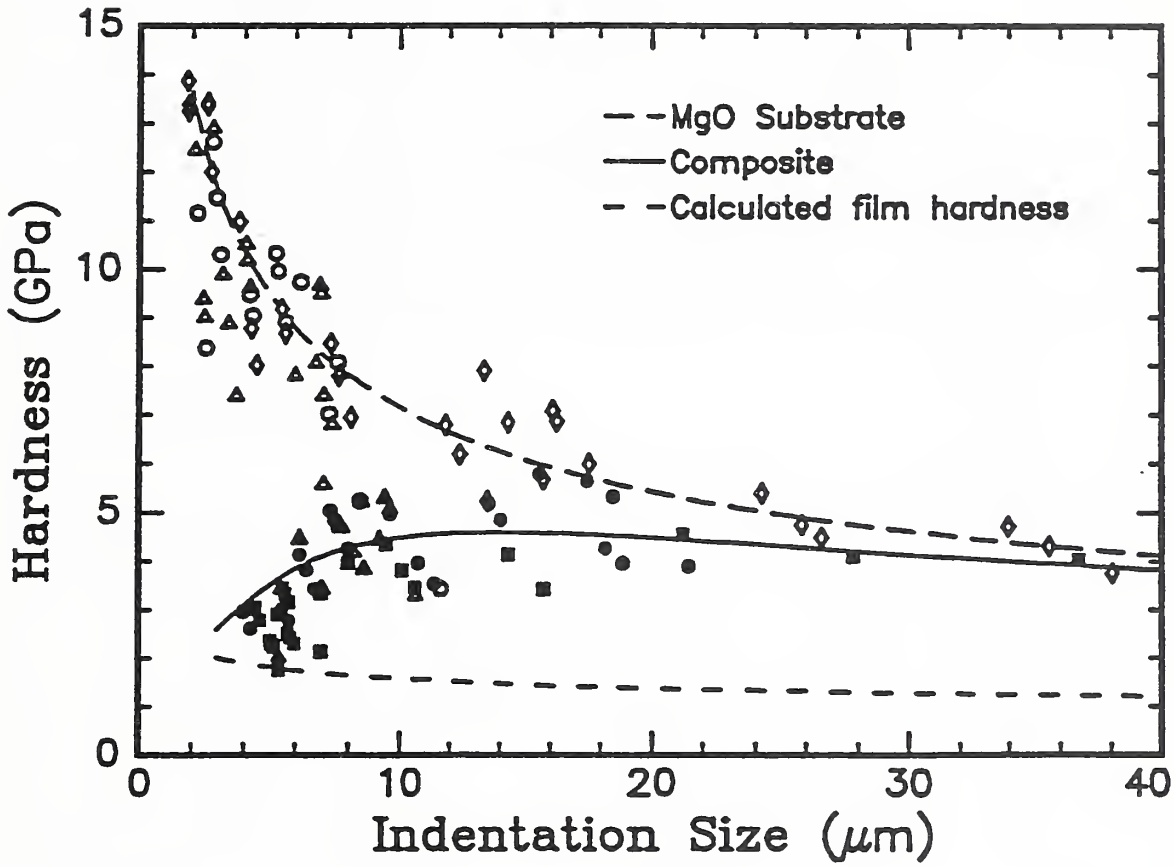

Figure IV-2. Hardness of a Bi-Sr-Ca-Cu-O film on MgO substrate as a function of indentation dimensions.2

Figure IV-3. Schematic of test methodologies for determining toughness of ceramic matrix composites.

SiC-Reinforced Alumina Matrix Composites - Crack Front Phenomena

Stable crack propagation towards uncoated fibers, during applied tensile loading, was observed in SiC reinforced alumina matrix composites (low volume fraction fibers). The fiber plane pinned the crack front, and a three fold increase in load was required to propagate the crack past the fiber plane. The load increase required to propagate the crack front past the pinning fibers resulted in a toughness increase from 2.3 MPa.$m^{1/2}$ to 4.3 MPa.$m^{1/2}$ (Figure IV-4a).

SiC Reinforced Alumina Matrix Composites - Crack Wake Phenomena

Crack-wake toughening mechanisms were investigated on the polymer/gold coated fiber composites by extending the precrack in air beyond the fiber plane. Fibers in the crack wake bridge the crack and thereby enhance the crack resistance by shielding the crack tip from the applied load. A gradual increase in applied load propagated the crack in a stable manner. Toughness increased with increasing crack length to a maximum at failure of 7.35 MPa.$m^{1/2}$ (10% areal fraction of fibers) (Figure IV-4b). Grain and fiber bridging in the crack wake were responsible for the observed increase in toughness. Measured fiber pullout lengths of 30-50 μm, after specimen fracture, suggest debonding along the fiber matrix interface during crack propagation.

SiC Reinforced Si_3N_4 Matrix Composite

The indentation-strength response of a Si_3N_4 matrix/SiC fiber-reinforced composite with 0 (monolith), 14 and 29 vol % fibers was determined. Crack-front and crack-wake behavior were investigated using the indentation-strength technique (See Figure IV-5). Low indentation loads correspond to small, short cracks in the material, while high indentation loads correspond to large, long cracks in the material. The indentation strength response of the monolithic Si_3N_4 followed an indentation load$^{-1/3}$ dependence as expected for a material with no stabilizing resistance curve behavior (no R-curve). The strength of the material was strongly dependent on the indentation load, i.e. the size of the initial crack. The indentation-strength response of the Si_3N_4 matrix 14 vol % SiC fiber-reinforced composite material, however, showed a transition from flaw-sensitive to flaw-tolerant behavior. Indentation cracks produced at very low loads (5 - 50 N) in the composite material did not intersect and bridge the fibers prior to stressing or during stabilized growth (due to indentation residual field), and therefore, the strength was strongly dependent on the indentation load. However, indentation cracks produced at high loads in the composite material (100 - 300 N) intersect and bridge the fibers prior to stressing. These data show pronounced flaw tolerance, and the strength was independent of the indentation load. The indentation-strength response of the Si_3N_4 matrix 29 vol % SiC fiber-reinforced composite shows pronounced flaw tolerance over the entire range of indentations loads (5 - 300 N). The indentation cracks intersect and bridge the fibers prior to stressing at all indentation loads in these higher volume fraction (smaller fiber spacing) composites.

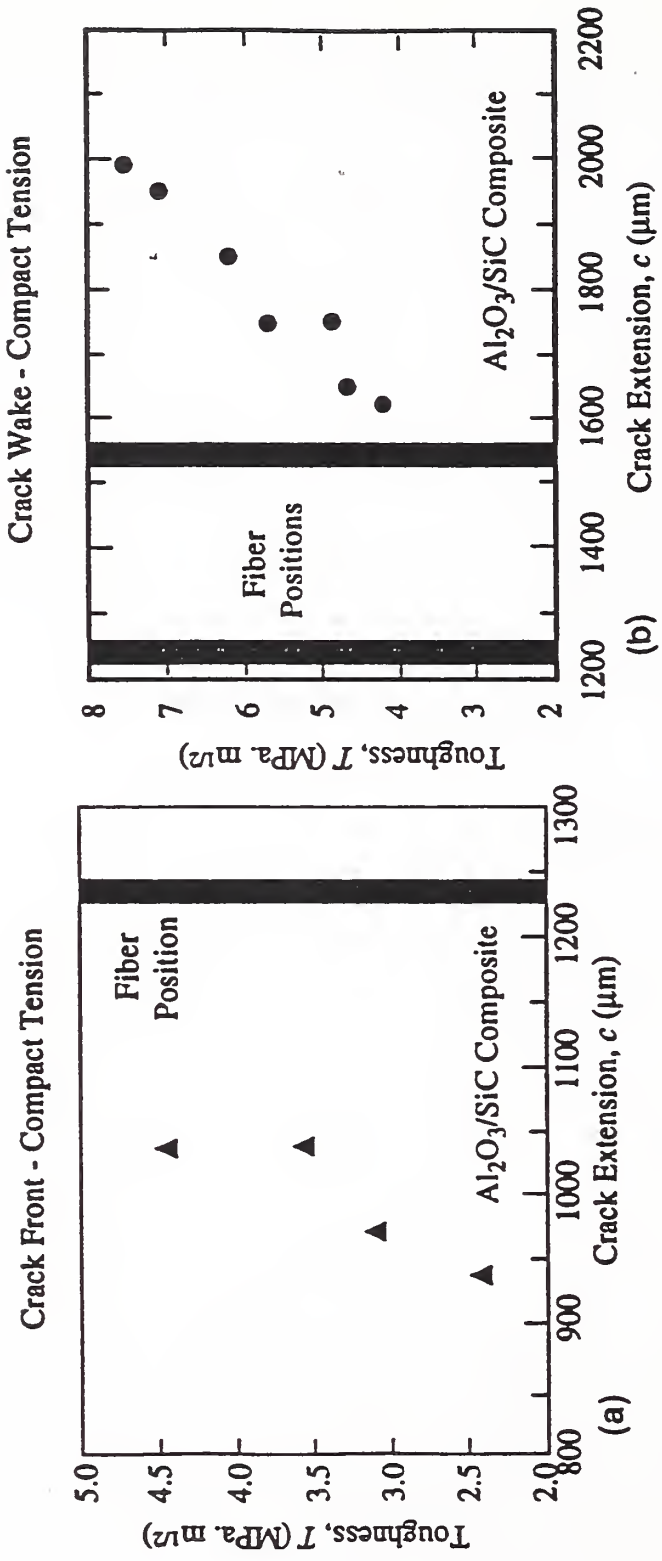

Figure IV-4. Measured fracture toughness of ceramic matrix composites as a function of crack/fiber position

(a) Crack front toughening
(b) Crack wake toughening

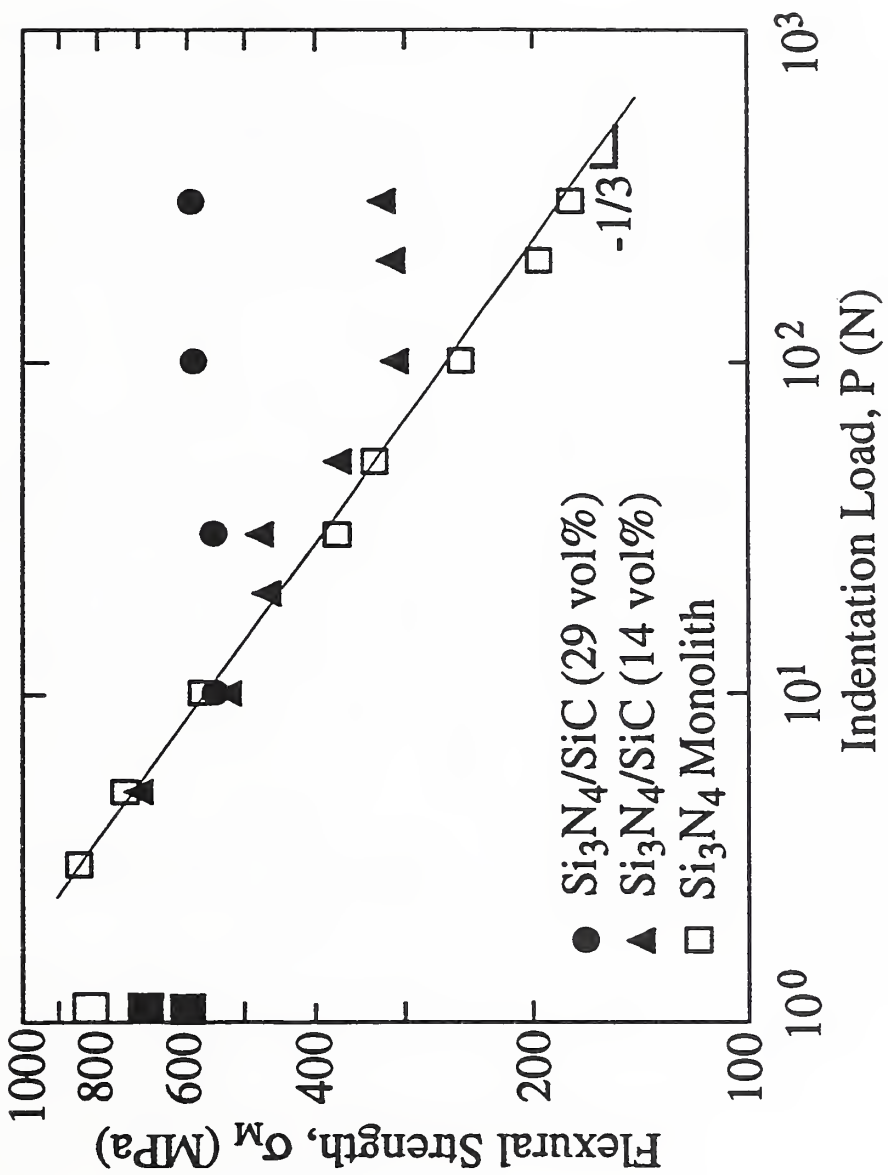

Figure IV-5. Indentation-strength behavior for monolithic Si_3N_4 and Si_3N_4/SiC composites.

Short-Crack Toughness-Curves and Flaw Tolerant Ceramics

L. M. Braun, B. R. Lawn[1], S. J. Bennison[2], and R. F. Cook[3]

[1] MSEL Scientist
[2]E.I. DuPont de Nemours & Co. Inc.
[3]IBM, T.J. Watson Research Center

Toughness-curves or resistance-curves (T-curves, K_R-curves, R-curves), which describe a functional dependence of toughness on crack size, are known to have a profound influence on the mechanical properties of ceramics. Traditional T-curve measurements are made with long cracks in notched specimens. However, some of the most important mechanical properties, notably strength and wear resistance, are determined in the domain of short cracks, i.e. cracks on a scale comparable with that of the microstructure. As intimated in measurements of crack extension from natural and controlled surface flaws in several ceramics, the critical short-crack region of interest lies below the lower limits of valid extrapolation from long-crack data.

A methodology was developed for evaluating short-crack toughness-curves (T-curves) of ceramics using indentation flaws. Two experimental routes were considered: (i) conventional measurement of inert strength as a function of indentation load; (ii) in situ measurement of crack size as a function of applied stress. Central to the procedure is a proper calibration of the indentation coefficients that determine the K-field of indentation cracks in combined residual-contact and applied-stress loading, using data on an appropriate base material with single-valued toughness. A key constraint in the coefficient evaluation is an observed satisfaction of the classical indentation strength-load$^{-1/3}$ relation for such materials, implying an essential geometrical similarity in the crack configurations at failure. T-curves for any ceramic material (similar to base material) without single-valued toughness can then be generated objectively from inert-strength or in situ crack-size data. Advantages of this procedure are 1) it provides an objective determination of the T-curve without reference to specific models of the underlying shielding mechanism or parametric evaluations using any presupposed analytical function, 2) T-curve behavior can be measured in the critical short-crack strength controlling region from a minimum number of specimens, and 3) crack-microstructure interactions fundamentally responsible for the T-curve can be directly observed during stressing to failure.

This procedure allows for investigation of the role of microstructure in the strength and toughness of structural ceramics. Experiments on materials with strong toughness-curves from grain-localized crack bridging (alumina-based materials), transformation toughening (Y-TZP), and fiber bridging/pullout (SiC fiber-reinforced ceramic matrix composites) demonstrate the versatility of this approach. The short-crack toughness curves due to these three different toughening mechanisms are currently being examined and compared.

Tests on a fine-grain alumina with single-valued toughness were used to calibrate the indentation coefficients. T-curves for coarse-grained aluminas and an alumina-matrix material with aluminum titanate second-phase particles were then generated from inert-strength and in situ crack-size data. The alumina-matrix material with aluminum titanate second-phase particles showed pronounced flaw tolerance and strong T-curve behavior. In situ observations of crack-

microstructure interactions in these two-phase materials revealed evidence for copious grain-interlock bridging at crack interfaces. The attendant crack stabilization from grain-bridging allowed the material to tolerate multiple damage accumulation during loading to failure.

Tensile Creep and Creep Rupture of Structural Ceramics

B. J. Hockey and S. M. Wiederhorn*

*MSEL Senior Scientist

Structural ceramics are generally recognized as viable materials for use in heat engines for transportation and power generation. In these applications, expected operating temperatures range from the ambient to over 1400 C. Currently, silicon nitride-based ceramics are regarded as prime candidates for these applications due to their excellent thermal shock and oxidation resistance in combination with high strength and fracture toughness at moderate temperatures. However, as successful application in heat engines requires service for extended periods under load at high temperatures, the evaluation of these materials ultimately depends on their creep and creep rupture behavior.

In this program, we are investigating the creep/creep rupture behavior of various grades of silicon nitride in collaboration with their industrial producers and users (Norton/TRW, Allied Signal, and Allison). The aim of this work is both to assist in the evaluation of current grades of this material and to help guide the development of improved grades for high temperature uses.

The program is divided into three tasks: (1) development of a tensile test configuration and methodology suitable for ceramics; (2) development and evaluation of a tensile creep and creep rupture data base; and, (3) microstructural and defect analyses by analytical transmission electron microscopy (AHEM) and other characterization techniques.

(1) Tensile Test Methodology

Current capabilities allow measurement of tensile strain rates of about $10^{-10}S^{-1}$ at temperatures up to 1500 °C; at 1400 °C, reliable creep data have been obtained for periods exceeding 4,000 hours. Work on this phase of the program is now directed toward test standardization. A draft standard for creep testing of ceramics is under consideration by ASTM Committee C 28. A commercial version of the equipment developed at NIST is available from Applied Test Systems.

(2) Creep and Creep Rupture Results

In a creep test, tensile strain is measured as a function of time over regions of stress and temperature appropriate to the material. These tests are generally continued until rupture occurs to determine creep lifetime under the imposed conditions. To date, creep and creep rupture data have been obtained for five different grades of silicon nitride. By specifying both the deformation and rupture behavior, the results have allowed preliminary lifetime predictions, which specify service life under combined stress and temperature conditions. Comparison of the results on this basis clearly establishes significant differences in high temperature behavior

and provides a useful criterion for material selection. Our results have also established that the tensile creep of these materials occurs in a transient manner, in that the strain rate continuously decreases with time; steady state creep is never realized. As a consequence, creep results obtained over different regions of stress and temperature can not be readily normalized to provide a global description for creep behavior. Therefore, as our database is augmented by results for still other materials, the development of a transient creep model will be emphasized.

(3) Microstructural Analysis

Examination of the various grades of silicon nitride by transmission electron microscopy has shown that extensive interfacial cavitation occurs during creep, indicating the importance of cavity nucleation and growth to both creep deformation and creep rupture. Moreover, two distinctly different types of cavitation are found to occur depending on microstructure. One type, which can be generally associated with superior creep/creep rupture behavior, results in discrete, ellipsoidal-shaped cavities by diffusive growth; creep rupture eventually occurs with the development of a critical density of such cavities. The other type, generally associated with inferior creep behavior, results in narrow crack-like cavities by either diffusive growth or, at higher temperatures, by a viscous "hole-growth" process; creep rupture results directly from the linking of these cavity cracks. This difference in cavity growth behavior can be related to observed differences in the thickness and composition of the interfacial glass phase present in these otherwise similar materials. Both of these microstructural parameters are known to determine interfacial ahem and transport; these properties, in turn, govern the rate of cavity growth by surface diffusion and, hence, cavity morphology. Currently, we are assessing the use of precision density measurement, small angle neutron scattering (SANS), and small angle X-ray scattering (SAXS) in determining accumulated cavity damage with creep strain (See Figure VII-3). This data is critical to the development of a predictive lifetime model under transient creep conditions.

Versailles Advanced Materials and Standards (VAMAS)

G. Quinn

The ceramics division is responsible for coordinating the activities of Technical Working Area (TWA) #3, Ceramics, in the Versailles Advanced Materials and Standards (VAMAS) project. VAMAS is an international collaboration to share prestandardization research. 1992 was an especially active year in TWA #3. A twenty-two nation round robin coordinated by NIST and the Japan Fine Ceramic Center on fracture toughness measurements was concluded and a comprehensive report prepared. Three test methods were used on two materials. Consistent results were obtained with the indentation strength and single-edged precracked beam methods, and important refinements to test technique and interpretation were made. This round robin is having a significant influence on the new initiative to standardize fracture toughness testing within ASTM.

In the meantime, a second round robin continued on high-temperature fracture toughness evaluation based on the single-edge precracked beam and chevron notch methods. A third round robin using the controlled surface flaw in bending method commenced in late 1992. The latter

project is a joint undertaking of NIST and EMPA, the Swiss Federal Laboratory for Materials Testing and Research. Twenty-two laboratories in Europe and the United States are participating.

VAMAS TWA #3 also cosponsored, with the European Standards Committee (CEN), a twenty five laboratory quantitative microscopy round robin. NIST coordinated the USA participation. Line and circle methods were used to determine mean linear intercept length for two aluminas and a computer generated microstructure. Grain size distribution and percent porosity were also measured using grid methods. The project was organized, performed, and analyzed (with a draft final report) in the remarkably short time of 6 months. The findings of the study show the influence of random sampling effects as opposed to variations due to specimen preparation and operator procedures. A draft European standard has been prepared based upon the methods used in the round robin, which themselves are based upon earlier ASTM standards prepared for metallic materials.

Fracture Toughness

A new initiative to standardize fracture toughness testing has commenced in ASTM committees C 28, Advanced Ceramics, and E 24, Fracture Testing (see schematic in Figure IV-6). The Ceramics Division is contributing to this effort by coordinating two VAMAS round robin projects. Refinements to the indentation strength and single-edge precracked beam methods have resulted from one round robin. Intensive work has focussed on the controlled surface flaw method in which an artificial flaw is created in a flexure specimen by a Knoop microhardness indentation. The residual stress and damage zones are removed by polishing and the specimen is fractured in flexure. Fractography is performed to measure the crack size at fracture and toughness is computed from the appropriate equations for semielliptical surface flaws in bending. Techniques have been devised to make the precracks more readily detectible and measurable on the fracture surface. A round robin exercise is underway.

Hardness

Hardness, one of the most commonly measured characteristics of advanced ceramics, is prone to high scatter and uncertainty. These problems were highlighted in a twenty laboratory, VAMAS international round robin conducted by the National Physical Laboratory in the United Kingdom in 1988. Errors of as much as 10-15% (and sometimes more) were reported for Vickers and Knoop tests. The VAMAS study has prompted the Ceramics Division, NIST, to develop a hardness standard reference material (SRM). Certified hardness blocks that are commercially available are hardened metals with HK or HV hardness numbers in the range of 500-700. A ceramic SRM with a known and certified hardness numbers in the range of 1500-2000 will enable users to refine their measurement techniques and will contribute significantly to improved accuracy and precision in ceramic hardness measurements. This work ultimately will contribute to a hardness standard for advanced ceramics.

Figure IV-6. Schematic of various test configurations involved in fracture toughness round robin.

Fractography

Mechanical testing to evaluate strength presents only a partial characteri zation of structural ceramics. Fractography is essential in order to identify the strength limiting flaws. It is especially important to determine whether flaws are surface or volume distributed, and whether more than one flaw population is active. Design data generated in the laboratory which represents one flaw type, may not be pertinent to component performance whereby alternative flaws are active. Fractography can resolve many of these issues, but has been heretofore very subjective and often incomplete. The Ceramics Division collaborated with the U.S. Army Materials Technology Laboratory in creating a new handbook: "Fractography and Characterization of Fracture Origins in Advanced Structural Ceramics." This document will serve many users, including beginners, mechanical testers, materials scientists, designers, and data base organizers. It is in essence a standard for fractographic analysis of strength limiting flaws in structural ceramics.

Modeling Fracture of Advanced Ceramic Materials

Hongda Cai[1], Tze-Jer Chuang, Edwin R. Fuller, Jr., Narayanaswamy Sridhar[2], and David J. Srolovitz[2]

[1]Guest Scientist, Lehigh University
[2]The University of Michigan

Ceramic materials can have significant positive impact on innumerable heat-resisting applications where higher operating temperatures equate to more energy-efficient operation. Brittleness, however, is a major concern in designing with these materials. A general stratagem has been to improve the fracture toughness, and indeed, much progress has been achieved in the last few years in developing ceramic microstructures, including ceramic composite systems, which lead to improved fracture resistance.

Understanding the mechanisms that influence fracture resistance of ceramics is typically formulated in terms of idealized micro-mechanics models. Statistical aspects of these mechanisms, related to the stochastic nature of a ceramic microstructure, are rarely considered. such considerations are crucial to the development of new improved materials and to structural design with these materials. Knowledge about these stochastic aspects is most readily attained from statistically generated microstructures and micro-mechanical descriptions of the toughening mechanisms, thereby relating grain-boundary properties and their distributions to processing variables and structural performance. Mimicking physical phenomena with simplistic algorithms, these simulations will explore the stochastic influence of complex microstructural phenomena, such as thermal-expansion-anisotropy, microcracking, crack deflection and crack bridging, on strength and fracture toughness.

The research involves the development of micro-mechanics models and the use of these models in computer simulation studies to elucidate the influence of various microstructural aspects on strength and fracture toughness behavior of advanced ceramic materials. The models are based upon a spring-network approach in which simple springs are interconnected at nodes to form an

network. The spring elements can have either linear-elastic properties to model elastic effects, or other constitutive properties to model various micromechanical processes (e.g., the frictional pull-out of a microstructural "reinforcement"). Similar spring-network models, except for the "microstructural" constitutive elements, have been successfully used to simulate fracture at the atomistic level.

Polycrystalline aspects of the ceramic microstructure are introduced into the spring network models by "overlaying" a random, "digitized" ceramic microstructure on the spring network. Accordingly, different spring elements with different constitutive properties and breaking strengths are used to represent various microstructural features, e.g., transgranular versus and intergranular properties. Thermal-expansion-anisotropy (TEA) effects are introduced into the models by using springs of different initial lengths. Such effects can also be correlated with digitized microstructures of actual advanced ceramics. Microcracking is simulated by discrete spring failures, as influenced by breaking strength distributions and TEA effects. Crack bridging is simulated by surviving springs, or clusters of springs, in the wake of the crack tip.

Two random-microstructure, spring-network models have been developed: (1) A two-dimensional model in which a "straight-through," but non-planar crack propagates through a random, two-dimensional microstructure with TEA-induced strains to elucidate the influence of residual thermal stresses and interface properties on microcracking and crack propagation behavior; and (2) A quasi-three-dimensional model in which a planar crack interacts with a random microstructure in the third dimension (the crack front is not constrained to remain straight) to elucidate bridge-formation processes in the crack wake and their influence on the fracture toughness. The models have been formulated, initial computer codes have been written, and several simulations have been performed.

Non-Planar, Two-Dimensional Fracture Model

This model, developed in collaboration with N. Sridhar and Professor David Srolovitz at the University of Michigan, simulates TEA-induced microcracking and TEA-influenced crack propagation in a microstructural simulation of a polycrystalline advanced ceramic. It consists of a two dimensional, triangular network of springs upon which a polycrystalline microstructure is mapped. The energy of each spring (or bond) has both a bond-stretching and a bond-bending component. The total energy of the system is a sum over all the bonds.

The simulation is periodic in a direction parallel to the tensile axis and has free surfaces in the transverse directions. It thus simulates a sample with an effectively infinite gage length. The network is stressed by applying a fixed strain over the gage length and relaxing the node positions with a double-precision conjugate gradient algorithm to minimize the total energy. Bond rupture is affected via a critical bond-strain-energy criterion, and thus mimics a critical strain-energy-release-rate or fracture surface energy criterion for failure. (Bulk and grain-boundary bonds are assumed to have different critical strain energies.) When a bond fractures, the system is re-equilibrated at the existing applied strain, and additional bonds are allowed to fracture, if required, before applying a further strain increment.

Thermal expansion anisotropy effects are introduced into the simulation by randomly selecting

Thermal expansion anisotropy effects are introduced into the simulation by randomly selecting a high-expansion direction in each grain and initially contracting the network spring in this direction. This contraction was applied gradually, testing for localized fracture (microcracks) at each (misfit) strain step. Initial studies have examined the influence of the size of this misfit strain, the grain size and Poisson's ratio on microcrack density.

Planar, Three-Dimensional Crack-Front Model

This model simulates a planar crack propagating in a "quasi-three-dimensional" polycrystalline ceramic microstructure. The (planar) crack front is able to meander through the microstructure as local stresses and fracture criteria dictate, thereby developing a three-dimensional crack front. The model consists of two two-dimensional rectangular networks of springs which are jointed across the fracture plane by a network of cohesive springs. A planar crack is initially introduced into the fracture plane by "cutting" the appropriate cohesive bonds. Stress are applied normal to the fracture plane, and as before the node positions are relaxed via a conjugate gradient algorithm to minimize the total energy. Bond fracture, which give rise to crack advance, is determined by a critical cohesive bond-strain.

Thus far, this model has been formulated algebraically and initial computer code has been developed. No polycrystalline microstructure has yet been superposed on the simulation, but rather each cohesive bond has been assumed to represent a grain boundary. Accordingly, the cohesive strength of each bond represents a grain-boundary strength, which is then selected from a equal-probability distribution. Initial studies for this simulation have examined the fracture resistance as a function of crack length (i.e., R-curves behavior) for different dispersion in the distribution of grain-boundary strengths.

Crack Bridging by Inclined Fibers/Whiskers in Ceramic Composites

Hongda Cai[1], Elizabeth P. Butler[1], K. T. Faber[2], and Edwin R. Fuller, Jr.

[1]Guest Scientist, Lehigh University
[2]Northwestern University

Significant increases in the fracture toughness of brittle ceramics can be achieved by incorporating whiskers or fibers into a ceramic matrix. In studies of whisker-reinforced ceramic composites, crack bridging has been identified as a major toughening mechanism. Studies of large-grain polycrystalline alumina have shown a similar toughening mechanism, i.e., crack bridging by grains. Even though these studies have analyzed the micro-mechanics of crack bridging, either the reinforcements are assumed to be perpendicular to the crack plane or else a simplistic relation is used between the bridging force and inclination angle. These assumptions are made due to the lack of information regarding the dependence of the bridging force on the whisker inclination angle. Alternatively, inclined whiskers are neglected because they are considered to fail by bending and therefore result in negligible toughening. In reality, reinforcing whiskers can be of any orientation with respect to the crack plane. In fact, a majority of whiskers are not perpendicular to the crack plane. A more realistic model should consider whiskers of all orientations. Indeed, recent in-situ observations for a SiC-whisker

reinforced alumina have indicated the importance of inclined whiskers to the bridging process.

In the present work, we examine the influence of fiber inclination angle on reinforcement bridging by studying fiber bridging of a crack under conditions which closely simulates those in an actual composite. The double cleavage drilled compression (DCDC) fracture mechanics specimen was used for this purpose. We have previously used the DCDC specimen to study crack interactions with aligned fibers and to quantify the toughening effect of aligned fibers which had ductile interfacial layers. In the present studies SiC fibers were placed in the path of the DCDC crack at inclination angles that varied from normal to 40° off normal. The bridging toughness from these fibers was quantified in terms of the change in the applied stress intensity from that of the base toughness of the matrix.

For a quantitative analysis of the bridging relation, the key information is in the relation between the bridging force and the crack opening displacement. The crack opening displacement was measured directly using a displacement gauge. The bridging force must be extracted from the measured change in the stress intensity. For an inclined fiber bridging a crack, the bridging force consists of a component perpendicular to the crack plane and another component parallel to the crack plane. The present treatment neglects the second component because we are primarily concerned with mode I loading. With this simplification, the bridging action of a fiber behind the crack tip is approximated by self-equilibrated traction forces acting at a bridging distance behind the crack tip. For bridging forces very close to the crack tip (small bridging distance) the near crack-tip solution can be used. However, for general values of the bridging distance, the crack bridging relation in the DCDC specimen is not available. A finite element analysis was used to obtain this relationship. In this analysis, the change in the stress intensity was computed as a function of the bridging force, the crack length, and the bridging distance.

Results of this analysis for experiments on a model composite system of SiC fibers and a borosilicate glass matrix show that the bridging force decreases with increasing fiber inclination angle in the range of crack opening displacement observed. This finding is in qualitative agreement with a theoretical analysis of Leung and Li which showed that the total crack bridging force consists of contributions due to: 1) the bending force on the inclined fiber and 2) the resistance to fiber pullout. The contribution from fiber bending increases with fiber inclination angle initially but decreases at higher angle. Localized matrix cracking relaxes the more heavily stressed fibers and thus reduce the difference between fibers lying at different angles. The contribution from the resistance to fiber pullout in the direction normal to the crack plane decreases with inclination angle.
However, there were still strong contributions to the bridging force from inclined fibers at angles up to 40° and fiber failure due to bending was not significant. For example, crack bridging by fibers inclined by 40° is sustained more than 6 mm behind the crack tip (or more than 40 times the fiber diameter). Further crack propagation and larger COD's would be required for fiber fracture. In actual whisker-reinforced materials, the majority of the whiskers are inclined with respect to the crack plane. Therefore, in the near tip wake region where the COD's are small, bridging by inclined whiskers is expected to make up the main portion of toughening. If the present results can be extended to whisker-reinforced ceramic composites, toughening predictions based on aligned whiskers would represent overestimates. In addition, the dependence of bridging force on the whisker inclination angle and crack opening displacement also has a

profound effect on the shape of the crack resistance of the composite. Compared with predictions for composites with aligned whiskers, the crack resistance curve would be flatter if the bridging force at a given COD is reduced as a result of whisker inclination.

Comparison of matrix cracking between smaller and large fiber inclination angles shows that localized matrix cracking is related to fiber inclination. We observed that larger fiber inclination angles result in a greater degree of matrix cracking. Matrix cracking reduces the severity of fiber bending and has the benefit of delaying fiber breakage. Accordingly, the fiber can maintain its integrity for a greater distance behind the crack tip as a result of matrix cracking. At the same, matrix cracking modifies the force-displacement relation. Matrix spalling has also been reported recently by Hillig, who observed progressive matrix spalling at an inclined fiber as the crack was opened.

Machining of Advanced Ceramics

S. Jahanmir, T. Strakna*, H. Liang*, G. Zhang*, S. Jain*

*Guest Scientist, University of Maryland

A comprehensive survey of industry has confirmed that high cost of machining is a primary impediment to the widespread utilization of advanced ceramics. The goal of the ceramic machining program is to provide measurement methods, data, and mechanistic information needed by industry to develop innovative cost-effective methods for machining of advanced structural ceramics. Research projects are carried out jointly with industry, academic institutions, and the Precision Machining Research Facility of NIST under the auspices of Ceramic Machining Consortium. Currently, the Ceramic Machining Consortium has seventeen members. Current projects include: 1) Grinding Optimization for Advanced Ceramics, 2) Characterization of Machining Damage, 3) Nano-precision Grinding of Silicon Nitride Bearing Materials, 4) Chemo-mechanical Effects in Drilling and Grinding of Ceramics, and 5) Polishing of Silicon Carbide Ceramics. Consortium members participate in these projects by providing materials, testing, advice, and other in-kind contributions. Highlights of these projects are described below.

The primary goal of the Grinding Optimization Project is to develop a database for machining of advanced ceramics. It is planned to collect data on the effect of grinding parameters on properties and performance of advanced ceramics. Data will be collected from joint research with several industrial companies who are members of the Ceramic Machining Consortium; some data will also be collected from the published literature. In the first phase of this project, the participating members were asked to use their experience in selecting the grinding conditions. Each participant machined one set of flexure test bars, which were then tested and characterized at NIST for surface integrity and fracture strength. The results for a reaction bonded silicon nitride (RBSN) and a sintered reaction bonded silicon nitride (SRBSN) are shown in Figure IV-7. It is clear that the characteristic strength is unaffected by the volumetric material removal rate. It was, however, found that some grinding conditions, particularly those with a larger grit wheel, resulted in a higher surface roughness. Nevertheless, the results suggest that it is possible to increase the removal rate by a factor of 30. This will undoubtedly

lower the cost of machining for ceramic components. In phase two a statistical experimental design will be employed to analyze the effect of various grinding parameters. The aim of this study is to achieve high removal rates while maintaining an acceptable level of surface roughness and strength. It is also planned to use fractography to identify the fracture initiation sites, and identify possible material removal mechanisms as a function of grinding parameters.

The objective of the second project is to compare various techniques for detection and evaluation of machining damage. Taper-sectioning has been used for this purpose, and plans are in place for damage detection by ultrasonic techniques, acoustic microscopy, thermal wave analysis and x-ray residual stress measurements. The results of taper-sectioning and fractography on the fractured samples tested in Project No. 1 have been complementary in showing no machining damage under the various grinding conditions used in the first phase of this project. It is planned to analyze these test bars by ultrasonic and thermal wave techniques.

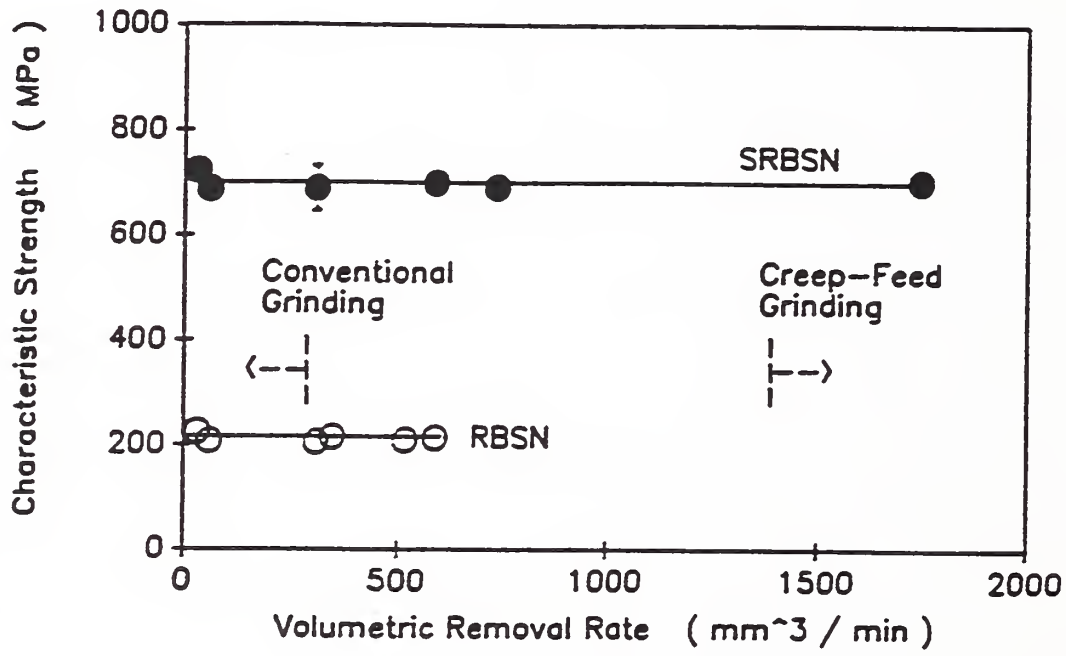

Figure IV-7. Effect of volumetric material removal rate during grinding on characteristic strength of two types of silicon nitride ceramics. The figure clearly shows that it is possible to increase the removal rate by a factor of 30 over conventional grinding practice.

The goal of the third project is to elucidate the chemo-mechanical interactions during machining in order to increase the machining rate through proper use of additives in cutting fluids. Recent results obtained in core-drilling of alumina with diamond-impregnated tools have shown that certain chemical compounds are effective in increasing the drilling rate, as shown in Figure IV-8. Two commercial cutting fluids were compared with the compounds tested in drilling. The results indicated that although one of the commercial fluids increased the drilling rate over that observed with water, the percent increase was not as large as the rates obtained with compounds A and F. A patent disclosure has been submitted, and the most promising compounds will be

evaluated by the consortium members in grinding. Analysis of the machined surface and the diamond particles indicated that removal of material from alumina occurs by a brittle fracture process, and the wear of the diamond particles take place by a micro-fracture process within each particle. It is believed that the compounds tested adsorb on the diamond surface and reduce the coefficient of friction and the rate of heat generation during machining. The diamonds will then remain sharp for a longer period of time, thereby increasing the machining rate. The details of this process is presently under investigation.

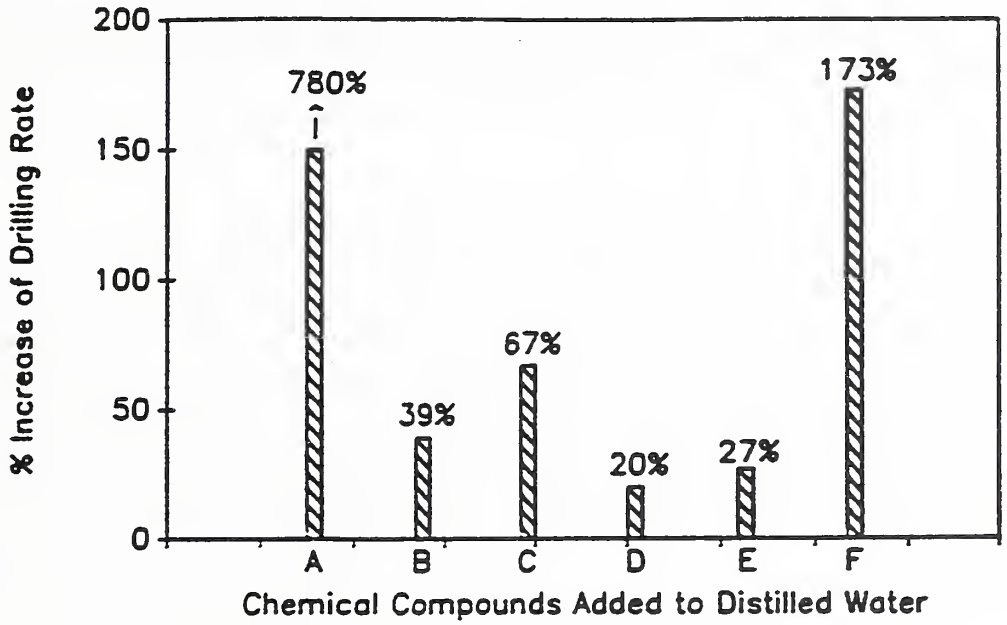

Figure IV-8. The effect of several chemical compounds on the drilling rate of alumina is shown in the figure. Two compounds show a dramatic effect on the drilling rate. These compounds increase the drilling rate several folds over the rate achieved in distilled water.

In the fourth project, ultra-precision (or ductile regime) grinding is used to finish-grind silicon nitride bearing materials. This project is conducted jointly with Chris Evans in the Precision Machining Research Facility. The results have been very positive. A surface roughness of one nanometer has been obtained on a HIPed silicon nitride bearing material. In the next phase of this project, fracture strength and rolling contact fatigue of silicon nitride machined by this technique will be determined. It is, also, planned to analyzed the mechanism of material removal and identify the parameters that control the transition from a conventional removal process to the ductile regime mode. The effect of microstructure on material removal process and the "machinability" of several high strength silicon nitrides will be determined.

The goal of the polishing project is to develop an understanding and the technology for polishing of silicon carbide ceramics. Particular interest is in polishing of two-phase materials such as reaction bonded silicon carbide. Multi-phase materials are difficult to polish because of the differences in mechanical properties of the different phases. Polishing parameters such as

diamond particle size, type of polishing cloth, rotational speed, and applied load must be selected properly to avoid fracture in the most brittle phase.

VAMAS Wear Test Methods

S. Jahanmir

The objectives of the Wear Test Methods Technical Working Area of VAMAS are improvements in the reproducibility and comparability of wear test methods, and characterization of the wear behavior of advanced materials. Two previous round robin interlaboratory comparisons have resulted in several publications and standard test methods adopted by ASTM and DIN. Under NIST leadership, four projects are currently underway: 1) Standard format for organizing and reporting wear data, 2) Interlaboratory wear volume measurement comparison, 3) Compilation of standard wear test methods, and 4) Interlaboratory wear testing of Inorganic coatings.

The goal of project No. 1 (coordinated by A. W. Ruff, NIST) is to define a uniform format for organizing and reporting wear data with application to computerized databases. This project is very important and timely, because of recent interests in using computer databases for storing materials property data and searching the databases to retrieve data for research, design and material selection. There are large differences between the databases being used by different people in the U. S. and also in other countries. If a uniform format is developed, then it will be much easier to exchange data among organizations interested in the same type of data. In fact, recent international efforts on data exchange (PDES) is an excellent example of the need for a standardized database format. Other benefits of the proposed project include agreements on important variables and units, as well as methods for reporting data precision. At the completion of this project a VAMAS report will be issued, which will contain recommendations for a uniform format for reporting of wear data. A preliminary format was prepared at NIST and was sent to the participating laboratories for evaluation and comments. The format was revised base on the comments received and has been mailed to participants for a second evaluation. This project is coordinated with a similar activity in progress by the G-2 Committee of ASTM.

The goal of project No. 2 (coordinated by M. Gee, NPL) is to evaluate and compare different methods used for wear volume measurement. Two sets of specimens worn under different conditions will be prepared by the lead laboratory to produce a range of wear volumes. These specimens will be circulated among the participating laboratories with instructions for wear volume measurements by two or three different techniques, for example, weight loss measurement, surface profiling by stylus method, optical microscopy measurement, and other unique methods that may be available in the participating laboratories. Presently, the samples are being prepared, and the detail plans and instructions are being drafted. A total of 24 laboratories have expressed interest in participating in this project.

The purpose of project No. 3 (coordinated by P. J. Blau, ORNL) is to compile and publish a report containing a listing of standard wear test methods in countries participating in VAMAS. A questionnaire was prepared and distributed to the participating laboratories. Over 325 friction

and wear testing standards, guidelines, and practices were received and compiled. More than 12 standard producing organizations are represented in the compiled standards. The information has been analyzed and a first draft of a VAMAS report has been prepared.

The goal of project No. 4 (coordinated by E. Santner, BAM) is to obtain information on reproducibility of test results for the preparation of an internationally agreed test methodology for wear and friction of inorganic coatings. This project is currently in the planning stage. A pin on disk geometry, similar to the previous round robin exercise, will be used. The tests will be conducted with bearing steel balls sliding against silicon nitride disks. TiN has been tentatively selected as the coating material. The coatings will be characterized before testing, and the samples will be distributed to the participating laboratories. The test conditions, i. e., load, speed, duration of sliding, etc., will be similar to those used in the first two interlaboratory tests.

Glass Science and Technology

D. C. Cranmer, D. A. Kauffman, and D. H. Blackburn[1]

[1]Consultant

NIST has been involved in glass science and technology since 1910, including the large-scale production of glasses for lenses and mirrors during World War II. The primary efforts at the present time are focussed on the formulation and preparation of special glasses which are used as standards or as model materials on which other research programs are carried out. The following represents a listing of on-going projects being carried out collaboratively by this group.

- Laser-induced gratings in glass: Oklahoma State University
- Thermal neutron shielding glass: NIST-CSTL
- Microanalytical standards: NIST-CSTL/OSRM
- X-ray fluorescence spectrometry: NIST-CSTL/OSRM
- Nuclear track detectors: NIST-CSTL
- UV transmitting Faraday rotators: Naval Research Laboratory
- Refractive index standards for asbestos identification: NIST/CSTL
- Dental restorative materials: NIST-MSEL, ADA
- Radiation dosimeter: NIST-CSTL
- UV fluorescence standards: NIST-PL

and wear testing standards, guidelines, and practices were received and compiled. More than 12 standard producing organizations are represented in the compiled standards. The information has been analyzed and a first draft of a VAMAS report has been prepared.

The goal of project No. 4 (coordinated by E. Santner, BAM) is to obtain information on reproducibility of test results for the preparation of an internationally agreed test methodology for wear and friction of inorganic coatings. This project is currently in the planning stage. A pin on disk geometry, similar to the previous round robin exercise, will be used. The tests will be conducted with bearing steel balls sliding against silicon nitride disks. TiN has been tentatively selected as the coating material. The coatings will be characterized before testing, and the samples will be distributed to the participating laboratories. The test conditions, i. e., load, speed, duration of sliding, etc., will be similar to those used in the first two interlaboratory tests.

Glass Science and Technology

D. C. Cranmer, D. A. Kauffman, and D. H. Blackburn[1]

[1]Consultant

NIST has been involved in glass science and technology since 1910, including the large-scale production of glasses for lenses and mirrors during World War II. The primary efforts at the present time are focussed on the formulation and preparation of special glasses which are used as standards or as model materials on which other research programs are carried out. The following represents a listing of on-going projects being carried out collaboratively by this group.

- Laser-induced gratings in glass: Oklahoma State University
- Thermal neutron shielding glass: NIST-CSTL
- Microanalytical standards: NIST-CSTL/OSRM
- X-ray fluorescence spectrometry: NIST-CSTL/OSRM
- Nuclear track detectors: NIST-CSTL
- UV transmitting Faraday rotators: Naval Research Laboratory
- Refractive index standards for asbestos identification: NIST/CSTL
- Dental restorative materials: NIST-MSEL, ADA
- Radiation dosimeter: NIST-CSTL
- UV fluorescence standards: NIST-PL

V. ELECTRONIC MATERIALS

Grady White

Increasing demands upon electronic components, both of sophistication and reliability, place concomitant demands upon our basic understanding of electronic ceramics and upon our ability to measure critical properties. In response to these needs, the Electronics Materials Group provides information on basic properties and measurement procedures to the ceramics community.

For example, the Ceramics Division has a history of developing phase equilibria which, in the past year, has focussed on high temperature superconductors and high dielectric microwave materials. In the high T_c area a need exists for phase diagrams describing all of the major ceramic systems of interest. Similarly, for microwave applications, there is a need for phase diagrams which might serve to predict new compositions which will have a temperature independent, high dielectric constant. Ongoing work continues in these areas, in collaboration with both other NIST scientists as well as with personnel in industry who are developing manufacturing processes for such materials.

The second thrust of the Electronic Materials Group is the development of measurement techniques to determine critical materials properties. The Group has a background in measuring traditional bulk mechanical, thermal, and dielectric properties. These capabilities are being extended to include measurements of effects of cyclic loading, interactions between electric field and mechanical loads, thermal properties of films, and thermoelectric power (Seebeck) coefficients. In addition, the ability to measure grain texture, i.e., the degree of grain orientation, has been achieved for both bulk and film geometries. Finally, the capability to measure residual stresses quantifiably over distances of a few micrometers is being developed. While these capabilities are valuable for a wide range of applications and materials, they have been acquired specifically to evaluate ferroelectric actuator materials, which undergo cyclic strains and large electric fields, ferroelectric films, whose properties (electronic or optical) can be enhanced by appropriate texturing of the grains, and ceramics for thermoelectric power applications, whose efficiencies depend upon both thermal and electrical conductivities. Finally, stress measuring capabilities are being developed because residual stresses between films and substrate, ceramic and electrode, or at ceramic/ceramic interfaces are known to have a major impact upon lifetime and reliability of ceramic components.

Finally, the Electronic Materials Group is expanding capabilities in modeling, at both the atomic and microstructural level. First principles calculations are being used to predict phase diagrams in ferroelectric oxide systems. Such predictions could result in a major reduction in effort and time required to produce phase diagrams, and could lead the way to higher undiscovered compounds. Molecular orbital calculations are being used to evaluate how environments interact with strained ceramic bonds; this effort could result in the ability to predict how a particular ceramic composition will survive under load in all environments. Finally, surface energy models relating grain growth and faceting to the presence and composition of glassy phases at grain boundaries should have an important impact on the development of processing techniques to design particular textures into ceramic components.

Significant Accomplishments

- A self consistent topological sequence (equilibrium progression of phases with temperature) of reaction equilibria has been determined between the minimum melting temperature of the $BaO\text{-}1/2Y_2O_3\text{-}CuO$ system to the melting of the green phase in air. These results also lead to a quantitative liquidus diagram around the $Ba_2YCu_3O_{6+x}$ region.

- A compilation of the powder x-ray diffraction patterns of the high T_c superconductor and related phases including potential container reaction products and cation substituted products in the systems of Ba-R-Cu-O, Sr-R-Cu-O and Ca-R-Cu-O, where R=yttrium and lanthanides, has been made. A cross correlation of these phases with those reported in Phase Diagrams for Ceramists (PDFC) has also been successfully completed.

- It has been determined that when more than about 5 wt% Zn is added to $BaTi_4O_9$, a common microwave dielectric, the high temperature form of $BaZn_2Ti_4O_{11}$ forms as a second phase. As $BaZn_2Ti_4O_{11}$ has a positive temperature coefficient of the dielectric constant, whereas $BaTi_4O_9$ has a negative temperature coefficient, a mixture of the two can result in a zero temperature coefficient of the dielectric constant, which is essential for microwave dielectric applications.

- Molecular orbital calculations simulating environmental reactions at crack tips have shown that a major effect of crack tip strain is the reduction of steric hindrances which would inhibit access of the environmental molecules to the crack tip bonds. Silicon, in particular, appears to require very large strains at the crack tip to remove steric hindrance. These results could explain the observed lack of environmentally enhanced crack growth in silicon.

- An SN (strength vs number of cycles) curve has been obtained in PZT specimens cycled mechanically at room temperature. Discrepancy between the experimental data and a theoretical fit to the curve suggests that true cyclic fatigue processes are occurring simultaneously with environmentally enhanced fracture to cause mechanical failure. These results indicate that lifetime models for PZT cannot assume traditional slow crack growth as the only failure mechanism.

- Micro-focus Raman measurements have been made on alumina specimens as a function of stress in a diamond anvil cell. The results provide a calibration mechanism for measuring residual stresses on a local scale.

- Theoretical and experimental results have been obtained which explain facetting and wetting behavior of polycrystalline grain in contact with a glassy grain boundary. These results can be used to predict whether adjacent grains will grow together or be separated by a glassy phase.

- Alumina fiber growth experiments using flux melting/directed solidification has achieved aspect ratios of 50:1. In related work, alumina tapes seeded with oriented grains achieved a 90% orientation of the final fired material. These results have important implications in the manufacture of grain-oriented ceramics.

- Strong (001) or (111) texturing has been achieved in $BaTiO_3$ formed by laser ablation on Pt coated Si substrates. The texturing was obtained for large laser fluences and the choice of (001) or (111) appeared to depend upon the degree of (111) texture of the substrate. Texturing of ferroelectric films could lead to less residual stress in the film during poling and, perhaps, to a lower aging rate.

- Transparent γ-alumina has been prepared from nanosized powder. The first values of strength and of fracture toughness in γ-alumina have been obtained.

PHASE DIAGRAMS

NIST has long been recognized for providing reliable phase diagrams to the ceramics community. This year, experimental efforts on formulating phase diagrams have focussed on high T_c and high dielectric materials. In addition, we have begun developing the capability to calculate phase diagrams from first principles. These calculations are in their initial stages and, presently, are aimed at ferroelectric materials. Finally, we continue to investigate effects of high pressure on phase transformations and phase stability in ceramics formed from nano-sized powders, using γ-alumina as a model system.

Phase Equilibria and Crystal Chemistry in Ceramic Systems

C. J. Rawn, C. G. Lindsay[1], and R. S. Roth[2]

[1]Postdoctoral
[2]Guest Scientist

Experimental investigation of phase equilibria and solid state chemistry of oxide ceramics focused this year on three systems. The quaternary system $\frac{1}{2}Bi_2O_3$:SrO:CaO:CuO (BSCCO) contains at least three high-temperature superconducting phases; during 1992, two of the bounding ternary systems were examined in detail, and work continued on one of the bounding binary systems. Studies of two systems containing microwave dielectric materials, BaO:ZnO:TiO_2 and $\frac{1}{2}La_2O_3$:$\frac{1}{2}Al_2O_3$:$\frac{1}{2}Nb_2O_5$:TiO_2, were also conducted.

Studies of the $\frac{1}{2}Bi_2O_3$:SrO:CaO:CuO system have yielded structure determinations, by x-ray and neutron diffraction, of $CaBi_2O_4$ and $Ca_6Bi_6O_{15}$ (the latter in collaboration with J.B. Parise, State University of New York at Stony Brook, and C.C. Torardi, E.I. DuPont de Nemours), and phase relations in the ternary systems CaO:$\frac{1}{2}Bi_2O_3$:CuO and SrO:CaO:$\frac{1}{2}Bi_2O_3$. Results of x-ray diffraction analysis indicated non-stoichiometry in $CaBi_2O_4$, consistent with the results of earlier phase equilibria studies, so that the formula is better written $Ca_{1-x}Bi_{2+y}O_4$. In $Ca_6Bi_6O_{15}$, Bi is in an unusual three-fold coordination as in $Ca_4Bi_6O_{13}$, and in fact these two compounds are structurally similar. The system CaO:$\frac{1}{2}Bi_2O_3$:CuO was found to contain no ternary phases that form in air between 700°C and 950°C. These studies also gave corrected stoichiometries for two previously reported binary compounds: "$Ca_7Bi_{10}O_{20}$" is actually $Ca_4Bi_6O_{13}$ and "$Ca_7Bi_6O_{16}$" is actually $Ca_2Bi_2O_5$. In the system SrO:CaO:$\frac{1}{2}Bi_2O_3$, a new ternary phase has been identified in addition to the high- and low-temperature phases with Sr:Ca:Bi = 49.5:16.5:34.0 identified last year. This new phase is a solid solution described tentatively by the formula $Sr_{6-x}Ca_{6+x}Bi_{14}O_{33}$, $0 \leq x \leq 3$ (approximate limits). A detailed crystal structure study of this phase is in progress. These results will aid in identification of stability limits and secondary phases in syntheses of BSCCO-type high-temperature superconducting materials, particularly as our program embarks on the study of the five-component $\frac{1}{2}Bi_2O_3$:PbO:SrO:CaO:CuO system during 1993.

In the BaO:ZnO:TiO_2 system, ternary phases have been identified having ideal formulas $BaZn_2Ti_4O_{11}$, $Ba_4ZnTi_{11}O_{27}$, $Ba_2ZnTi_5O_{13}$, and $Ba_xZn_xTi_{8-x}O_{16}$. The first of these, earlier

reported with the formula $Ba_3Zn_7Ti_{12}O_{34}$, exists as two phases, one high- and one low-temperature form. The high-temperature form occurs as a second phase when more than about 5 wt% Zn is added to $BaTi_4O_9$, a commonly-used microwave dielectric material. As $BaZn_2Ti_4O_{11}$ has a positive temperature coefficient of the dielectric constant whereas $BaTi_4O_9$ has a negative temperature coefficient, the presence of $BaZn_2Ti_4O_{11}$ with $BaTi_4O_9$ can result in the desired zero temperature coefficient of the dielectric constant. A crystal structure determination showed that Zn occupies some tetrahedral interstices as well as octahedral interstices in the anion network. Considering that Mg is divalent like Zn and that the two cations form bonds to O of about the same length, it would seem that Mg could also be used to form a phase isostructural with $BaZn_2Ti_4O_{11}$. However, it turns out that Mg occupies none of the tetrahedral interstices in the structure, hence hollandite-structure $Ba_xMg_xTi_{8-x}O_{16}$ forms instead of $BaMg_2Ti_4O_{11}$. Like its Zn counterpart, this material has a high dielectric loss and is useless as a microwave dielectric. All attempts to grow single crystals of the low-temperature form of $BaZn_2Ti_4O_{11}$ have been unsuccessful, so its crystal structure has not yet been determined.

In the $\frac{1}{2}La_2O_3$:$\frac{1}{2}Al_2O_3$:$\frac{1}{2}Nb_2O_5$:TiO_2 system, phase relations in the binary system $La_{1/3}NbO_3$:$La_{2/3}TiO_3$ have been developed (Figure V-1). The Ti-rich end member is used as a microwave dielectric material, and has one of the highest dielectric constants among such materials. It does not form with this stoichiometry, but is stabilized with other cations, primarily Al, which tends to lower the dielectric constant. Early attempts to stabilize $La_{2/3}TiO_3$ with Nb as an alternative to Al were not successful, but this year, we were able to make a perovskite- structure compound with the approximate composition $La_{2/3}Nb_{0.07}Ti_{0.93}O_3$ within a narrow temperature band, approximately 1375°C to 1400°C or slightly higher. Larger amounts of Nb lead to formation of monoclinic $LaNbTiO_6$ as a second phase. Investigations of structures in the compositional region $La_{2/3}Nb_xAl_yTi_{1-x-y}O_3$ are now being made to see if a stable perovskite-like structure can be formed with the highest possible dielectric constant in the system. The two $LaNbTiO_6$ phases, a high-temperature monoclinic and a low-temperature orthorhombic form, have also been examined this year. We have demonstrated reversibility of the orthorhombic-monoclinic phase transformation with temperature. Attempts were made to synthesize single-phase specimens of each for more complete structural and electrical characterization. It appears that these have been successful for the orthorhombic phase and that our earlier difficulties may have been due to incomplete standard powder patterns rather than to our techniques. This may also be true for the monoclinic phase. These compounds are of interest because of their tendency to form as second phases with the perovskite-like end members of the binary system. Study of phase relations has begun in other regions of the ternary system $La_{1/3}NbO_3$:$La_{2/3}TiO_3$:$LaAlO_3$ and in the parts of the quaternary system from the aforementioned ternary system toward $\frac{1}{2}La_2O_3$.

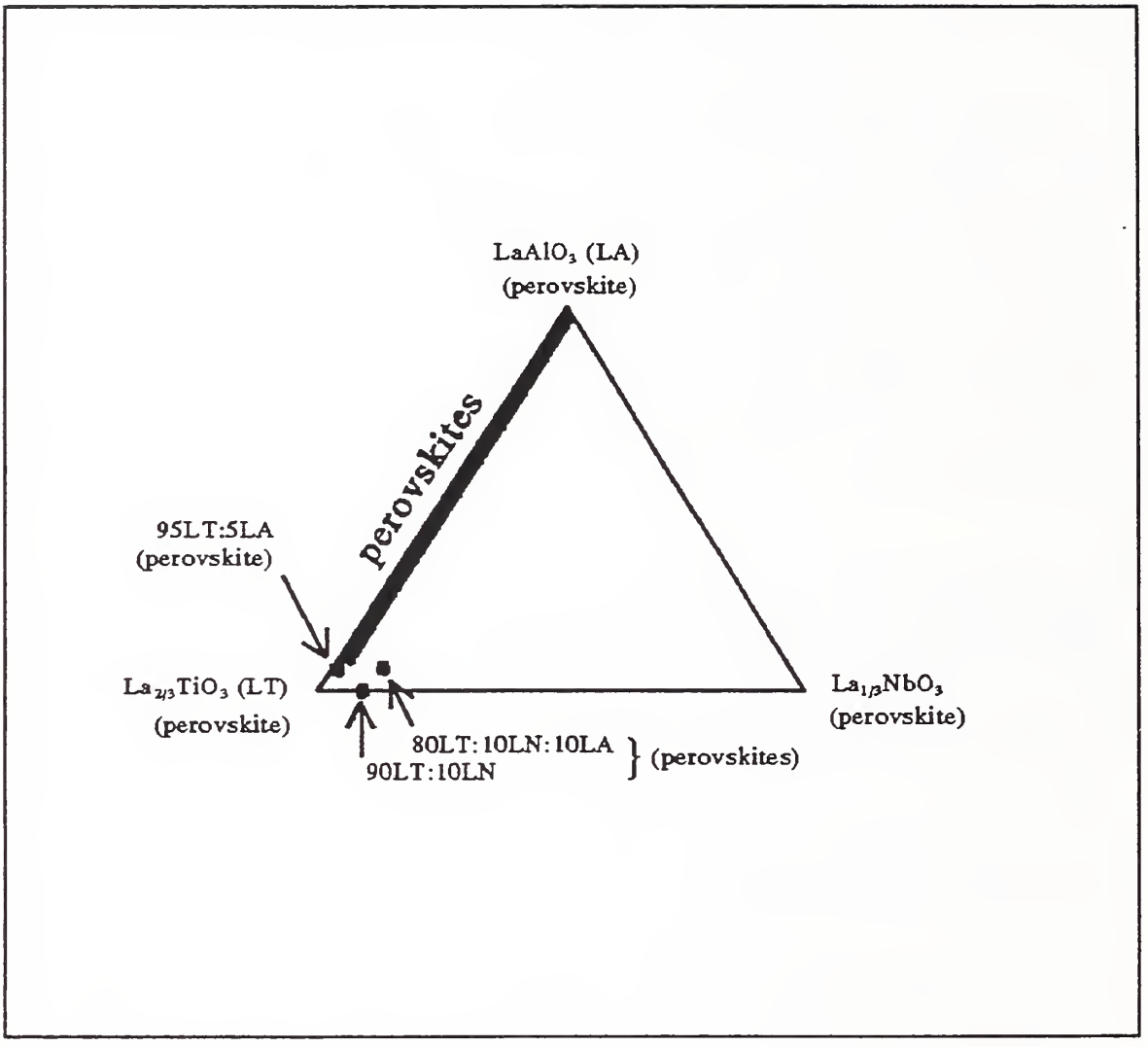

Figure V-1. The system $La_{2/3}TiO_3$-$La_{1/3}NbO_3$-$LaAlO_3$ (LT-LN-LA), whose end-members all have similar crystal structures, is being explored to discover other materials potentially useful as microwave dielectrics. Two materials apparently isostructural with LT, 90LT:10LN and 80LT:10LN:10LA, were recently synthesized and appear to occur within narrow ranges of temperature and composition.

Superconducting Ceramic: Crystal Chemistry and Melting Studies of the Ba-Y-Cu-O System

W. Wong-Ng, L. P. Cook and B. Paretzkin[1]

[1]Guest Scientist

In the past year, efforts to study the liquidus phase diagram of the BaO-Y-Cu-O system have continued. As mentioned elsewhere (see Melt Processing of Y-Sm-Ba-Cu-O Superconductors), melt processing appears to offer greater critical currents and enhanced flux pinning. However, to optimize melt processing, a detailed knowledge of the liquidus phase diagram is necessary. To that end, substantial progress has been made in the quantitative determination of the BaO-½Y_2O_3-CuO liquidus in air. Various invariant (at constant pressure) reactions of this system have been successfully investigated. These reactions include the minimum melting of the system, melting of compounds such as $Ba_2YCu_3O_{6+x}$, BaY_2CuO_5 (green phase), $BaCuO_2$, $Y_2Cu_2O_5$, and of invariant reactions involving tie-line switching of the system. The primary phases produced by these reactions were identified and the melt compositions quantified. Using these data a self consistent topological sequence (equilibrium progression of phases with temperature) of invariant equilibria has been determined between the minimum melting temperature of the system to the melting of the green phase. In addition, these results also lead to a quantitative diagram around the $Ba_2YCu_3O_{6+x}$ region. Figure V-2 shows the current version of the low temperature melting equilibria. These results indicate that (1) The primary phase field of $Ba_2YCu_3O_{6+x}$ was confirmed to be narrow, therefore stoichiometry must be precisely controlled to maximize yield of $Ba_2YCu_3O_{6+x}$ by single crystal growth technique. (2) Low temperature melts have low yttrium, indicating the growth rate and the size of single crystals may be restricted as a result. (3) Loss of oxygen accompanies melting, indicating melt needs adequate oxygen during crystallization, and as a result, P_{O2} can be used as a control variable during melt processing.

We also continued to study the effect of two important factors, namely, the progressively decreasing size of the lanthanides, known as the lanthanide contraction, as well as the role which the stability of different oxidation states of these elements plays in governing compound formation in the Ba-R-Cu-O systems, where R=lanthanides and yttrium.

In addition to the above activities, a compilation of the powder X-ray diffraction patterns of the high T_c superconductor and related phases in the systems of Ba-R-Cu-O, Sr-R-Cu-O and Ca-R-Cu-O, where R=yttrium and lanthanides, has also been made. In addition to the patterns of compounds found in these systems, other related compounds included are cation substitution products of the high T_c phases of $Ba_2RCu_3O_{6+x}$, potential reaction products with different types of sample containers, and selected thin-film substrates.

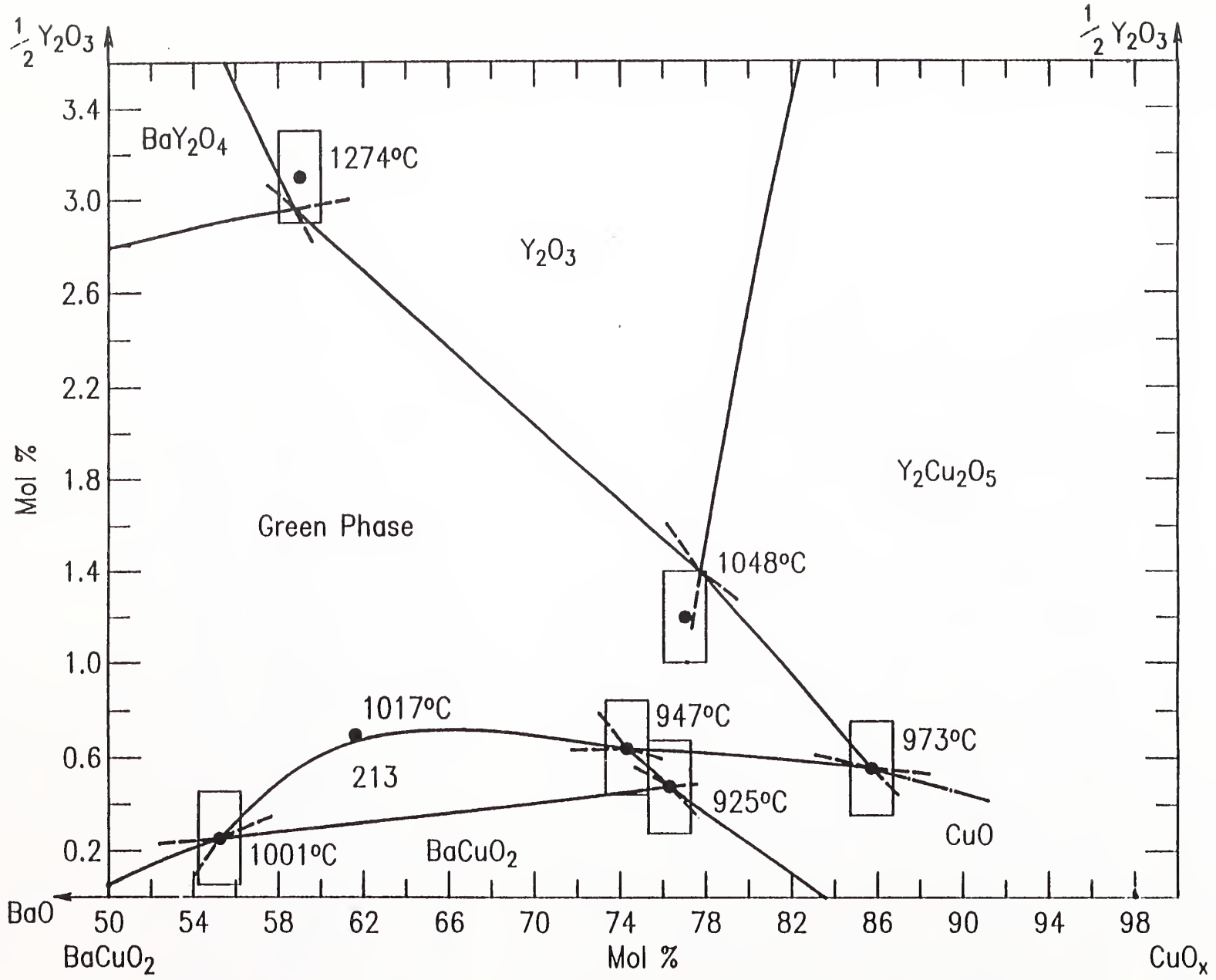

Figure V-2. Preliminary liquidus diagram showing the primary phase fields in the copper rich end of the diagram. Diagram is slightly distorted in that the right bottom angle should be 89°.

Single Crystal X-ray Diffraction Studies

W. Wong-Ng, R. S. Roth[1], and C. J. Rawn[2]

[1] Guest Scientist
[2] Now at Arizona State University

Crystallographic structural characterization has been shown to be essential for understanding phase equilibria. Previously, during the phase equilibrium study of the Ba-Zn-Ti-O system, three new ternary oxides with formulas $Ba_4ZnTi_{11}O_{27}$, $BaZn_2Ti_4O_{11}$ and $Ba_2ZnTi_5O_{13}$ have been discovered. We have successfully determined the crystal structure of these compounds by using single crystal X-ray diffraction methods. While these three structures are substantially different, they all consist of 3-dimensional interconnecting network of octahedral TiO_6 and ZnO_6 (tetrahedral ZnO_4 also in $BaZn_2Ti_4O_{11}$). Mutual substitution of Zn and Ti were found in some octahedral sites in all three compounds.

In collaboration with Stephen Sunshine of AT&T Bell Laboratory, the crystal structure of the potential optical wave-guide material, chromium doped $Zr_2(Si,Cr)O_4$, and the undoped willemite analog Zn_2SiO_4 have been investigated by using single crystal X-ray diffraction techniques. $Zn_2(Si,Cr)O_4$ is a metastable phase quenched from the liquid of the same composition at above the melting point. The structure of Zn_2SiO_4 is rhombohedral with space group R-3 while $Zn(Si,Cr)_2O_4$ is monoclinic with space group $P2_1/c$. About 3.7% of Cr was found to substitute the tetrahedral Si sites. It appears that the result of doping is to force the Cr ion to change from a Cr^{3+} state into a Cr^{4+} state, thereby changing the optical property of the zinc silicate. Both compounds can be described by interconnecting 3-dimensional network of ZnO_4 and $SiO_4/(Si,Cr)O_4$ with open channels running throughout the structures. The structure of the Cr-doped compound is relatively more distorted.

With regard to superconductor compounds, fruitful collaborations have also been extended to outside research laboratories. In collaboration with Bai-Hao Chen, Bryan Eichgorn of University of Maryland and Phillip E. Fanwick of Purdue University, structures of a new series of compounds of $Ba_{n+1}A_nS_{3n+1}$, where A = Hf and Zr have been determined. Ruddlesden-Popper type structures play an important role in high T_c superconductor series, i.e. in the Bi and Tl containing compounds of $(Tl,Bi)_m(Ba,Sr)_2Ca_{n-1}Cu_nO_{2n+m+2}$, where m=1 or 2 for the Tl system and m=2 for the Bi system. To our knowledge, only compounds with $n \leq 3$ have been reported and well characterized. In this new series of compounds of $Ba_{n+1}A_nS_{3n+1}$, n has been observed as high as 5. Our collaborative results also showed a progression of symmetry of these compounds from tetragonal to more distorted orthorhombic as n increases. The possibility of producing superconductivity in these compounds by doping is currently under investigation.

First Principles Phase Diagram Calculations

B. P. Burton, A. Pasturel[1], and R. E. Cohen[2]

[1]CNRS, Grenoble France
[2]The Geophysical Laboratory, Carnegie Institute of Washington, D.C.

Relaxor ferroelectrics are a technologically important class of solid solution materials in which the ferroelectric properties are sensitive functions of composition and cation order (heat treatment). A first principles phase diagram (FPPD) calculation for the relaxor system $(1-x)Pb(Sc_{½}Sc_{½})O_3$-$xPbTiO_3$ is in progress, and preliminary results predict new and unexpected ordered phases at compositions $x=0.5$ and $x=0.75$. These calculations constitute an important test of the validity of FPPD calculations when they are applied to complex ceramic systems.

A FPPD calculation was also used to study metastable bcc based ordering in the system Fe-Be. These calculations combine first principles electronic structure calculations of the cohesive energies of ordered compounds (to obtain a model Hamiltonian) with a cluster variation method phase diagram calculation. For the first time in a FPPD calculation, both chemical and magnetic ordering were considered. It was demonstrated that: 1) Magnetic ordering is responsible for the observed B2 (CsCl structure) ordering in metastable bcc solutions (without magnetism B32 ordering would occur); 2) The energetic cost of mixing atoms of very different sizes is responsible for observed spinodal ordering/phase separation in metastable bcc solutions.

The application of FPPD calculations has been extended to the relaxor ferroelectric system $(1-x)Pb(Sc_{½}Sc_{½})O_3$-$xPbTiO_3$, and new ordered phases have been predicted at compositions $x=0.5$ and $x=0.75$.

Ceramic Processing of Nanosize Powder of γ Alumina

G. J. Piermarini and M. R. Gallas[1]

[1]Guest Scientist

Nanosize γ-Al_2O_3 powder (20 nm average diameter) was compacted at various pressures up to 3 GPa utilizing a diamond anvil high pressure cell (DAC). The compaction, done at RT and also under liquid N_2, produced a transparent green state. The transparent green state was retrieved to 1 atmosphere and sintered in a tube furnace at 800°C for 10 hours in vacuum. The quality of the compacts before and after sintering was evaluated by microindentation hardness measurements and also by optical transparency. Green state optical transparency was preserved on sintering in some cases and the hardness increased to a maximum value of 10 GPa. The crystallographic structure of the compacts was determined by energy dispersive x-ray diffraction measurements and showed that transparency was retained only in those cases where the γ phase did not transform to the α alumina phase. This is the first example of the production of hard, transparent γ alumina compacts.

Compression measurements were performed for the first time on nanocrystalline γ-alumina using a diamond anvil cell (DAC) and the energy dispersive x-ray diffraction method . The cubic unit cell (a = 0.7924 nm) for γ-alumina was found to have a volume compression of about 2.4% over the pressure range from 1 atm to 3.8 GPa at room temperature. Using a linear fit with the Birch equation of state, the isothermal bulk modulus (B_o) was determined to be 213 $\pm$ 20 GPa. The Young's modulus (E) was estimated to be 337 $\pm$ 32 GPa assuming a Poisson's ratio for γ-alumina of 0.236, a value which is typical for polycrystalline α-alumina with 0% porosity. These moduli represent the first values to be obtained on γ-alumina.

HIGH T_c SUPERCONDUCTORS

Work studying high T_c superconductors has involved phase equilibria research (see Phase Diagram section), processing studies, and investigations of mechanical properties.

Melt Processing of Y-Sm-Ba-Cu-O Superconductors:

M. D. Hill, J. E. Blendell and W. Wong-Ng

A series of experiments were performed to examine properties of melt processed barium yttrium cuprate (123) containing 5% excess Y or Sm (211) 'green' phase. This material shows consistently large magnetic J_c's as well as excellent flux pinning and, with the optimization of processing conditions to minimize sample deformation, may be able to retain its pre-melt processed net shape. Near net shape materials would have enormous potential in applications such as superconductive bearings.

A series of melt processed Y-123 samples were cooled in Ar to suppress the tetragonal to orthorhombic transition. The tetragonal to orthorhombic transition in this material upon cooling involves an increase in the oxygen content of the unit cell and is dependant on a sufficiently high oxygen partial pressure. It is this transition and its associated unit cell volume change that is believed to be responsible for the microcracks observed in melt processed material cooled in air. For the melt processed material cooled in Ar, optical microscopy revealed that the aligned microcracks present in samples cooled in higher oxygen partial pressures were absent. This suggests that the tetragonal to orthorhombic phase transition is responsible for the formation of aligned microcracks on cooling. After the tetragonal material was annealed in oxygen at 420°C, the superconducting orthorhombic phase was formed although the microcrack density was significantly lower than material cooled in air or oxygen from the melt processing stage. Material processed with reduced microcrack densities may be better suited for applications requiring higher transport current densities in addition to the strong flux pinning.

A trapezoidal section of the phase diagram Y-Sm-Ba-Cu-O containing the Y-123 Phase, the Sm-123 phase, the Y-211 phase and the Sm-211 phase as end members was investigated to determine the compatibility relations. It was discovered that the equilibrium phase assemblage for initial compositions containing Sm-211 and Y-123 consists of the (Y,Sm)-211 and the (Y,Sm)-123 phases with most of the Sm going into the 123 phase. The

Sm-123 material and its mixed lanthanide solid solutions have poor superconducting properties relative to the Y-123 material, so it is important that the composition does not reach equilibrium. This information is significant in that melt-processed material in the Y-Sm-Ba-Cu-O system shows promise as a candidate material for superconducting bearing applications.

Mechanical Properties of 110 K Pb-BSCCO Superconductors

M. D. Hill and S. W. Freiman

One of the most promising candidate materials for superconducting wires is Ag clad-110 K Pb-BSCCO. This material has a sufficiently high transport current density and can be fabricated into wires. However, little is known of the mechanical behavior of the 110 K Pb-BSCCO superconductor.

Test specimens were fabricated by the solid state reaction of oxide or carbonate precursors with the nominal composition being $Bi_{1.68}Pb_{0.32}Sr_{1.75}Ca_{1.83}Cu_{2.82}O_x$. Powder x-ray diffraction revealed that the final material contained about 15-20 % of the 80 K phase with the remainder being the 110 K superconducting phase. The powder was then uniaxially pressed into bars at 4 MPa, cold isostatically pressed at 300 MPa, and sintered in air at 858°C for 40 hours.

The bars were indented with a Vickers indentor under range of loads and stressed to failure in four-point bending. By plotting the logarithm of the failure stresses as a function of the logarithm of the indentation load, a fracture toughness (K_{Ic}) of 1.21 $MPa \cdot m^{1/2}$ was obtained as shown in Figure V-3. This value of K_{Ic} is similar to that for Y-Ba-Cu-O and is quite low compared to other ceramics.

TEXTURE/GRAIN ORIENTATION

Ceramics are used in many applications in which expense or availability prohibits use of single crystals. However, the randomly oriented grains in polycrystalline ceramics unavoidably dilute many properties of interest, e.g., domain orientation in ferroelectrics or conducting plane orientations in high T_c superconductors. In such instances, an improvement in properties of interest could be achieved if the individual grains in the ceramic could be aligned during processing. A substantial effort in the Electronics Materials Group has been made to address grain alignment; this effort includes investigations of grain growth, ranging from such basic questions as the energetics associated with liquid-solid interfaces to more applied questions of zone-refining, and extends to the development of tools to determine grain orientation in bulk or thin film geometries. The goal of this work is the understanding of how ceramics can be processed to obtain preferred alignments and how those alignments can be measured on a local, microscopic scale.

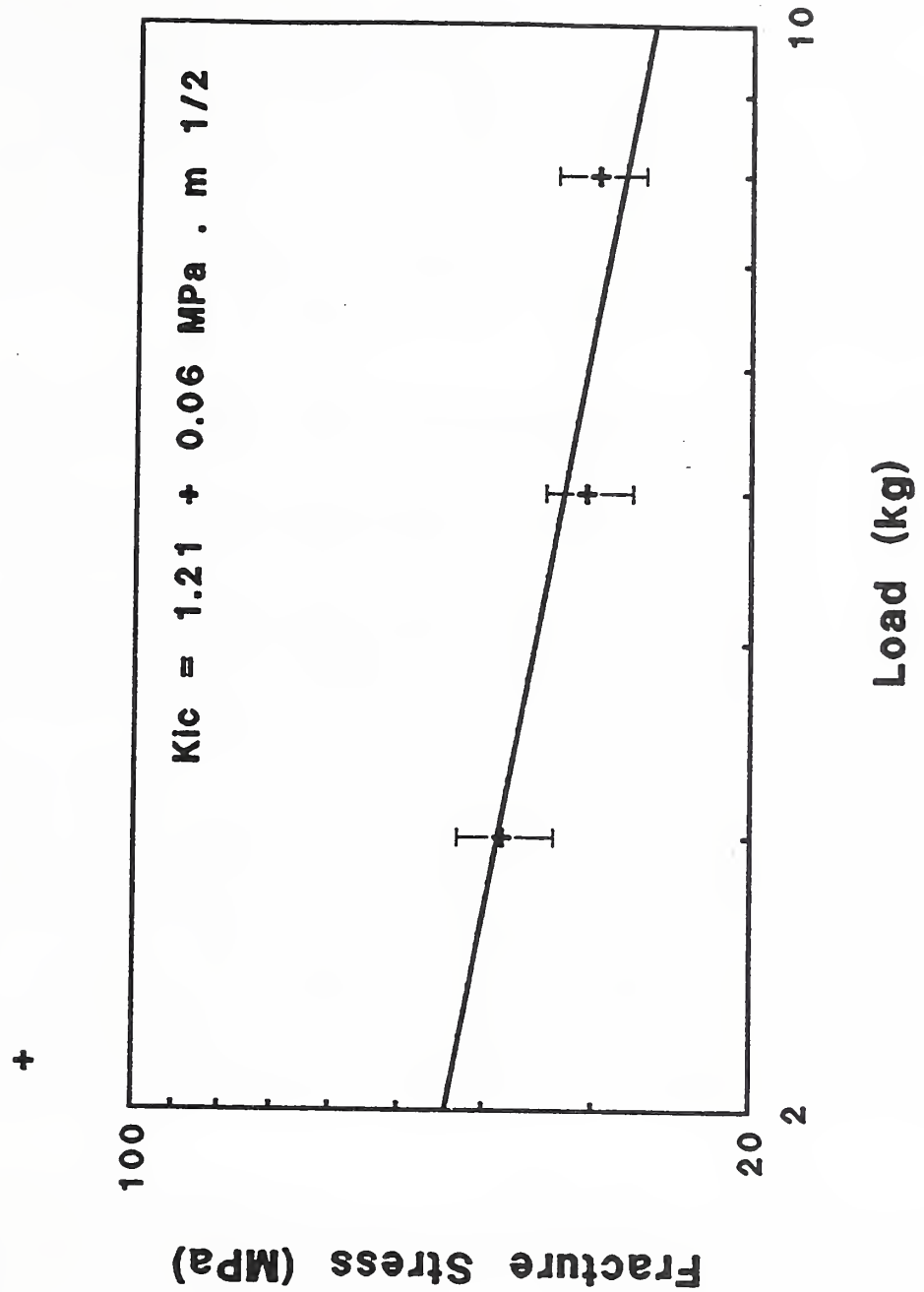

Figure V-3. Indentation-Strength curve for the Bi-110 K phase. The toughness (K_{Ic}) is determined from the y-intercept of the linear fit of the data presented.

Surface Energy Anisotropy in Al_2O_3-Anorthite

J. E. Blendell, C. A. Handwerker[1], J. W. Cahn[1], S. M. Wiederhorn[2], B. J. Hockey[3], M. D. Vaudin, W. C. Carter[4] and D. Y. Kim[5]

[1]Metallurgy Division
[2]Materials Science and Engineering Laboratory
[3]Mechanical Properties Group, Ceramics Division
[4]Powder Processing and Characterization Group, Ceramics Division
[5]Seoul National University

While researchers have known that ceramics exhibit surface energy anisotropy, they have been unable to measure this anisotropy directly or to use it as an aid to obtain improved processing and properties. Many of the properties of advanced ceramics are critically dependent on the nature and distribution of an intergranular film. For example, bulk ceramic superconductors have very poor critical current densities due to the presence of thin intergranular films of non-superconducting phases. We have studied the wetting and dewetting of Al_2O_3 grain boundaries by anorthite ($CaO{\cdot}Al_2O_3{\cdot}2SiO_2$) glass. The orientation dependance of the wetting has been determined for a low angle tilt boundary and as a result of new theoretical developments, we are able to suggest a method for a direct determination of the solid-liquid surface energy.

Low-angle tilt boundaries (7° about $<10\bar{1}0>$) were produced by annealing a layer sample containing tape-cast Al_2O_3 between two near basal (0001) plane sapphire crystals. The Al_2O_3 tapes contained 4% anorthite glass. As the sapphire grew and consumed the polycrystalline tapes, a liquid layer was formed at the boundary. At long times a low-angle tilt boundary was formed. The nature of this boundary was found to be different from predictions based on a model of wetting or non-wetting, where it is assumed that the glass either completely wets the surfaces or a dry grain-boundary is formed. We found that boundary structures which contained both wetted and non-wetted regions were stable. The orientation of the boundary relative to the sapphire crystal structure determined what type of boundary was stable.

Based on these observations, we have developed a method for determining the shape of a partially wetted interface. Using the equilibrium shape of a crystal in contact with the liquid (the Wulff shape), the shape of a fully wetted interface can be determined. This can be combined with the Wulff shape of the grain boundary (which can be calculated for low-angle boundaries) to give the shape of the partially-wetted interface. This shape can then be used to predict when wetting will occur and to what degree. The implications for improving the properties of advanced ceramics are clear, in that using these shapes, the degree of texture needed either to prevent or to allow wetting is known. Thus, the properties of ceramics can be tailored by controlling the orientation of the boundaries in the samples.

Also, this technique has allowed us to determine the surface tension of Al_2O_3 in a direct method. Based on the observation of when the boundaries are fully dewetted and the Wulff shape of the crystals, the surface tension can be determined. For the basal plane of Al_2O_3 in

contact with anorthite, the surface energy was found to be 0.9 J/m^2. This is in good agreement with the estimates of the surface energy from a variety of other studies.

These results, though preliminary, suggest that compositions of glass phases might be modified either to eliminate or to enhance wetting between chosen grain facets. This property could possibly be used, for example, to enhance electrical conductivity in oriented structures by making it energetically favorable for the glass to wet grain boundaries parallel, rather than perpendicular, to the conduction path.

Grain Growth in Textured Al_2O_3 Tapes

J. E. Blendell, C. A. Handwerker[1], M. D. Vaudin, J. P. Cline[2] and K. J. Bowman[3]

[1]Metallurgy Division
[2]Powder Processing and Characterization Group, Ceramics Division
[3]Purdue University

One technique which can be used to improve the high temperature toughness and creep resistance of advanced ceramics is the addition of single crystal whiskers or fibers to coarse grained materials. The large grain size lowers the creep rate, but also degrades the strength. The whiskers or fibers act as bridging elements across the cracks and increase the toughness. Among the many problems with processing such composites to have improved properties, is the very high cost or unavailability of these whiskers and fibers. In an effort to address this issue in the Al_2O_3 system, DARPA has funded a study of texture development and anisotropic grain growth in tape-cast Al_2O_3 samples in an attempt to grow oriented polycrystalline fibers whose behavior would approximate that of single crystal fibers. Because of the anisotropy of the mechanical properties of Al_2O_3, fibers oriented along $<0001>$, the basal direction, are needed. However, the growth of Al_2O_3 in most cases leads to platelets oriented normal to $<0001>$. We have looked at the effect of different rare-earth dopants on lowering the anisotropic growth in orientations normal to the $<0001>$ and increasing growth in $<0001>$.

Additions of the rare-earths Sm, Ce, Nd and La were studied. They were added to tape-cast Al_2O_3 samples which also contained 5% Al_2O_3 platelets as seeds for exaggerated grain growth. Seeded tape-cast samples were used to determine the conditions which favored the growth of Al_2O_3 needles (whiskers) rather than Al_2O_3 plates. Samples which contained 4% glass (anorthite) were also studied. The degree of texture was measured by x-ray diffraction and compared to results from x-ray pole figures. Because x-ray diffraction determination of texture is not very accurate for highly textured samples, the distributions of the orientations of individual grains was determined by backscattered Kikuchi patterns (see Backscatter Kikuchi Diffraction Patterns, below). It was found the large seed grains, which grew, were textured and the fine grains regions were randomly oriented. The grain shape was determined by optical microscopy.

We found that the initially random orientations were dominated at later times by the growth of the large seed grains. The seed grains were oriented during the tape casting and therefore

the samples developed a texture upon annealing. As the orientation of the seed grains was known, the anisotropy in the growth rate could be determined. It was found that in the presence of glass Sm promoted isotropic growth while Ce enhanced the anisotropic growth. Both Nd and La induced porosity and this reduced the amount of grain growth which occurred.

These results suggest that ceramics with preferentially oriented grains might be obtained by appropriately doping seed crystallites. At this time, however, the oriented grain growth has not resulted in oriented whiskers.

Ceramic Fibers by Flux Growth / Directed Solidification

L. P. Cook, B. W. Lee[1] and W. Wong-Ng

[1]Guest Scientist

As part of the DARPA funded effort to obtain fibers with oriented grain structures, a methodology and apparatus was established for the systematic study of alumina fiber growth by flux melting/directed solidification (DS). Dense ingots of various diameters were prepared for DS experiments by inductively premelting a eutectic mixture and causing it to flow into a graphite mold, from which it was easily removed. Using these ingots, experiments were completed by placing the ingot in a temperature gradient furnace such that the a liquid/solid interface is caused to move through the sample at a controlled rate. Furnaces of two types were constructed for this purpose. In one type, a very stable thermal gradient was obtained by using a furnace with relatively large thermal inertia, and producing a directed cooling by the use of flowing gas at one end of the sample cell. With this type of furnace, it was established that directed solidification was achieved under one set of conditions (thermal gradient 50 °C/cm, interface velocity ~ 1 cm/min). This was inferred from the highly oriented nature of the cryolite matrix. However, to date, only platelets, rather than fibers, of alumina have been produced. Theory indicates that the ratio of phases at the eutectic is appropriate for alumina fiber formation (< 30 vol%), and that the lamellar to rodlike morphological transition may be achieved under the appropriate combination of liquid thermal gradient (G) and interface velocity (R). To this end a motorized gradient microfurnace was constructed to allow more efficient reconnaissance of a large range in R (and to a lesser extent, variation in G). Once the matrix region of stable interface conditions is known, further experiments will be completed in the larger gradient furnaces to determine if the lamellar to rodlike transition can be achieved under any conditions.

The effect of liquid/solid surface tension may also play a role. To this end static experiments are being completed to investigate the effect of various cationic and anionic additives on the alumina eutectic morphology, to the extent that fiber vs. platelet morphology can be encouraged independently of the DS-related lamellar to rodlike transition.

Backscatter Kikuchi Diffraction Patterns

M. D. Vaudin, J. F. Kelly[1], J. E. Blendell, W. C. Carter[1] and C. A. Handwerker[2]

Backscatter Kikuchi Diffraction Patterns

M. D. Vaudin, J. F. Kelly[1], J. E. Blendell, W. C. Carter[1] and C. A. Handwerker[2]

[1]Powder Processing and Characterization Group, Ceramics Division
[2]Metallurgy Division

Backscatter Kikuchi diffraction patterns (BKDPs) have been used to study texture in sintered alumina processed in different ways. The texture of hot-pressed alumina samples has been determined and compared with data collected using x-ray diffraction. The texture was found to be strongly [0001] (i.e. c-axis); x-ray measurements are not as accurate in the strong texture regime so corroboration from other techniques is desirable. Tapes of fine grained alumina have been seeded with large c-axis platelets to promote grain growth and produce a highly textured microstructure. BKDP has shown the texture of the large grain fraction to be strongly c-axis and the small grain fraction to be approximately random.

In order to obtain this type of information, substantial improvements in obtaining and analyzing the BKDP patterns have been made. Software has been written to process digitized patterns using a frame grabber and high speed frame processor and thus to create much clearer diffraction patterns. It is now possible to: (1) average the diffraction pattern video image to remove the noise; (2) subtract the background from the image to remove effects of imperfections in the phosphor and video camera; (3) expand the contrast of the image for maximum visibility and accurate analysis; (4) save images in various formats for transfer to hard copy. A video distortion correction based on a look-up table technique has been implemented. The software for crystal orientation determination has been improved to the point where the automatic indexing algorithm takes a maximum of two seconds to index any pattern once the positions of three or more zone axes have been determined. The results of this development for Cr_2O_3 are shown in Figure V-4.

FERROELECTRIC MATERIALS

Ferroelectric ceramics are becoming increasingly more important with such potential applications as non-volatile memory, smart materials, and high strain actuators. This past year, we have continued looking at ferroelectrics in both film and bulk forms, investigating texturing, mechanical properties, and failure mechanisms.

Crystal Structure and Texture in $BaTiO_3$ Thin Films

M. D. Vaudin, D. L. Kaiser[2], L. H. Robins[2], and P. K. Schenck[1]

[1]Metallurgy Division
[2]Optical Materials Group, Ceramics Division

High quality films of $BaTiO_3$ are of interest in areas such as hard, non-volatile computer memory and electro-optic devices. Thin films of $BaTiO_3$ have been deposited in crystalline form by pulsed laser ablation on heated Pt/Si substrates and by MOCVD on fused quartz

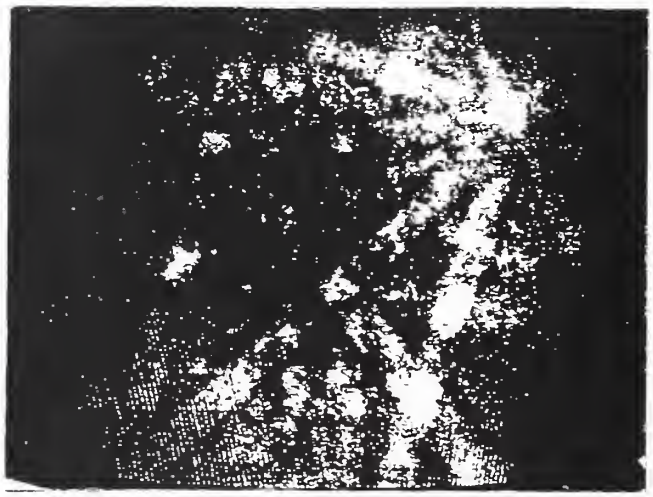

Backscattered Kikuchi Pattern from Cr_2O_3

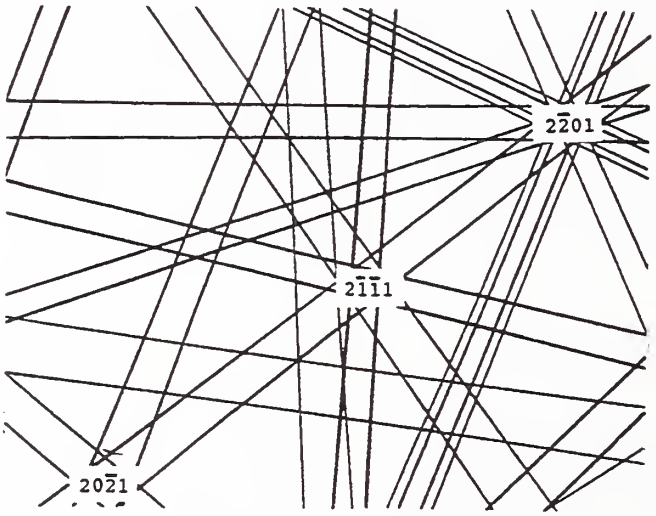

Indexed simulation of above BKP

Figure V-4. Comparison of measured (SEM) and simulated backscatter Kikuchi pattern for Cr_2O_3.

substrates. For all envisioned applications, the crystalline texture of the film is of great importance; ferroelectric applications require that the c-axis be preferentially oriented normal to the film whereas a film with the c-axis lying in the plane of the film is desirable for dielectric applications. The crystal structure and texture of the deposited films have been characterized by both conventional and glancing angle x-ray powder diffraction and the microstructure has been studied in the SEM. Films with small thicknesses and/or small grain size are often observed to be cubic instead of the equilibrium tetragonal structure. Preliminary Raman spectroscopy results have confirmed this. Strong (001) or (111) texture has frequently been observed and the causes of the texture have been studied by varying the deposition conditions, in particular film growth rate and substrate temperature. For laser deposited films, high fluences (laser energy density) promote texture; the nature of the texture (i.e. (001) or (111)) appears to be related to the degree of (111) texture of the Pt/Si substrate.

Ferroelectric Thin Films by Pulsed Laser Deposition

L. P. Cook, B. W. Lee[1], C. K. Chiang, W. Wong-Ng, M. D. Vaudin, H. M. Lee[1], P. K. Schenck[2], and P. S. Brody[3]

[1]Guest Scientist
[2]Metallurgy Division
[3]Army Research Laboratory, Adelphi, MD

Work has concentrated on three thin film materials: (Mg, W) - modified $PbTiO_3$, PZT ($PbZr_{0.53}Ti_{0.47}O_3$), and $BaTiO_3$,. Two principal types of experiments have been completed: a) deposition and crystallization on resistively self-heated Pt-coated Si wafers and b) controlled post-depositional annealing experiments on amorphous films deposited on room temperature substrates. The heated depositions have produced films with varying degrees of preferred orientation, which apparently are related to the preferred orientation of the underlying platinum coating. For both $BaTiO_3$ and $PbTiO_3$, [111] oriented platinum tends to favor a tendency for [111] orientation in the deposited film. Interestingly, the effects on the ferroelectric properties of the two materials are not the same, however. Whereas in $BaTiO_3$, [111] orientation tends to enhance ferroelectricity, in $PbTiO_3$, [100] films show the greatest ferroelectricity. For PZT self heated films, work has concentrated on preparing materials with various levels of Nb dopant to investigate the effect on the problem of ferroelectric fatigue. Preliminary indications are that Nb improves the ferroelectric fatigue resistance of PZT thin films.

By completing controlled post-depositional annealings on initially amorphous films, it has been possible to determine the best temperatures for processing (including depositions on heated substrates). At temperatures below 550°C, crystallization rates appear to be too slow for practical use. Above 650°C, crystallization of a large volume fraction of the films is largely instantaneous. In PZT and $PbTiO_3$, the process is complicated by the precipitation of an unwanted pyrochlore phase; however this can be removed by extended annealing, or very careful choice of temperature. Indeed, extended annealing appears to improve the crystallinity of the films regardless of the crystallization temperature, up to 750°C. For

$BaTiO_3$, two rate phenomena appear to be operative, based on crystalline fraction vs. log time curves obtained during the post depositional anneals. At 600-650°C both processes are operative, judging from a break in slope of the kinetic data. X-ray evidence suggests that $BaTiO_3$ may crystallize initially as the hexagonal form, then assume a cubic symmetry. Investigations are under way to clarify the relations between kinetics, phase equilibria, and grain size.

Cyclic Fatigue and Mechanical Properties of PZT

G. S. White and M. D. Hill

We have continued investigating the mechanical properties of bulk lead zirconate titanate (PZT) under a program from ONR, particularly focussing on failures resulting from cyclic loading. Since this material is presently the most common actuator and transducer material in use, its reliability under cyclic loading conditions is of great importance. Material degradation under electrical cycling at resonance frequency has been observed and would limit the number of potential applications for this material and its overall reliability. Consequently, our interest has been to understand the mechanical behavior of cycled PZT and to quantify those variables which will aid understanding of the mechanical properties.

The strength, toughness (K_{Ic}), and sensitivity to environmental fracture (N-value) were measured for a PZT-8 material and were found to be 123 $\pm$ 8 MPa, 1.19 MPa-$m^{1/2}$, and 37, respectively. For mechanically generated cyclic stress tests, the mean stress was set to half of the mean failure strength obtained above. One side of the billet was kept continually in tension, while the other was kept in compression. No attempt was made to isolate the tensile surface from the environment. The S-N curve was derived from a semi-log regression fit (Figure V-5). The poor quality of the straight line fit, based on the Fuller Evans model suggests that, while environmentally enhanced fracture certainly occurs in this material (i.e. N = 37), it appears that true cyclic phenomena are affecting the lifetimes of the cycled specimens as well. At this time, however, the cyclic phenomena have not been identified. Similarly, measurements of the velocity of sound in the materials loaded at resonance demonstrate that cyclic loading is affecting the elastic properties of the material, particularly in the high stress region. Again, the source of the change in sound velocity has not yet been identified.

STRESS MEASUREMENTS MADE BY MICRO-RAMAN SPECTROSCOPY

G. J. Piermarini, Y. C. Chu[1], G. S. White, and L. M. Braun[2]

[1]Guest Scientist
[2]Mechanical Properties Group

The ability to measure stresses over distances comparable to microstructural dimensions is critical both for evaluating the quality of monolithic and composite structures and for providing input into processing models to design new generations of materials. In particular, residual stresses associated with thermal expansion mismatches in layered electronic systems

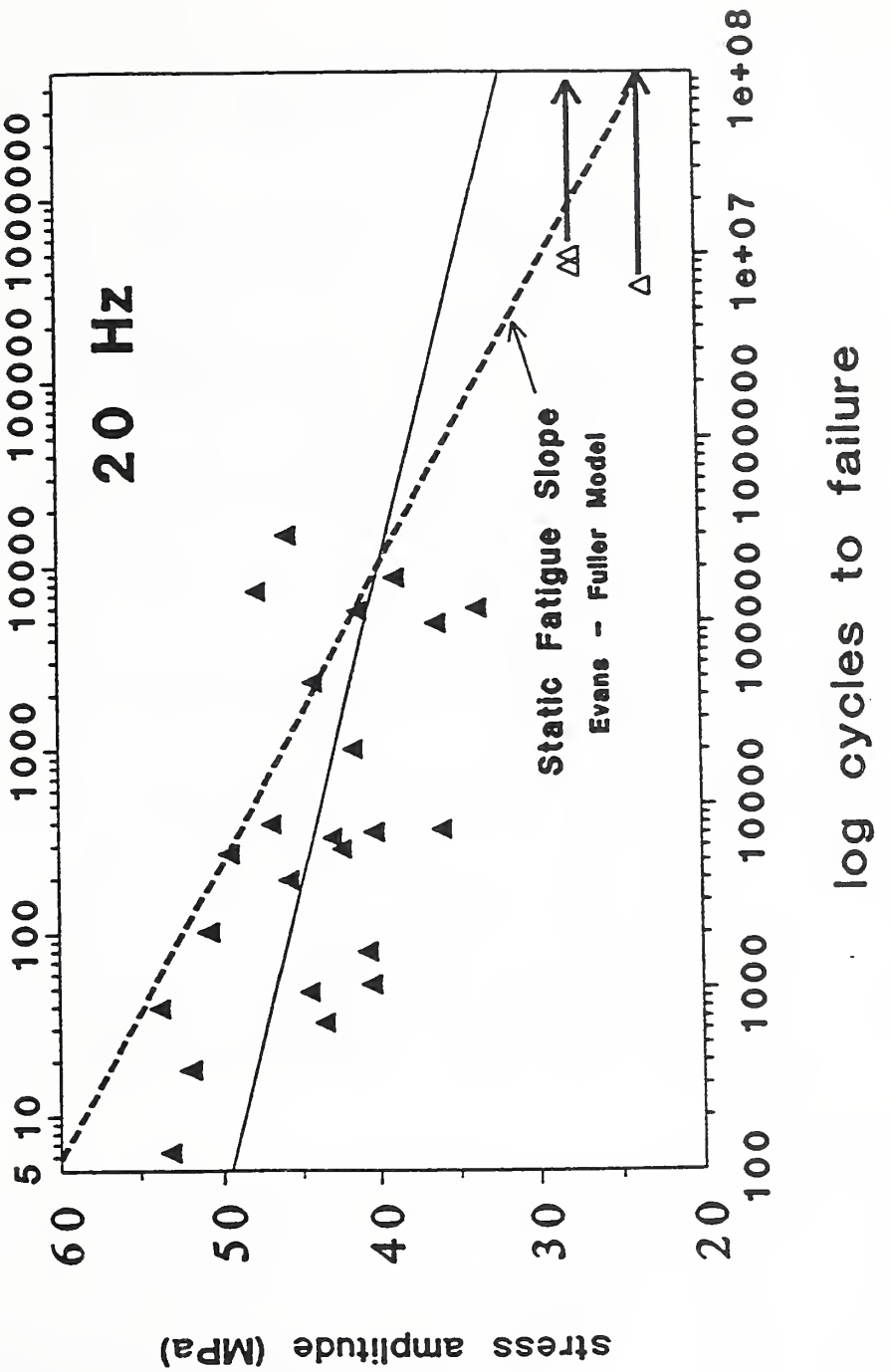

Figure V-5. Fatigue Curve for PZT in four point bending. The solid line indicates a linear regression fit of the fatigue data while the dashed line is the simulated curve for the Evans-Fuller model. The data points represented by open triangles with arrows are tests where the experiment was halted before fracture occurred.

is known to be a serious problem in system reliability. Therefore, we have begun using a micro-focus Raman system, Figure V-6, to measure stresses in ceramics. The technique involves measuring stress-induced shifts in the Raman spectra of the material.

To quantify the stress, precise curves relating the peak shift to known stress values are required. We have obtained preliminary curves for alumina and aluminum titanate powders exposed to hydrostatic compressive stresses in a diamond anvil cell. In addition, we have had a biaxial loading rig constructed which will allow us to generate well known tensile stresses on the surface of disk-shaped specimens. The combination of these two systems will allow us to calibrate shifts due to hydrostatic or directionally dependent stresses.

We have obtained spectra from unstressed alumina disks which show very sharp, well defined peaks on a flat background. Such spectra are ideal for the detection of small peak shifts associated with residual stresses. Currently, work is in progress to calibrate peak shifts in alumina and to determine the limits of the sensitivity of the system.

Alumina and aluminum titanate ceramics have been chosen as model materials, because we have extensive experience in varying, in a qualitative manner, residual stresses in these materials by varying processing conditions.

MOLECULAR ORBITAL SIMULATIONS OF ENVIRONMENTALLY ENHANCED FRACTURE

W. Wong-Ng, G. S. White, C. G. Lindsay, and S. W. Freiman

Molecular orbital (MO) calculations, used to model effects of environmental molecules on the rupture of strained crack tip bonds, have been continued for the silica system, which exhibits this behavior, and have been started for silicon, which appears impervious to environmental effects.

Silica: Calculations involving a water, ammonia, formamide, nitrogen, or argon molecule near the strained crack tip bond have been made. As expected, the energy barrier to the approach of the environmental molecules increased in the order water, ammonia, formamide, nitrogen and argon as shown in Figure V-7. These results are consistent with known crack growth behavior of silica in these environments. The calculations determined that strain of the crack tip bond has two important effects. As expected, strain further polarizes the Si-O bond, making it more attractive to the environmental molecule. In addition, however, an important aspect of the strain is that it reduces steric hindrance to the approach of the environmental molecule caused by the oxygen atoms adjacent to the crack tip. Therefore, strain not only makes the crack tip bonds more attractive to the environmental molecules, it also makes the crack tip accessible.

Silicon: In order to understand the fact that silicon appears to remain inert towards environmental molecules such as H_2O and NH_3 under strain, in the past year, MO calculations have also been performed on a model silicon molecule with and without the environmental molecule of H_2O. Factors such as the size of crack tip and net charge on the

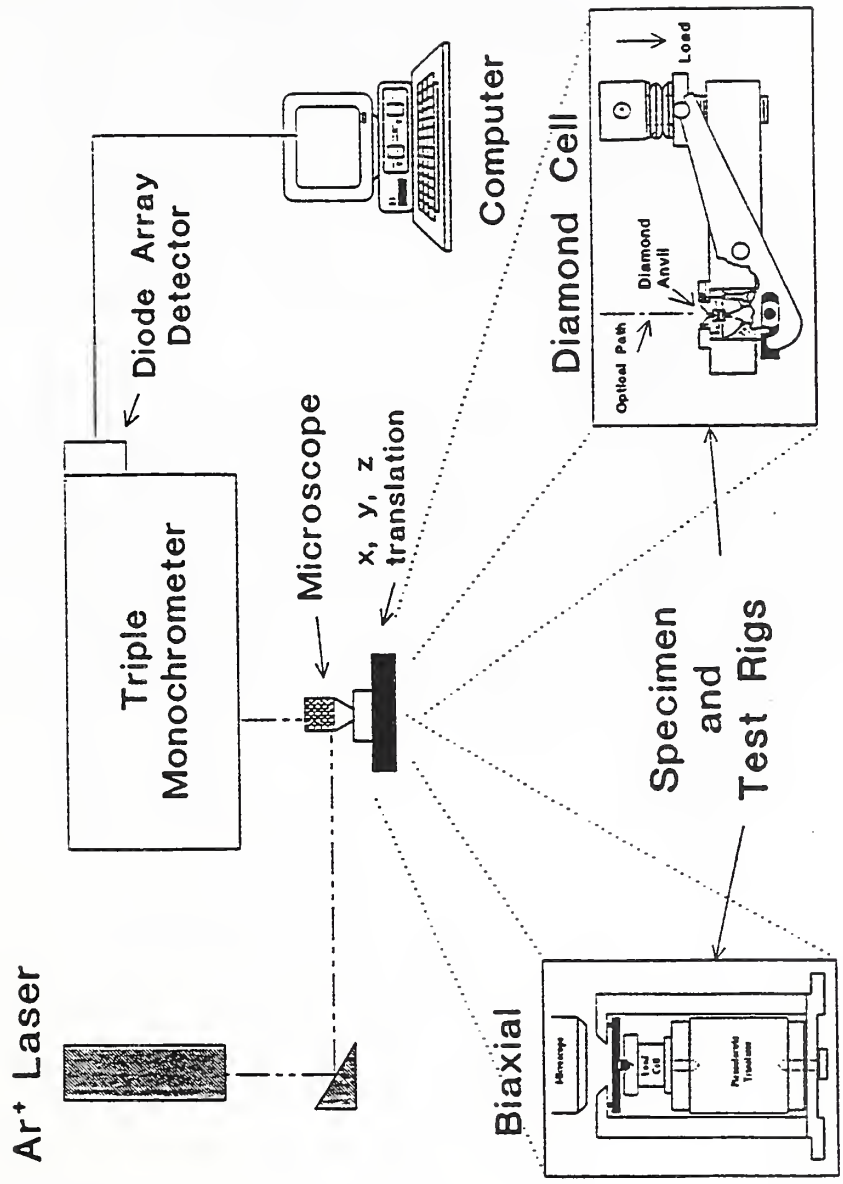

Figure V-6. Schematic diagram of μ-Raman system showing both the in situ biaxial stressing rig and the diamond cell.

crack-tip atoms as a result of applying strain were investigated. Model molecules of Si_8H_{18} [H_9Si_4-Si_4H_9] and $Si_8H_{18}O$ [H_9Si_4-$Si_4H_8(OH)$] have been used. The crack-tip is assumed to have one Si-Si bond unit. The latter model is used to simulate situation in which an hydroxyl group remained at the crack wall.

It was found that the size of the crack tip is too small to accommodate environmental molecules, and strain is necessary to widen the crack tip and at the same time attract and orient the molecule to move in. An enhanced reaction of the crack-tip Si-Si bond with H_2O leading to its breakage is, however unlikely, because as tensile strain was applied along the Si-Si crack-tip bond, the strained band did not polarize regardless of the manner in which the strain was applied (ie. with or without angle distortion, and whether the strain was distributed evenly in the neighborhood of the crack-tip bonds). This is different from the situation of silica in which when the crack-tip Si-O bond is strained, the net charge of Si becomes more positive and O becomes more negative, enhancing the interaction with an environmental molecule containing both atoms which donate (O,N) and accept electrons (H).

The absence of chemical reaction in Si with environmental molecules is also demonstrated from the geometry optimization calculations of the system $Si_8H_{18}O+H_2O$. In the absence of strain, the water molecule is about 5 Å away from the crack-tip Si [$O(H_2O)...Si$], whereas under 15% strain (15% elongation of the Si-Si bond), the molecule is able to move closer towards the crack-tip (still at a relatively great distance of 2.9 Å, which is slightly less than the sum of the Van der Waal's radii of Si (1.7 Å) and O(1.4 Å)). Comparing with a O-H bond of $\approx$1.0 Å, this great separation indicates no chemical reaction takes place. Therefore, despite the fact that strain widens the size of the crack-tip, the result of charge redistribution at the crack-tip does not favor chemical reaction. Calculations are underway examining the reaction between $Si_8H_{18}O$ and NH_3.

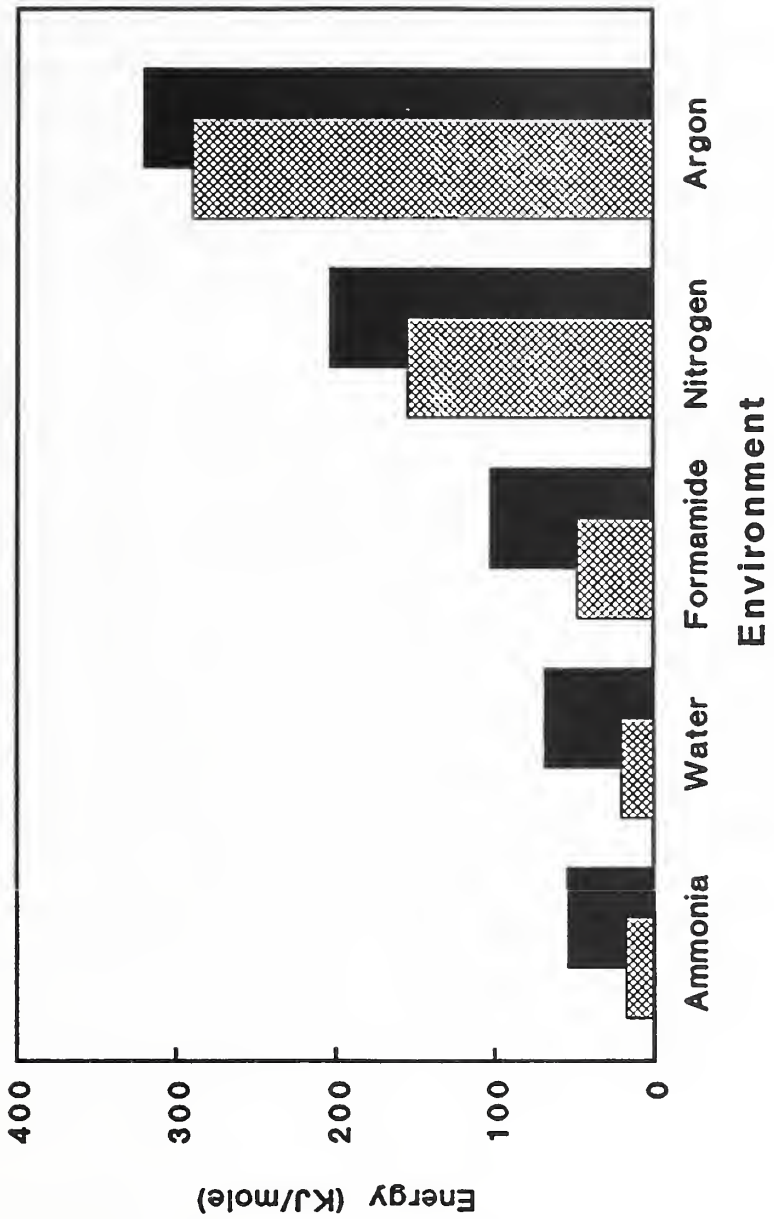

Figure V-7. Histogram showing trend in energy of approach to crack tip in silica for different environments. Hashed regions represent the system under strain, solid is unstrained.

VI. OPTICAL MATERIALS

Albert Feldman

The objectives of the Optical Materials Group are to provide data and their evaluation, measurement methods, standards and reference materials, concepts, and technical information on the fundamental aspects of processing, structure, properties, and performance of optical and photonic materials for industry, government agencies, universities and other scientific and technical organizations. The program supports generic technologies in crystalline, glassy, and thin film inorganic optical and photonic materials in order to foster their safe, efficient and economical use. Research in the group addresses the science base underlying advanced optical and photonic materials technologies together with associated measurement methodology.

The principal activity of the Optical Materials Group is being directed toward materials for photonic technology related to data processing and storage. Three aspects of this technology to be addressed are modulator materials, storage media materials, and material for short wavelength radiation sources to increase storage density. In area of modulator materials, we are evaluating new processing methods that would result in thin film materials with superior properties such as enhanced electro-optic modulator characteristics. In the area of storage media materials we are addressing the development of thin film photorefractive materials, in which the storage method involves modification of the refractive and absorptive properties upon exposure to optical radiation. Ferro-electric oxides (more specifically barium titanate) are the materials we are studying in the latter two aspects because they possess large electro-optic coefficients and a large photorefractive effect. In the area of materials for short wavelength sources, our studies are being directed toward crystalline materials with large band gaps. This is because a large bandgap is required if a material is to emit radiation at short wavelengths. We have been studying diamond, a wide band-gap material; we expect to extend this work to other wide band-gap materials that hold greater promise as optical sources, such as gallium-nitride, aluminum nitride, silicon carbide, and quantum well structures of these materials. Diamond possesses numerous superior properties make it an excellent material for a variety of photonic applications. In addition to its optical transparency, it has the highest thermal conductivity making and excellent substrate material for solid-state semiconductor laser sources.

Significant Accomplishments

- Metalorganic chemical vapor deposition (MOCVD) is a new method of producing electro-optic thin film ceramic materials that is expected to play an important role in the development of photonic devices for future information technology systems. The first polycrystalline films of the electro-optic material barium titanate ($BaTiO_3$) have been deposited in a newly constructed metalorganic chemical vapor deposition (MOCVD) facility. The MOCVD system, which was designed and constructed in the Ceramics Division, allows for precise control of the process conditions that affect the microstructural, electrical and electro-optic properties of the films.

- The performance of this material will be determined by its structure; however, common structure determination techniques, such as x-ray diffraction, cannot easily distinguish between the different phases that may be present in the films. Raman spectroscopy is a useful alternative method because several Raman lines have been uniquely associated with the desirable tetragonal ferroelectric phase. Because of the high spatial resolution of the Raman probe beam, maps of the tetragonal phase distribution can also be obtained. In a $BaTiO_3$ film deposited by laser evaporation and examined by Raman spectroscopy, a mapping of the tetragonal-phase lines showed that the phase composition was not uniformly distributed. This type of data is providing a means of evaluating and improving the deposition process.

- Chemical vapor deposition (CVD) of diamond is expected to have a significant economic impact in the near future and Raman spectroscopy has become the standard method of evaluating diamond quality. A Raman spectrum usually consists of several components or lines that have been individually attributed to crystalline diamond, amorphous carbon, structures of unknown origin. In examining a series of diamond films, we found that the width of the Raman line attributed to crystalline diamond line initially increased with increasing nondiamond carbon content, but then saturated to a constant value. Because the width can be inversely related to the average size of a crystalline domain, the upper limit to the linewidth implies a lower limit to the size of the crystalline diamond domains in these films.

- Defects introduced during the growth of diamond by chemical vapor deposition (CVD) can play a major role in the rate of growth and in the performance of the material in a many applications. For example, the size and distribution of noncoherent twin boundaries is expected to affect the fracture strength of the diamond. High resolution lattice images of CVD diamond have revealed the twinning defect structure. Moire-fringe patterns observed in the micrographs can be interpreted as overlapping twins with noncoherent boundaries that are inclined to the electron beam. A computer graphic simulation has duplicated the periodicities and orientations of these boundary images.

- Spatially resolved cathodoluminescence (CL) spectroscopy is proving a valuable means for finding defects that may affect the performance of diamond in optical and electronic applications. In developing cathodoluminescence as a useful diagnostic tool for evaluating the quality of diamond, spatially resolved CL spectra were obtained from a large single-crystal diamond wafer that had been characterized previously by x-ray topography and etch pit analysis. Two CL spectral bands were found to be localized in regions of the wafer with high dislocation densities. Because one of the bands had previously been attributed to nitrogen and atomic vacancy complexes, this work suggest that these types of defects are more prevalent in regions of high dislocation density rather than in other regions of the material.

- The performance of high temperature superconductors will depend strongly on the flux pinning behavior of the material. A new, high-resolution magneto-optical imaging system for obtaining real-time, quantitative magnetic flux distribution maps

has been set-up. This imaging technique permits direct correlation of microstructural features with flux flow dynamics at a range of temperatures and applied magnetic fields. An examination of $YBa_2Cu_3O_{6+x}$ (YBCO) single crystals has revealed highly anisotropic flux pinning by twin boundaries; the flux gradient across twin boundaries was more than ten times the flux gradient along twin boundaries. Measurements on bicrystals demonstrated for the first time that flux penetrated along many grain boundaries at very low applied magnetic fields (3.5 mT).

FERROELECTRIC OXIDE THIN FILMS FOR PHOTONICS

Photonic devices made of ferroelectric oxide films that have large electro-optic coefficients are expected to have a major role in future information technology systems. U.S. dominance in these advanced technologies will be important for maintaining the future economic health of the nation. Pioneering new methods of materials fabrication and characterizing the materials produced is an important means of promoting U.S. dominance in these technologies.

Metalorganic Deposition of Barium Titanate

D.L. Kaiser, M.D. Vaudin, L.D. Rotter and L.H. Robins

The advancement of ferroelectric oxides for photonics requires two research components: 1) a practical thin film deposition process suitable for mass production of optical-quality films; and 2) methods to characterize the nature of defects in such films and the effect of these defects on electric and electro-optic properties. The deposition technique selected for this study is metalorganic chemical vapor deposition (MOCVD), a technique currently used for the manufacture of electronic devices made of III-V semiconductor films and for fabrication of high-quality superconducting oxide films. The ferroelectric oxide chosen for our initial efforts is $BaTiO_3$, a material with one of the largest known electro-optic coefficients.

A specialized MOCVD system to deposit ferroelectric oxide films has been designed, constructed, and placed into operation. Polycrystalline films of $BaTiO_3$ have successfully been deposited on fused silica substrates. Process variables are the metalorganic source temperatures, the carrier gas flow rates through the source bubblers, oxygen gas flowrate, substrate temperature and total pressure. Stoichiometric $BaTiO_3$ films were deposited; the films were approximately 1.2 μm thick, X-ray diffraction indicated that the films did not have a preferred crystallographic orientation. Energy dispersive x-ray analysis gave a molar ratio Ba:Ti=1.1. The grain size was $\sim$ 100 nm. The films were translucent and white-colored due to light scattering from the grain boundaries.

Additional microstructural characterization and identification of defect structures will be performed by backscattered electron diffraction, wavelength and energy dispersive x-ray spectrometry, scanning and transmission electron microscopy, and Raman spectroscopy. Electrical, optical and electro-optical properties of the films will be measured and correlated with the defect structures. The information from these characterization studies will provide

guidance for optimizing the deposition process in order to improve the quality of the films. The next phase of this program will be a collaborative effort with the Electromagnetic Technology Division (Boulder) to fabricate and test devices from well-characterized, high-quality films.

Characterization of Barium Titanate Films

L. H. Robins, D. Kaiser, L. Cook, P. Schenck and M. Vaudin

Microcrystalline films of $BaTiO_3$ are being deposited by laser ablation and by the MOCVD method discussed above. In laser ablation, an excimer-laser beam is used to evaporate $BaTiO_3$ from a target and deposit a film of the material on a remotely located substrate.

Transmittance and reflectance spectroscopy in the 0.5-6.5 eV spectral range is being used to obtain thicknesses, refractive indices, and optical absorption spectra of these films. Because the laser-ablated films are deposited on platinum-coated silicon substrates, they could only be characterized by reflectance and only thickness and refractive index dispersion could be calculated from these measurements. An MOCVD film, which was deposited on fused-silica substrates, was characterized by both transmittance and reflectance. By fitting both the transmittance and reflectance spectra to a model function, values for the film thickness, refractive index, and optical absorption coefficient were obtained. Because the MOCVD film was amorphous according to X-ray diffraction, the optical properties were not expected to match those of crystalline $BaTiO_3$.

Raman spectroscopy has been used to characterize the structure of the laser-ablated films. It is capable of distinguishing between different crystalline phases of $BaTiO_3$, in particular the nonferroelectric cubic phase and the ferroelectric tetragonal phase. This is because some of the lines in the Raman spectrum are uniquely associated with the tetragonal phase. In bulk single crystals of $BaTiO_3$, the tetragonal phase is stable from below room temperature up to about 100° C, and the cubic phase is stable at higher temperatures. However, the behavior of thin films is more complicated because a variety of phases can be quenched into the film when it is deposited. Raman spectroscopy of $BaTiO_3$ is more sensitive to the cubic-tetragonal phase transition, which involves very small atomic displacements, than x-ray diffraction.

Because Raman spectroscopy has a much higher spatial resolution than x-ray diffraction, it can be used to map the phases present in the film. In one laser-ablated film characterized by spatially resolved Raman spectroscopy, the magnitudes of the lines associated with the tetragonal phase were found to decrease with increasing distance from the center of the deposited area. This preliminary experiment shows that Raman spectroscopy can be used to obtain structural information not readily obtainable by x-ray diffraction. As part of future work, we will begin to characterize the MOCVD-grown films by Raman spectroscopy.

DIAMOND THIN FILMS

Chemical vapor deposition of diamond will have a significant economic impact in the near future on a range of commercial products including durable cutting tools and heat dissipating substrates for electronics and opto-electronics. Diamond is an enabling technology because its economic impact will be greater than the market for the material itself, creating markets that might not otherwise develop. Thus, CVD diamond research at NIST is important for helping U.S. industry obtain a competitive edge. In addition to research on materials characterization methods, NIST has been making an significant impact by organizing standards related workshops at which representative of U.S. companies come together to decide on generic issues important to diamond technology.

Optical and optoelectronic characterization of CVD diamond films

L. H. Robins, E. N. Farabaugh, A. Feldman, and David Black

Synthetic diamond is a potentially superior optical material for a number of applications because of its wide transparency range, from deep-ultraviolet to far-infrared, and because of its mechanical, thermal, and chemical properties, which lead to good survivability in severe environments. Diamond also shows promise for optoelectronic applications, such as a full-color solid-state display, which would be based on the visible light emission (luminescence) of defects. Chemical vapor deposition (CVD) techniques developed in the last decade have enabled the growth of diamond particles and films at low pressure. In our research, we utilize several types of optical spectroscopy to investigate the relationships between the optical properties of CVD diamond specimens and the deposition conditions for these specimens. The goal of this research is to optimize the properties of CVD diamond for selected optical or optoelectronic applications. A major theme of this work has been the influence of imperfections, such as point defects, extended lattice defects, chemical impurities, and non-diamond phases, on the optical properties.

We have used CL imaging and spectroscopy to study small diamond crystallites grown by hot-filament CVD. These experiments focussed on the near-bandgap luminescence (4.7 eV to 5.5 eV) which was due primarily to exciton recombination. Two types of excitons, distinguished by different spectral characteristics, can be present: free excitons, which are intrinsic excitations of the defect-free crystal, and bound excitons, which are localized at defects or impurities. Two specimens containing diamond crystallites were grown and examined. One specimen contained about 500 ppm boron, and the other specimen was nominally undoped. In both specimens, the temperature dependence of the exciton CL spectra over the temperature range 80 K to 300 K was used to obtain the binding energy of the bound excitons. The dominant component of the exciton luminescence in the boron-doped crystallites came from boron-acceptor bound excitons. In addition to the expected free-exciton features, the exciton CL spectra from the undoped crystals contained several bound-exciton lines that have not been observed before, to our knowledge. We have not yet identified the defects or impurities that give rise to these bound excitons.

We have also used CL imaging and spectroscopy to characterize large single-crystal diamond specimens grown by the high-temperature high-pressure method at the General Electric Company. A detailed mapping was made of a 0.5 × 0.5 cm wafer that had been characterized previously by x-ray topography and etch-pit defect analysis. Both the exciton CL and the deep defect CL were examined. The deep defect CL showed a greater spatial variation than the exciton CL, which was dominated by free excitons. Two of the observed defect CL bands were found to be localized in regions of high dislocation density. One of the spatially localized bands is thought to arise from intrinsic dislocation-related defects such as dangling bonds. The other spatially localized band is attributed to a defect complex that contains nitrogen and atomic vacancies. Thus, nitrogen and atomic vacancy complexes can be associated with dislocation sites. This type of information cannot be obtained by x-ray topography alone.

Raman spectroscopy is widely accepted as the technique for evaluating the quality of CVD diamond. It is especially sensitive to contamination of specimens by disordered nondiamond carbon phases. We have carefully examined the form of the Raman spectra of a number of diamond specimens grown by hot-filament and microwave-plasma CVD. All of the Raman spectra could be accurately represented by four components: a narrow Lorentzian line due to crystalline diamond; two broader Gaussian lines attributed to nondiamond carbon; and, a broad photoluminescence (PL) background. The width of the diamond line first increased with increasing nondiamond carbon content, but to then reached a maximum width of 15 cm^{-1}. This behavior is shown in Fig. VI-1, where the full width at half maximum of the diamond Raman line is plotted as a function of the intensity of the PL background; the PL background, in these films, increases with increasing nondiamond carbon content. The diamond Raman linewidth is believed to vary inversely with the average size of a crystalline domain; thus, the observation of an upper limit to the diamond linewidth implies that there is a lower limit to the size of the crystalline diamond domains.

High Resolution Electron Microscopy of Diamond Film Growth Defects and Their Interactions[1]

Dan Shechtman[2], A. Feldman, M. Vaudin, and J.L. Hutchison[3]

[1]Supported in part by the Office of Naval Research
[2]Technion (Israel), Guest Scientist at NIST and at the Johns Hopkins University
[3]Oxford University (UK)

Defects introduced during the growth of diamond by chemical vapor deposition (CVD) can play a major role in the rate of growth and in the performance of the material in a many applications. For example, twins, stacking faults and grain boundaries may increase the rate of growth while at the same time causing unwanted optical absorption that would not occur if the material were perfect. In addition, the size and distribution of noncoherent twin boundaries is expected to affect the fracture strength of the diamond. High resolution transmission electron microscopy (HRTEM) has been used to examine the nature of lattice defects in CVD diamond at atomic dimensions. During the past year, previously unexplained features in HRTEM lattice images of CVD diamond have been explained as Moire fringes

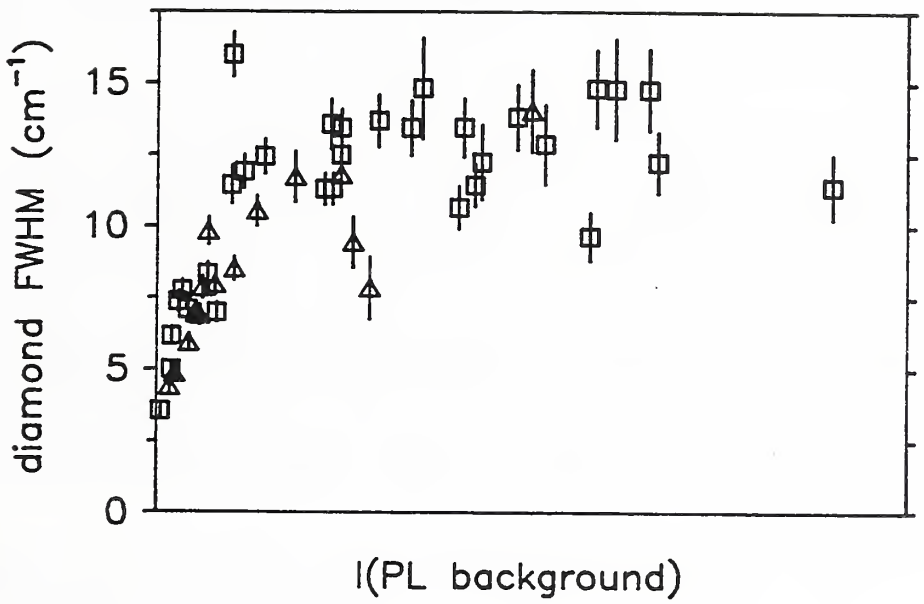

Figure VI-1. Full width at half maximum of the diamond Raman line as a function of photoluminescent background intensity for a series of CVD diamond films demonstrating saturation in the value of the line width. The saturation of the linewidth implies a minimum size to the diamond crystallites within the films.

that occur when a noncoherent boundary between two twins is not parallel to the viewing direction, resulting in a superposition of images. In general, we have observed four types of twin boundaries in CVD diamond. In terms of the coincidence site lattice (CSL) notation these twin boundaries are called $\Sigma=3$, $\Sigma=9$, $\Sigma=27$, and $\Sigma=81$.

Figure VI-2 shows both coherent and noncoherent twin boundaries in the CVD diamond specimen. The coherent boundaries are all of type $\Sigma=3$. A noncoherent boundary can be observed meandering across the micrograph. Where the boundary is parallel to the electron beam (**V**), its image is lighter than the images of coherent boundaries because of preferential ion thinning; this suggests that the noncoherent boundary has greater energy than the coherent boundaries. From the relative orientations of the {111} planes on opposite sides of a boundary, we have identified noncoherent boundaries of types $\Sigma=3$ and $\Sigma=9$. Noncoherent twin boundaries of types $\Sigma=27$ and $\Sigma=81$ can be seen in Fig. VI-3, which shows a region containing a twin quintuplet (discussed below).

In CVD diamond, $\Sigma=9$, $\Sigma=27$ and $\Sigma=81$ boundaries are usually observed to be noncoherent. This is in marked contrast to observations made in silicon, where $\Sigma=9$ and $\Sigma=27$ boundaries are usually coherent. Noncoherent boundaries arise when the free surfaces of two twin-related crystals grow toward each other and meet at an arbitrary surface. The boundary that is formed results from the detailed kinetics and energetics of the diamond growth specific to a particular specimen. Thus, a noncoherent boundary can even occur when two crystals of the same orientation grow together. There may be some slight displacement of the two crystals relative to each other and there is insufficient energy to allow the boundary to annihilate. Such a displacement is seen in Fig. VI-2 (**W**), where two crystals of identical orientation have formed an interface of relatively low density.

Noncoherent boundaries can arise during the early stages of the nucleation and growth of a diamond twin quintuplet, a structure frequently observed to be the origin of growth of a grain. An example is shown in Fig. VI-3 where the center of the twin quintuplet is marked ★. Figure VI-4(a) shows a computer simulation of the twin quintuplet in $<110>$ projection; in three dimensions, the twin quintuplet consists of five successive tilt boundaries radiating from a common $<110>$ rotation axis. Four of the boundaries are coherent twin boundaries of type $\Sigma=3$ with a tilt angle of 70.53°. The fifth boundary is of type $\Sigma=81$ with a tilt angle of 77.88°. The difference between the $\Sigma=81$ tilt and the $\Sigma=3$ tilt leaves a small mismatch angle of 7.35° between {111} planes in the twins separated by the $\Sigma=81$ boundary as shown in Fig. VI-4. The $\Sigma=81$ boundary can be modeled as a $\Sigma=3$ twin boundary containing regularly spaced secondary dislocations to accommodate the mismatch angle. However, because this boundary is the last to form during nucleation of a twin quintuplet, the boundary forms in a noncoherent manner inherent to the quintuplet structure.

Several regions associated with the noncoherent boundary in Fig. VI-2, such as is indicated by **X** and **Y**, do not exhibit the typical appearance of $<110>$ oriented diamond evident throughout most the micrograph. These regions can be interpreted as Moire-fringe patterns that result when the twin boundaries are inclined with respect to the electron beam so that the beam passes through two overlapping twins. Region **X** is a boundary of type $\Sigma=3$ whereas region **Y** is a boundary of type $\Sigma=9$.

We have modeled the periodicities observed in the images of the inclined $\Sigma=3$ and $\Sigma=9$ noncoherent boundaries using a graphical projection of the diamond lattice viewed along the <110> direction. In the twin quintuplet modeled in Fig. VI-4(a) 5 twin domains are labeled **A**, **B**, **C**, **D** and **E**. If we enlarge the twin in region **A** to overlap the entire twin quintuplet, we obtain overlap patterns with the periodicities of the CSLs having $\Sigma=3$ (**A** overlap with **B**), $\Sigma=9$ (**A** overlap with **C**), $\Sigma=27$ (**A** overlap with **D**) and $\Sigma=81$ (**A** overlap with **E**) misorientations (Fig. VI-4(b)). The overlap of region **A** with region **B** shows a striped pattern having the same periodicity as region **X** in Fig. VI-4. The overlap of region **A** with region **C** shows a centered hexagonal pattern having the same periodicities as the $\Sigma=9$ overlap region labeled **Y** in Fig. VI-4. Furthermore, the relative orientations of the $\Sigma=3$ CSL, the $\Sigma=9$ CSL, and the non-overlapping regions seen in Fig. VI-4(b) are the same as the relative orientations of the stripes in region **X**, the hexagonal patterns in region **Y**, and the non-overlapping crystals seen in Fig. VI-4.

HIGH T_c SUPERCONDUCTING CRYSTALS

Large scale commercial applications of high temperature superconductions will depend our ability to produce material that can sustain high critical current densities (J_c). Our ability to control a prime factor in promoting high J_c, flux pinning, is the motivation of the research discussed below.

Mapping of Magnetic Flux Distributions by a Magneto-Optical Imaging Technique

D.L. Kaiser, M. Turchinskaya[1], F.W. Gayle[2], A. Shapiro[2], A. Roytburd[3], A.A. Polyanskii[4], V.K. Vlasko-Vlasov[4] and V.I. Nikitenko[4]

[1]Consultant
[2]Metallurgy Division
[3]University of Maryland
[4]Institute for Solid State Physics, Russian Academy of Sciences

Real-time, quantitative mapping of magnetic flux distributions in high temperature superconductors is critical to understanding the effect of microstructural defects on the dynamics of magnetic flux flow. Such information is essential in the search for strong flux pinning centers required to attain the high critical current densities needed for high magnetic field applications. Through a collaborative effort with researchers from the Russian Academy of Sciences, we have set up a high-resolution, magneto-optic imaging facility that is capable of mapping flux distributions in superconducting materials. The imaging system described below has been used to study the effect of twin and grain boundaries on flux flow in $YBa_2Cu_3O_{6+x}$ (YBCO) crystals.

The magneto-optical imaging technique has been developed and improved by our Russian collaborators. In the technique, a Bi-doped yttrium iron garnet film is placed atop a superconducting specimen that is located in a miniature liquid helium cryostat. The temperature of the cryostat is controlled from 4.2 to 400 K by means of a heater. A constant magnetic field is applied to the specimen via an external electromagnet. A magnetic flux

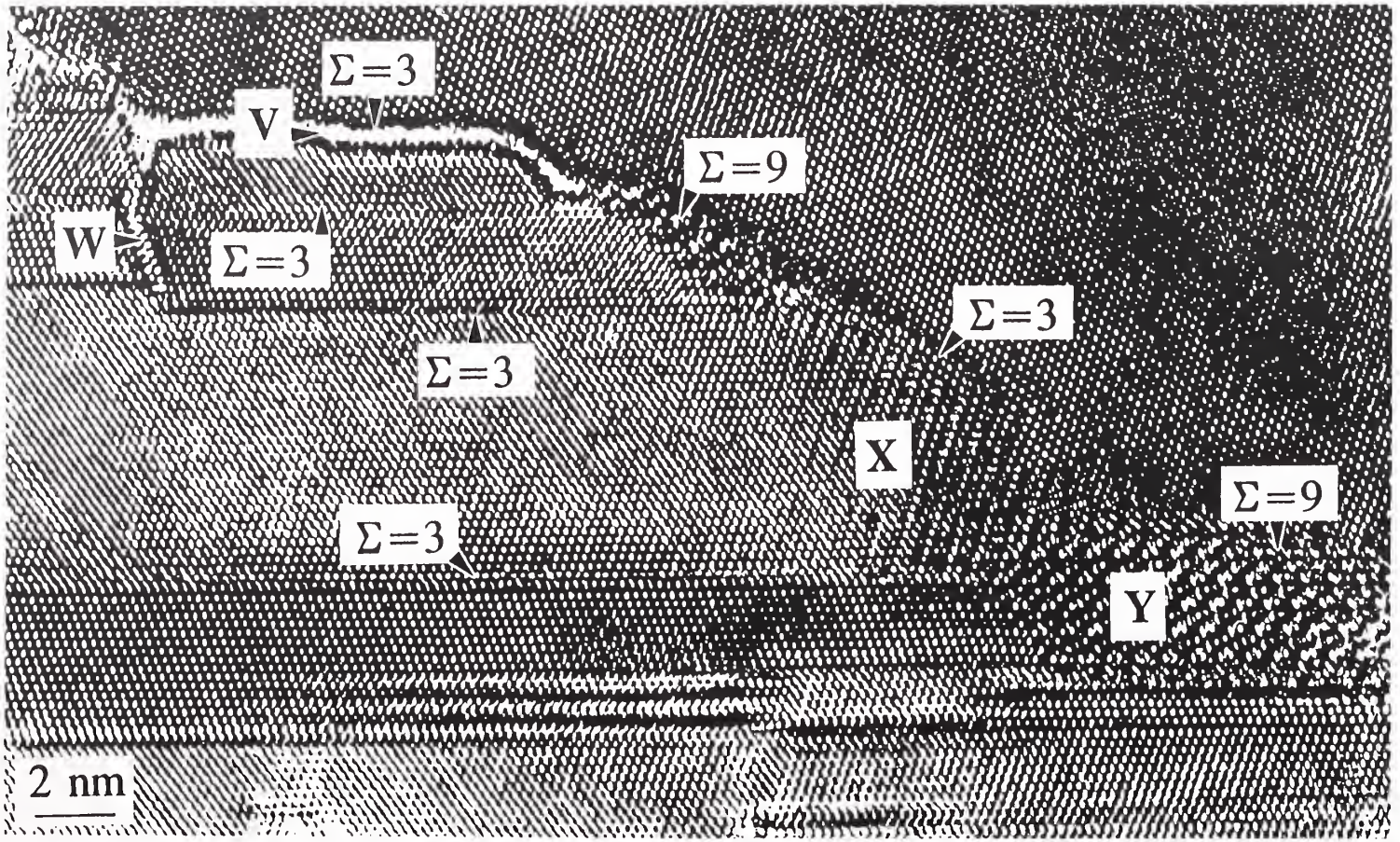

Figure VI-2. Lattice image of a CVD diamond specimen observed in a <110> direction. The figure shows coherent twin boundaries of type Σ=3, noncoherent boundaries of types Σ=3 and Σ=9, and Moire fringes. V - a noncoherent twin boundary, W - boundary showing a small relative displacement of twins of the same orientation, X - region of Moire fringes corresponding to a Σ=3 coincident site lattice, Y - region of Moire fringes corresponding to a Σ=9 coincident site lattice.

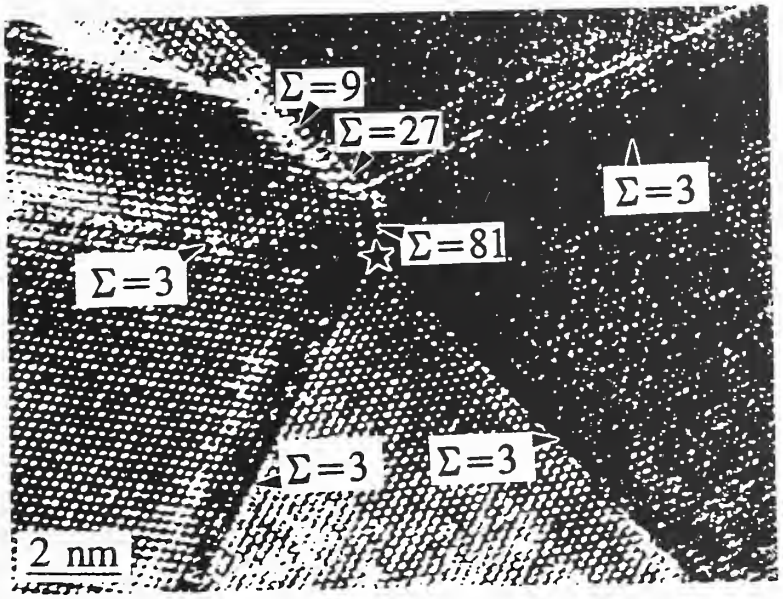

Figure VI-3. Lattice image of CVD diamond containing a twin quintuplet observed in a <110> direction. Σ=3, Σ=9, Σ=27, and Σ=81 boundaries can be observed.

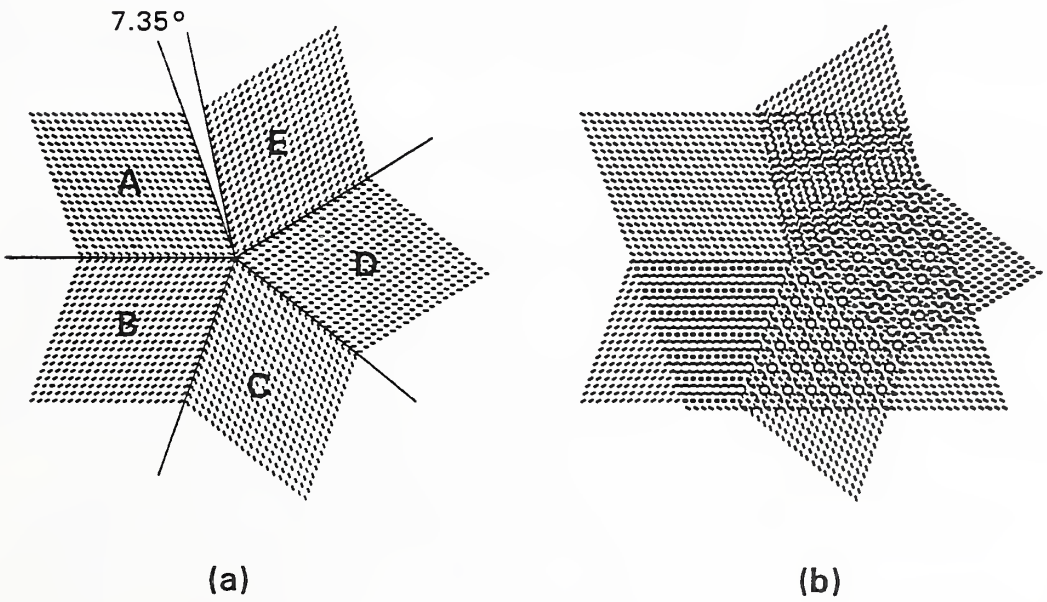

Figure VI-4. Computer model of a twin quintuplet where the {111} planes bounding in each of the twins are indicated by the lines. (b) Overlapping twins having coincidence site lattices of types Σ=3, Σ=9, Σ=27 and Σ=81. The simulations are observed along a <110> direction.

distribution is induced in the superconductor by the applied a magnetic field. This induced flux passes into the garnet indicator film and modifies the garnet domain structure. Polarized optical radiation passes through the garnet film. Because of the Faraday effect, the polarization of light propagating through the film is rotated. The amount of rotation depends on the strength of the magnetic flux in the film; thus, an image of the flux distribution can be obtained from observation of this light through light polarizing components. In this particular system, dual-color maps are produced wherein the color indicates the field direction and the intensity is directly related to magnetic field strength.

The flux map of an indicator film is imaged in a polarizing light optical microscope with an attached video system, permitting direct, real-time observation and recording of flux flow dynamics. The intensity level is correlated to magnetic induction by in-situ calibration of the indicator film in various magnetic fields. The maps are then processed in an image analysis system to generate contour maps of magnetic induction as well as induction profiles along a selected line.

Flux penetration studies on YBCO crystals have yielded new results on the effect of twin structure and grain boundaries on flux flow. Flux pinning was found to be lowest in twin-free material and increased with increasing twin density. In a twinned region, flux penetrated preferentially along the direction of the {110} twin boundaries. Pinning by twin boundaries was highly anisotropic: the flux gradient across twin boundaries was estimated to be ten times higher than that along twin boundaries at 17 K.

Bicrystals with {001} tilt grain boundaries were mechanically polished and examined in the imaging system. Flux penetrated along many grain boundaries at applied fields as low as 3.5 mT. The depth of subsequent flux penetration into the grain depended on the twin density and twin boundary orientation along the grain boundary. Penetration depth was greatest when twin boundaries were normal to the grain boundary and the resistance to flux flow increased with increasing deviation from this normal.

Photonic Materials Workshop - S. W. Freiman and J. A. Carpenter, Jr.

A Photonic Materials Workshop, sponsored by NIST and the Optoelectronics Industry Development Association (OIDA), was held at NIST August 26-27, 1992. The objective of the workshop was to identify and prioritize materials R&D issues relevant to photonic products expected to appear in commercial markets over the next 3-15 years. Organized by a steering committee of industrial, Department of Commerce (DOC), and NIST personnel, the by-invitation-only workshop was attended by a total of 87 persons from 27 industrial firms, academia, DARPA, SDIO, the Sandia and Lawrence Livermore National Laboratories, and NIST. Key overview presentations identified issues in the key material areas of semiconductors, polymers, and ceramics. A view of the Japanese efforts in photonics relative to that in the U.S. was also presented. Dr. Robert White, Undersecretary for Technology of the Department of Commerce, addressed the workshop on various federal government efforts aimed at promoting the R&D of U.S. industrial firms in the photonics area.

Working Group Sessions were held in six areas: sources and detectors, display, storage, active devices (other than the four previously listed), packaging, and passive devices (other than packaging); specific materials R&D needs and opportunities were identified by each group. the major conclusion of the workshop was that for commercial applications the major materials R&D issues of importance over the next 3-15 years will be those associated with reductions in costs of the products. An initial, oral report to the OIDA was made at one of their meetings on September 17, 1992; a full report is being prepared by NIST.

VII. MATERIALS MICROSTRUCTURE CHARACTERIZATION

Gabrielle Long

Materials Characterization is the fundamental link in the processing/microstructure/properties chain which enables next-generation advances in technological materials. To support a characterization program of the highest quality, the Materials Microstructure Characterization Group operates the two NIST/MSEL x-ray beamports at the National Synchrotron Light Source where group members carry out state-of-the-art measurements on ceramic, semiconductor, photonic and other materials of high-current interest. There is also an active research program involving in situ microstructure development at the NIST Research Reactor. Taken together, the x-ray synchrotron and the neutron scattering programs provide a unique portfolio of advanced characterization techniques for scientists from the Ceramics Division, from NIST, and from the greater scientific community.

The range of scientific problems which the Group addressed this year has been exceptionally broad. Substantial progress has been made in understanding processing of ceramic oxides and porous materials, hydration of cements and mortars, creep cavitation in ceramics, atomic scale structure of surfaces and interfaces of metal to III-V semiconductors, and the electronic structure of high T_c superconductors as a function of chemistry. In addition, the Group has collaborated in research involving the in situ observation of the nucleation of zeolites, imaging of defects in III-V and II-VI single crystals and man-made diamonds, and fundamental studies in catalysis. The x-ray beamline capabilities were enhanced such that this year we supported forefront research in biology involving x-ray scattering in liquid cells and in humid environments. In another remarkable experiment, the ultra-low-angle x-ray scattering instrument was used to provide data overlapping static light scattering and conventional small-angle x-ray scattering to achieve data ranging from 100 μm to 1 nm on a technologically-important foam.

The long term goal of research in crystal regularity is to enable photonic and electronic device manufacturers to produce superior devices on the basis of innovative structural information not available elsewhere. This goal determines two long term objectives: (1) Identification of those crystal structure irregularities that most affect critical device performance parameters, and (2) Understanding of the genesis of these structural irregularities during crystal growth, subsequent crystal handling, and device processing so that these processes can be optimized.

Achievement of these objectives requires highly sensitive techniques for surveying the presence and spatial distribution of various crystal irregularities, determination of their precise nature, and development of an understanding of their genesis. For those effects that are transitory, which are essential for photonic and electronic devices for information processing, the development of techniques for real time observation is a key component of a comprehensive program.

Overall, the combined measurement capabilities which are now available are unique in the world in sensitivity, size range, analysis and imaging capacity. In the coming year, new equipment will be commissioned so that the mechanical capacity of the beamline can keep pace with ever more demanding scientific opportunities.

Significant Accomplishments

- Measurements were made with the high resolution ultra-low-q small-angle x-ray scattering camera which bridge the gap between static light scattering and conventional pin-hole x-ray scattering. The data, on a microporous polyacrylonitrile foam, span the microstructural size range from 100 μm to 1 nm scales. This extraordinary size range capability is essential for the characterization of modern technological materials.

- By microscopically manipulating the Ångstrom-scale x-ray interference fields produced during Bragg diffraction, the x-ray standing wave technique was used to determine perpendicular atomic distances to host substrate planes at surfaces and interfaces with unprecedented accuracy. Our structural determinations include: the bond-length conserving rotation model for clean III-V semiconductor surfaces, the epitaxial continued layer structure for Sb/Si(111) and Sb/Si(100), and the amphoteric nature of In bonding at the Si(111)$\sqrt{3}$x$\sqrt{3}$-In interface. Structures such as these are of critical importance for next-generation submicron electronics and optics.

- High resolution small-angle x-ray and neutron scattering measurements have proven that the microstructure of microporous silicas can be successfully engineered from the micrometer scale down to the nanometer scale. These custom materials are important in emerging technologies for filters and membranes, catalysis supports, sensors, transparent insulators, and matrix materials for second phase infiltration.

- Studies of the microstructure evolution during sintering of silicon nitride have elucidated the role of various dopants in the densification process. Silicon nitride is a prime candidate for components in heat engines, and the mechanisms operative during the processing of this material must be well understood before product reproducibility and reliability will be achieved.

- Oxygen K near-edge fluorescence-yield spectroscopy was successfully used to characterize the bulk oxygen hole-state density of high temperature superconductors. The hole state density was measured as a function of superconductor composition and was correlated to x-ray diffraction and critical temperature results. A knowledge of the hole state density is essential toward developing an understanding of high T_c materials.

- Small-angle neutron and small-angle x-ray scattering measurements have been performed in-situ during the nucleation of zeolite A and zeolite X, with and without template molecules present. Because of our unusual size-range capability, both the development within the gel and the nucleating populations of crystals could be followed as a function of time. These are the first successful measurements of the microstructural evolution during nucleation and the results show graphic evidence of the supporting role of the template.

- Scattering studies of creep cavity development in silicon nitride have indicated the importance of an unsuspected small population of large cavities (0.6-1 μm) in the creep process. This kind of information is expected to lead to an improved model of the failure law in this important material.

- In situ observation of pressure figures in single crystals indicate that the percussion figure in calcite is nucleated by elastic twinning. The twinning becomes locked in when the stress concentration at the head of the twin lamalla reaches cleavage fracture value. These studies are used to assess the cohesive strength and structural stability of single crystals.

- The first direct observation of crystal lattice deformation associated with optically induced fields in photorefractive materials has been made. High resolution diffraction images of the piezoelectric strain pattern induced by the mixing of two laser beams display distinct gratings. This is the first major step in the determination of the influence of various crystalline irregularities on such optical interactions, which are of major potential importance in the processing and storage of optical information.

- Gallium arsenide wafers grown by a new commercial technique, vertical gradient freeze, have been shown to have a dramatically lower density of the cellular irregularities characteristic of the current liquid encapsulated Czochralski (LEC) process, and none of the very low angle grain boundaries typical of LEC material. This latter observation undoubtedly explains the substantially greater resistance of the new material to fracture.

- The triglycine crystal grown on space shuttle IML-1 has been examined with high resolution diffraction imaging, both before and after slicing for the formation of infrared detectors; the local acceptance angle for diffraction from the uncut crystal, 1-2 arc seconds, indicates extraordinary crystal regularity. Observation of the cut edge of the final crystal shows continuity between the seed and the space growth, indicating a high degree of epitaxy of the space growth.

The Role of Zirconia Addition in Pore Development and Grain Growth in Alumina Compacts

G. G. Long, S. Krueger[1], Y-M. Pan[2], and R. A. Page[2]

[1]Reactor Radiation Division
[2]Southwest Research Institute

The sinterability of ceramics and the properties of the product material depend on their internal structure. The effect of grain growth on pore stability has been extensively discussed by a number of investigators. As pointed out by Kingery and Francois and others, pore stability depends on both the value of the dihedral angle and the pore/grain size ratio; and there is a critical pore coordination number above which the pore is stable, and below which it is unstable. In earlier studies at NIST, the evolution of the porous phase within alumina during sintering, with and without the addition of magnesia, was measured using multiple small-angle neutron scattering (MSANS) and small-angle x-ray scattering. The results of those investigations indicated that the role of MgO as a sintering aid lies, at least in part, in prolonging the stability of intermediate-stage sintering such that the body achieves greater density before the transition to isolated porosity takes place, leading to a finer-grained finished ceramic. In our current program, we have measured the microstructure evolution of undoped alumina and of an alumina/10 vol.% zirconia using MSANS and stereological analysis to follow both the porous phase and the crystalline phases during sintering of the alumina compacts.

The effects of zirconia inclusions on the grain growth and sinterability of alumina has been studied by Lange and others. They found that alumina compacts containing enough zirconia (> 5 vol %) to fill a majority of four-grain junctions in the alumina matrix showed more effective grain-growth control than those of low zirconia compositions (< 2.5 vol. %) with partially-filled four-grain junctions. Until now, however, the evolution of the pore-size and grain-size distributions had not been characterized together, and thus the trajectory in microstructure space was unknown.

The effective pore radius (Fig. VII-1) and the effective grain size (Fig. VII-2) as a function of density indicate a delay in the onset of the final sintering stage for alumina/zirconia (96% TD) compared to alumina (92% TD), and show that the zirconia second phase is very effective in inhibiting growth of the alumina grains. SEM observations on both polished and fracture surfaces showed that abnormal grain growth develops in the single-phase alumina at a relatively low density (86% TD), and some of the pores were separated from grain boundaries and trapped inside grains. Such abnormal grain growth and pore-grain boundary separation were not observed in the alumina/zirconia composite. Thus, the zirconia phase was very effective in controlling grain growth and in preventing pore-grain boundary separation. It appears that both the dragging force exerted on the alumina by the zirconia and the kinetics influence the microstructure development during the densification of alumina/zirconia.

Future research will focus on the role of particle size in sintering. We will be measuring the porous phase and crystalline phase evolution as a function of grain size in bimodal powder compacts. Results from that research are expected to yield direct information on the

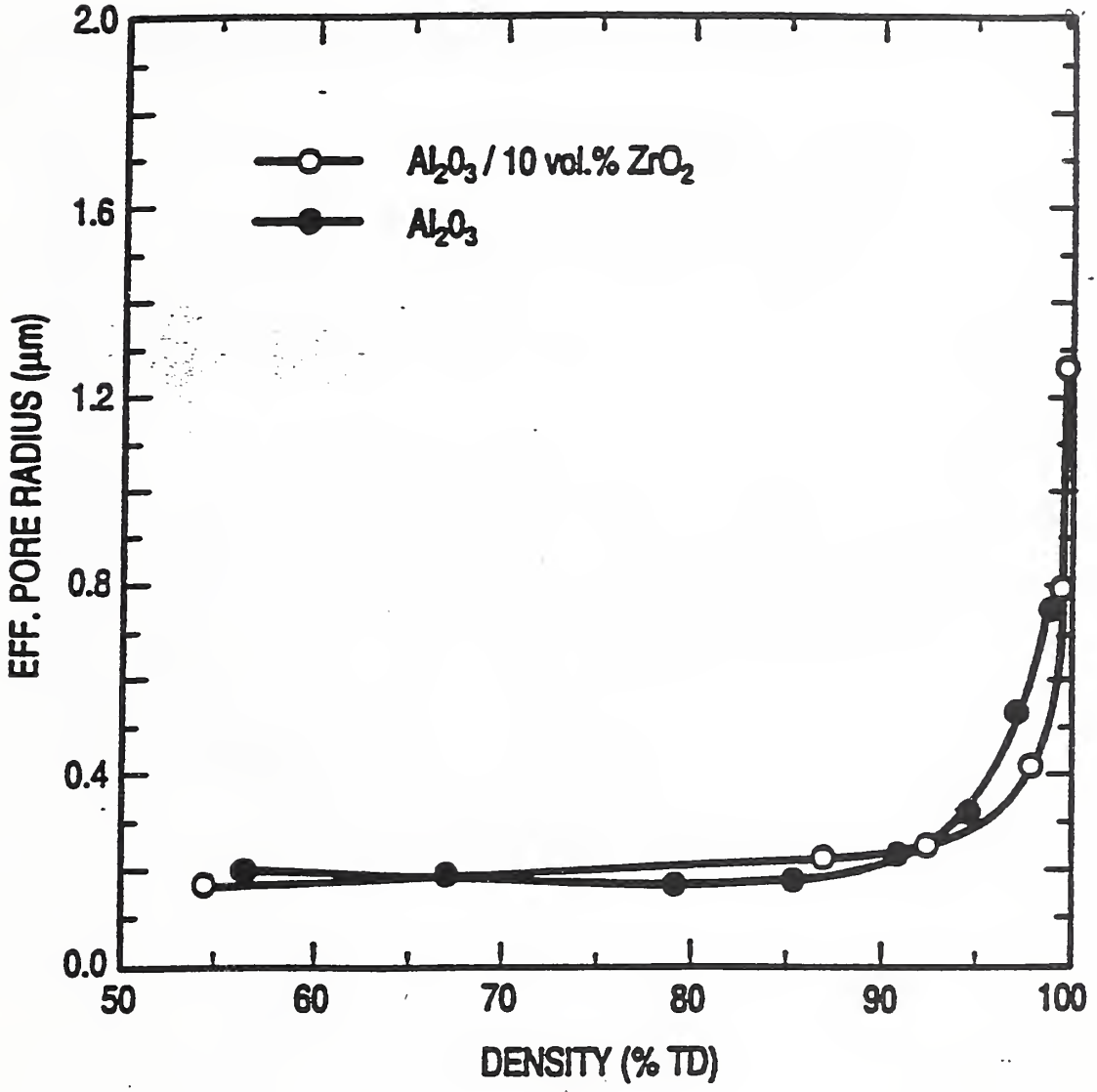

Figure VII-1. Effective pore radius as a function of percent theoretical density for $A\ell_2O_3$ and $A\ell_2O_3$/10 vol. % ZrO_2

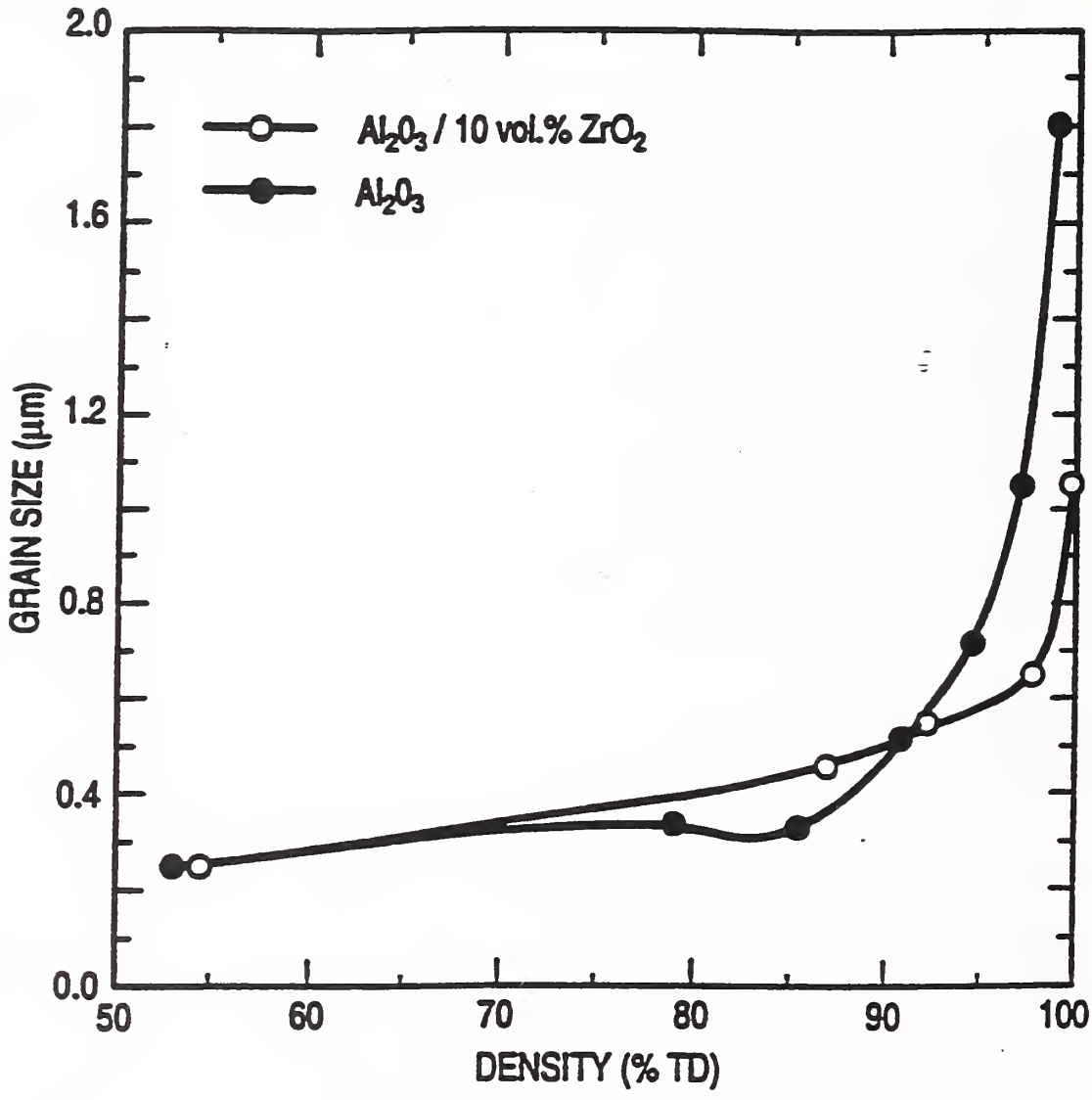

Figure VII-2. Effective grain size as a function of percent theoretical density for $A\ell_2O_3$/10 vol.% ZrO_2.

mechanisms by which powder size and size distributions affect green density, pore channel size during intermediate stage sintering, densification rate, the required sintering temperature, and the onset density at the transition to final stage sintering.

Small-angle X-ray Scattering Study of Creep Cavity Development and Creep Lifetime of Silicon Nitride

G. G. Long, W. E. Luecke, S. M. Wiederhorn and B. J. Hockey

Accurate lifetime prediction is essential to the acceptance of advanced ceramic materials for high-temperature applications. Our research is aimed at gaining an understanding of the microstructural origins of processes that limit the lifetimes of such ceramics. Under low stress at elevated temperatures, many advanced ceramics fail by a process known as creep rupture in which they show up to several percent strain-to-failure over a lifetime of tens to thousands of hours.

In an attempt to understand the microstructural origins of creep rupture, we characterized the creep rupture process for a single commercially available Si_3N_4 (Norton NT154). By testing several dozen specimens in uniaxial tension creep, we thoroughly mapped out the stress-strain rate-temperature-lifetime response of the material. From the suite of deformation conditions we chose four specimens for further characterization by SANS, TEM and SAXS. Especially important was the fact that we were able to examine using TEM the same specimens characterized by SAXS. The results of the SAXS analysis gave us new insight into the cavitation process. Specifically, we found that large (0.6-1 μm), rare cavities at three-grain junctions were dominating the volume fraction distribution, even though smaller (0.1-0.2 μm) cavities on two-grain junctions were much more common. A maximum entropy analysis of the SAXS curves is shown in Fig. VII-3. Subsequent TEM analysis confirmed the bimodality of the cavity size distribution. With this information in hand, we are currently attempting to determine the mechanism by which the cavities evolve with increasing strain by characterizing specimens that have not been tested to failure. Knowledge of the cavity evolution mechanism will enable us to model the failure law, and better predict lifetimes for this class of materials.

Microstructure Evolution of Silicon Nitride During Sintering

A. J. Allen[1], S. Krueger[2], J. Hwang[3] and G. G. Long

[1]University of Maryland
[2]Reactor Radiation Division
[3]Dow Chemical Corporation

Among modern light-weight ceramics with outstanding wear-resistance, strength and thermal stability, silicon nitride is one of the most promising. It combines good high-temperature properties (such as high strength, corrosion resistance against fused metals, chemical inertness and oxidation resistance in air) with excellent thermal-shock resistance and fracture toughness. For these reasons, silicon nitride is increasingly being considered for the high-temperature components in gas turbine or automotive applications. A major goal in silicon nitride processing

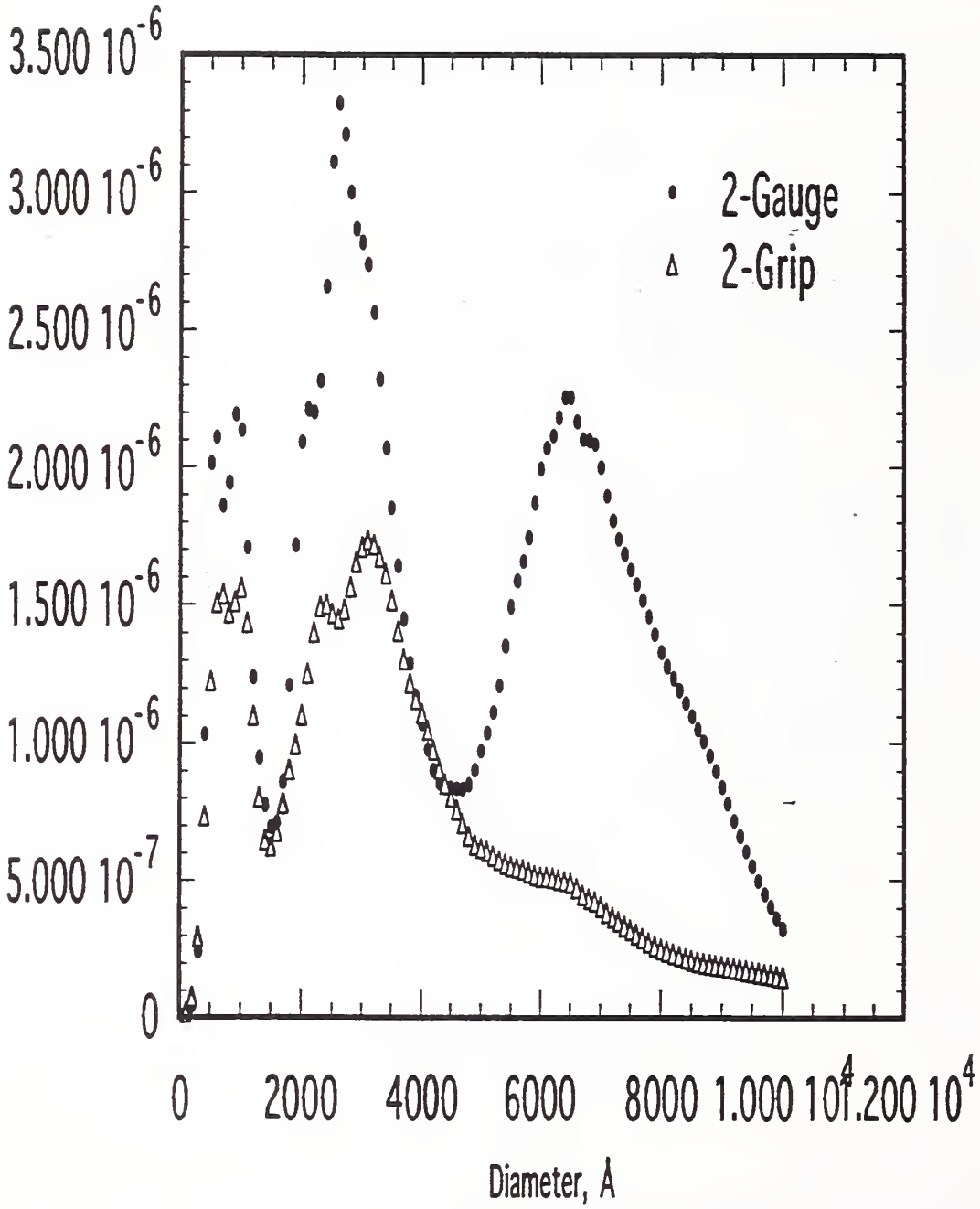

Figure VII-3. Volume distribution of cavities (dV/dD) as a function of their diameter (D). Both the uncrept (grip) and the crept (gauge) results are shown for sample 2.

is to achieve at minimum cost a high density and reproducible product with a microstructure tuned to deliver optimal material properties for the particular application required.

Densification of silicon nitride during sintering varies significantly when different sintering additives are used, and these differences often give rise to variations in the microstructural development and mechanical properties. Thus we have been interested in correlating the pore evolution of silicon nitride from initial through intermediate and final-stage sintering with the viscosity of the glass or liquid phases derived from different sintering additives. Using small-angle neutron scattering (SANS) and multiple-small-angle neutron scattering (MSANS) methods to determine the pore surface area and mean pore diameter respectively as a function of sintered density, we have studied the microstructural evolution during sintering with both yttria and magnesia additives.

Figure VII-4 shows that the reduction in pore surface area with sintered density is the same for both the Si_3N_4-MgO and Si_3N_4-Y_2O_3 systems. However, the pore diameters determined by MSANS, (Fig. VII-5) reveal opposite trends for the two additives. The increasing pore-size for Si_3N_4-MgO is probably associated with a relatively low viscosity liquid phase, a low liquid eutectic temperature and a slow transformation from the α-Si_3N_4 phase to β-Si_3N_4. Thus there is little to interfere with the stable growth of solid agglomerates and the associated coarsening of the pore gaps between them. For Si_3N_4-Y_2O_3, the liquid phase is more viscous and is formed at a higher eutectic temperature. Furthermore, the system has a somewhat higher α-β transformation rate. The early stage during which there is an apparent rise in pore diameter, is probably associated with the loss of small pores. This is similar to an effect observed previously in glassy silica. However, the combined effects of the different eutectic mix, particularly the α-β transformation which gives rise to fibrous β-phase Si_3N_4 grains, seem to result in continued pore filling of the larger pores to high sintering densities.

Controlled Porosity Ceramics

H. M. Kerch[1], G. G. Long, S. Krueger[2], A. J. Allen[3], H. E. Burdette, D. B. Minor, E. J. Garboczi[4], and F. Cosandey[5]

[1]Guest Scientist, John Hopkins University
[2]Reactor Radiation Division
[3]Guest Scientist, University of Maryland
[4]Building Materials Division
[5]Rutgers University

Controlled porosity materials are an important family of ceramics in which microstructure and performance are strongly correlated. These custom-engineered systems are currently being developed as filters and membranes, catalysis supports, sensors, transparent insulators, and matrix materials for second phase infiltration. The success of controlled porosity materials in these applications depends on our ability to produce pore volumes tailored to specific pore sizes and size distributions. The desired microstructure is commonly achieved by heat treatment of an appropriate precursor material. While there exist theoretical predictions of microstructure evolution during sintering, little statistically-significant experimental data is available concerning

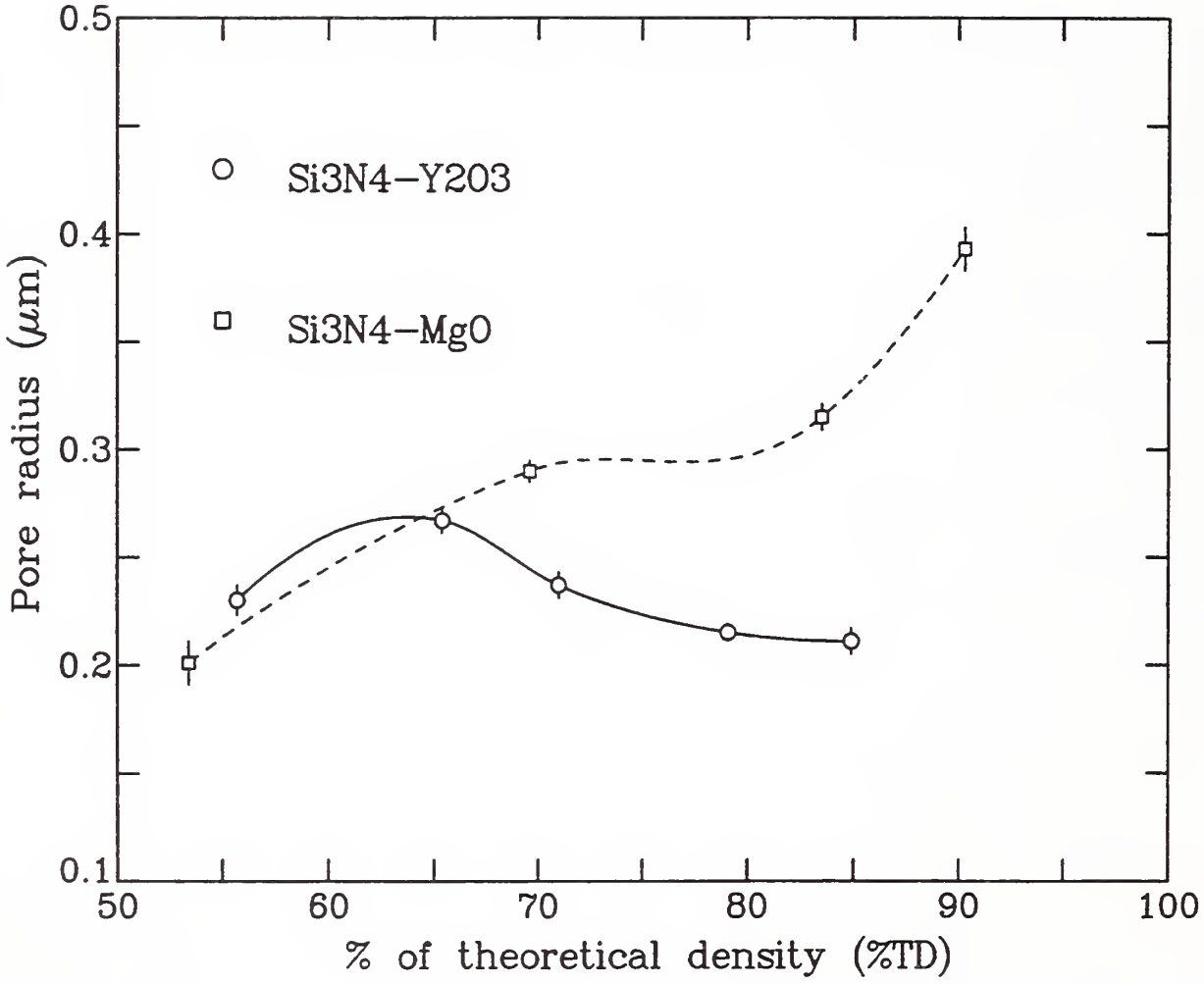

Figure VII-5. Pore radius as a function of density for both systems.

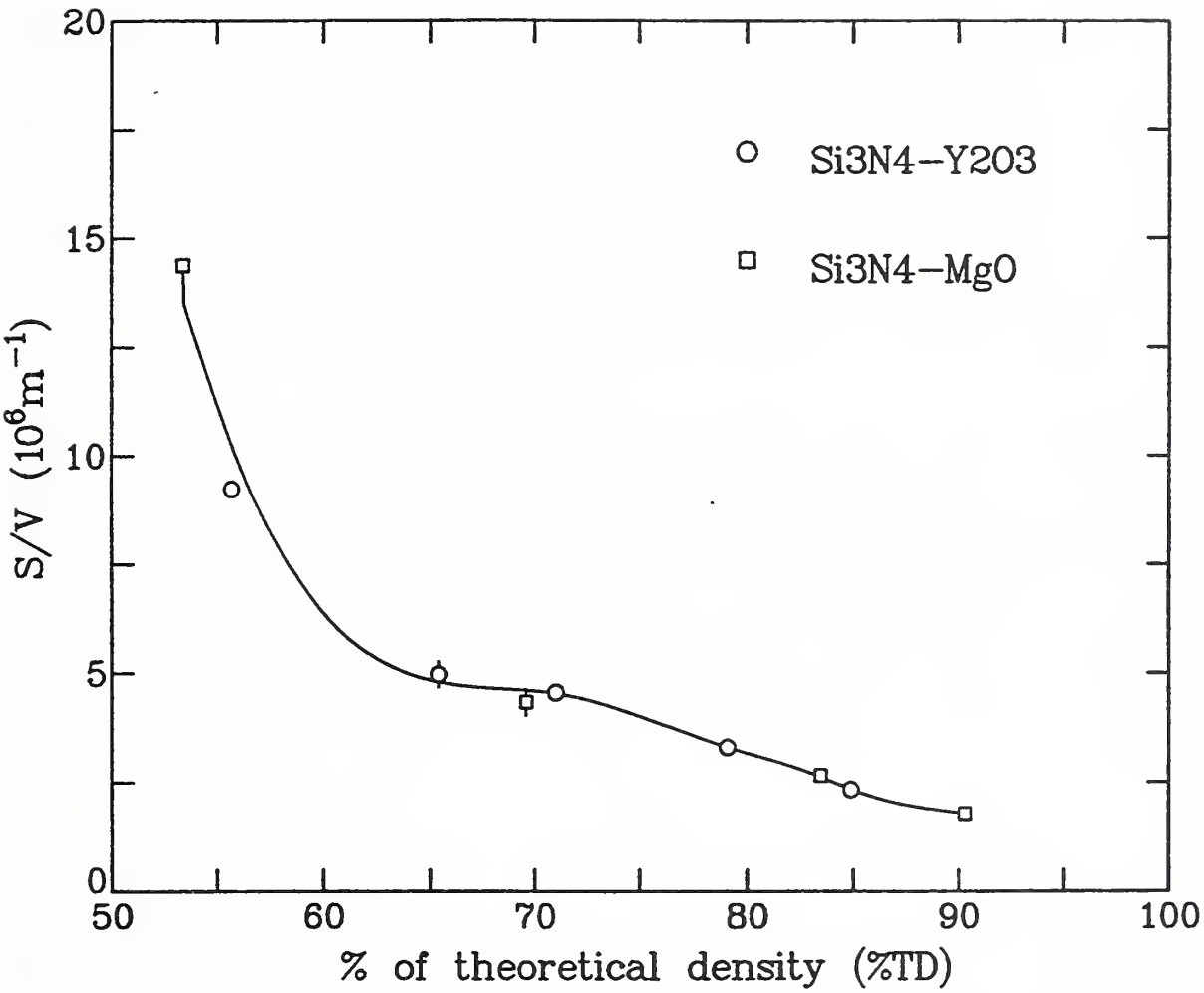

Figure VII-4. Pore surface area per unit volume as a function of density for both systems.

the development of the highly-porous intermediate microstructures. To this end, we are carrying out a small-angle-neutron and small-angle x-ray scattering investigation of the interdependent effects of precursor microstructure and thermal treatment on a model porous-ceramic system. The current work is focusing on pore-size distribution and its influence on microstructure development. The goal of the work is to enable optimization of the microstructural design of these materials though predictive processing schemes.

The first goal of this project is to synthesize a suite of reproducible, porous specimens with a broad range of average pore sizes and distributions. A colloidal-silicate sol-gel formulation is being utilized for this purpose. Preliminary scattering experiments on the as-prepared monoliths show the gel to possess scattering entities from the nanometer to the micrometer scale. Through control of the volume-percent seed colloidal particles, both the average cluster size and the nature of their polydispersity can be engineered (Fig. VII-6). The underlying pore structure has been shown to scale with the solid-phase microstructural trends. Scattering results also indicate that fine scale nanoporosity can be manipulated by leaching treatments on the gel. These initial studies have proven that by monotonically varying the chemical synthesis parameters, the required specimen microstructures can be produced.

Microstructural studies of sintered and quenched specimens have indicated some unexpected pore size and morphology transitions for the gel with the most polydisperse microstructure. Radii of gyration obtained from multiple-scattering data and Porod surface-area analysis show the pore size to remain constant during intermediate-stage sintering with an increase in pore diameter at the highest densities (see Fig. VII-7). Topological analysis of the scattering data indicates that this is due to a transition from spherical to disc-like pores at the later stages of sintering. While additional work is required to understand the mechanisms behind this microstructural development, the results already demonstrate the richness of microstructural detail afforded by small-angle scattering that extends well beyond the realm of simply obtaining the average pore size.

The future goals of this project include: an examination of the pore-structure evolution as a function of pore-size distribution for the synthesized gels, an extension of the investigation of the thermal treatment of the gel by performing in-situ small-angle scattering using the newly-commissioned SANS furnace, further quantification of the nanoscale microstructure of the gel using small-angle scattering coupled with stereological measurements of high-resolution TEM images, a utilization of computer-simulation modeling to elucidate the microstructural mechanisms responsible for the observed pore-structure evolution during densification, and testing of the long term applicability of the methodology by performing in-situ experiments with other porous systems.

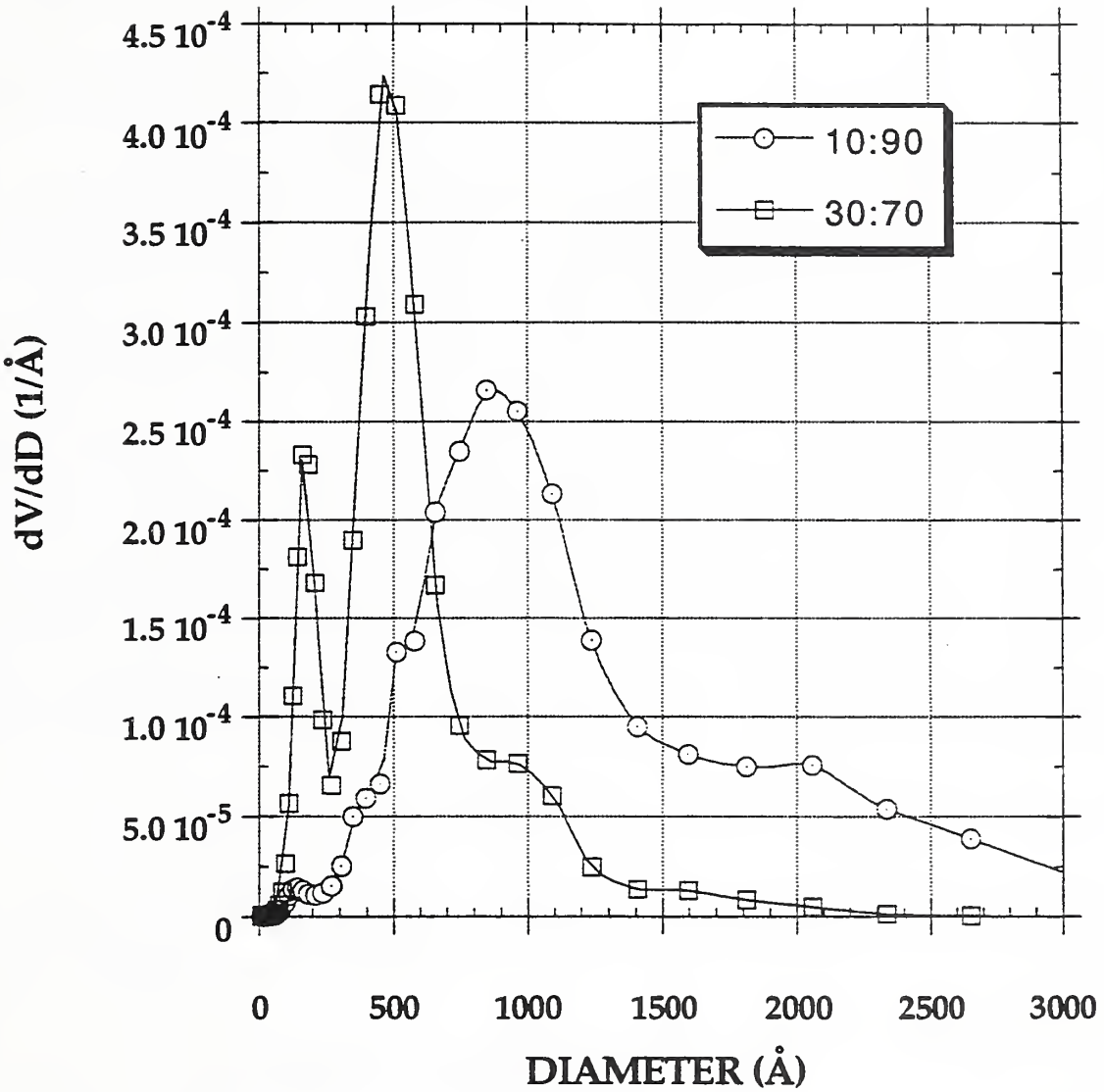

Figure VII-6. Volume distribution of pores for the 10:90 and the 30:70 porous materials which has not been leached.

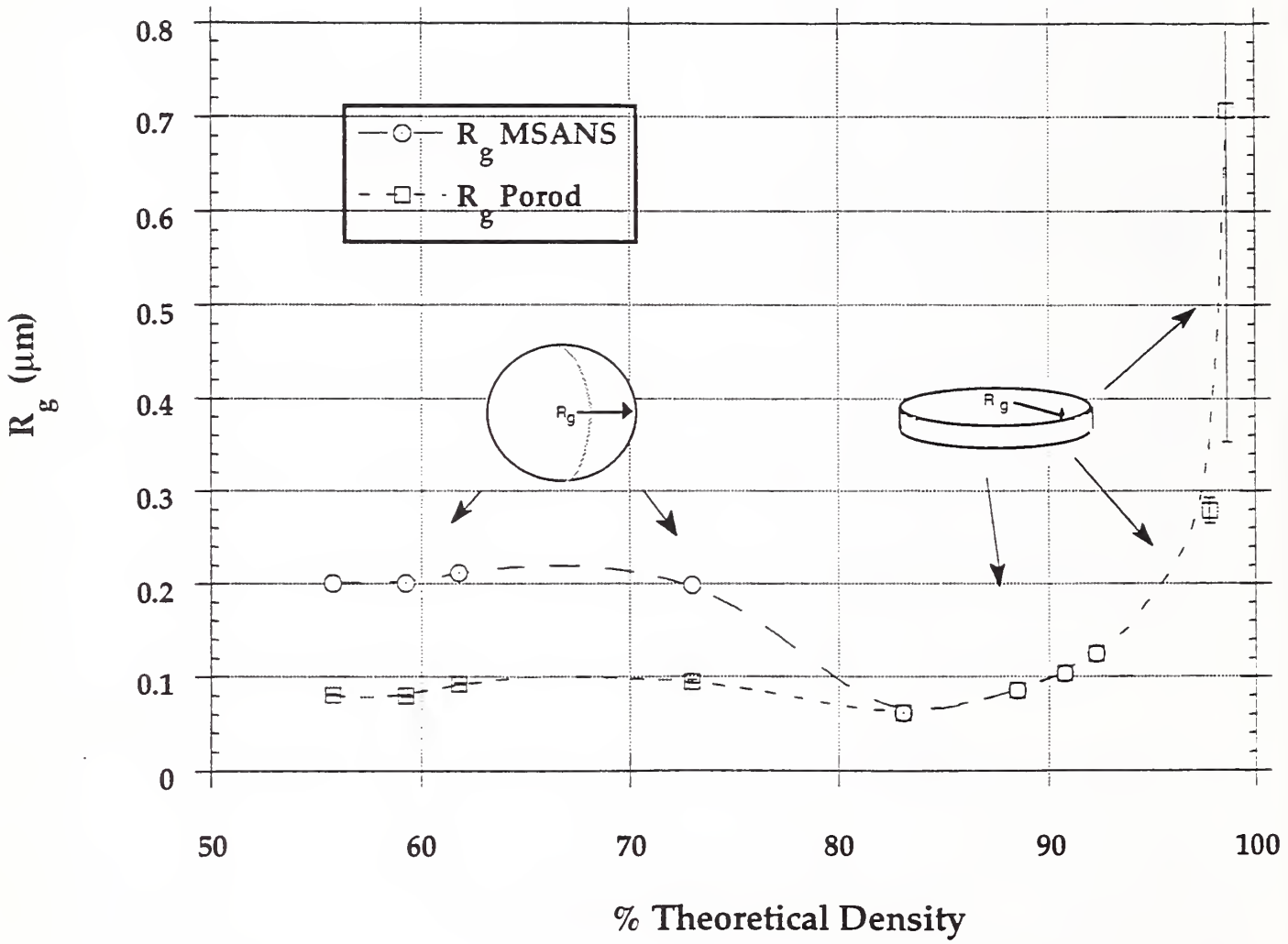

Figure VII-7. Radii of gyration of pores in porous silica as a function of density, indicating a morphological transition at about 83% TD.

Surface Extended X-ray Absorption Fine Structure Characterization of the One-Monolayer Sb/GaP (110) Interface

J. C. Woicik, K. E. Miyano[1], T. Kendelewicz[1], M. Richter[2], P. Pianetta[2], and W. E. Spicer[1]

[1]Stanford Electronics Labs
[2]Stanford Synchrotron Radiation Laboratory

The ordered interfaces achieved by depositing Sb or Bi on cleaved III-V semiconductor surfaces have been the focus of recent theoretical and experimental activity. The structural models currently proposed for this interface, shown in Fig. VII-8, involve zigzag chains of Sb atoms running along the (110)-direction of the surface. Scanning tunneling microscopy studies have indeed imaged such chains. The distinction between the various models involves the registry and orientation of these chains with respect to the substrate. Determining their correct structure is of keen interest because, as Fig. 8 makes clear, the models differ substantially in their hybridization and their means of dangling bond saturation. It has been established that these Sb overlayers inhibit the reactivity of the III-V surfaces; at least for certain substrates these monolayers tie up the dangling bonds without creating interfacial band gap states that pin the Fermi level. The ECLS and EOTS models (see Fig. VII-8 for a definition of model acronyms) propose three-fold coordinated adatoms, leading to the saturation of dangling bonds. On the other hand, in the p^3 structure the Sb-anion bond is not formed, and such a model has been actively discussed for the phosphide substrates because of the absence of Sb-P bonds in any known compounds. There has been a report that the V / III-V interface can switch from ECLS to a structure with the adatom chains on top of the surface-most substrate chains (EOTS or EOCS) as the lattice constant of the substrate is expanded with respect to the chain dimensions.

It is also of interest to look at the quantitative structural details of these Sb / III-V interfaces such as the bond lengths or the degree of tilt of the Sb chains. Specifically, the experimental measurements of these parameters can be compared to the results of total energy minimization. For example, there has been some disagreement between the calculated values for the Sb-P bond length, specifically, the Sb-P repulsion has been difficult to model because of the lack of standard Sb-P bonds.

In this study, surface extended x-ray absorption fine structure was measured at the Sb L_3 edge for the ordered interface between 1 ML Sb and the cleaved GaP (110) surface. The Sb adatoms are bonded to three species, P, Ga, and Sb. Because these three backscatterers are well separated in atomic number, their contributions to the first shell absorption fine structure are distinct and separable. The Sb-P, Sb-Ga, and Sb-Sb bond lengths were determined to be 2.60 ± 0.05 Å, 2.79 ± 0.05 Å, and 2.88 ± 0.05 Å, respectively. Each value correlates well with the sum of covalent radii. These bond lengths demonstrate that the adatom chains are not strongly tilted with respect to the GaP surface, and the polorization dependence of both the L_3 fine structure and the L_1 near edge structure supports this finding.

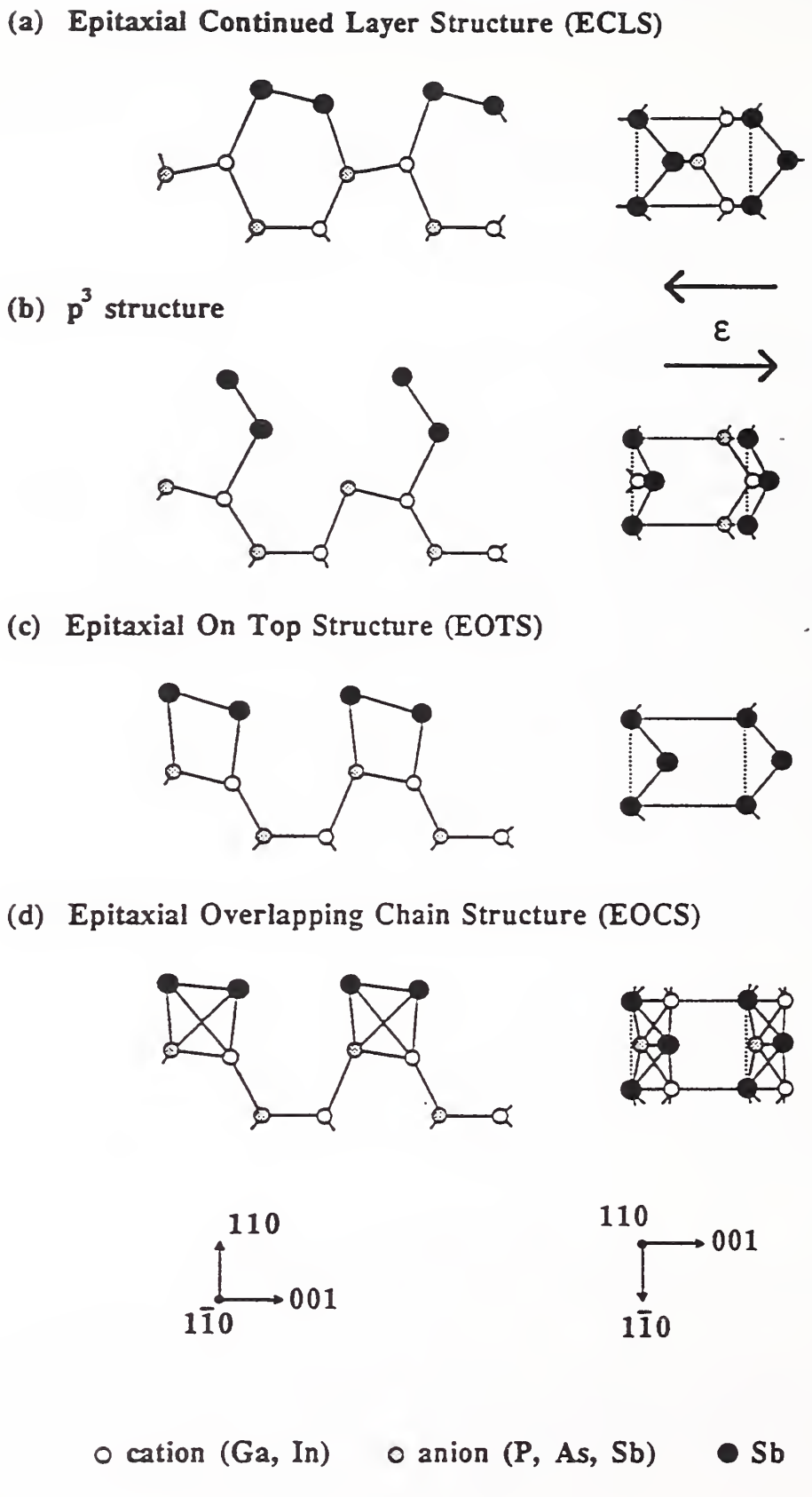

Figure VII-8. Structural models proposed for the Sb atoms on cleaved III-V semiconductor surfaces.

To summarize, bond lengths and coordination numbers were extracted for the 1 ML Sb / GaP interface from SEXAFS above the Sb L_3 edge. The presence of a P backscattering contribution verifies the presence of the Sb-P bond in these interfaces between Sb and this III-V phosphide. The bond lengths and polorization dependence of the coordination numbers further suggest that the Sb chains are nearly parallel to the GaP (110) planes. The SEXAFS parameters effectively rule out the p^3 structure and EOCS models for this particular interface. These numbers can be combined with results from a recent x-ray standing-wave measurement to derive a full set of atomic coordinates in the context of the ECLS and EOTS structures. The measurement-based ECLS better resembles the corresponding minimum-energy structure than the EOTS case. This along with the smaller surface contraction derived for the ECLS favors this particular structure for the Sb/GaP system.

Ultra Soft X-ray Fluorescence Yield XAFS: An In Situ Photon-in Photon-out Spectroscopy

D. A. Fischer, J. L. Gland[1], T. S. Rufael[1]

[1]Chemistry Department, University of Michigan

We have developed ultra-soft fluorescence-yield XAFS is an important extension of a traditionally hard x-ray technique for structural determination of low Z elements (C,N,O,F) in materials. Until recently soft x-ray XAFS studies have been accomplished solely by electron yield methods which usually must be done under ultra-high vacuum conditions. The fluorescence technique is particularly useful in surface chemistry applications for in situ monitoring (kinetics) of transient surface species under real reaction conditions of temperature and pressure. This was exemplified this year by two experiments: the reaction kinetics of NiO/Ni(100) with hydrogen, and the reaction kinetics of sulfur carbon bond cleavage of methylthiolate on Pt(111) in the presence of hydrogen. These reaction-kinetic surface-science experiments are the first of their kind (a milestone in surface science) since they involve in-situ characterization which was not possible with traditional surface science techniques such as XPS, EELS, or LEED.

Mechanistic studies of hydrogen-induced C-S bond activation are interesting because of the important role C-S bond activation plays in a wide range of catalytic hydrodesulfurization processes. This study represents an initial step in our effort to examine the role of hydrogen in bond activation on metal surfaces. In conventional reactivity studies separation of the elementary reaction steps involved in complex processes is often difficult. By studying the hydrogenolysis of the well-characterized methylthiolate (CH_3S) surface intermediate we have been able to isolate a single elementary reaction step so that detailed kinetic studies can be performed. A series of in-situ isothermal methylthiolate hydrogenolysis experiments were performed over the temperature range 305 to 330 K for hydrogen pressures from 0.01 - 1 Pa so that the kinetics of hydrogen induced C-S bond activation could be characterized. The hydrogenolysis of methylthiolate (CH_3S) was found to be first order with respect to surface carbon coverage and roughly half order with respect to hydrogen pressures. The C-S bond activation energy in presence of 1 Pa hydrogen was found to be approximately 18.0 kcal/mol.

In Situ X-Ray Diffraction Imaging of Non Linear Optical Interactions in Photorefractive Crystals

Bruce Steiner, Mark Cronin-Golomb,[1] Gerard Fogarty,[1] Uri Laor,[2] John Martin,[3] Dana Anderson,[4] Cardinal Warde,[5] Thomas Mark Garrett,[5,6] and Ronald C. Dobbyn[7]

[1]Electro-Optics Technology Center, Tufts University
[2]Guest Scientist from the Nuclear Research Center of the Negev
[3]Deltronics, Inc.
[4]University of Colorado/Joint Inst. for Laboratory Astrophysics
[5]Massachusetts Institute of Technology
[6]Sandoz Optoélectronique
[7]Consultant

Signal processing capacity and speed may be facilitated by the development of in optical approaches, which incorporate parallelism with relative ease. One promising technique for processing optical signals uses photorefractive crystals; however this is complicated by photorefractive amplified scattering (fanning). The scattering centers responsible for seeding the fanning noise have been presumed to be traceable to crystal lattice irregularities. These defects have not been previously examined in detail, and the relative importance of various specific imperfections and the role that they play in crystal optics is not known. An understanding of these defects should lead to improvement in optical signal processing through growth of more satisfactory photorefractive crystals. We thus set out two years ago to address these issues through direct, *in situ*, observation of photorefractive crystals and optical interactions in them.

We have recently been successful in imaging the lattice deformation due to photorefractive space charge fields. Two beams split from a 50 mW frequency-doubled YAG laser at 532 nm have been used to form high contrast fringe patterns (modulation 96%) with fringe periods between 7 and 50 μm in barium titanate. Diffraction images were obtained for the piezoelectric strain pattern induced by the resulting charge redistribution.

Moreover, we have observed directly for the first time 180° domains in a variety of barium titanate crystals. We have confirmed the identification of these domains by observing the phase shift across the domain wall. The prevalence of these domains proves to be far greater than had been suspected, and may well explain the aging of thin barium titanate crystals with time, a phenomenon that had not been understood.

Dislocations also have been observed in barium titanate. Both pure edge dislocations running and pure screw dislocations running in the [010] direction are visible in images in Laue geometry. Clearly visible also are strains resulting from faceted growth of the crystal boule. Examination of the boundaries between the facets reveals evidence of competition between adjacent facets during growth.

We are working with crystal growers and device physicists to reduce the most critical irregularities and to optimize photorefractive performance.

Defects in Epitaxial Layers: Their Genesis and Effects on Semiconductor Device Performance

Bruce Steiner, Uri Laor,[1] Krishna Rajan,[2] James Comas,[3] Wen Tseng,[3] Ronald C. Dobbyn,[4] G. Metze,[5] A. Cornfeld,[5] P. B. Klein,[6] G. K. Gaskill,[6] W. Xia,[7] and S. S. Lau[7]

[1]Guest Scientist from the Nuclear Research Center of the Negev
[2]Rensselaer Polytechnic Institute
[3]NIST Electronics and Electrical Engineering Laboratory
[4]Consultant
[5]Comsat
[6]Naval Research Laboratory
[7]University of California, San Diego

Commercially available semi-insulating gallium arsenide and indium phosphide wafers have a very high density of severely strain-inducing crystallographic irregularities such as dislocations, anti-phase boundaries, low angle grain boundaries, stacking faults, etc. ($> 10^3$ cm^{-2} etch pit density). Epitaxial layers grown on the surfaces of such irregular substrates contain defects, some of which propagate from the underlying wafers into the layers grown on them. Moreover, other crystal defects are introduced by device fabrication and processing. We are examining the various types of defects in such systems, both before and after layer deposition, and their propagation from the underlying substrates into epitaxial layers. In this way we separate process-induced irregularities from those grown in. These results are compared where helpful with those obtained by electron microscopy.

The imaging of layered semiconducting crystals over the past two years has resulted in the development of criteria for the nucleation and propagation of irregularity in layered systems. Lattice mismatch is demonstrated in each system by warping after layer deposition. In two of the systems, one severely mismatched while the other is not, no arrays of dislocations are obvious. Elaborate sets of mixed linear dislocations are found in two other systems with intermediate degrees of mismatch. The nucleation of extensive arrays of dislocations during *uniform* one micrometer layer deposition thus appears to depend not only on the extent of lattice mismatch and layer thickness but also on the regularity of the substrate. Establishment of a non-pseudomorphic layer mismatched with the substrate by several tenths of a percent is an important factor, as previously determined. However, localized irregularity, either dislocations in the substrate or surface scratches, appears to assist nucleation of arrays of interface mismatch dislocations. Moreover, the absence of nominally equivalent orthogonal array suggests that propagation of these arrays depends on the character of the unit cell.

Images of a special series of high electron mobility transistor (HEMT) structures have displayed five types of accommodation to lattice mismatch, depending on its extent: 1) lattice warping, 2) the formation of an non pseudomorphic layer, 3) the formation of extended arrays of linear mismatch dislocations at the interface between the substrate and a non pseudomorphic layer, 4) the formation of oval regions of tweed-like local lattice variation imbedded among these arrays, and 5) extended tweed-like local lattice variation over large peripheral areas in which the formation of straight mismatch dislocation arrays is not observed.

In closely lattice matched HEMT systems, all of the irregularities observed resemble those of the substrate. Thus effective epitaxy can indeed be achieved. However, warping of the lattice is found in mismatched systems, both those with pseudomorphic layers and those that are non pseudomorphic. A non pseudomorphic layer without visible misfit dislocations is formed with a mismatch of 0.27 %. With increase of the mismatch to 0.5 %, the other three forms of accommodation are observed: arrays of <011> mismatch dislocations; oval regions of tweed-like irregularity, oriented in the [011] direction; and peripheral regions of extended tweed-like local lattice variation.

High resolution diffraction images of a heterojunction consisting of a HgCdTe grid on a uniform layer of CdTe, on a GaAs buffer, on a Si substrate, have displayed the induction of pure edge dislocations by the grid that extend down through both uniform layers into the substrate. The pure edge character of these dislocations is in sharp contrast to the lattice mismatch dislocations noted above for uniform systems. These irregularities thus are expected to have a strong affect on the electronic properties of irregular layered systems.

Residual Defects in Substrates: Their Genesis and Effects on Semiconductor Device Performance

Bruce Steiner, Uri Laor,[1] James Comas,[2] Wen Tseng,[2] Morris Young,[3]
William Graham,[4] and Ronald C. Dobbyn,[5]

[1]Guest Scientist from the Nuclear Research Center of the Negev
[2]NIST Electronics and Electrical Engineering Laboratory
[3]President, American Xtal Technology, Inc.
[4]President, Xsirius, Inc.
[5]Consultant

A reduction by several orders of magnitude in the irregularity density in gallium arsenide wafers grown by a new commercial process has recently been reported. Since the work in the preceding section shows that the formation of mismatch dislocations in layered systems is strongly influenced by substrate regularity, the characterization of these new substrates is particularly important. In close collaboration with the crystal grower, we have initiated a diffraction imaging study of these wafers. We find that the incidence of the cellular structure characteristic of Czochralski-grown gallium arsenide is indeed severely reduced. Perhaps even more important, the formation of the low angle subgrain boundaries also characteristic of Czochralski material is completely suppressed in these wafers. This observation explains a substantial reduction in fracture sensitivity of these new wafers.

High resolution diffraction images of a commercial liquid encapsulated Czochralski gallium arsenide wafer have confirmed predictions of the antiphase boundary model proposed earlier but not yet confirmed. In the new sample, the cells of high irregularity density are sufficiently isolated that the predicted edge dislocations are clearly distinguishable when not aligned with the diffraction vector. Moreover, the filling in of the cellular structure in the newly observed asymmetric diffractions indicates that the cells of irregularity have a columnar structure whose axis is aligned with the crystal growth.

A high quality commercial substrate of LEC InP has been observed in high resolution diffraction imaging in the first such study to have been completed. This material does not display the very low angle grain boundaries characteristic of LEC GaAs. However, the individual features resemble those in LEC GaAs under comparable diffraction conditions. The antiphase boundary model attributed to GaAs thus appear applicable to this material as well. Nevertheless, in contrast to their appearance in GaAs, the sharp irregularities in InP do not display a pure edge character: they are visible even when aligned with the diffraction vector. More important, these features and their accompanying linear streak-like features suggesting antiphase boundaries are not arranged in cells. These results all suggest that these substrates may be far more satisfactory than previously believed.

We have also initiated a study of sapphire substrates of particular interest as substrates for high temperature superconducting devices. Early results indicate that the irregularities present are strongly influenced by the processing.

Irregularities in Crystals Grown in Microgravity and Related Terrestrial Crystals: Their Nature, Genesis, and Effects on Device Performance

Bruce Steiner, Uri Laor,[1] Lodewijk van den Berg,[2] Ravindra Lal,[3] David Larson,[4] and Ronald C. Dobbyn[5]

[1]Guest Scientist from the Nuclear Research Center of the Negev
[2]EG&G Energy Systems
[3]Alabama A&M University
[4]Grumman
[5]Consultant

Crystals grown in microgravity have previously been found to have properties superior to those of directly comparable terrestrial crystals and have led to substantial interest in crystal growth in space. For example, the charge carrier mobility of x- and gamma-ray mercuric iodide detectors made from space-grown crystals was a least six times higher than for similar detectors made from ground-grown crystals. Neither the structural nature of the differences nor their origins in crystal growth had been determined prior to the initiation of the current program. Since both issues are important to the realization of the space crystal growth program and indeed to improvement in the effectiveness of crystal growth in general, we have established a collaborative program with commercial and academic crystal growers of NASA's Microgravity Sciences and Applications Program.

We have focussed this year on the two materials grown on IML 1 in February 1992: vapor-grown mercuric iodide and solution-grown triglycine sulfate; and on preparations for observation of the four materials grown on USML 1 in April 1992: three derivatives of cadmium telluride and Bridgman-grown gallium arsenide.

In the initial ground-grown mercuric iodide crystals observed in high resolution diffraction imaging, more than one phase in the form of arrays of non diffracting inclusions was observed. These apparently stiffened the lattice, giving an observed long range regularity to it. However,

this precipitate formation apparently was suppressed in the initial growth in microgravity and on the ground when higher purity source material was used, which appears to have led in each instance to the formation of extremely soft materials displaying a very low degree of long range lattice regularity. However, it has been unclear whether the long range irregularity observed was characteristic of the growth process, or simply a result of the slicing and polishing process for what was now a very soft material. We have therefore inaugurated a study of the effects of various surface treatment steps. The results appear initially to bear strongly on other aspects of the material, which may determine its hardness.

A triglycine sulfate crystal grown on space shuttle IML-1 has been examined with high resolution diffraction imaging, both before and after slicing for the formation of infrared detectors. The local acceptance angle for diffraction from the uncut crystal, 1-2 arc seconds, which indicates extraordinary crystal regularity. Polystyrene fluid flow markers that had been included in the space growth are observed as small imperfections. Also clearly distinguishable in was a faceted growth mode during space growth. Two sets of edge dislocations in the seed, one [101]-oriented and the other [001]-oriented, were noted as well in images taken in Laue geometry; but they appear not to have affected the space growth.

Observation of the cut edge of the space crystal, shows continuity between the terrestrial seed at the bottom and the space growth at the top, indicating a high degree of epitaxy of the space growth. The demarkation between the seed and space growth is indistinct.

Preceding high resolution imaging of terrestrial crystals had shown that the surface treatment of the seed crystal was critical to growth perfection. As a result, the quality of the space growth had been optimized through the earlier NSLS imaging.

RESEARCH STAFF

DATA BASE ACTIVITIES

Begley, Edwin F.	• Database management methods • Engineering database structures • Digital video interactive technology
Munro, Ronald G.	• Material properties of advanced ceramics • Data evaluation and validation • Analysis of data relations

POWDER CHARACTERIZATION AND PROCESSING

Carter, Craig W.	• Materials thermodynamics • Advanced mathematical and computational techniques • Computation of materials processes
Cline, James P.	• Standard reference materials • High-temperature x-ray diffraction • Microstructural effects in x-ray diffraction • Rietveld Refinement of XRD data
Kelly, James F.	• Quantitative scanning electron microscopy • Image analysis • Microstructure analysis • Powder standards
Lum, Lin-Sien H.	• Powder characterization • Instrumental analysis
Malghan, Subhas G.	• Powder and dense slurry characterization • Colloidal processing and forming • Interfacial and surface chemistry of powders • Standards development
Minor, Dennis B.	• Analytical SEM of ceramics and particulates • Powder test sample preparation • Powder characterization
Pei, Patrick T.	• Spectroscopic and thermal characterization • Chemical coating • Powders characterization

Ritter, Joseph J.	• Chemistry of powders synthesis • Specialty powders synthesis • Powder preparation and compositional evaluation
Pechenik, Alexander	• Novel powder processing • High pressure, low temperature powder compaction • Powder processing science
Wallace, Jay S.	• Processing and microstructure • Silicon nitride densification • Thermal analysis
Wang, Pu Sen	• Solid state NMR • Surface characterization by x-ray photoelectron and Auger electron spectroscopy

SURFACE PROPERTIES

Gates, Richard S.	• Tribo-chemistry • Surface chemical properties of ceramics • Machining of ceramics
Hsu, Stephen M.	• Ceramic wear mechanisms • Engineered ceramic surfaces • Lubrication and machining of ceramics
Ives, Lewis K.	• Wear of materials • Transmission electron microscopy • Mechanical properties
Ruff, Arthur W.	• Wear of materials • Microstructure effects • Mechanical behavior

MECHANICAL PROPERTIES

Braun, Linda	• Raman stress measurements • Ceramic matrix composites • Toughening mechanisms

Chuang, Tze-Jer	• Creep/creep rupture • Fracture mechanics • Finite-element modeling • Lifetime predictions
Cranmer, David C.	• Ceramic and glass composite fabrication • Composite test development • Ceramic composite properties • Glass viscosity • Properties of glass
Hockey, Bernard J.	• Electron microscopy • High-temperature creep
Horn, Roger G.	• Surface forces • Fracture mechanics • Colloidal processing • Adhesion
Jahanmir, Said	• Ceramic Machining Research • Machining Data
Kauffman, Dale A.	• Glass melting
Krause, Ralph F., Jr.	• Creep in flexure and tension • Fracture mechanics • Hot pressing • Chemical thermodynamics
Quinn, George	• Mechanical Property Test Standards • Standard Reference Materials • Creep Testing
Ostertag, Claudia P.	• Influence of heterogeneities on sintering • Processing and sintering of reinforced ceramics • Investigation of toughening mechanisms in pressureless sintered composites • Measurement of residual stresses by cathodoluminescence and in situ high temperature X-ray diffraction

Smith, Douglas T.	• Surface forces • Charge transfer at interfaces • Adhesion and friction • Colloidal processing

ELECTRONIC MATERIALS

Blendell, John E.	• Ceramic processing and clean-room processing • Sintering and diffusion controlled processes • Processing high T_c ceramic superconductors • Activation chemical analysis
Burton, Benjamin P.	• Calculated phase diagrams • Ferroelectric ceramics
Chiang, Chwan K.	• Electronic ceramics • Superconductivity • Electrical measurements
Clevinger, Mary A.	• Phase diagrams for ceramists • Computerized data
Cook, Lawrence P.	• High temperature chemistry • Phase equilibria • Electronic ceramic films
Hill, Michael D.	• Mechanical properties of PZT • Superconducting materials • Ceramic processing
Lindsay, Curtis G.	• Phase equilibria of high dielectric ceramics • Phase equilibria of high T_c ceramics • MO calculations of environmentally enhanced fracture
Piermarini, Gasper J.	• Ceramic processing and high pressure sintering • Pressure-induced transformation toughening • High pressure physical properties and structures • High pressure X-ray diffraction and spectroscopy

Rawn, Claudia J.	• Phase diagrams • X-ray diffraction
Vaudin, Mark D.	• Electron microscopy of ceramic superconductors and of ceramic-ceramic and ceramic-metal composites • Microscopy and diffraction studies of interfaces • Computer modelling of grain boundary phenomena
White, Grady S.	• Thin films • Nondestructive evaluation • Subcritical crack growth • Stress measurements • Cyclic fatigue
Wong-Ng, Winnie	• X-ray analysis • X-ray standards • Molecular orbital calculations

OPTICAL MATERIALS

Farabaugh, Edward N.	• Chemical vapor deposition of diamond • Structure and morphology analysis • Scanning electron microscopy • X-ray diffraction • Thin film deposition • Surface analysis
Feldman, Albert	• Chemical vapor deposition of diamond • Thermal properties • Modelling thermal wave propagation • Thin film optical properties
Kaiser, Debra L.	• Bulk single crystal growth • Phase equilibria • Physical properties and structures of high temperature superconductors • Interfaces in high temperature superconductors • Chemical vapor deposition of ferroelectric oxide thin films

Robins, Lawrence H.	• Defect identification and distribution in CVD diamond • Stress in ceramics • Cathodoluminescence imaging and spectroscopy • Photoluminescence spectroscopy • Optical properties • Raman spectroscopy • Scanning electron microscopy
Rotter, Lawrence D.	• Measurement of electro-optic coefficients • Photorefractive effect • Optical spectroscopy of thin films

MATERIALS MICROSTRUCTURE CHARACTERIZATION

Black, David R.	• Defect microstructure in diamond • Polycrystalline diffraction imaging • X-ray imaging of photonic materials
Bouldin, Charles E.	• X-ray absorption spectroscopy • Diffraction anomalous fine structure • GeSi heterojunction bipolar transistors
Burdette, Harold E.	• X-ray optics • X-ray diffraction imaging • Crystal growth • Instrumentation
Fischer, Daniel A.	• X-ray absorption fine structure • X-ray scattering • Surface science
Long, Gabrielle G.	• Small-angle x-ray and neutron scattering • Ceramic microstructure evolution as a function of processing • X-ray optics
Spal, Richard D.	• X-ray optics • Diffraction physics • X-ray scattering
Woicik, Joseph C.	• UV photoemission • X-ray standing waves • Surface and interface science

DIVISION OFFICE

Carpenter, Joseph A., Jr.,	• Functional ceramics applications • Technical assessments • Industrial liaisons
Dapkunas, Stanley J.	• Structural ceramics applications • Technical assessments
Freiman, Stephen W.	• Electronic ceramics • Mechanical properties • Superconductivity
Fuller, Edwin, R., Jr.	• Influence of microstructure on fracture and other physical properties of materials • Toughening mechanisms in ceramics and ceramic composites, and their relations to processing • Interfacial fracture and toughening mechanisms in reinforced ceramic composites • Processing/property relations and phase equilibria of high T_c ceramic superconductors
Steiner, Bruce W.	• High resolution diffraction imaging • Nature, genesis, distribution, and effects of irregularities in monolithic crystals and multilayers • Non linear optical processes

GUEST SCIENTISTS AND GRADUATE STUDENTS

Allen, Andrew	University of Maryland
Bell, Michael I.	Naval Research Laboratory
Blackburn, Douglas	Consultant
Block, Stanley	Consultant
Bogatin, Oleg	Institute of Nonmetallic Materials
Butler, Elizabeth	Lehigh University
Cedeno, Christina	American Ceramic Society
Chapel, Jean-Paul	Ecole Normale Superieure, Paris
Chen, Yung-Mien	University of Maryland
Chen, Wei	Alfred University
Chu, Yuan-Chao	Howard University
Coker, Eric	Worcester Polytechnic Institute
Craig, Charles	Defense Tech Security
Dally, James	University of Maryland
Domingues, Louis	Trans-Tech, Inc.
Dong, Xiaoyuan	University of Maryland
Frederikske, Hans	Consultant
Gallas, Marcia	Instituto de Fisica da Ufrgs
Green, Thomas	American Ceramic Society
Grabbe, Alexis	Postdoc (ex - University of North Carolina at Chapel Hill)
Gu, Jia-Ming	University of Maryland

Hackley, Vince	University of Wisconsin
Haller, Wolfgang	Abbott Laboratories
Harmer, Martin	Lehigh University
He, Chuan	University of Maryland
Hill, Kimberly	American Ceramic Society
Hong, William	Institute for Defense Analysis
Hu, Zu-Shao	East China University
Jemian, Peter	Illinois Institute of Technology
Kerch, Helen	Johns Hopkins University
Krebs, Lorrie	Johns Hopkins University
Kruger, Jerome	Johns Hopkins University
Laor, Uri	Nuclear Research Center of the Negev
Larsen-Basse, Jorn	National Science Foundation
Lee, Byeong	Hanyang University
Lee, Hsien-Ming	University of Maryland
Lee, Soo Wohn	University of Illinois
Liang, Hong	University of Maryland
Liu, Hanyan	Northwestern University
McMurdie, Howard	Joint Center for Powder Diffraction Studies
Messina, Carla	American Ceramic Society
Ondik, Helen	American Ceramic Society
Pan, Yi-Ming	Southwest Research Institute

Paretzkin, Boris	Joint Center for Powder Diffraction Studies
Paulik, Steven	Northwestern University
Pechenik, Alex	Air Force Office of Scientific Research
Perez, Joseph	Department of Energy
Peterson, Marshall	Wear Sciences
Premachandran, Ramannair Sarasamma	Indian Institute of Technology, Madras
Roth, Robert	Consultant
Russell, Thomas	Naval Surface Warfare Center
Sater, Janet	Institute for Defense Analysis
Shechtman, Dan	Johns Hopkins University
Shen, Ming	University of Illinois
Shin, Hung Hyangjae	University of Maryland
Smith, Wallace	Office of Naval Research
Strakna, Timothy	University of Maryland
Sun, Jian-Xia	Shanghai University of Science and Technology
Swanson, Nils	American Ceramic Society
Vandiver, Pamela	Smithsonian Institute
Vinod, Natarajan	University of Maryland
Wang, Yushu	University of Maryland
Xu, Huakun	University of Maryland
Ying, Tsi-Neng	University of Maryland
Zhang, Guangming	University of Maryland

OUTPUTS AND INTERACTIONS

TECHNICAL PUBLICATIONS

DATA BASE ACTIVITIES

Munro, R. G and Begley, E. F., "Materials Properties for Advanced Structural Ceramics", NISTIR 4885 (1992).

Munro, R. G., "A Units Conversion Routine for Use in the Computerized Structural Ceramics Database," NISTIR 4728 (1992).

Begley, E. F. and Munro, R. G., "User's Guide to the Structural Ceramics Database Version 2.0", NISTIR 4861 (1992).

Begley, E. F. and Munro, R. G., "Preview of the Database on High-Temperature Superconductors," NISTIR 4926 (1992).

Munro, R. G., "Expert System Technology for Natural Gas Resource Development," submitted to Fuel (1992).

Munro, R. G., Malghan, S. G., and Hsu, S. M., "Variances in Ceramic Powder Characterization Measurements," submitted to J. Am. Cer. Soc. (1992).

Rumble, J. Jr. and Carpenter, J. Jr., "Materials 'STEP' into the Future," Advanced Materials and Processes, Vol. 142, No. 4, October 1992, pages 23-27.

Clevinger, M. A. and Hill, (Editors), "Phase Equilibria Diagrams, Phase diagrams for Ceramists, Cumulative Indexes, Volumes I-IX, Annuals 91-92, High Tc Monograph," The American Ceramics society, 1992.

McHale, A. E. (Editor), "Phase Equilibria Diagrams, Phase Diagrams for Ceramists," Annual 92, The american Ceramic Society, 1992.

Clevinger, M. A., Hill, K., and Ondik, H. (Editors), "Phase Equilibria Diagrams, Phase Diagrams for Ceramists, 1992 Bibliographic Update," The American Ceramics Society, 1992.

Shingfellow, G. B., (Editor), "Phase Equilibria Diagrams, Phase Diagrams for Ceramists, Vol. IX, Semi Conductors and Chalcoguides," The American Ceramoc Society, 1992.

POWDER CHARACTERIZATION AND PROCESSING

Cline, J. P., Schiller, S., and Jenkins, R., "Introduction of a NIST Instrument Sensitivity Standard Reference Material for X-Ray Powder Diffraction," Advances in X-Ray Analysis, 35, 1992.

Hackley, V. A., Malghan, S. G., and Premachandran, R., "Electrokinetic Sonic Analysis of Silicon Colloidal Nitride Suspensions," American Ceramic Society Symposium Proceedings: Spring 1992 Meeting, Characterization of Ceramic Powders, Ed. J. Adair, May 1992.

Malghan, S. G., Pei, P. T., and Wang, P. S., "Interface Chemistry of Silicon Carbide Platelets During Alumina Coating," Ceramic Eng. and Sci. Proceedings, Am. Cer. Soc., 12, No. 9-10, Part 2, 2115-2123, 1991.

Malghan, S. G., Sivakumar, A., Wang, P. S., and Somasundaran, P., "Deposition of Adsorption of Colloidal Sintering-Aid Particles on Silicon Nitride," accepted for publication in Composites and Interfaces, August 1992.

Malghan, S. G., Lum, L.-H. S., Lagergren E., Kelly, J. F., and Kacker, R., "Statistical Analysis of Parameters Affecting Measurement of Particle Size Distribution of Silicon Nitride Powders by Sedigraph," accepted for publication in Powder Technology, June 1992.

Malghan, S. G., "Process Design for Ceramic Materials," accepted for publication in Symposium Proceedings "Quality Through Engineering Design, Bangalore, India, January 1993."

Malghan, S. G., Paik, U., and Minor, D. B., "Polymeric Interactions in Aqueous Suspensions Silicon Nitride Powders," "Dispersion and Aggregation of Particles" to be published in Conference Proceedings by Engineering Foundation, May 1992.

Pechenik, A., Piermarini, G., "Fabrication of Transparent Ceramics from Clusters," Proceedings of DOE Fossil Energy Materials Conference at Oak Ridge, TN, May 1992.

Pei, P. T., Kelly, J. F., and Malghan, S. G., "Surface Modification and Slip Casting of SiC Platelets in $A\ell_2O_3$," Ceramic Engineering and Science Proc. Am. Cer. Soc., 13, No. 7-8, 1992.

Ritter, J. J., Minor, D. B., McMichael, R., and Shull, R., "Nanostructured Magnetic Materials Through Molecular Chemical Syntheses," Proceedings, 1992 Annual Mtg., TMS, San Diego, CA.

Ritter, J. J., "In Situ Characterization of the Pulsed Laser Deposition of Magnetic Thin Films," Proceedings of the Symposium on Photons and Low Energy Particles in Surface Processing, Materials Research Society, Fall Meeting, Boston, MA, December 2-6, 1991.

Roth, R., Cline, J. P., and Ritter, J. J., "Influence of PO_2 on Thermodynamic Stability During Formation of BYCO Superconducting Phases," Proceedings of the International Workshop on Superconductivity, June 23-26, 1992, sponsored by ISTEC/MRC.

Wang, P. S., Malghan, S. G., and Hsu S. M., "Surface Oxidation Kinetics of an α-Si_3N_4 and an Amorphous Si_3N_4 Powder," Proceedings of the Matls. Res. Soc. Fall Meeting, December 1991.

Wang, P. S., Malghan, S. G., Hsu, S. M., and Wittberg, T. N., "Effect of a-Silicon Nitride Powder Processing on Surface Oxidation Kinetics," accepted for publication in Journal of Materials Research, May 1992.

Wang, P. S., Minor, D. B., and Malghan, S. G., "Binder Distribution in Si_3N_4 Ceramic Green Bodies Studied By Stray-Field NMR Imaging," accepted for publication in Journal of Materials Research, October 1992.

MECHANICAL PROPERTIES

Chuang, T.-J., Chu, J.-L., and Lee, S., "Asymmetric Tip Morphology of Creep Microcracks Growing along Bimaterial Interfaces," **Acta Metall. Mater.** 40 [10] 2683-91 (1992).

Chuang, T.-J., "A Generic Model for Creep Rupture Lifetime Estimation on Fibrous Ceramic Composites,"Fracture Mechanics of Ceramics, Vol.10, pp. 441-457, Plenum Press, New York, 1992.

Chuang, T.-J., Chu, J.-L., and Lee, S., "Diffusive Crack Growth at a Bimaterial Interface", Proc. 33rd AIAA/ASME/ASCE/AHS/ASC Structures, Structural Mechanics and Materials Conf. Dallas, TX, April 13-15, 1992 Eds. G.L. Giles, O. Hal Burnside and W. Rogers, pp. 2964-2969 (1992).

Chuang, T.-J., Chu, J.-L., and Lee, S., "Diffusional Crack Growth in Dissimilar Media" Proc. 5th HITEMP Conference, Vol. III: Turbine Materials, pp. 64-1— 64-16, Westlake, OH, Oct.27-28, 1992.

Chuang, T.-J., Wang, Z.-D., and Wu, D., "Analysis of Creep in a Si-SiC C-Ring by Finite Element Method," ASME Trans. **J. Eng. Mater. Tech.** 114 [3] 311-316 (1992).

Chuang, T.-J., Chu, J.-L., and Lee, S., "A Microcrack Growth Theory for a Bimaterial System at Elevated Temperatures" **J. Appl. Mech.** to be submitted.

Chuang, T.-J., Chu, J.-L., and Lee, S., "High Temperature Crack Growth in Dissimilar Media," Proc. 8th International Conference on Fracture, Keiv, Ukraine, June 8-14, 1993.

Chuang, T.-J., and Duffy, S. F., "A Methodology to Predict Creep Life for Advanced Ceramics Using Continuum Damage Mechanics Concepts" to be published in ASTM STP 1201, 1993.

Grabbe, A., "Double-Layer Interactions Between Silylated Silica Sheets," Langmuir, in press. Grabbe, A., and Horn, R.G., "Double-Layer and Hydration Forces Measured Between Silica Sheets Subjected to Various Surface Treatments," J. Colloid Interface Sci., submitted.

Horn, R.G., and Smith, D.T., "Contact Electrification and Adhesion Between Dissimilar Materials," Science, **256**, 362-364 (1992).

Smith, D.T., "Measuring Contact Charge Transfer at Interfaces: A New Experimental Technique," J. Electrostat., **26**, 291-308 (1991).

SURFACE PROPERTIES

Hsu, S. M., "Boundary Lubrication of Advanced Materials," MRS Bulletin, XVI, 10, 54-58, 1991.

Cho, S. J., Moon, H., Hockey, B. J., and Hsu, S. M., "Wear Transition Mechanism in Alumina during Sliding," S. J. Cho, H. Moon, B. J. Hockey and S. M. Hsu, Acta Metall. Mater., 40, 1, 185, 1992.

Deckman, D. E., Jahanmir, S., and Hsu, S. M., "Wear Mechanisms of α-Alumina Lubricated with a Paraffin Oil," Wear, 149, 155-168, 1991.

He, C., Wang, Y., Wallace, J. S., Hsu, S. M., and Lacey, P., "The Effect of Microstructure on the Wear Transition of Zirconia Toughened Alumina," accepted for publication in the Wear of Materials 93.

Hu, Z. S., Hsu, S. M., and Wang, P. S., "Tribochemical Reaction of Stearic Acid on Copper Surface Studied by Surface Enhanced Raman Spectroscopy," Tribology Trans., 35, 3, 417, 1992.

Hu, Z. S., Hsu, S. M., and Wang, P. S., "Tribochemical and Thermochemical Reactions of Stearic Acid on Copper Surfaces," in Surface Science Investigations in Tribology: Experimental Approaches, ACS Symposium Series No. 485, edited by Y. W. Chung, A. M. Homola, and G. B. Street, 1992.

Hu, Z. S., Hsu, S. M., and Wang, P. S., "Tribochemical and Thermochemical Reactions of Stearic Acid on Copper Surfaces Studied by Infrared Micro-spectroscopy," Tribology Trans., 35, 1, 189, 1992.

Ives, L. K., "Abrasive Wear by Coal-Fueled Diesel Engine and Related Particles," NISTIR 4811, September 1992.

Ives, L. K., "Mechanisms of Galling and Abrasive Wear," in Fossil Energy Advanced Research and Technology Development Materials Program Semiannual Progress Report for the Period Ending September 30, 1991, ONRL/FMP-91/2, Oak Ridge National Laboratory, Oak Ridge, TN, April 1992, pp. 313-327.

Ives, L. K., "Wear by Coal-Fueled Diesel Engine Particles," in Proceedings of the Fifth Annual Conference on Fossil Energy Materials, Oak Ridge, TN September 1991, Conf. 9105184, ORNL/FMP-91/1, pp. 367-376.

Jahanmir, S., Ives, L. K., Ruff, A. W., and Peterson, M. B., "Ceramic Machining: Assessment of Current Practice and Research Needs in the United States," NIST SP-834 (1992).

Lee, S. L., Shen, M., and Hsu, S. M., "Wear Maps: Zirconia," accepted for publication in the J. Cera. Sci.

Malghan, S. G., Hsu, S. M., Dragoo, A. L., Hausner, H., and Pompe, R., "Analysis of Physical Properties of Ceramic Powders in an International Laboratory Comparison Program," in the 4th International Symposium on Ceramic Components for Engines, Ed. by R. Carlsson, T. Johnson, L. Kahlman, Elservier Applied Science, London, 1992.

Ruff, A. W., "Introduction to Laboratory Characterization Techniques," ASM Handbook - Friction, Lubrication, and Wear Technology, Vol. 18 (ASM International, OH, 1992).

Ruff, A. W., "Tribology of Materials and the Effect of Microstructure," Proceedings of the NATO Institute on Ultrafine Microstructure Materials, Portugal, (NATO, 1992). In press.

Ruff, A. W., "Wear Measurement," ASM Handbook - Friction, Lubrication, and Wear Technology, Vol. 18 (ASM Intern., OH, 1992).

Ruff, A. W., and Lashmore, D. S., "Effect of Layer Spacing on Wear of Nickel-Copper Multi-layer Alloys," Wear Journal, 151, 245-253 (1991).

Ruff, A. W., and Peterson, M. B., "Tribological Investigations of Composites and Other Selected Materials Sliding Against Vacuum-deposited MoS_2 Coatings," NIST IR-4959 (1992).

Ruff, A. W., and Peterson, M. B., "Wear of Self-lubricating Composite Materials vs. MoS_2 Films," Proceedings of the Conference on Wear of Materials-1993 (Elsevier Publ., 1993). In press.

Wang, J. C., and Hsu, S. M., "Chemically Assisted Machining of Ceramics," submitted to J. of Tribology.

Ying, T., and Hsu, S. M., "Asperity-asperity Contact Model," an invited paper for the International Micro-Tribology Conf. to be held at Morioka, Japan, Oct. 12-14, 1992.

Zhang, Y., Pei, P., Perez, J. M., and Hsu, S. M., "Tendency of Liquid Lubricants by Differential Scanning Calorimetry," Lubrication Engineering, 48, 3, 189-195, 1992.

Zhang, Y., Perez, J. M., Pei, P., and Hsu, S. M., "The Deposit Forming Tendencies of Diesel Engine Oils: Correlation between the Two-Peak Method and Engine Tests," Lubrication Engr., 48, 3, 221-226, 1992.

ELECTRONIC MATERIALS

Bennett, L. H., Swartzendruber, L. J., Kaiser, D. L., Gayle, F. W., Blendell, J. E., Habib, J. M., and Seyoum, H. M., "Thermoremanence and Meissner Effect in QMG and Single Crystal YBCO," Journal of Magnetism and Magnetic Materials, p. 539-540, (1992).

Brody, P., Rod, B., Cook, L. P., and Schenck, P., "Photovoltaic Effect in Thin Ferroelectric Films," Ferroelectric Thin Films II, eds., E. Myers and B. Tuttle) Materials Research Symposium proceedings, Vol 243, p. 27-31, 1992.

Carpenter, J., Piermarini, G. J., Dickens, B., Manning, J., Read, D., Kreider, K., Mattis, R., and Evans, R., "NIST/NCMS Program on Electronic Packaging: First Update," submitted for publication in the Proceedings of the International Electronics Packaging, Conf. Austin, TX.

Chen, B. H., Wong-Ng, W., and Eichhorn, B. W., "Preparation of New $Ba_4M_3S_{10}$ Phases (M=Zr,Hf) and Single Crystal Structure Determination of $Ba_4Zr_3S_{10}$," to be published in the Journal of Solid State Chemistry (1993).

Chiang, C. K., Wong-Ng, W., Cook, L. P., Schenck, P., Lee, H. M., Brody, P., Bennett, K., and Rod, B., "Post Processing of Pulsed Laser Deposited PZT Thin Film, " published, Mat. Res. Soc.(book) Ferroelectric Thin Films II, Symposium held December 2-4, 1991, Boston, Mass., Vol. 243, p. 423-428 (1992).

Cook, L. P., Chiang, C. K., Schenck, P., Wong-Ng, W., and Vaudin, M. D., "Ferroelectric Thin Films Prepared by Pulsed Laser Deposition: Processing and Characterization," NISTIR 4844 (1992).

Cook, L. P., and Plante, E., "Phase Diagram of the System Li_2O-Al_2O_3," published in Lithium Ceramics-III, a book edited by I. Hasting and G. Hollenberg, Ceramic Trans., Vol.27, p 193-222.

Deb, K., Hill, M. D., and Kelly, J., "Pyroelectric Characteristics of Modified Barium Titanate Ceramics," published in Journal of Materials Research, Vol. 7, No. 12, (1992).

Feldman, A., Vaudin, M. D., Shechtman, D., and Hutshson, J., "Moire Twin Boundary Images in Chemical Vapor Deposited Diamond," was accepted for publication to the Applied Physics Letters.

Freiman, S. W., and White, G. S., " Cyclic Fatigue in Piezoelectric Ceramics," published in Active Materials and Adaptive Stuctures (Gareth J. Knowles, ed.) pp 81-86, IOP Publishing Ltd. (1992).

Hill, M. D., Wong-Ng, W., Chiang, C. K., Fuller, E., Paretzkin, B., Blendell, J. E., Lagergren, E., and Kacker, R., "Effect of Composition of Superconducting Properties in the System Ba-Y-Gd-Cu-O," Amer. Ceram. Soc. Journal, 75 (No.9), 2390 (1992).

Hsieh, T. J., Smilgys, R. V., Chiang, C. K., Robey, S. W., Arsenault, R. J., and Salamanca-Riba, L., "Characterization of $DyBaCu_3O_7$ Thin Films Prepared by Ozone Asisted Co-Exporation Technique," Materials Research Symposium Proceedings, Conference, San Francisco, CA., Vol.275, p. 519 (1992).

Parise, J. B., Torardi, C., Rawn, C. J., Roth, R. S., Burton, B. P., and Santoro, A., "The Synthesis and Structure of $Ca_6BiO_6O_{15}$: Its Relationship to $Ca_4Bi_6O_{13}$," Journal of Solid State Chemistry, 101 [1] (1993).

Pechenik, A., Piermarini, G. J., and Danforth, S., "Fabrication of Transparent Silicon Nitride from Nanosize Particles," J. of the Amer. Ceram. Soc., January 1993.

Rawn, C. J., Roth, R. S., Burton, B. P., and Hill, M. D., "Phase Equilibria and Crystal Chemistry in Portions of the System SrO-CaO-$\frac{1}{2}Bi_2O_3$-CuO, Part IV--The System SrO-CaO-$\frac{1}{2}Bi_2O_3$," to be published in the Journal of the Amer. Ceram. Soc.

Roth, R. S., "Experimental Determination of Phase Equilibria Diagrams in Ceramic Systems," to be published in the International Summer School for Crystal Growth-8 Proceedings.

Roth, R. S., Rawn, C. J., Lindsay, C. G., and Wong-Ng, W., "Phase Equilibria and Crystal Chemistry of the Binary and Ternary Barium Polytitantes and Crystallography of the Barium Zinc Polytitantes, " accepted for publication, Journal of Solid State Chemistry: J. S. Anderson Memorial Issue.

Tez, E., Schroeder, T., and Wong-Ng, W., "Micro Raman Characterization of Impurity Phases in Ceramic and Thin Films Samples of the Y-Ba-Cu-O High T_c Superconductor, " published in Microbeam Analysis - 1991, p. 113-118.

Vaudin, M. D., Cook, L. P., Wong-Ng, W., Schenck, P., Broady, P., Rod, B., and Bennett, K., "Texturing and Dielectric Properties of Laser Deposited $BaTiO_3$ Thin Films Grown on Heated Substrates," eds., Angus Kingon, Edward Myers, and Bruce Tuttle, MRS Proceedings, Ferroelectric Thin Films II, Vol 243, p 513-518 (1992).

White, G. S., "TW NDE of Advanced Ceramics," published in proceedings of the CUICAC Workshop on NDE of Advanced Ceramics, ed. by Tom Coyle.

White, G. S., and Vaudin, M. D., "Fracture Behavior of Cyclically Loaded PZT, II.," submitted to J. Amer. Ceram. Soc.

Whitler, J., and Roth, R. S., "Phase Diagram for High T_c Superconductors", (book) published by the Amer. Ceram. Soc., 757 Brooksedge Plaza Drive, Westerville, OH, September 1991.

Wong-Ng, W., "The ICDD/PDF Coverage of the High T_c Superconductor and Related Compounds in the A-R-Cu-O Systems A=Ba, Sr and Ca and R=Lanthanides and Y," published in the Powder Diffraction, 7(3), 125 (1992).

Wong-Ng, W., Chiang, C. K., Freiman, S. W., Cook, L. P., and Hill, M. D., "Phase Formation of High-T_c Superconducting Oxide in the Bi-Pb-Sr-Ca-Cu-O Oxides," Bulletin of the American Ceramic Society, 1261 August 1992.

Wong-Ng, W., Cook, L. P., Chiang, C. K., Vaudin, M. D., Bennett, L., and Fuller, E., "Correlation of the Structural Phase Transformation of the High T_c Superconducting Materials, $Ba_2TCu_3O_{6+x}$ in Air," submitted to J. Amer. Ceram. Soc.

Wong-Ng, W., Cook, L. P., Schenck, P., Vaudin, M. D., Chiang, C. K., and Robins, L., "Powder X-Ray Diffraction Characterization of Ferroelectric Thin Films," Advances in X-Ray Analysis, 35A, 211 (1991).

Wong-Ng, W., and Cook, L. P., "Phase Equilibria and Crystal Chemistry of High T_c Superconductor Cuprates," Engineering Superconductors published by AICHE, 88, 11 (1992).

Wong-Ng, W., and Cook, L. P., "Oxidation/Reduction Melting Equilibria in the System $BaO\text{-}\frac{1}{2}Y_2O_3\text{-}CuO_x$, II. Powder X-Ray Analysis," Advances in X-Ray Analysis, 35A, 633 (1991).

Wong-Ng, W., and Cook, L. P., "Crystal Chemistry and Phase Equilibria Studies of the $BaO\frac{1}{2}R_2O_2\text{-}CuO$ System in Air VII. Single Crystal Structural Analysis of BAR_2CuO_5(R=Nd and Dy)," submitted to Acta Crystallogr., 1992.

Wong-Ng, W., and Mighell, A., "Crystallographic Databases for Chemical and Materials Analysis," published workbook distributed at the Pacific International Congress on X-Ray Analytical Methods, Hawaii, August (1991).

OPTICAL MATERIALS

Diamond Films

Feldman, A., "Properties of Diamond," in Handbook of Laser Science and Technology, CRC Press, in press

Feldman, A., "Use of Diamond as an Optical Material," in Proceedings of the 38th Sagamore Army Materials Research Conference, Plymouth, MA, Sept. 10-12, 1991. in press.

Feldman, A., Beetz, C. P., Drory, M., and Holly, S., "Workshop on Characterizing Diamond Films", NISTIR 4849, 1992.

Feldman, A., Beetz, C. P., Drory, M., and Holly, S., "Workshop on Characterizing Diamond Films", Conference Report, J. of Res. NIST, **97**, 387-391 (1992).

Feldman, A., Farabaugh, E. N., and Robins, L. H., "Chemical Vapor Deposited Diamond," chapter in Ceramic Films and Coatings, J.B. Wachtman, Editor, in press.

Feldman, A., and Holly, S., Proceedings SPIE, Vol. 1534 - *Diamond Optics IV*, Chairs/Editors (SPIE, Bellingham WA, 1991).

Feldman, A., Robins, L. H., Farabaugh, E. N., and Shechtman, D., "Diamond as an Optical Material," chapter in Characterization of Optical Materials, G. Exarhos, Editor, Manning-Butterworth, in press.

Robins, L. H., Farabaugh, E. N., Feldman, A., "Determination of the optical constants of thin chemical-vapor-deposited diamond windows from 0.5 to 6.5 eV", in Diamond Optics IV, A. Feldman and S. Holly, Editors, Proc. SPIE, 1534, 105-116 (1991).

Robins, L. H., Farabaugh, E. N., and Feldman, A.,"Spatially and Spectrally Resolved Cathodoluminescence of Hot-Filament Chemical-Vapor-Deposited Diamond Particles," J. Mater. Res. 7, 394-403 (1992).

Robins, L. H., Farabaugh, E. N., and Feldman, A., "Spatially and Spectrally Resolved Cathodoluminescence Measurements of CVD-Grown Diamond Particles and Films," Proc. of the 2nd Int. Symp. on Diamond Materials, ed. by A. J. Purdes et al., Electrochem. Soc. Proc. 91-8 (The Electrochemical Society, 1991), pp. 427-34.

Robins, L. H., Feldman, A., and Farabaugh, E. N., "Re-examination of the Raman Lineshapes of Diamond Films Grown by Hot-Filament or Microwave-Plasma Chemical Vapor Deposition," in Diamond Optics V, ed. by A. Feldman and S. Holly, Proc. SPIE 1759 (1992).

Shechtman, D., Farabaugh, E. N., Robins, L. H., Feldman, A., and Hutchinson, J. L., "High Resolution Electron Microscopy of Diamond Film Growth Defects and their Interactions," in Diamond Optics IV, A. Feldman and S. Holly, Editors, SPIE Proc. 1534, 26-43 (1991).

Shechtman, D., Hutchinson, J. L., Robins, L. H., Farabaugh, E. N., and Feldman, A., "Growth Defects in Diamond Films", J. Mater. Res., in press.

Shechtman, D., Feldman, A., Vaudin, M. D., and Hutchinson, J. L., "Moire-Fringe Images of Twin Boundaries in Chemical Vapor Deposited Diamond", submitted to Appl. Phys. Letters.

Superconducting $YBa_2Cu_3O_{6-x}$ Crystals

Babcock, S. E., Zhang, N., Gao, Y., Cai, X. Y., Kaiser, D. L., Larbalestier, D. C., and Merkle, K., "Microstructure and Composition of Electromagnetically-Characterized $YBa_2Cu_3O_{7-x}$ Grain Boundaries," Journal of Advanced Science, 4, 119 (1992).

Bennett, L. H., Swartzendruber, L. J., Kaiser, D. L., Gayle, F. W., Blendell, J., Habib, J. M., and Seyoum, H. M., "Thermoremanance and Meissner Effect in QMG and Single Crystal YBCO," J. Magnetism and Magnetic Matls., 104, 539 (1992).

Dorsinskii, L. A., Nikitenko, V. I., Polyanski, A. A., Vlasko-Vlasov, V. K., Roytburd, A., Kaiser, D. L., and Gayle, F. W., "Kinetics of Twin Boundary Migration in $YBa_2Cu_3O_{7-x}$," submitted to Physica C.

Kaiser, D. L., Swartzendruber, L. J., and Fiori, C. E., "Chemical Doping of $YBa_2Cu_3O_{7-x}$ Single Crystals," Proc. of the Workshop on Superconductivity, International Superconductivity and Technology Center and Materials Research Society (1992), p. 134-137.

Larbalestier, D. C., Babcock, S. E., Cai, X. Y., Field, M. B., Gao, Y., Heinig, N. F., Kaiser, D. L., Merkle, K., Williams, L. K., and Zhang, N., "Electrical Transport Across Grain Boundaries in Bicrystals of $YBa_2Cu_3O_{7-x}$," Physica C., 185-189, 315 (1991).

MATERIALS MICROSTRUCTURE CHARACTERIZATION

Black, D. R., Burdette, H. E., and Banholzer, W., "X-ray Diffraction Imaging of Man-Made and Natural Diamond," Proceeding of the Third International Conference on New Diamond Science and Technology, Heidelberg, August 30-September 4, 1992.

Black, D. R., Kuntz, T. A., and Wadley, H. N. G., "Measurement of Internal Residual Strain Gradients in Metal Matrix Composites Using Synchrotron Radiation," Proceedings from Review of Progress in Quantitative Nondestructive Evaluation, July 28 - August 2, 1991, Brunswick Maine.

Black, D. R., Long, G. G., Spain, I. L., "Soft X-ray Reflectivity at the Carbon K-Edge of Glassy Carbon," submitted to Phys. Rev. B.

Black, D. R., Long, G. G., and Spain, I. L., "X-ray Raman Scattering by Glassy Carbon: Investigation of Short-Range Order and Bonding," submitted to Phys. Rev. B.

Bouldin, C. E., Brewe, D. L., Pease, D. M., Budnick, J. I., and Tan, Z., "Pin Diode Detector for a Glancing-Emergence-Angle EXAFS Technique," submitted to Review of Scientific Instruments.

Fischer, D. A., Castner, D., Lewis, K., Ratner, B., and Gland, J., "Surface Structure and Orientation of Polymerized Terafluoroethylene Films," in press Langmuir.

Fischer, D. A., Chen, J. G., Hardenburg, J. H., and Hall, R. B., "A Fluorescence Yield Near Edge Spectroscopy (FYNES) Investigation of the Reaction Kinetics of NiO/Ni(100) with Hydrogen," in press Surface Science.

Fischer, D. A., Davis, S. M., Zhou, Y., Freeman, M. A., Meitzner, G. M., and Gland, J. L., "Carbon K-Edge X-ray Absorption Spectroscopy of Zeolite Coke Deposits," submitted to J. of Catalysis.

Fischer, D. A., Donovan, R., Jiang, L. Q., and Strongin, M., "Deuteration of Propylene Over Palladium Overlayers on Tantalum," Surface Science, 276, 95-98 (1992).

Fischer, D. A., Gland, J. L., and Rufael, T., "Ultra-Soft X-ray Absorption Detected by Fluorescence Yield: An In-Situ Method for Characterizing Adsorbates and Surface Reactions," submitted to ACS Surface Science of Catalysis: In-Situ Probes and Reaction Kinetics edited by Fritz Hoffman, pg. 183-201 (1992).

Fischer, D. A., and Meitzner, G., "Distortions of Fluorescence Yield X-ray Absorption Spectra Due to Sample Thickness," submitted to J. Solid State Comm.

Fischer, D. A., Meitzner, G., Sinfelt, J. H., "X-ray Absorption Studies of the Electronic Structure of Nickel-Copper Catalysts," Catalysis Letters, 15, 219-229 (1992).

Fischer, D. A., and Phillips, W., "Soft X-ray Transmission of Thin Film Diamond: Applications to Detectors and High Pressure Gas Cells," J. of Vacuum Science and Technology, A10, 2219-2221 (1992).

Fischer, D. A., Rufael, T., Prasad, J., and Gland, J. L., "Hydrogen Induced C-S Bond Activiation in the Pt(111) Surface: Transient In-Situ C K_{α} Fluorescence Yield Measurements of Methylthiolate Hydrogenolysis," Surface Science, 278, 41-50 (1992).

Kerch, H. M., Cosandey, F., and Gerhardt, R., "Imaging of Fine Porosity in Low Density Amorphous Materials by Defocus Contrast Microscopy," Journal of Non-Crystalline Solids, in press.

Long, G. G., Black, D. R., Feldman, A., Farabaugh, E. N., Spal, R. D., Tanaka, D. K., and Zhang, Z., "Structure of Vapor-Deposited Yttria and Zirconia Thin Films," Thin Solid Films, 217, 113-119 (1992).

Long, G. G., Kruger, J., Zhang, Z., and Tanaka, D. K., "Reflection X-ray Absorption Fine Structure Study of the Passive Films on Cast and Rapidly Solidified Mg Alloys," X-ray Methods in Corrosion and Interfacial Electrochemistry, ed. by A. Davenport and J. G. Gordon II. The Electrochemical Society, N.J (1992), pp. 298-305.

Long, G. G., Shaeffer, D., Oliver, D., Ashley, C. S., Richter, D., Farago, B., Frick, B., Hrubesh, L., Van Bommel, M. J., and Krueger, S., "Structure and Topology of Silica Aerogels," Noncryst. Solids, 145, 105-112 (1992).

Spal, R. D., Klaffky, R., Singh, O., and Link, H., "Characterization of White Beam Position Fluctuations at NSLS X23A3," submitted to Nuclear Instruments and Methods in Physics Research A.

Steiner, B., Dobbyn, R. C., Black, D., Burdette, H., Kuriyama, M., Spal, R., van den Berg, L., Fripp, A., Simchick, R., Lal, R., Batra, A., Matthiesen, D., and Ditchek, B., "High resolution synchrotron x-radiation diffraction imaging of crystals grown in microgravity and closely related terrestrial crystals" Proc. SPIE, **1557**, 156-167 (1991).

Steiner, B., Dobbyn, R. C., Black, D., Burdette, H., Kuriyama, M., Spal, R., Simchick, R., and Fripp, A., "High resolution x-ray diffraction imaging of lead tin telluride" J. Crystal Growth, **114**, 707-714 (1991).

Steiner, B., Tseng, W., Comas, J., Laor, U., Dobbyn, R. C., and Rajan, K., "Defect Formation in Semiconductor Layers during Epitaxial Growth," J. Crystal Growth, in press (1992).

Tseng, W. F., Comas, J., Steiner, B., Metze, G., Cornfeld, A., Klein, P. B., Gaskill, D. S., Xia, W., and Lau, S. S., "Growth and Characterization of Ternary and Quaternary Compounds of $In_y(Al_xGa_{1-x})_{1-y}As$ on (110) InP, Mat. Res. Soc. Symp. Proc **240**, 117-122 (1992).

Woicik, J. C., Karlin, B. A., and Cowan, P. L., "X-ray, Soft X-ray, and VUV Beam Position Monitor," Rev. Sci. Instrum., 63, 526 (1992).

Woicik, J. C., Kendelewicz, T., Miyano, K. E., Cowan, P. L., Bouldin, C. E., Richter, M., Karlin, B. A., Pianetta, P., and Spicer, W. E., "Extended X-ray Absorption Fine Structure and X-ray Standing Wave of the Clean InP(110) Surface Relaxation," J. Vac. Sci. Tech. A. (Vacuum, Surfaces & Films) Vol. 10, 4 Pt. 2, 2041-2045 (1992).

Woicik, J. C., Miyano, K. E., Kendelewicz, T., Cowan, P. L., Karlin, B. A., Bouldin, C. E., Pianetta, P., and Spicer, W. E., "Structural Characterization of the 1 ML Sb/GaP(110) Interface Using X-ray Standing Waves," Phys. Rev. B (Condensed Matter) Vol. 46, 11 6869-6874 (1992).

Woicik, J. C., Zhengquan, T., Heald, S. M., Rapposch, M., and Bouldin, C. E., "Gold Induced Germanium Crystallization," Phys. Rev. B. [Condensed Matter], Vol. 46, 15 9505-9519 (1992).

Woicik, J. C., Stragier, H., Cross, J. O., Rehr, J. J., Sorensen, L. B., and Bouldin, C. E., "Local Atomic Structures from New Resonance X-ray Diffraction Harnessing the Virtual Photoelectrons," Phys. Rev. Lett., Vol. 69, 21 3064-3067 (1992).

Woicik, J. C., Kendelewicz, T., Miyano, K. E., Richter, M., Bouldin, C. E., Pianetta, P., and Spicer, W. E., "Extended X-ray Absorption Fine Structure Determination of Bond Length Conservation at the Clean InP(110) Surface," Phys. Rev. B [Condensed Matter], Vol. 46, 15 9869-9872 (1992).

Woicik, J. C., Kendelewicz, T., Miyano, K. E., Herrera-Gomez, A., Cowan, P. L., Karlin, B. A., Bouldin, C. E., Pianetta, P., and Spicer, W. E., "X-ray Standing Wave Study of Monolayers of Sb on GaAs(110)," Physical Review [Condensed Matter], Vol. 46, 11 7276-7279 (1992).

Woicik, J. C., Terry, J., Liu, H., Cao, R., Pianetta, P., Yang, X., Wu, J., Richter, M., Maluf, N., Pease, F., Robinson, M. B., Dillon, A., and George, S., "A Photoemission Study of Electrochemically Etched Light Emitting Silicon," Chemical Surface Preparation Passivation and Cleaning for Semiconductor Growth and Processing, eds. R. J. Nemanich, C. R. Helms, M. Hirose and G. Rubloff, Volume 259, Symposium Proceedings of the Matls. Res. Soc., 1992.

CERAMICS DIVISION PATENTS

1992

Novel Method of Bonding Materials Together - "Nanoglue" (P)	D. T. Smith R. G. Horn, A. Grabbe
Coprecipitation Synthesis of Precursors to Bismuth-Containing Superconductors (I)	J. Ritter
A Super Stable High-Temperature Liquid Lubricant Containing a Unique Antioxidant and Additive Solulubilizing Ternary System (D)	J. Perez, C. Ku, Y. M. Zhang
A Chemical Assisted Process for Rapid Machining of Tough Ceramics (D)	J. Wang, S. M. Hsu
A Cutting Fluid Additive for Machining of Ceramics (D)	S. Jahanmir, G. Zhang
Hydroxyl Containing Organic Compounds as Boundary Lubricants for Silicon Nitride Ceramics (D)	R. S. Gates, S. M. Hsu
A Process to Lubricate Titanium with Chlorinated Hydrocarbons (D)	J. Wang, S. M. Hsu
A Process to Machine Titanium Using Chlorinated Hydrocarbons (D)	J. Wang, S. M. Hsu
Methods of Reducing Wear on SiC Ceramic Surfaces (P)	D. E. Deckman S. M. Hsu
Detergent and Dispersant Type Organic Compounds as Boundary Lubricants for Silicon Nitride Ceramics (D)	R. S. Gates S. M. Hsu

1991

Diamond Coated Laminates and Methods of Producing Same (D)	A. Feldman E. N. Farabaugh
High Resolution X-Ray Microtomographic Detector (P)	R. D. Spal R. C. Dobbyn M. Kuriyama

A Colloidal Processing Method for Coating Ceramic Reinforcing Agents (I) U.S. Patent No. 5,039,550, August 1991	S. Malghan C. Ostertag
Process for the Fabrication of Ceramic Monoliths by Laser-Assisted Chemical Vapor Infiltration (I)	J. Ritter
A Method for Making Translucent High Purity Transparent Silicon Nitride (P)	A. Pechenik G. Piermarini S. Block S. Danforth

1990

Novel Synergistic Additive Packages Containing High Molecular Weight Antioxidants for High Temperature Lubricants (P)	S. Hsu J. Perez C. Ku Y. Zhang
Low Energy (Thermal) Neutron Absorbing Glass (A)	D. Blackburn (Retired) C. Stone D. Cranmer D. Kauffman J. Grudl
Process for Elimination of Twins in Perovskite-Type Superconducting Single Crystals (D)	D. Kaiser F. Gayle
A Method for Fabrication of Materials from Nano-Sized Particles Using High Pressure and Cryogenic Temperatures (I)	A. Pechenik G. Piermarini
Aluminum Hydroxides as Solid Lubricants U.S. Patent 4919829, issued April 24, 1990	R. Gates S. Hsu

1989

Ultraviolet Transmitting Glass for 308mm Ring Dye Laser (D)	D. Blackburn D. Cranmer D. Kauffman
Buffered Cell for Sintering of High T_c Thallium Containing Ceramics (D)	L. Cook
Polished Plates of Chemical Vapor Deposited Diamond (A)	A. Feldman E. Farabaugh
Additive Packages Containing High Molecular Weight Antioxidants for High Temp Lubricant (D)	S. Hsu J. Perez C. Ku
A Novel Fluid to Solubilize High Temperature Liquid Lubricant Antioxidants (D)	J. Perez C. Ku S. Hsu
A Process for the Controlled Preparation of a Composite of Ultra-Fine Magnetic Particles Homogeneously Dispersed in a Dielectric Matrix (P)	J. Ritter R. Shull
Optical Sensor: Molecular Orientation and Viscosity of Polymeric Materials (D)	A. Bur R. Lowry R. Roth
Elimination of Twins in Perovskite-Type Superconducting Single Crystals (D)	F. Gayle D. Kaiser

1988

Stress-Free Sintering of Fiber-Reinforced Ceramic Composites (D)	C. Ostertag
Electrode Array for Analysis of Particles in Slurries (D)	A. Dragoo
Quantitative & Qualitative Technique for Assessing Stresses During Densification (D)	C. Ostertag
Process for the Preparation of Fiber-Reinforced Ceramic Matrix Composites (A)	W. Haller U. Deshmukh

A Process for the Chemical Synthesis and Forming of BiPbSrCaCuO and BiSrCaCuO High Temperature Superconductors Materials (D)	J. Ritter
Low Temperature Chemical Synthesis of Precursors to $BiCaSrCuO_x$ High Temperature Superconductor Powders (D)	J. Ritter
High Pressure Process for Producing Transformation Toughened Ceramics (I)	S. Block G. Piermarini
Superconductor-Polymer Composite (D)	A. DeReggi C. Chiang G. David

(D) = INVENTION DISCLOSURE
(P) = PENDING DECISION BY PATENT OFFICE
(A) = INVENTION ALLOWED BY PATENT OFFICE
(I) = PATENT ISSUED

CONFERENCES AND WORKSHOPS SPONSORED

Conference Diamond Optics IV, at 35th Annual International Technical Symposium on Optical and Optoelectronic Applied Science and Engineering, A. Feldman, Chairman, July 20, 21, 1992. Conference to review the status of the use of diamond for optics.

Workshop on Characterizing Diamond Films, A. Feldman, Organizer and Chairman, February 27, 28 (1992). A NIST sponsored workshop for U.S. companies covering in depth issues related to applications of diamond and the need for standards.

Workshop on "Small-angle X-ray Scattering for Materials Science," organized by G. Long, May 18, 1992, at the National Synchrotron Light Source User's Meeting.

Workshop on "Advances in EXAFS Application," organized by C. Bouldin, May 18, 1992, at the National Synchrotron Light Source User's Meeting.

Symposium on Smart Materials, Grady S. White, Co-organizer, April 13-14, 1992 Minneapolis, MN. Sponsored by American Ceramic Society to review status of ceramics in "Smart Materials."

Lubrication Technologies for Future Energy Conversion Systems, an invited workshop held at Northwestern University, Evanston, IL on September 21-23, 1992. The workshop was organized and chaired by S. M. Hsu on behalf of the Department of Energy, Office of Transportation Technologies, Office of Transportation Materials, in conjunction with NIST, and Northwestern University. Some 44 industrial representatives attended to identify current and future research needs as well as to prioritize future activities. A conference proceeding is being prepared.

Workshop on Thermal Spray Research, at NIST July 20, 1992, organized by S. J. Dapkunas to identify research issues critical to the reproducibility and performance prediction of thermal spray coatings.

Workshop on Intelligent Processing of Ceramic Powders, at NIST July 17-18, 1992, oganized by S. G. Malghan to determine measurement research needs for process control.

Workshop on Photonic Materials, at NIST August 26-28, 1992, organized by J. A. Carpenter and S. W. Freiman in cooperation with the OIDA to identify material issues of importance to photonic systems.

STANDARD REFERENCE MATERIALS

The Division provides science, industries, and government a central course of well characterized materials certified for chemical composition of physical or chemical properties. These materials are issued with a certification and are used to calibrate instruments, to evaluate analytical methods, or to produce scientific data which can be referred to a common base.

DESCRIPTION	SRM NUMBER
Abrasive Wear	1857*
Alumina Elasticity	718
Alumina Glass Anneal Point	714
Alumina Glass Anneal Point	715
Alumina Melting Point	742
Aluminum Magnetic Susceptibility	763-1
Aluminum Magnetic Susceptibility	763-2
Aluminum Magnetic Susceptibility	763-3
Barium Glass Anneal Point	713
Borosilicate Glass Composition	93(A)
Borosilicate Glass Thermal Expansion	731L1
Borosilicate Glass Thermal Expansion	731L2
Borosilicate Glass Thermal Expansion	731L3
Cadmium Vapor Pressure	746
Catalyst Package for Engine Simulation (IIID)	1817
Catalyst Package for Engine Simulation (IIID)	1817b
Catalyst Package for Engine Simulation (IIIE)	8500
Catalyst Package for Engine Simulation (IIIE)	8501
Catalyst Package for Engine Simulation (IIIE)	8500a
Chlorine in Base Oil	1818
Container Glass Composition	621
Container Glass Leaching	622
Container Glass Leaching	623
Copper Thermal Expansion	736L1
Fused Silica Thermal Expansion	739L1
Fused Silica Thermal Expansion	739L2
Fused Silica Thermal Expansion	739L3
Glass Analytical Standard	1835
Glass Dielectric Constant	774
Glass Electrical Resistance	624
Glass Fluorescence Source	477
Glass Liquidus Temperature	773
Glass Refractive Index	1820

Glass Sand (High Iron)	81A
Glass Sand (Low Iron)	165A
Glass Stress Optical Coefficient	708
Glass Stress Optical Coefficient	709
Glass Viscosity Standard Renewal	717
Gold Vapor Pressure	745
High Boron Glass Viscosity	717
Intensity XRD Set	674
Lead Barium Glass Composition	89
Lead Glass Anneal Point	712
Lead-Silica Glass High Temperature Resistivity	1414
Lead Glass Viscosity	711
Line Profile	660
Liquids Refractive Index	1823
Low Boron Glass Composition	92
MNF_2 Magnetic Susceptibility	766-1
Mica X-Ray Diffraction	675
Neutral Glass Anneal Point	716
Nickel Magnetic Susceptibility	772
Opal Glass Composition	91
Palladium Magnetic Susceptibility	765-1
Palladium Magnetic Susceptibility	765-2
Palladium Magnetic Susceptibility	765-3
Platinum Magnetic Susceptibility	764-1
Platinum Magnetic Susceptibility	764-2
Platinum Magnetic Susceptibility	764-3
Refractive Index Glass	1822
Respirable Cristobalite	1879
Respirable Quartz	1878
Ruby EPR Absorption	2601
Sapphire Thermal Expansion	732
Silicon X-Ray Diffraction	640(b)
Silicon Nitride Particle Size	659*
Silver Vapor Pressure	748
Soda Lime Flat Glass Composition	S620
Soda Lime Float Composition	1830
Soda Lime Float Viscosity	710
Soda Lime Sheet Composition	1831
Soda-Lime-Silica Glass	710a
Sulfur in Oil	1819
Toluene 5 ML	211C
Total Nitrogen in Oil	1836
Tungsten Thermal Expansion	737
Total Nitrogen in Oils	1836
Wear Metals in Oil	1084a
Wear Metals in Oil	1085a

X-Ray Diffraction Instrument Sensitivity	1976*
X-Ray Diffraction Intensity	676*
X-Ray Diffraction Intensity Set	674a

*New in FY-1992

SELECTED TECHNICAL/PROFESSIONAL COMMITTEE LEADERSHIP

American Association for the Advancement of Science

- Physics Section
  - B. Steiner, Representative of the Optical Society of America

American Ceramic Society

- Program and Meetings Committee
  - S. Freiman, Incoming Chairman
- Glass Division
  - Committee on Glass Standards Classification and Nomenclature
    - M. Cellarosi, Chairman
  - Editorial Committee
    - S. Wiederhorn, Subchairman
- Basic Science Division
  - Editorial Committee
    - B. Lawn, Chairman
  - Program Committee
    - E. Fuller, Jr., Chairman
- Communication of the American Ceramic Society
  - E. Fuller, Jr., Contributing Editor
- Engineering Ceramics Division
  - D. Cranmer, Vice-Chairman

ASM International

- Energy Division
  - S. Dapkunas, Past Chairman, Division Council Member
- Journal of Materials Engineering and Performance
  - S. Dapkunas, Editorial Board
- Washington D.C. Chapter Education Committee
  - J. A. Carpenter, Jr., Chairman

American Society for Engineering Education

- Postdoctoral Review Committee
  - A. Feldman, Member

American Society for Testing and Materials

- C14: Glass and Glass Product
  - M. Cellarosi, Chairman
- C14.01: Nomenclature of Glass and Glass Products
  - M. Cellarosi, Chairman

C28. Advanced Ceramics
G. D. Quinn, Vice-Chairman
C28.05: Powder Characterization
S. Malghan, Working Group Chairman
C28.07: Ceramic Matrix Composites
D. C. Cranmer, Chairman
D2: Petroleum Products and Lubricants
E24.07: Fracture Toughness of Brittle Nanmetallic Materials
G. D. Quinn, Member
E29.01: Advanced Ceramics, Organizational Meeting
M. Cellarosi
E42: Surface Science
G. G. Long, Member
Fl:02: Lasers
A. Feldman, Subcommittee Editor
G2.2.02: Solid Particle Erosion
A. Ruff, Task Group Leader
G2.4.04: Pin-on-Disk
A. Ruff, Chairman
G2.12: Computerization in Wear and Erosion,
A. Ruff, Chairman

American Society of Mechanical Engineers

Journal of Tribology
S. Jahanmir, Associate Editor
Research Committee on Tribology
S. Jahanmir, Member
S. Hsu, Member
Wear of Materials Conference Steering Committee
A. Ruff, Member

COMAT Subcommittee on Structural Ceramics
S. J. Dapkunas, Member

Diamond Films and Technology
Editorial Advisory Board
A. Feldman, Member

IEEE Lasers and Electrooptics Society
Washington-Northern Virginia Chapter
B. Steiner, Treasurer

International Advisory Committee of Topical Symposium V on structural ceramics, 8th CIMTEC
S. Hsu, Member

International Energy Agency
Task II - International Standards
S. Hsu, Overall Task Leader on Powder Characterization
Subtask 6 Powder Characterization Subgroup
S. Malghan, U. S. Task Leader

International Union of Crystallography (IUCr)
Commission on Crystallographic Studies at Controlled Pressures and Temperatures
G. Piermarini, Chairman

Minerals and Metallurgical Processing Journal
Editorial Board
S. G. Malghan, Member

National Materials Advisory Board, National Academy of Sciences
Committee on Superhard Materials
A. Feldman, Member

National Synchrotron Light Source
Housing Committee
C. E. Bouldin, Member
User Executive Committee
G. G. Long, Member
EXAFS Special Interest Group
C. E. Bouldin, Chairman
Proposal Study Panel
D. A. Fischer, Chairman
Housekeeping Committee
J. C. Woicik, Member

NIST Cold Neutron Research Facility
G. G. Long, Program Advisory Committee Member

Optical Society of America
Meggers Award Committee
B. Steiner, *ex officio* member as former chairman

Powder and Bulk Engineering Journal
S. Malghan, Member Editorial Advisory Board

Society of Photooptical Instrumentation Engineers
Kingslake Award Committee
B. Steiner, Chairman

Society of Tribologists and Lubrication Engineers
Annual Meeting Program Committee
S. Jahanmir, Member
Board of Directors
S. Hsu, Director
Ceramics and Composite Committee
S. Jahanmir, Chairman

Strategic Defense Initiative Organization Technology Applications Office (SDIO/TA)
Materials and Electronics Panel
J. A. Carpenter, Jr., Member

Superconductor Applications Association
E. Fuller, Jr., Member of Advisory Board

Versailles Project on Advanced Materials and Standards (VAMAS)
Technical Working Area on Ceramics
G. D. Quinn, U. S. Representative and International Chairman

Technical Working Area on Wear Test Methods
S. Jahanmir, U. S. Representative and International Leader

INDUSTRIAL AND ACADEMIC INTERACTIONS

INDUSTRIAL

ACTIS, Inc.

An agreement has been signed between NIST and ACTIS, Inc. for a joint research and development activity related to comprehensive computerized tribology databases. These databases will be evaluated by NIST and marketed by ACTIS, Inc. Other participants in the program are DOE, U.S. Army, U.S. Air Force, ASME and STLE.

AKZO Chemical Co.

A Cooperative Research and Development Program continues to utilize the NIST technology (S. M. Hsu, NIST; T. Marolewski, AKZO) in development of a high temperature liquid lubricant for evaluation in low heat rejection engines.

Allied Signal Corporation

A joint research program is underway to determine the role of impurities in superconducting ceramic powders on limiting the critical current density in the final product. Allied (A. Trivedi) is supplying superconducting powders containing various quantities of carbon and other impurities. NIST (S. Freiman) is processing these powders and determining critical current densities. The work will be published as a joint paper.

S. G. Malghan is conducting collaborative studies with B. Busovne and J. Pollinger of Garrett Ceramic Components (an Allied subsidiary) on the interactions of powder-binder-sintering aid in the processing of silicon nitride powders. Garrett intends to utilize the results developed at NIST.

A collaborative effort between NIST (Benjamin Burton) and S. P. Greiner, Allied Signal has begun to conduct first principles phase diagram calculations of BCC based ordering in Ca-Mg-Li alloys.

Allison

D. C. Cranmer has been collaborating in a program started to completely evaluate the creep and creep rupture behavior of PY6, a grade of silicon nitride made by GTE. This work is being done in collaboration with Pramod Khandelwal of Allison Gas Turbine.

American Xtal Technology, Inc.

Collaboration in the characterization of gallium arsenide substrates grown with a greatly increased degree of regularity by a new commercial process: vertical gradient freeze (Bruce Steiner, NIST, and Morris Young, President, AXT, Inc.)

Applied Physics Laboratory (APL)

A collaboration between NIST (L.H. Robins) and Johns Hopkins Applied Physics Laboratory (A. Wickendon) to characterize the optoelectronic properties of epitaxial films and heterostructures of the aluminum gallium nitride ($Al_xGa_{1-x}N$) system. These films, grown at APL by metalorganic chemical vapor deposition, show promise for applications as blue-violet/UV laser and non-laser light sources, photoconductive light detectors, and electro-optic modulators. Spectroscopic characterization techniques to be applied to these films include cathodoluminescence, photoluminescence, photoconductivity, and electroabsorption; preliminary cathodoluminescence measurements have already been carried out.

AT&T (Bell Laboratories)

Dr. Cliff King is collaborating with J. C. Woicik (NIST) and C. E. Bouldin (NIST) on the structure of boron-doped SiGe heterojunction bipolar transistors.

Battelle Columbus Laboratories

A joint activity is underway to prepare a wear atlas from selected literature and research findings at Battelle Columbus Laboratories, NIST, and the West German Bundesanstalt fur Materialprufung. Battelle (W. Glaeser) and NIST (A. W. Ruff) are evaluating publications in wear and friction to select authoritative findings that relate wear and friction with materials properties and surface morphology.

Brookhaven National Laboratory

Arnie Moodenbaugh (BNL) and Dan Fischer (NIST) are collaborating on oxygen K near edge fluorescence yield spectroscopy to characterize the oxygen hole state density of high temperature superconductors. The hole state density was measured as a function of superconductor composition and was correlated with measurements of T_c and x-ray diffraction.

Catalyst Research Corp.

D. Schrodt (CRC) has obtained laboratory procedures from J. Ritter for designing tests for Li-batteries.

Caterpillar Company

The Surface Properties Group at NIST is working with Caterpillar Company in several areas. F. Kelly is working with S. M. Hsu in the area of advanced lubrication, diesel particulate reduction and engine simulations. He is also working with A. W. Ruff to improve the wear resistance of tractor under-carriage linkage. S. M. Hsu is also working wth K. Bruk, B. Hockman, and R. Nevinger on the design of ceramic valve seat inserts.

As part of the DOE sponsored study on diesel particulates formation, S. M. Hsu and R. S. Gates at NIST is working with the CRC study group to jointly evaluate the effects of fuel type, engine design and service duty on diesel particulate formation. The study group consists of the major oil companies, engine manufacturers and component suppliers. Various particulate samples were received from the study group who is currently conducting various engine tests and full-scale field tests of different engine and fuel combinations.

Crystallume

Unique samples of thick homoepitaxial diamond films were provided to D. R. Black, The defect microstructure of these films was examined by x-ray topography and correlated to the substrate microstructure.

William Phillips and Dan Fischer (NIST) have measured for the first time the soft x-ray absolute transmission function of thin film diamond (as supplied commercially). The thin film diamond will be used as a high pressure and high temperature contamination barrier in more demanding applications of our low Z fluorescence yield technique.

Cummins Engine Company

S. M. Hsu is working with J. Wang, M. Naylor, and T. Gallant of Cummins Engine on the lubrication of new materials, evaluation of chemistries and development of advanced lubrication concepts for future engines. In conjunction with Akzo Chemicals Company under a DOE contract, new chemistries are being developed and these chemistries are being evaluated in prototype engines by Cummins.

Deere and Company

A collaborative research project is in progress between Deere and Company (P. A. Swanson) and NIST (L. K. Ives) to determine the influence of crystal structure on galling resistance of nitrided 4140 steel.

Delco Products (Division of General Motors)

Dr. V. Ananthanarayanan, Delco Products, has collaborated with S. Malghan in developing test procedures for evaluating the dispersion of strontium ferrite in aqueous environment. Two scientists spent two months at NIST to conduct experimental research. Based on these results, a development program is being carried out at the Delco Products production facility.

DOW Chemical Company

Gary Mitchell and Ben Dekoven of the Dow Chemical Company have begun a research collaboration with Dan Fischer (NIST) to study polymer surfaces and metal polymer interfaces using ultra soft x-ray absorption spectroscopy. The concentrations and orientations of functional groups have been characterized at and near the surface for a series of model polymeric materials. The materials studied include poly(acrylic acid), poly(butyl methacrylate), polystyrene, polycarbonate, poly(ethylene terephthalate), and model acrylic coatings.

Eaton

S. M. Hsu is working with J. Edler and M. Leydet of Eaton to jointly evaluate ceramic material for gas-fuelled co-generation engines. NIST conducts wear tests and mechanistic studies and provides feedback to Eaton. This is part of the study sponsored by GRI.

Eastman Kodak Company

D. T. Smith (NIST) has been collaborating informally with Ravi Sharma of Kodak's Polymer Research Laboratory to study the surface charging properties of thin insulating films of potential industrial interest in Kodak.

EG&G Energy Systems

Collaboration in diffraction imaging on irregularities in mercuric iodide crystals and detectors grown in space and on the ground. (Bruce Steiner, NIST, and Lodewijk van den Berg, EG&G)

E. I. DuPont de Nemours & Co.

DuPont (D. Roach) has provided alumina and alumina-zirconia fibers to C. Ostertag for incorporation into ceramic, ceramic-metal, and glass matrix composites.

NIST (Lawrence Cook) has collaborated with the High T_c group at DuPont on characterization of thallium-based high T_c thin films and substrates.

C. Torardi of AT&T Bell Laboratories has assisted R. Roth and C. Rawn of NIST in determining crystal structures of calcium bismuth oxides that occur in the Bi-Sr-Ca-Cu oxide system. This system is currently of major interest as it contains important high-temperature superconducting materials.

Edge Technology Inc.

Artificial diamonds to be used as machine tools were supplied to D. R. Black. Topographic examination of these crystals was correlated to optically observed defects for quality control.

Electric Power Research Institute

EPRI (W. Bakker) funded a program in the Ceramics Division (S. Freiman) to develop superconducting ceramics for conductor applications. The program involves determining the effects on critical current density of substituting other rare earth ions for yttrium in Ba-Y-Cu-O superconducting ceramics. Phase equilibria and processing data relevant to the production of these materials were obtained.

Exxon Research and Engineering Company

George Meitzner (ER&E) and Mark Davis (Exxon Research and Development Lab) have a research collaboration with Dan Fischer (NIST) to study the electronic structure of carbonaceous deposits (coke) in zeolite cataysts using near edge spectroscopy above the carbon K edge. This work has highlighted our ability to understand the coke deposits at a molecular level without physically removing the coke from the zeolite catalyst as had been done before using more standard (destructive) chemical analysis.

Ford Motor Company

Ford Motor Company (K. Carduner and M. Rokosz) have been active in the application of NMR spectroscopy and imaging to characterize ceramic materials. Collaborative effort with P. S. Wang involves data exchange of Si-27 CP/MAS NMR for phase composition determination of silicon nitride and carbide powders. In the future, we plan to exchange imaging capabilities.

Gas Research Institute and Center for Advanced Materials, Pennsylvania State University

The Structural Ceramics Database project was funded in part by the Gas Research Institute through the Center for Advanced Materials at Pennsylvania State University, as an important step towards the use of advanced ceramics in heat exchangers and gas-fueled engines.

General Electric Corporate Research and Development

A collaborative research program to study the microstructure of large artificial diamond has been established with D. R. Black in the Materials Microstructure Characterization Group.

Geophysical Laboratory, Carnegie Institute of Washington, DC

NIST (Benjamin Burton) has been working with R. E. Cohen, The Geophysical Laboratory, Carnegie Institute of Washington, D.C. on a first principles study of cation ordering in the relaxor ferroelectric system $Pb(Sc_{½}Ta_{½})O_3$-$PbTiO_3$.

Grumman Corporation

Collaboration in diffraction imaging on the crystal perfection of zinc cadmium telluride crystals grown in space and on the ground. (Bruce Steiner, NIST, and David Larson, Grumman) Grumman Corporation

GTE Laboratories, Inc.

GTE (J. Baldoni) has provided whisker-reinforced and whisker-free silicon nitrides to S. Wiederhorn and D. Cranmer for evaluation of creep and creep rupture, and changes in microstructure as a result of creep.

Collaboration in diffraction imaging on irregularities in gallium arsenide. (Bruce Steiner, NIST, and David Matthiesen and Brian Ditchek, GTE)

Hughes Research Laboratories

Collaboration in the crystal growth of barium titanate. (Bruce Steiner, NIST, Mark Cronin-Golomb and Gerard Fogarty, Tufts University, and Barry Wechsler, Hughes)

IBM, Almaden Research Laboratory

Interactions between NIST (Winnie Wong-Ng) and T. C. Huang of IBM focused on the investigation of the X-ray property of PZT and $BaTiO_3$ thin films which were prepared at NIST using the laser deposition technique.

International Centre for Diffraction Data (ICDD)

Winnie Wong-Ng, chairperson of the Ceramics Subcommittee, initiated the organization of the inorganic materials of the X-ray Powder Diffraction File (PDF) into minifiles according to their functions, properties or structure at the ICDD. W. Wong-Ng also serves as a consulting editor for the PDF.

Kennemetal Inc.

S. M. Hsu is cooperating with the machining group at Kennemetal (R. F. Upholster) on jointly developing chemically assisted technology of ceramics. Samples were exchanged and many discussions were held. Some of the more promising chemistries may be tested at their facility. Kennemetal is the largest US manufacturer of ceramic wear inserts.

Lawrence Livermore Laboratories

As part of a study with Pat Johnson of Lawrence Livermore Laboratories, of the cohesive strength of grain boundaries in Ni_3Al as a function of grain boundary misorientation and symmetry, alloy stoichiometry and boron concentration, grain orientations in test bars have been measured at NIST (Mark Vaudin) prior to mechanical testing.

Matec Applied Sciences

This cooperative research is related to the development of electrokinetic sonic amplitude measurement for dispersion of powders in dense slurries. Research at NIST under the direction of S. Malghan will be utilizing hardware and software developed by Matec Applied Sciences for on-line measurement of dispersion.

Morgan-Matroc

NIST (Mike Hill, Grady White, and Steve Freiman) is working with Craig Near from Morgan-Matroc studying the mechanical properties of PZT.

Nanophase Technology, Inc.

Collaborative research is being undertaken between J. Parker and A. Thomas of Nanophase Technology and S. Krueger (NIST/Reactor Radiation Division) and G. Long of NIST on nanocrystalline yttria, zirconia, ciria and alumina.

NASA Consortium for Commercial Development

Cooperative research is aimed at understanding fundamentals of zeolite nucleation, growth of CdTe single crystals and strain development during growth of GaAs. G. G. Long, D. R. Black, H. E. Burdette, and S. Krueger (Reactor Radiation Division) are working with E. Coker, H. Wiedemeier and D. Larson on this research.

Naval Research Laboratory

S. Lawrence and B. Bender (NRL) are collaborating with J. Wallace on the thermochemical treatment of polymer-derived SiC fibers and the degradation mechanisms of these fibers during high temperature heat treatments. A joint publication is planned.

NIST (Mike Hill and Grady White) is collaborating with Dr. Sadananda at the Naval Research Laboratory investigating cyclic fatigue of piezoelectric material. Mechanical properties are investigated at NIST and TEM will be done at NRL.

Naval Surface Weapon Center (NSWC)

NIST (Winnie Wong-Ng) and I. Talmy of NSWC are in collaborating in the study of the phase diagram of barium and strontium feldspar solid solutions, $(Ba,Sr)Al_2Si_2O_8$. Revised phase diagrams and standard X-ray powder diffraction patterns were obtained based on these collaborations.

Tom Russell, Naval Surface Warfare Center (NSWC) has been working with NIST (Gasper J. Piermarini) collaborating on the study of energetic materials and Buckminsterfullerenes at high pressure.

A joint research project with D. R. Black has been developed to supply and characterize copper single crystal substrates for use as substrates for heteroepitaxial growth of diamond films.

Norton Company

In one collaborative project V. Pujari and C. Willkens of Norton Company, and S. Malghan of NIST are studying the characteristics of agitation milled silicon nitride powders in aqueous environment. Norton Company has provided silicon nitride powder samples. Based on the results of first stage of collaboration, a second stage of research was initiated with an intent to compare the performance of agitation ball milling to large-scale processing by conventional methods.

Thermal conductivity measurements are important for characterizing diamond films. Interaction with Norton (K. Grey) involved learning to use the NIST (A. Feldman and H.P.R. Frederikse) photothermal radiometry facility for the purpose of setting up such a facility at Norton. We plan to collaborate in the analysis of the data generated at Norton.

Dr. Vimal Pujari is cooperating with S. M. Hsu on the effects of machining on tensile strength of silicon nitrides. Tensile bars were received from Norton and were subjected to chemical assisted machining. These bars are being tested.

Norton/TRW Co.

Norton/TRW (R. Yeckley) has provided a Y_2O_3-containing silicon nitride to S. Wiederhorn and D. Cranmer for evaluation of creep and creep rupture, and changes in microstructure as a result of creep.

S. M. Hsu is working with Brian McEntire at Norton-TRW to jointly evaluate ceramic materials for valve seat insert application. The program is a joint program with the Gas Research Institute (GRI), Caterpillar, and Southwest Research Institute (SWRI). A Full-scale engine test is being conducted at SWRI to evaluate different materials for the valve seat inserts in a gas-fuelled Caterpillar 3500 series engine.

Research Triangle Institute

A joint research project was developed with D. R. Black to study the microstructure of diamond substrates to be used for homoepitaxial growth of diamond films by chemical vapor deposition.

Rockwell International

A collaboration between NIST (A. Feldman) and Rockwell International (S. Holly) to organize the Diamond Optics IV conference sponsored by the Society of Photo-Optical Instrumentation Engineers (SPIE).

Rotem, Inc.

Collaboration in the characterization of sapphire substrates. (Bruce Steiner and Uri Laor, NIST, and Shlomo Biderman and Yezekiel Einav, Rotem)

Russian Academy of Science

Cooperative activities under the NIST-Russian Academy of Science Agreement have continued in the areas of tribology and materials science. Current emphasis is on a joint US-USSR book on tribology (A. W. Ruff and S. Jahanmir). Future benefits to NIST and the Division include exchange of tribology data, exchange of computer software for surface analysis, and future exchange of technical staff.

A collaborative program between the Russian Academy of Sciences and NIST Ceramics (D. Kaiser) and Metallurgy Divisions is underway to map flux distributions in high temperature superconductors by a magneto-optical technique.

Sanders Corporation

Collaboration on the crystal growth of barium titanate single crystals (Bruce Steiner, NIST, Mark Cronin-Golomb and Gerard Fogarty, Tufts University, and Tom Pollack, Sanders)

Schmidt Instruments

A collaborative research project was initiated with D. R. Black to grow heteroepitaxial diamond films and characterize their crystal perfection.

Southwest Research Institute

R. A. Page, Southwest Research Institute and S. Krueger, Reactor Division, NIST, are collaborating with G. G. Long on multiple angle small angle neutron scattering (MSANS) studies of pore evolution in research-grade alumina.

Trans-Tech Inc.

NIST (Robert S. Roth and Curtis G. Lindsay) in collaboration with T. Negas of Trans-Tech, Inc. Negas provides NIST with advice on what microwave dielectric materials are of primary industrial interest. NIST in turn develops phase equilibria and crystal structure data. Measurement of electrical properties is a joint effort between NIST and Trans-Tech.

Ube Industries, Japan

Ube Industries (T. Yamada) has collaborated with S. Malghan by providing powder samples for studying the high energy agitation milling of silicon nitride powders. The specific interest lies in the development of an understanding of morphological and surface chemical changes taking place to the milled powders.

U. S. Army Research Laboratory

NIST (Lawrence Cook, Mark Vaudin, and C. K. Chiang) has collaborated with the U. S. Army Research Laboratory on measurements of ferroelectric and dielectric properties of $BaTiO_3$, PZT and $PbTiO_3$ thin films, prepared by pulsed laser deposition.

U.S. Bureau of Mines at Albany

The main goal of the collaboration between N. Gokcen of U.S. Bureau of Mines and (W. Wong-Ng) NIST was to investigate the effect of high oxygen pressure on the structural and superconducting properties of the $Ba_2RCu_3O_{6+x}$ superconductors, R=neodymium and yttrium.

Xsirius, Inc.

Collaboration in the characterization of sapphire substrates for high temperature superconducting devices. (Bruce Steiner and Uri Laor, NIST, and William Graham, President, Xsirius, Inc.)

ACADEMIA

Alabama A&M University

Collaboration on the crystal growth of triglycine sulfate in space and on the ground (Bruce Steiner, NIST, and Ravindra Lal and Ashok Batra, Alabama A&M)

University of Colorado/Joint Institute for Laboratory Astrophysics

Collaboration in the surface treatment and characterization of barium titanate single crystals (Bruce Steiner, NIST, Mark Cronin-Golomb and Gerard Fogarty, Tufts University, and Dana Anderson, U. Col.)

Auburn University

A collaboration between NIST (A. Feldman) and Auburn University (Y. Tzeng) to organize the First International Conference on the Applications of Diamond Films and Related Materials, ADC'91.

Clemson University

B. I. Lee is collaborating with S. Malghan on surface chemical characteristics of silicon nitride powders in aqueous environment in the presence of organic surface active agents.

Cleveland State University

Professor Stephen Duffy is collaborating with T.-J. Chuang in the area of continuum damage mechanics on continuous fiber reinforced ceramic composites for high-temperature applications.
Columbia University

P. Somasundaran has been collaborating with S. Malghan on a research project to study basic parameters affecting the preparation of dense suspensions of silicon nitride powder containing sintering aids.

Drexel University

This is a joint program between Drexel University (M. Barsoum) and NIST (D. Cranmer) to investigate and control the fracture behavior of ceramic and glass matrix composites.

East China University of Chemical Technology

This is a joint effort to use finite-element techniques to analyze creep behavior of ceramic c-rings at elevated temperatures. ECUCT (D. Wu and Z-D Wang) is developing the finite element model for C-rings and a computational algorithm for creep and NIST (T.-J. Chuang) is providing a theoretical framework and experimental data to support the program.

Professor D. Wu and Dr. Z Wang are collaborating with T.-J. Chuang in the area of finite element method and numerical analysis for mechanical evaluation of advanced ceramics.

Howard University

Gasper Piermarini of NIST has been working with George Walrafen and Dr. Chu, Chemistry Dept., Howard University, Washington, DC. Raman scattering to detect residual stresses in ceramics.

Johns Hopkins University

Professor J. Kruger and L. Krebs are collaborating with G. G. Long, NIST, and C. Majkrazak (Reactor Division, NIST) on in situ polarized neutron reflectometry studies of the nature and structure of passive films.

Dan Shechtman of Johns Hopkins is collaborating with NIST (A. Feldman and E. Farabaugh) in the high resolution TEM analysis of CVD diamond nucleation and growth.

Illinois Institute of Technology

P. R. Jemian is collaborating with G. G. Long and S. Krueger (Reactor Division) on neutron and x-ray scattering by novel materials.

Lehigh University

This is a collaboration to determine the effect of microstructure on the fracture resistance of monolithic ceramic materials. The materials under study have been manufactured at Lehigh University (H. Chan, M. Harmer) and are being characterized at NIST (B. Lawn).

Massachusetts Institute of Technology

Collaboration in diffraction imaging on the crystal growth of barium titanate (Bruce Steiner, NIST, and Mark Garrett, MIT)

Interaction with R. Hallock and W. Rhine of MIT (W. Wong-Ng of NIST) was conducted to characterize the $BaTiO_3$ precursor material, $BaTi(O)(C_2O_4)_2 \cdot 5H_2O$ by x-ray diffraction method.

National Tsing Hua University

Professor S. Lee and Dr. J.-L. Chu are collaborting with T.-J. Chuang, NIST in the project of creep life prediction.

Northwestern University

S. M. Hsu is collaborating with Profs. M. Fine and Birl on optimization of ceramic wear resistance by introducing compressive stress into the surface and interfaces. A previous study by Prof. Fine has demonstrated that introduction of a compressive surface layer increased the wear resistance of ceramic material significantly.

Oklahoma State University

Collaborative research between OSU and NIST (R. Powell and D. Cranmer) is being conducted to investigate the properties of permanent, laser-induced refractive index gratings based on Eu-containing glasses. The end result of this effort will be a device for processing optical signals.

Pennsylvania State University

S. M. Hsu is collaborating with Profs. Duda, Klaus, Philips, and Christen on a variety of projects. Duda and Klaus are working on lubrication, development of lubricants for alternative fuels and ceramic lubrication. Philips is working on synthesis of nano-sized particles of ceramic materials using a microwave assisted plasma reactor. Christen is working on computer simulation of grain growth.

Purdue University

Mark D. Vaudin of NIST is collaborating with Keith J. Bowman of Purdue University on texture studies in Al_2O_3. The texture of a hot-forged alumina sample was determined using BKPDP and compared with data collected at Purdue using x-ray diffraction. The texture was found to be strongly [0001] (i.e. c-axis); x-ray measurements are not as accurate in the strong texture regime so corroboration from other techniques was desirable. Grain boundary misorientations in gallium-embrittled aluminum are being measured using BKDP with the intention of assessing interface strength as a function of the misorientation parameters.

Rensselaer Polytechnic Institute

Collaboration on the diffraction imaging of semiconducting multilayers (Bruce Steiner, NIST, and Krishna Rajan, RPI)

Rutgers University

S. C. Danforth (Rutgers) has provided A. Pechenik (NIST) with nano-sized Si_3N_4 powder. The powder is processed at NIST using our diamond cell.

S. M. Hsu is collaborating with Profs. Niesz and Wachtman on microstructural design for wear resistance on silicon nitrides. Variation of grain size, shape and interface strength are being examined. The materials processed are evaluated both at NIST and at Rutgers.

H. Han is collaborative with G. G. Long (NIST) and S. Krueger (NiST/Radiation Reactor Division), A. Allen and H. Kerch in the study of nanophase powders and processing.

NIST (Linda Braun, Grady White, and Gasper Piermarini) has begun a collaborative effort with Roger Cannon to investigate toughening mechanisms in ceramics via micro-focus Raman spectroscopy measurements.

Grady White of NIST has been interacting with Steve Garofalini at Rutgers University investigating environmental effects on crack growth in silica.

Seoul National University

NIST (John E. Blendell) is collaborating with Doh-Yeon Kim of Seoul National University, Korea on the wetting of grain boundaries in Al_2O_3.

Stanford University

Professor W. Spicer is collaborating with J. C. Woicik, NIST, on the structure of metal/semiconductor interfaces and clean semiconductor interfaces.

State University of New York at Stony Brook

Collaboration on the observation of four wave mixing and related optical phenomena in non linear optical crystals (Bruce Steiner, NIST, and Mark Cronin-Golomb and Gerard Fogarty, Tufts)

Tufts University

Collaboration on the observation of four wave mixing and related optical phenomena in non linear optical crystals (Bruce Steiner, NIST, and Mark Cronin-Golomb and Gerard Fogarty, Tufts)

University of California at Berkeley

Professor Andrea M. Glaeser is collaborating with T.J. Chuang, NIST, on microdesign of interfacial defects for creep crack growth experiment.

University of California at Santa Barbara

Joint experiments between University of California (J. N. Israelachvili, P. McGuiggan) and NIST (R. Horn and D. Smith) are being conducted to investigate frictional properties of silica surfaces under dry conditions and with a variety of thin (< 10 nm) intervening liquid films.
University of Colorado/Joint Institute for Laboratory Astrophysics

Collaboration in the surface treatment of barium titanate single crystals (Bruce Steiner, NIST, Mark Cronin-Golomb and Gerard Fogarty, Tufts University, and Dana Anderson, U. Col.)

University of Dayton Research Institute

Using UDRI's x-ray photoelectron spectrometer (XPS) and Auger electron spectrometer (AES), T. Wittberg, UDRI, is conducting studies on surface structures and reactivities with P. S. Wang, NIST. A variety of powders and ceramic materials have been investigated and the results have been published.

University of Florida

B. Moudgil is studying the characterization techniques and structure of flocs in dense slurries with G. G. Long and S. G. Malghan. Primary emphasis is placed on interfacial, rheological, and scattering (neutron and x-ray) techniques.

University of Grenoble

NIST (Benjamin P. Burton) has been working with Prof. A. Pasturel, CNRS/University of Grenoble, to make first principles phase diagram calculations of BCC based ordering in Ni-Al-Ti and Fe-Be alloys.

University of Illinois

Prof. S. Danyluk is collaborating with S. M. Hsu on wear mechanisms of ceramic materials and the definition of surface quality in terms of strength as a result of machining damage.

University of Illinois and Rockwell Science Center

NIST (Grady White and Steve Freiman) has written a joint proposal with Dwight Viehland of the University of Illinois and Ratnaker Neurgaonkar of Rockwell Science Center to investigate mechanical and electronic properties of piezoelectric and electrostrictive materials for use in smart material applications.

University of Maryland

A collaborative study between the University of Maryland (A. Roitburd) and NIST (D. Kaiser, F. Gayle, L. Swartzendruber, L. Bennett) involves theoretical aspects of twin boundary migration under an applied stress and flux pinning by twin boundaries in $YBa_2Cu_3O_{6+x}$.

L. Chang and Y. Zhang, U. MD, are collaborating with P. S. Wang on a project to investigate ceramic surface reactivities with surface lubricants at high temperature by TGA/DSC as well as surface film formations. The lubricant oxidation is studied through free radical formation and recombinations by the electron spin resonance (ESR) method.

R. K. Khanna is conducting joint research with S. Malghan on the Raman and FTIR Spectroscopy of silicon nitride, silicon carbide, zirconia and aluminum nitride powders.

Collaborative research between L. K. Ives (NIST) and L. Salamanca-Reba (University of Maryland) is being conducted to investigate 5the microstructure of tribo-oxide films.

M. Wuttig is collaborating with S. M. Hsu on wear resistance of materials and the micromechanical mechanisms of asperity interactions.

A joint study is underway concerning the mechanics of indentation of materials down to the nanoscale of size and forces (A. W. Ruff, NIST; R. Armstrong, J. Dally, University of Maryland).

Bai-Hao Chen and Bryan Eichgorn of UM are collaborators in the structural investigation of new superconductor related single crystal materials (with W. Wong-Ng, NIST). For examples, members of a new Ruddlesten-Popper series of compounds $Ba_{n+1}A_nS_{3n+1}$, where A = Hf and Zr have been successfully studied.

University of Michigan

J. Schwank is carrying out specialized characterization of conductive ceramic powders by ESCA and Auger spectroscopy in collaboration with J. Ritter, NIST. These powders are synthesized at NIST for NASA.

Investigators at NIST (Mike Hill, Grady White, and Steve Freiman) are collaborating with Isabelle Lloyd investigating mechanical and electrical effects of cyclic loading of PZT. Mike Hill is using the research as partial fulfillment of requirements for a PhD in materials science.

John Gland (U. of M) and Dan Fischer (NIST) are collaborating on a carbon K near edge fluorescence yield study of the hydrogenolysis of the well characterized methylthiolate (CH_3S) surface intermediate. We have been able to isolate the carbon sulfur bond cleavage elementary reaction step so that detailed kinetic studies could be performed.

University of Pennsylvania

P. Davies of the University of Pennsylvania has been working with NIST (Robert S. Roth, Claudia J. Rawn, and Curtis G. Lindsay) on high-resolution transmission electron microscopic images of microwave dielectric materials. The possibility is envisioned that he may become involved in thermochemical analysis of high-temperature superconducting materials in the Bi-Pb-Sr-Ca-Cu oxide system to determine phase stability.

University of Virginia

NIST (Mark D. Vaudin) and John Wert, Univeristy of Virginia, have been investigating the orientation of grains adjacent to a fracture surface in a brittle intermetallic (Al_3Ti) as part of a project to test a model of fracture in these materials.

University of Washington

Professor Larry Sorenson is collaborating with C. E. Bouldin and J. C. Woicik on XAFS and diffraction studies of strained semiconductor materials.

University of Western Ontario

A collaboration was initiated this year between H. H. Schloessin and R. A. Secco of the Geophysics Department and R. D. Spal, NIST, involving the study of geological samples by means of x-ray diffraction topography and the asymmetric Bragg diffraction microscope.

University of Wisconsin

V. Hackley, Water Chemistry Program, Civil Eng. Department at the University of Wisconsin is conducting joint research with NIST on the electrokinetic sonic amplitude (ESA) measurement technique for dispersion of powders. The results of this research are to be used for the application of ESA technique for on-line monitoring of ceramic slurry properties.

A joint activity is underway between the University of Wisconsin (S. Babcock, X. Cai, D. Larbalestier) and NIST (D. Kaiser) to characterize the microstructural, magnetic and electrical transport properties of single crystals and bicrystals of superconducting $YBa_2Cu_3O_{6+x}$.

University of Washington

David Castner, Buddy Ratner, and Dan Fischer (NIST) have used the polarization dependence of carbon and fluorine NEXAFS to understand the orientation of flurocarbon groups and proteins on polymeric biomaterials used in medical implants. The orientation of surface species was shown to differ for various polymeric preparation techniques which also correlated with protein film growth, an important consideration in bio compatibility of these materials.

FACILITIES

FACILITIES

POWDER CHARACTERIZATION AND PROCESSING

High Temperature X-ray Diffraction - J. P. Cline

The x-ray diffraction facility at NIST consists of a high temperature machine of theta-two theta geometry equipped with an incident beam monochrometer and a position sensitive proportional counter. The incident beam monochrometer removes the Kα2 radiation and results in diffraction profiles that are more sensitive to effects of sample character. The position sensitive detector allows for data collection at a rate two orders of magnitude faster than conventional detectors. The furnace is an enclosed high vacuum chamber capable of reaching 3000 K, it is equipped with a mass flow controller for atmospheric control. This equipment is used for the study of high temperature phase equilibria, high temperature reaction kinetics, sintering of monolithic ceramics, and strain development during sintering of ceramic composites. Additional equipment consists of four automated and updated Philips diffractometers which are used for certification of standard reference materials (SRMs), studies on the effects of microabsorption and extinction, and the development of the Rietveld method for a conventional, sealed tube,
X-ray diffraction equipment.

Electrokinetic Measurements - V. A. Hackley and S. G. Malghan

The Matec ESA-8000 system has the unique capability for measuring colloidal properties in dense slurries. The analytical capabilities of the ESA system include performance in the following modes: potentiometric titration, conductometric titration, time-series titration, and concentration series titration. In the selected mode, the equipment can monitor: electrokinetic sonic amplitude, zeta-potential, electrophoretic mobility, electrical conductivity, isoelectric point, surface charge density, and phase angle of the material with the specified experimental conditions.

Slurry Rheology - S. G. Malghan and V. A. Hackley

The RTI rheometer allows for viscosity as well as rheology characterization of ceramic slurries. Rheological measurements are more informative and flexible with respect to the various slurry properties: Newtonian, pseudoplastic, plastic, dilatant, and thixotropic. The modeling of these rheological properties as a function of sample treatment, surface chemical properties is paramount in developing and improving the slurry processing technology.

Physical Properties Characterization Laboratory - L. Lum, D. Minor, P. Pei and S. Malghan

The physical properties characterization laboratory is equipped with state-of-the-art techniques for the measurement of particle size distribution, specific surface area, specific gravity, tap density, and porosity. The particle size distribution is measured by three techniques -- gravity sedimentation by Sedigraph, centrifugal sedimentation by Joyce-Loeble, laser diffraction by Horiba LA-900. The range of particle size distribution covered by these techniques is 0.01 μm to 200 μm. The specific surface area determination is carried out by nitrogen adsorption and the BET method. The porosity of powders and ceramics is measured by mercury intrusion.

Colloidal Processing of Powders - S. Malghan, D. Minor and P. Pei

The focus of this laboratory is to develop data and understanding of non-oxide powders processing in aqueous environment. The laboratory is equipped with instruments and equipment for studying deagglomeration, dispersion, suspension stability, slurry casting, and green body microstructure evaluation.

Agitation Milling of Powders - D. Minor and S. Malghan

High energy agitation milling of silicon nitride powders is carried out with a minimum contamination by the use of a specially designed milling system. This milling device allows for the size reduction of silicon nitride powder by milling at high slurry densities in approximately 1/6th to 1/10th of the time required by the conventional tumbling ball mill. The mill is lined with silicon nitride and the media are made of silicon nitride materials. Hence, external sources of contamination can be minimized.

Nuclear Magnetic Resonance (NMR) - P. S. Wang

The solid state NMR facility includes a Bruker MSL-400 NMR system capable of studying almost all NMR active nuclei in the periodic table in both solid and liquid states as well as performing NMR imaging in proton and carbon-13 frequencies. Currently, the operation parameters for both states at proton, deuterium, carbon-13, and aluminum-27 have been defined and proved by documented NMR spectra of organic and inorganic molecules. The equipment has been tuned to Si-29, Cu-63, and Y-89.

Scanning Electron Microscope/Image Analysis (SEM) Facility - J. F. Kelly

This laboratory is equipped with an Amray 1830 digital scanning electron microscope with LaB_6 source and a Leitz optical microscope. The SEM is equipped with a solid state backscatter detector and an ultrathin window x-ray detector. A Kevex Delta V EDS x-ray analysis and image analysis system is interfaced to both the SEM and optical microscopes. Automated imaging capabilities enable rapid size and shape analysis of a variety of imaged features,

including ceramic powder particles and second phase regions in composite structures. Fracture stages have been developed for real time observation and measurement of in-situ crack propagation in ceramic specimens. The addition of an interior mounted phosphore screen with video camera imaging provides the capability of imaging single grain electron backscatter diffraction patterns from bulk specimens. This permits the measurement of crystallographic orientation in ceramic specimens.

Thermal Analysis Facility - J. Wallace and J. Blendell

This facility includes equipment for measurement of behavior of ceramic materials in a wide range of atmospheres and temperatures. The equipment is comprised of a computer-controlled differential pushrod dilatometer capable of measuring thermal expansion or sintering shrinkage in vacuum, inert, oxidizing or reducing conditions from room temperature to 1600 °C. The atmosphere can be monitored using either a zirconia oxygen cell or an external mass spectrometer using its own associated computerized data acquisition system.

The second major piece of equipment is a simultaneous thermal analysis (STA) system which is capable of performing simultaneous thermogravimetric and differential thermal analysis from room temperature to 1700 °C. Atmospheres can be varied from vacuum to single and mixtures of gases using a four channel mass flow controller. The STA is also connected to the mass spectrometer system and it's associated data acquisition system. The quadrapole mass spectrometer system has a capability of analyzing to 512 AMU.

Chemical Laboratory Facilities - J. J. Ritter

Chemical synthesis of powders is carried out in a well-equipped laboratory, which consists of controlled atmosphere glove boxes, preparative chemical vacuum systems, and a chemical flow reactor. A range of powders can be synthesized for exploratory purposes.

Ceramics Powders Processing Laboratory - J. Wallace and J. Blendell

A processing laboratory for processing and sintering well controlled ceramic powders has been assembled. This facility consists of: equipment for chemical powder synthesis routes; attrition mills; ball mill; jet mill; pressure slip caster; uniaxial presses; cold isostatic press; spray dryers; drying ovens; hot presses; air furnaces to 1700°C; controlled atmosphere furnaces with associated gas flow systems and oxygen sensors for temperatures to 1600°C; graphite furnace for temperatures to 2300°C and a hot isostatic press/gas pressure sintering furnace capable of 2300°C and 200 MPa using graphite elements and insulation.

Nano-Size Powders Processing - W. Chen and S. Malghan

This is a new facility which consists of equipment for powder handling in inert environment, compaction of nano-size powders, and sintering under environment control. The compaction equipment was designed to facilitate the application of wide range of pressures (up to 5 GPa), temperatures (cryogenic to 1000°C) and environments. The size of green ceramic produced in this system is 3.0 mm diameter.

SURFACE PROPERTIES

Wear Tests - S. M. Hsu and S. W. Ruff

A state-of-the-art friction and wear testing laboratory is available for the evaluation of materials under different applications and conditions. Contact geometries include pin-on-disk, cross cylinders, ball-on-flat, ball-on-balls, flat-on-flat, and ring-on-block. Various motions and operating conditions are available to simulate many industrial applications. Environmental control includes temperature (room temperature to 1200°C), vacuum, and humidity.

Surface Analysis - S. M. Hsu, R. S. Gates, and S. W. Ruff

Many modern specialized instrumentation are available for the analysis of surface properties of materials. Mechanical property measurement include hot hardness tester, Vicker's indenter, nano-indentor, scratch test, and controlled depth micro-scratch test. Chemical property measurement include time-resolved micro-Raman spectroscopy, FTIR microscopic spectroscopy, GC-MS, SEM with EDX analysis, IR and UV spectroscopies with API compound identification files. A specially designed organo-metallic speciation facility is also available to detect surface reaction products at ppm level. Access to conventional surface analysis such as XPS, ESCA, AUGER, etc are also available through external contract.

Hydrocarbon Oxidation Facility - S. M. Hsu

Various oxidation apparatus are available to study the oxidation and degradation mechanisms of hydrocarbon mixtures. These include DSC, TGA, a simultaneous TGA/DTA, a specially designed chemiluminescence apparatus, hot tube, panel coker, micro-oxidation, TFOUT, and other engine simulation instruments.

STM/AFM - S. M. Hsu

A Digital commercial scanning tunnelling microscope (STM) and atomic force microscope (AFM) is available to measure surface properties at atomic level.

Time-Resolved Micro-Raman - S. M. Hsu

This versatile facility consists of a pulsed Nd-YAG laser, a CW Ar-ion laser, a triple monochromator, and a gated intensified diode array detector. This facility, therefore, provides a wide variety of Raman analysis techniques in both time-resolved and continuous operation modes, using either visible or ultra-violet excitation sources for either operation mode. In addition, either bulk macro-Raman or 5 μm resolution micro-Raman analysis is available.

MECHANICAL PROPERTIES

Surface Forces Laboratory – D. T. Smith

The surface forces laboratory consists of a semi-clean-room preparation facility and a crossed-cylinders surface force apparatus. The crossed-cylinder apparatus permits measurements of atomic-scale forces between surfaces. It can be operated with a variety of liquid or gaseous environments, thus allowing investigations of the effects of chemical changes on the forces between two surfaces. The apparatus includes several unique features that were developed and built by the surface forces group. First, sensitive custom electrometer circuits were built into the apparatus to allow in situ measurements of surface charges resulting from contact electrification. Second, the apparatus is being modified to permit the sliding of one surface over the other under constant applied load.

Nano-Indentation Apparatus – D. T. Smith

The Ceramics Division has purchased an instrumented indenter from Nano Instruments, Inc., which should be on site by the end of 1992. The indenter, under computer control, is capable of measuring loading–unloading indentation curves with displacement resolution better than 0.04 nm and load resolution better than 150 nN. This capability will allow detailed studies of the mechanical properties (hardness, Young's modulus, substrate adhesion) of very thin (tens of nanometers and up) ceramic films.

Instrumented Indenter - D. Cranmer

This apparatus is designed to enhance our ability to measure the properties of the fiber/matrix interface in ceramic matrix composites. The instrumented indenter permits us to measure the force on and displacement of a fiber directly during loading and unloading. Previous methods for examining these properties could only measure the maximum applied load and inelastic displacement.

High Temperature Creep Apparatus - D. Cranmer and S. Wiederhorn

A series of four high temperature creep rigs (T_{max} = 1550 °C) equipped with laser displacement sensors are available to determine the behavior of materials at elevated temperatures. Additionally, a rig capable of 1800 °C in air equipped with the same laser displacement sensor is available.

Analytical Electron Microscopy - B. Hockey

Several transmission and scanning electron microscopes are available for analysis of the changes in microstructure as a result of creep.

Glass Melting - D. Cranmer and D. Kauffman

Extensive glass melting and annealing facilities for production of melts up to 1600 °C are available. Batch sizes up to about 2.5 -3 kg can be produced using this equipment. Special facilities for melts containing heavy metals such as thallium and lead are also available.

Viscometers - D. Cranmer

Rotating bob, fiber elongation, and bending beam apparatuses for determining the complete range of viscosity from about 10^{14} to 10^{1} poise over the temperature range from room temperature to 1600 °C are available.

Microsphere Fabrication - D. Cranmer

This special facility is available to make relatively uniform diameter spheres of about 1 - 10 micrometers. Virtually any glass composition which can be melted below 1600 °C can be made into spheres with this apparatus.

ELECTRONIC MATERIALS

Ceramics Processing Laboratory - J. Blendell, J. Wallace, S. Malghan

A processing laboratory for the synthesis and production of well controlled ceramics has been assembled. Equipment includes: cold isostatic process, hot presses, furnaces, milling equipment, a sinter forge and tape caster.

Level 10 Clean Room - J. Blendell

A Level 10 Clean Room has been constructed for the processing of ceramics in a controlled environment where the presence of air low contaminants can seriously affect the final products properties. The room is provided with separated work stations to allow simultaneous conduct of experiments.

Thermal Wave Analysis Facility - A. Feldman and G. White

This facility is used for characterizations based on variations of thermal diffusivities. Equipped with both an Ar-ion and CO_2 laser, the facility permits analyses by infrared and Mirage methods. It is especially useful as a nondestructive method of detecting flaws in ceramics especially in near-surface regions.

OPTICAL MATERIALS

Diamond Film Deposition - E. Farabaugh and A. Feldman

Facilities consist of two hot filament CVD reactors, a microwave enhanced CVD reactor. The hot filament reactors can deposit diamond onto substrates up to 2.5 cm x 2.5 cm. The microwave reactor can accommodate substrates up to 10 cm in diameter. The reactant gases are hydrogen and methane. Growth rates typically range from 0.1 to 0.6 μm/hr.

Optical Characterization - L. Robins and A. Feldman

Facilities include a Cary spectrophotometer for measuring optical transmittance in the spectral range 0.2 μm to 2.5 μm, optical spectrometers for measuring photoluminescence and Raman spectra, and an argon ion laser.

Defect and Morphology Characterization - L. Robins and L. Cook

Facility consists of a scanning electron microscope (SEM) equipped with mirrors for cathodoluminescence detection allowing for simultaneous electron and cathodoluminscence imaging. A spectrometer for optical spectrum analysis of the cathodoluminescence radiation is attached to the SEM.

Single Crystal X-Ray Diffractometer - W. Wong-Ng

A commercial automated x-ray diffractometer suitable for single crystals is available. It is used by researchers from the Reactor Radiation and Polymers Divisions, in addition to those from the Ceramics Division, in investigations of the crystal structures of materials.

Thin Film Deposition and Characterization - E. Farabaugh

Facility consists of an electron beam deposition system equipped with multiple sources for codeposition. Attached to the deposition system is surface analysis chamber with capabilities for Auger spectroscopy, electronic energy loss spectroscopy, x-ray photoelectron spectroscopy, and secondary ion mass spectroscopy. Facility includes a HP-1000 computer for data acquisition.

Metallorganic Chemical Vapor Deposition (MOCVD) System - D. Kaiser

The system has been designed for depositing selected oxide materials by the method of MOCVD. The materials that can be deposited depend on the availability of metallorganic precursor materials. At present precursors suitable for depositing titanium dioxide and barium oxide are available. The substrate area is approximately 1 cm x 1 cm.

MATERIALS MICROSTRUCTURE CHARACTERIZATION

Synchrotron Radiation Beamlines - G. G. Long

The Materials Microstructure Characterization Group operates two beamstations on the X23A port at the National Synchrotron Light Source at Brookhaven National Laboratory in New York. These two beamstations offer access to dedicated instrumentation for small-angle x-ray scattering, x-ray diffraction imaging (topography) and EXAFS.

Small-angle x-ray scattering can be carried out in the energy range from 5 to 11 keV. The minimum wavevector is 4 x 10^{-3} nm^{-1} and the wavelength resolution is $\Delta\lambda/\lambda = 10^{-4}$, nomalous small-angle scattering with excellent resolution. Diffraction imaging of single crystals and powders is carried out with monochromatic photons between 5 and 30 keV. An energy-tunable x-ray image magnifier enables imaging of microstructure down to less than 1 μm. EXAFS experiments are also performed over an energy range from 5 - 30 keV.

Small-angle scattering measurements on ceramic and metallurgical materials are being used to characterize the microstructure in the 2 nm to 1 μm size range as a function starting chemistry and processing parameters. Diffraction imaging is being used to study imperfections and strains in single crystals and powder compacts. EXAFS is being used to study the structure of strained semiconductor interfaces and metal multilayers. A combination of EXAFS and diffraction will provide a capability for site-specific local structure determination in crystals.

SANS - Ceramics Furnace - G. Long

The SANS-Ceramic furnace is a unique facility that is now coming together. This system will allow in-situ densification studies of ceramic powders and SANS application. The experimental system has been designed to carry out densification studies of oxide powders at temperatures up to 2000 °C. In addition, the furnace will be equipped with a dilatometer.

APPENDIX

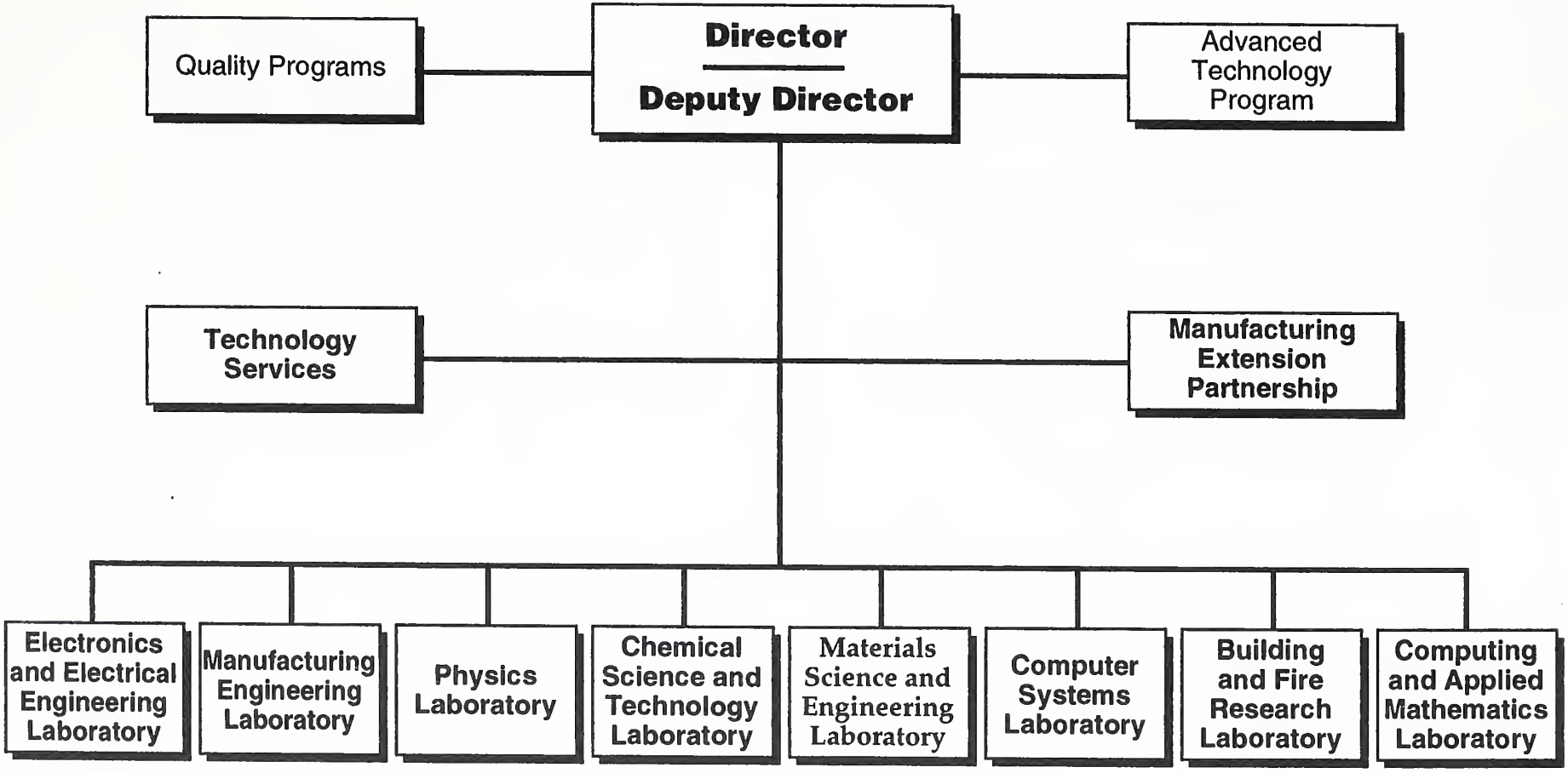
Director
Deputy Director
Quality Programs
Advanced Technology Program
Technology Services
Manufacturing Extension Partnership
Electronics and Electrical Engineering Laboratory
Manufacturing Engineering Laboratory
Physics Laboratory
Chemical Science and Technology Laboratory
Materials Science and Engineering Laboratory
Computer Systems Laboratory
Building and Fire Research Laboratory
Computing and Applied Mathematics Laboratory

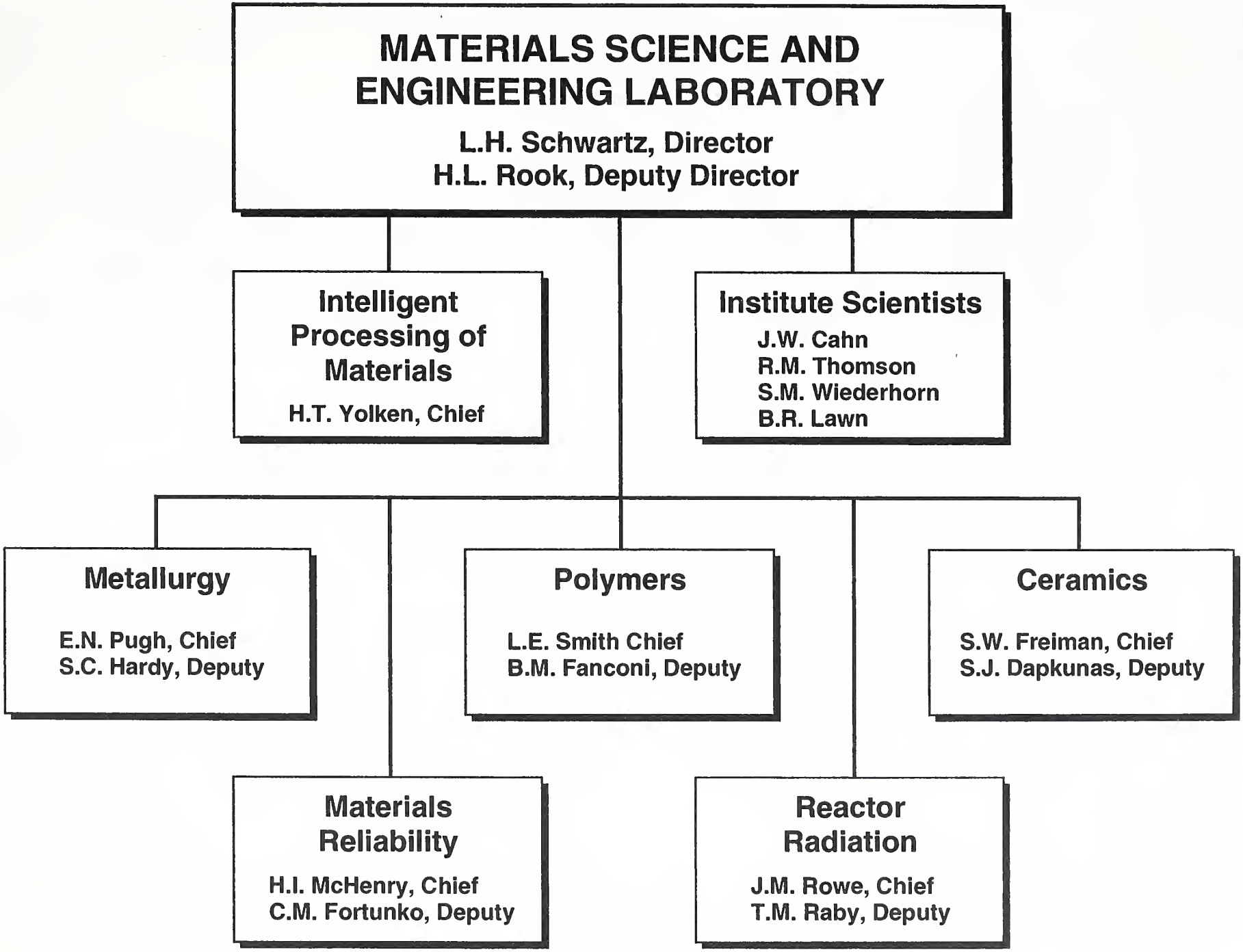
MATERIALS SCIENCE AND ENGINEERING LABORATORY
L.H. Schwartz, Director
H.L. Rook, Deputy Director
Intelligent Processing of Materials
H.T. Yolken, Chief
Institute Scientists
J.W. Cahn
R.M. Thomson
S.M. Wiederhorn
B.R. Lawn
Metallurgy
E.N. Pugh, Chief
S.C. Hardy, Deputy
Polymers
L.E. Smith Chief
B.M. Fanconi, Deputy
Ceramics
S.W. Freiman, Chief
S.J. Dapkunas, Deputy
Materials Reliability
H.I. McHenry, Chief
C.M. Fortunko, Deputy
Reactor Radiation
J.M. Rowe, Chief
T.M. Raby, Deputy

Ceramics Division

Division Office 975-6119, FAX 990-8729

Dr. Stephen Freiman, Chief
Mrs. Carolyn Sladic
Mr. S. J. Dapkunas, Deputy
Mrs. Vickie Love
Mr. Mario Cellarosi, x6123
Mrs. Wanda Warshaw, Admin. Officer, x6125
Mrs. Kimberly Herndon, Admin. Asst., x6126

Division Scientists
Fuller, E., Dr. x5795
Steiner, B., Dr. x5977

Guest Sci./Res. Assoc.
Butler, E., Ms., x5799
Cai, H., Dr. x5776

Databases
Begley, E. Mr. x6118
Carpenter, J., Dr. x6397
Clevinger, M., Mrs. x6109
Munro, R. Dr. x6127

ACerS Res. Assoc.
Cedeno, C., Ms., x6109
Green, T., Mr. x6112
Hayward, E., Dr. x6117
Hill, K., Mrs. x6111
Messina, C., Mrs. x6115
Ondik, H., Dr. x6115
Swanson, N., Mr. x6117

Powder Characterization and Processing

Malghan, S., Dr. x6101
Robinson, M., Ms. x6179

Carter, C., Dr. x3971
Cline, J., Dr. x5793
Kelly, J., Dr. x5794
Lum, L., Mrs. x3674
Minor, D., Mr. x5787
Pei, P., Dr. x3681
Ritter, J., Dr. x6106
Wallace, J., Dr. x5984
Wang, P., Dr. x6104

Guest Sci./Res. Assoc.
Chen, W., Dr. x5275
Dominquez, L., Mr. x6179
Hackley, V., Dr. x6790
Premachandran, R., Dr. x2168

Mechanical Properties

Freiman, S., Dr. x6119 (Acting)
Williams, V., Ms. x5736

Braun, L. Dr., x5777
Cranmer, D., Dr. x5753(Detailed)
Chuang, T., Dr. x5773
Hockey, B., Dr. x5780
Jahanmir, S., Dr. x3671
Kauffman, D., Mr. x5764
Krause, R., Mr. x5781
Osterlag, C., Dr. x6102
Quinn, G., Mr. x6766
Smith, D., Dr. x5766

Guest Sci./Res. Assoc.
Chapel, J., Dr. x6183
Blackburn, D., Mr. x5763
Daily, J., Dr. x3676
Dong, X., Mr. x5046
Gellings, R., Mr. x6673
Larsen-Basse, J., Dr. x5437
Liang, H., Dr x3675
Nguyen, T., Mr. x5773
Roberts, E., Mr. x5779
Salar, J., Ms. x5753
Strakna, T., Mr. x5022
Xu, H., Mr. x6784
Zhang, G., Dr. x3670

Electronic Materials

White, G., Dr. x5752
Northup, D., Mrs. x5741

Blendell, J., Dr. x5796
Burton, B., Dr. x6043
Chiang, C.K., Dr. x6122
Cook, L., Dr. x6114
Hill, M., Mr. x5798
Lindsay, C., Dr. x5786
Piermarini, G., Dr. x5734
Vaudin, M., Dr. x5789
Wong-Ng, W., Dr. x6781

Guest Sci./Res. Assoc.
Block, S., Dr. x5733
Chu, Y.,Dr. x5734
Craig, C.,Dr x5741
Gallas, M., Dr. x6129
Haller, W., Dr. x5767
Lee, B.W., Dr. x5714
Lee, H.M., Dr. x5279
McMurdie, H., Mr. x5782
Parelzkin, B., Mr. x5789
Roth, R., Dr. x6116
Russell, T. Dr., x5733
Smith, W., Dr. x5741

Optical Materials

Feldman, A., Dr. x5740
Hazel, L., Ms. x6385

Farabaugh, E., Dr. x5747
Kaiser, D., Dr. x6759
Robins, L., Dr. x6263
Rotter, L., Dr. x6603

Guest Sci./Res. Assoc.
Frederikse, H., Dr. x5749
Wilke, M., Mr. x5759

Materials Microstructural Characterization

Long, G., Dr. x5975
Brown, D., Ms. x5972

Black, D., Dr. x5976
Boudin, C., Dr. x2046
Burdette, H., Mr. x5979
Fischer, D., Dr., NSLS
Spal, R., Dr. x4028
Wolcik, J., Dr. NSLS

Guest Sci./Res. Assoc.
Allen, A., Dr. x5962
Coker, E., Dr., NSLS
Hahn, H., Dr. x5972
Jamian, P., Dr. NSLS
Karch, H., Dr. x3004
Krebs, L., Ms. x5972
Kruger, J., Mr. x5975
Pan, Y., Mr. x5972

Surface Properties

Hsu, S., Dr. x6120
Reginski, F., Mrs. x6029

Gates, R., Mr. x3677
Ives, L., Mr. x6013
Ruff, A.W., Dr. x6010

Guest Sci./Res. Assoc.
Bogatin, O., Dr. x6121
Chen, Y., Mr. x6389
Gu, J., Dr. x3672
He, C., Mr. x3046
Hu, Z., Dr. x5273
Lee, S., Dr. x5016
Liu, H., Dr. x3529
Perez, J., Dr. x3678
Peterson, M., Mr. x6012
Shen, M., Dr. x5294
Shin, H., Mr. x4087
Sun, J., Dr. x5271
Vinod, N., Mr. x4089
Wang, Y., Mr. x5280
Ying, T., Mr. x5278
Zutshi, A., Dr. x6029